

**ANALYSIS OF TAILPIPE EMISSIONS, THERMAL EFFICIENCY  
AND FUEL CONSUMPTION FOR URBAN REAL WORLD  
DRIVING USING A SI PASSENGER CAR AS A PROBE  
VEHICLE**

Ahmad M M Khalfan

Submitted in accordance with the requirements for the degree of  
Doctor of Philosophy

The University of Leeds  
School of Chemical and Process Engineering

November, 2016

## **ACKNOWLEDGEMENTS**

It takes more than an individual to carry out and successfully complete a PhD research, and towards this end, I would like to recognize the invaluable contributions of the following people, directly or indirectly during the last three years, towards this goal.

Firstly, I would like to thank the Almighty God for having given me the strength and guidance during this challenging period, and to have seen me through it. Without Him, none of this would be possible.

Secondly, I would like to thank my supervisors Prof. Gordon Andrews and Dr. Hu Li, for their wisdom, support and guidance throughout the journey to successful completion of my research. Also I would like to thank post graduate office and Postgraduate Research Tutor Dr. Darron Dixon-Hardy for their hard support.

Furthermore, I would specifically like to thank my family; my parents, my beautiful wife, and my adorable son for their encouragement and moral support always and more so during the period of my research. I will forever appreciate this.

I would like to thank colleagues and friends in the Energy Research Institute who have, in one way or another, been instrumental towards the successful completion of this research.

In summary, I would like to thank everyone for putting up with me for the last three years. I believe that this dissertation has made real contribution to the field of real driving emissions. I hope that everyone who reads this dissertation finds it useful in their work it has been a hard and challenging journey so far, even in developed processes. But I look forward to catching up with everyone and having good times after all this hard work.

## Abstract

Air quality issues in urban areas are always a big concern. Air pollution especially NO<sub>2</sub> and PM exceedances in cities are common. This is particularly true with congested traffic and the monitoring station is at the roadside. It is well known that road transport in the urban area is a major source of air pollution. Though all the vehicles have to comply the EU emission standards, the emissions were tested using the legislated standard driving cycles, which could not represent real world driving emissions. This is because compared to the legislated driving cycle, the real world driving uses different powers, different average speeds, different traffic congestion, different road gradients, different maximum acceleration rates, different cold start conditions, different numbers of stop/start events and occurs at different ambient temperatures and pressures and will inevitably have different emissions. In recognition of importance of real driving emissions, the EU plans to introduce RDE (Real driving emission) test procedure in 2017.

This work investigated real world emissions on a congested road by a roadside air quality monitoring station that exceeds European air quality standards for NO<sub>x</sub> and PM using a portable emissions measurement system (PEMS) and a Euro 4 SI passenger car. The PEMS used was the Temet FTIR with Horiba OBS pitot tube exhaust mass flow sensor and gas sampler. Twenty nine hot start repeat journeys were conducted at different times of the day (morning and evening rush hours, lunch time, night) so that a range of traffic conditions were included and eight cold start tests for the same journeys were conducted and compared with the hot start results and shown to give significantly higher emissions. The vehicle was equipped with thermocouple, lambda sensor and GPS for travel parameter analysis. The GHG including CO<sub>2</sub>, CH<sub>4</sub> and N<sub>2</sub>O, nitrogen species in the exhaust gases including NO, NO<sub>2</sub>, N<sub>2</sub>O, NH<sub>3</sub> and HCN and other emissions were analysed. The results were compared to the NEDC and WLTC. One of the suggestions from this work is that the proposal for the EU RDE test procedure do not include congested traffic driving and cold start which will compromise its expected purpose and effect.

The candidate confirms that the work submitted is his/her own, except where work which has formed part of jointly authored publications has been included. The contribution of the candidate and the other authors to this work has been explicitly indicated below. The candidate confirms that appropriate credit has been given within the thesis where reference has been made to the work of others.

This copy has been supplied on the understanding that it is copyright material and that no quotation from the thesis may be published without proper acknowledgement.



## **List of publications**

1. Li, H., Khalfan, A., & Andrews, G. (2014). Determination of GHG emissions, fuel consumption and thermal efficiency for real world urban driving using a SI probe car. SAE International Journal of Engines, 7(2014-01-1615), 1370-1381.
2. Khalfan, A., Li, H., & Andrews, G. (2014). Speciation of nitrogen compounds in the tailpipe emissions from a SI car under real world driving conditions. SAE International Journal of Engines, 7(4), 1961-1983.
3. Khalfan, A., Li, H., & Andrews, G. (2015). Cold Start SI Passenger Car Emissions from Real World Urban Congested Traffic. SAE technical paper series.
4. Khalfan, A., Li, H., & Andrews, G. E. (2016, August). Real Driving Emissions in Congested Traffic: A Comparison of Cold and Hot Start. In Conference Proceedings SAE International Powertrain, Fuels and Lubricants Meeting. SAE International.
5. Khalfan, A., Li, H., & Andrews, G. E. (2016, November). Micro trip analysis of emissions under real world congested driving. SAE World Congress Experience , Emissions Measurement and Testing.

## Table of Contents

List of Tables .....	IX
List of Figures.....	X
<b>1 Chapter One: Introduction .....</b>	<b>1</b>
1.1 Air quality and real world driving .....	1
1.2 Introduction .....	4
1.3 Objectives .....	5
1.4 Structure of the thesis .....	8
<b>2 Chapter Two: Literature review .....</b>	<b>9</b>
2.1 Introduction .....	9
2.2 Air Pollution in the UK.....	10
2.3 Measurements of air quality.....	11
2.4 Effects of vehicle exhaust emissions on global and local scales	12
2.4.1 Global scale-GHG and global warming .....	14
2.4.2 Local scale photochemical smog and its effects .....	16
2.5 Formation of pollutants in engines and their impacts on human health .....	17
2.5.1 Combustion in IC engines .....	18
2.5.2 CO (Carbon monoxide) .....	22
2.5.3 NO <sub>x</sub> (nitrogen oxides) .....	24
2.5.4 Volatile organic compounds (VOC) .....	26
2.6 Emission standards .....	35
2.7 Three-way catalytic converter (TWC) .....	36
2.7.1 Fundamentals of TWC.....	36
2.7.2 Lambda closed loop control.....	42
2.7.3 Development of TWC substrates for high conversion efficiency and fast light off.....	44
2.7.4 Lean warm up concept .....	44
2.7.5 NH <sub>3</sub> and HCN RDE emissions for TWC .....	45
2.8 Emission test cycles and measurement .....	46
2.8.1 Test cycles.....	46
2.8.2 Emission measurement methods .....	56
2.8.3 Chassis dynamometer test.....	58
2.9 Cold-start emissions .....	60
2.10 Real driving emissions (RDE).....	62
2.11 Realistic real world driving emissions tests .....	63

2.12	The crisis of air pollution in Europe.....	63
2.13	Real world tests .....	64
2.14	Car emissions testing facts .....	64
2.15	RDE test in practice .....	65
2.16	Equipment needed for RDE test .....	65
2.17	Implementation of RDE test.....	66
2.18	RDE conformity factors .....	66
2.19	RDE implementation and its impact on current technology .....	69
2.20	Impact of RDE .....	69
2.21	RDE testing for gasoline engines .....	70
2.22	RDE testing for diesel engines .....	70
<b>3</b>	<b>Chapter Three: Research methodologies.....</b>	<b>74</b>
3.1	Introduction .....	74
3.2	Experimental test car and thermal measurements .....	74
3.3	Measurements of fuel flow, air/fuel ratio and GPS .....	75
3.3.1	Fuel consumption measurement .....	75
3.3.2	Air/fuel ratio .....	76
3.3.3	Exhaust flow measurement using OBS .....	76
3.3.4	Geographical positioning system (GPS).....	77
3.4	Emission measurements system (EMS).....	77
3.4.1	Fourier transform infrared spectroscopy FTIR.....	77
3.4.2	Power for instruments.....	78
3.4.3	Sample conditioning .....	79
3.5	Mass emission and VSP calculations .....	80
3.5.1	Mass emission calculation.....	80
3.5.2	Vehicle specific power (VSP) .....	81
3.6	Test and routes.....	81
3.6.1	Test route procedure 1 .....	84
3.6.2	Test route and procedure 2 .....	87
3.6.3	Elevation calculation.....	88
3.6.4	Journeys route finder and drawing .....	92
<b>4</b>	<b>Chapter Four: Traffic flow analysis, determination of GHG emissions, fuel consumption and thermal efficiency .....</b>	<b>95</b>
4.1	Introduction .....	95
4.2	Traffic flow variations at different times of the day on the congested road .....	96

4.3	Analysis of driving parameter, fuel consumption and thermal efficiency .....	101
4.3.1	Velocity and acceleration.....	101
4.3.2	Fuel consumption and VSP.....	112
4.3.3	Overall thermal efficiency .....	114
4.4	GHG emissions.....	117
4.5	Conclusions .....	121
<b>5</b>	<b>Chapter Five: Speciation of nitrogen compounds in the tailpipe emissions from a SI car under realistic driving conditions .....</b>	<b>122</b>
5.1	Introduction .....	122
5.2	Results and discussions .....	124
5.2.1	Driving parameter analysis - velocity and acceleration ...	124
5.2.2	Concentration of nitrogen compounds.....	124
5.2.3	Time resolved mass emissions .....	124
5.2.4	Distance based cumulative mass emissions .....	126
5.3	Correlations between emissions and driving parameters .....	151
5.4	Conclusions .....	160
<b>6</b>	<b>Chapter Six: Cold start SI passenger car emissions from realistic urban congested traffic .....</b>	<b>163</b>
6.1	Introduction .....	163
6.2	Aim and objectives.....	165
6.2.1	Aim .....	165
6.2.2	Objectives.....	165
6.3	Experimental techniques .....	165
6.4	Results and discussions .....	166
6.4.1	Driving parameter analysis – velocity, acceleration and TWC light off during cold start .....	166
6.4.2	Fuel consumption and VSP.....	170
6.4.3	Greenhouse gases emissions (GHG).....	171
6.4.4	Nitrogen compound emissions .....	175
6.4.5	Legislated emissions .....	182
6.4.6	Correlations between emissions and driving parameters	188
6.5	Conclusions .....	194
<b>7</b>	<b>Chapter Seven: Real driving emissions (RDE) in congested traffic: a comparison of cold and hot start.....</b>	<b>197</b>
7.1	Results and discussions .....	197

7.1.1	Examples of real driving emission data vs time and distance .....	197
7.1.2	Emissions as a function of congestion .....	214
7.1.3	Emissions during the first minute and first 0.5 km of travel.....	226
7.2	Conclusions .....	229
<b>8</b>	<b>Chapter Eight: Micro trip analysis of emissions under real world congested driving .....</b>	<b>234</b>
8.1	Introduction .....	234
8.2	Congested traffic in urban area .....	237
8.3	Test route and procedure .....	239
8.4	The Number of stop/starts .....	242
8.5	The TWC temperature during the hot start.....	247
8.6	The emissions alongside the roadside air quality monitoring station. ....	247
8.6.1	CO <sub>2</sub> emissions.....	248
8.6.2	THC emissions .....	256
8.6.3	CO emissions .....	257
8.6.4	NO <sub>x</sub> emissions.....	258
8.6.5	Greenhouse gas emissions (GHG) .....	261
8.6.6	Toxic gas emissions .....	261
8.6.7	The role of idle in reducing the mean speed and increasing emissions.....	268
8.7	Conclusions .....	272
<b>9</b>	<b>Chapter Nine: Conclusion and future work.....</b>	<b>274</b>
9.1	Conclusions .....	274
9.2	Future work.....	277

## List of Tables

Table 2-1 Primary sources of air pollutants and their effects on human health [53].	13
Table 2-2 Content of exhaust gases according to the engine used during the combustion process [62].	21
Table 2-3 shows EU exhaust legislation for Euro 1-6 SI passenger cars [55].	35
Table 2-4 Test based on two different driving cycles as indicated [91].	54
Table 2-5 Descriptive parameters of the driving cycles [92].	56
Table 2-6: comparison between WLTP test cycles and RDE [96].	68
Table 2-7: Comparison of key parameters in test cycles and in real world driving.	72
Table 3-1 Start and end time of all the testing trips	86
Table 3-2 Directions of different driving routes.	87
Table 3-3 Start and end time of all the testing trips.	88
Table 4-1 Summary of driving parameters and GHG emissions for all journeys.	116
Table 5-1 Comparison of NH <sub>3</sub> emission (mg/km) from reference [88] and this research.	125
Table 6-1 EU exhaust legislation of EURO SI passenger cars.	165
Table 6-2 Summary of driving parameters and emissions species for all journeys.	169
Table 6-3 Comparison of NH <sub>3</sub> emission (mg/km) from reference [88] and this research	180
Table 7-1 Summary of driving parameters and emissions species for compared journey.	231
Table 7-2 Summary of driving parameters and emissions species for all journeys part A.	232
Table 7-3 Summary of driving parameters and emissions species for journey part B.	233
Table 8-1 Comparison of key parameters in test cycles and in real world driving.	235
Table 8-2 Directions of the two driving routes.	238
Table 8-3 Journey sections for locations in previous map.	240

## List of Figures

Figure 1-1 Comparison of measured and predicted annual averaged air quality data for various sites in Leeds. The Headingley roadside and background site measurements for midpoint of the studied route are indicated [1].	2
Figure 2-1 The relation between pollutant source, dispersion, chemistry and health impact [37].	9
Figure 2-2 Exhaust gases trend from the 1980's to 2015 in the UK [41].	11
Figure 2-3 Global CO <sub>2</sub> emissions caused by several source.	15
Figure 2-4 Sources of NO <sub>x</sub> and VOCs in our atmosphere [54].	17
Figure 2-5 Combustion of air fuel mixture[13].	20
Figure 2-6 Complete combustion without undesirable species (not NO <sub>x</sub> formation [13]).	20
Figure 2-7 Impact of NO <sub>x</sub> emissions.	26
Figure 2-8 Classification of hydrocarbons that belong to the category of volatile organic compounds (VOC).	28
Figure 2-9 Formation mechanisms of VOC from several sources [70].	29
Figure 2-10 Three-way catalytic converter located inside the tailpipe and their honeycomb internal structure [77].	37
Figure 2-11 Catalytic converter system [15].	39
Figure 2-12 Cross section of a 3 way catalytic converter [15].	40
Figure 2-13 Conversion efficiency for NO, CO and HC in 3 way catalyst [70].	41
Figure 2-14 Fuel conversion based on the air-to-fuel (A/F) ratio with classical three-way catalyst of stoichiometric petrol engines [62].	42
Figure 2-15 Catalytic efficiency and lambda sensor voltage relative to excess air factor [15].	43
Figure 2-16 US Test cycles for passenger cars and light commercial vehicles [91].	49
Figure 2-17 NEDC for passenger cars and light commercial vehicles.	51

Figure 2-18 Driving schedule of the NEDC cycle [92].	52
Figure 2-19 Japanese test cycles for passenger cars and light commercial vehicles [91].	53
Figure 2-20 Driving schedule of the JC08 cycle [92].	55
Figure 2-21 Driving schedule of the WLTC cycle [92].	55
Figure 2-22 Chassis dynamometer [93].	59
Figure 2-23 Chassis dynamometer cell [93].	59
Figure 2-24 Cold starts cause and effect diagram [20].	60
Figure 3-1 Scheme of the measurement system integration in a probe car Ford Mondeo.	75
Figure 3-2 Schematic diagram of sampling and data logging system.	80
Figure 3-3 Journey (A) map 1-2-3-4.	82
Figure 3-4 Journey (B) map 1-3-2-4.	83
Figure 3-5 Map and notations of driving routes.	85
Figure 3-6 Different manoeuvre at point 2 for route A (left) and B (right).	86
Figure 3-7 Map and notations of driving route.	88
Figure 3-8 Longitude and latitude data in excel sheet.	89
Figure 3-9 Saving file system in Google elevation.	90
Figure 3-10 Finding the elevation of journey on MAC computers.	91
Figure 3-11 Index file in Google elevation.	91
Figure 3-12 Data and name of the journey to find elevation.	92
Figure 3-13 Elevations data according to latitude and longitude.	92
Figure 3-14 Excel sheet show the longitude and latitude conversion.	93
Figure 3-15 Journey route on map.	93
Figure 3-16 Single point of journey on map.	94
Figure 4-1 Congested traffic driving route.	97
Figure 4-2 Mass emissions at junctions in real world driving [24-26].	97
Figure 4-3 Congestion as a function of traffic flow in vehicles per hour, vph. [107, 108].	98
Figure 4-4 Average road space per vehicle as a function of the average vehicle speed [107, 108].	99
Figure 4-5 Profiles for the trip 7:46A.	103
Figure 4-6 Profiles for the trip 8:30A.	104
Figure 4-7 Profiles for the trip 12:56A.	106



Figure 4-8 Profiles for the trip 19:25A. ....	107
Figure 4-9 Profiles for the trip 8:07B. ....	109
Figure 4-10 Profiles for the trip 8:53B. ....	110
Figure 4-11 Profiles for the trip 13:16B. ....	111
Figure 4-12 Profiles for the trip 19:41B. ....	112
Figure 4-13 Trip mean CO <sub>2</sub> emissions vs vehicle's average trip velocity. ....	119
Figure 4-14 Trip mean CH <sub>4</sub> emissions vs vehicle's average trip velocity. ....	119
Figure 4-15 Trip mean N <sub>2</sub> O emissions vs vehicle's average trip velocity. ....	120
Figure 5-1 Profiles for the trip 7:46A-a. ....	127
Figure 5-2 Profiles for the trip 8:30A. ....	128
Figure 5-3 Profiles for the trip 12:56A-a. ....	129
Figure 5-4 Profiles for the trip 19:25A-a. ....	130
Figure 5-5 Profiles for the trip 8:07B-a. ....	131
Figure 5-6 Profiles for the trip 8:53B-a. ....	132
Figure 5-7 Profiles for the trip 13:16B-a. ....	133
Figure 5-8 Profiles for the trip 19:41B-a. ....	134
Figure 5-9 Profiles for the trip 7:46A-b. ....	135
Figure 5-10 Profiles for the trip 8:30A-b. ....	136
Figure 5-11 Profiles for the trip 12:56A-b. ....	137
Figure 5-12 Profiles for the trip 19:25A-b. ....	138
Figure 5-13 Profiles for the trip 8:07B-b. ....	139
Figure 5-14 Profiles for the trip 8:53B-b. ....	140
Figure 5-15 Profiles for the trip 13:16B-b. ....	141
Figure 5-16 Profiles for the trip 19:41B-b. ....	142
Figure 5-17 Profiles for the trip 7:46A-c. ....	143
Figure 5-18 Profiles for the trip 8:30A-c. ....	144
Figure 5-19 Profiles for the trip 12:56A-c. ....	145
Figure 5-20 Profiles for the trip 19:25A-c. ....	146
Figure 5-21 Profiles for the trip 8:07B-c. ....	147
Figure 5-22 Profiles for the trip 8:53B-c. ....	148
Figure 5-23 Profiles for the trip 13:16B-c. ....	149
Figure 5-24 Profiles for the trip 19:41B-c. ....	150

Figure 5-25 Trip mean NO <sub>2</sub> emissions vs vehicle's average trip velocity.....	152
Figure 5-26 Trip mean HCN emissions vs vehicle's average trip velocity.....	152
Figure 5-27 Trip mean NH <sub>3</sub> emissions vs vehicle's average trip velocity.....	153
Figure 5-28 Trip mean N <sub>2</sub> O emissions vs vehicle's average trip velocity.....	153
Figure 5-29 Trip mean NO emissions vs vehicle's average trip velocity.....	154
Figure 5-30 Trip mean NH <sub>3</sub> emissions vs vehicle's average trip acceleration.....	154
Figure 5-31 Trip mean N <sub>2</sub> O emissions vs vehicle's average trip acceleration.....	155
Figure 5-32 Trip mean NO emissions vs vehicle's average trip acceleration.....	155
Figure 5-33 Trip mean NO <sub>2</sub> emissions vs vehicle's average trip acceleration.....	156
Figure 5-34 Trip mean HCN emissions vs vehicle's average trip acceleration.....	156
Figure 5-35 Trip mean NH <sub>3</sub> emissions vs vehicle's average trip vehicle specific power.....	157
Figure 5-36 Trip mean N <sub>2</sub> O emissions vs vehicle's average trip vehicle specific power.....	157
Figure 5-37 Trip mean NO <sub>2</sub> emissions vs vehicle's average trip vehicle specific power.....	158
Figure 5-38 Trip mean HCN emissions vs vehicle's average trip vehicle specific power.....	158
Figure 5-39 Trip mean NO emissions vs vehicle's average trip vehicle specific power.....	159
Figure 6-1 GHG Vs time profiles for the free flow trip 11:50.....	172
Figure 6-2 GHG Vs time profiles for the congested trip 16:24.....	173
Figure 6-3 GHG Vs distance profiles for the free flow trip 11:50a.....	174
Figure 6-4 GHG Vs distance profiles for the congested trip 16:24.....	175
Figure 6-5 Nitrogen species vs time profiles for the free flow trip 11:50.....	178
Figure 6-6 Nitrogen species Vs time profiles for the congested trip 16:24.....	179
Figure 6-7 Nitrogen species vs distance profiles for the free flow trip 11:50.....	181

Figure 6-8 Nitrogen species vs distance profiles for the congested trip 16:24. ....	182
Figure 6-9 Legislated species vs time profiles for the free flow trip 11:50. ....	184
Figure 6-10 Legislated species vs time profiles for the congested trip 16:24. ....	185
Figure 6-11 Legislated species vs Dist. profiles for the free flow trip 11:50. ....	186
Figure 6-12 Legislated species vs Dist. profiles for the congested trip 16:24. ....	187
Figure 6-13 Trip mean NH <sub>3</sub> emissions vs vehicle's average trip velocity. ....	188
Figure 6-14 Trip mean N <sub>2</sub> O emissions vs vehicle's average trip velocity. ....	189
Figure 6-15 Trip mean CO <sub>2</sub> emissions Vs vehicle's average trip velocity. ....	190
Figure 6-16 Trip mean CH <sub>4</sub> emissions vs vehicle's average trip velocity. ....	190
Figure 6-17 Trip mean NH <sub>3</sub> emissions vs vehicle's average trip velocity. ....	191
Figure 6-18 Trip mean THC emissions vs vehicle's average trip vehicle specific power. ....	192
Figure 6-19 Trip mean CO <sub>2</sub> emissions vs vehicle's average trip vehicle specific power. ....	192
Figure 6-20 Trip mean CH <sub>4</sub> emissions vs vehicle's average trip vehicle specific power. ....	193
Figure 7-1 GHG vs time profiles for low congested trip 9:13B. ....	198
Figure 7-2 GHG vs time profiles for high congested trip 17:40B. ....	199
Figure 7-3 GHG vs distance profiles for low congested trip 9:13B. ....	200
Figure 7-4 GHG vs distance profiles for high congested trip 17:40B. ....	201
Figure 7-5 Nitrogen species vs time profiles for low congested trip 9:13B. ....	202
Figure 7-6 Nitrogen species vs time profiles for high congested trip 17:40B. ....	203
Figure 7-7 Nitrogen species vs distance profiles for low congested trip 9:13B. ....	204
Figure 7-8 Nitrogen species vs distance profiles for high congested trip 17:40B. ....	205
Figure 7-9 Legislated species vs time profiles for low congested trip 9:13B. ....	206

Figure 7-10 Legislated species vs time profiles for high congested trip 17:40B.....	207
Figure 7-11 Legislated species vs distance profiles for low congested trip 9:13B.....	208
Figure 7-12 Legislated species vs distance profiles high congested trip 17:40B.....	209
Figure 7-13 Number of accelerations from idle vs mean trip velocity for cold and hot start trips.....	212
Figure 7-14 Number of accelerations not from idle ( $\geq 5$ kph initial vehicle speed) vs mean trip velocity for cold and hot start trips. ....	213
Figure 7-15 Trip mean CO <sub>2</sub> emissions vs vehicle's average trip velocity.....	215
Figure 7-16 Trip mean CO emissions vs vehicle's average trip velocity.....	216
Figure 7-17 Trip mean THC emissions vs vehicle's average trip velocity.....	216
Figure 7-18 Trip mean NO <sub>x</sub> emissions vs vehicle's average trip velocity.....	217
Figure 7-19 Trip mean NO <sub>2</sub> emissions vs vehicle's average trip velocity.....	217
Figure 7-20 Trip mean CH <sub>4</sub> emissions vs vehicle's average trip velocity.....	218
Figure 7-21 Trip mean N <sub>2</sub> O emissions vs vehicle's average trip velocity.....	218
Figure 7-22 Trip mean NH <sub>3</sub> emissions vs vehicle's average trip velocity.....	219
Figure 7-23 Trip mean HCN emissions vs vehicle's average trip velocity.....	219
Figure 7-24: Hot and cold CO emissions for the first km vs mean speed.....	220
Figure 7-25: Hot and cold NO <sub>x</sub> emissions for the first km vs mean speed.....	220
Figure 7-26: Hot and cold THC emissions for the first km vs mean speed.....	221
Figure 7-27: Congested traffic driving route.....	222
Figure 8-1 Map and notations of the driving route.....	238
Figure 8-2 Map of sections of the journey in Table 8-3.....	239
Figure 8-3 Velocity and acceleration records for high congestion (6 stop/starts per km) as a function of distance showing the 10 stages in Table 8-3.....	241

Figure 8-4 Velocity and acceleration records for low congestion (2.4 stop/starts per km) as a function of distance showing the 10 stages in Table 8-3. ....	242
Figure 8-5 Number of accelerations from idle vs mean trip velocity for cold and hot start trips.....	243
Figure 8-6 Number of accelerations from idle (<5km/h) per km for the 10 journey sections in Table 8-3. ....	243
Figure 8-7 The average thermal efficiency for each journey section as a function of the average velocity. ....	245
Figure 8-8 TWC upstream and downstream temperature for highly congested traffic. ....	246
Figure 8-9 TWC front and downstream temperature for lower congestion then in Figure 8-8. ....	247
Figure 8-10 CO <sub>2</sub> emissions for S <sub>2</sub> vs the mean velocity for S <sub>2</sub> . ....	249
Figure 8-11 THC emissions for S <sub>2</sub> vs the mean velocity for S <sub>2</sub> . ....	249
Figure 8-12 CO emissions for S <sub>2</sub> v. the mean velocity for S <sub>2</sub> . ....	249
Figure 8-13 NO <sub>x</sub> emissions for S <sub>2</sub> vs the mean velocity for S <sub>2</sub> . ....	250
Figure 8-14 CO <sub>2</sub> emissions for S <sub>9</sub> v. the mean velocity for S <sub>9</sub> . ....	250
Figure 8-15 THC emissions for S <sub>9</sub> vs the mean velocity for S <sub>9</sub> . ....	250
Figure 8-16 CO emissions for S <sub>9</sub> vs the mean velocity for S <sub>9</sub> . ....	251
Figure 8-17 NO <sub>x</sub> emissions for S <sub>9</sub> vs the mean velocity for S <sub>9</sub> . ....	251
Figure 8-18 CO <sub>2</sub> emissions for S <sub>1</sub> v. the mean velocity for S <sub>1</sub> . ....	251
Figure 8-19 THC emissions for S <sub>1</sub> v. the mean velocity for S <sub>1</sub> . ....	252
Figure 8-20 CO emissions for S <sub>1</sub> vs the mean velocity for S <sub>1</sub> . ....	252
Figure 8-21 NO <sub>x</sub> emissions for S <sub>1</sub> vs the mean velocity for S <sub>1</sub> . ....	253
Figure 8-22 CO <sub>2</sub> emissions for S <sub>1</sub> -S <sub>10</sub> vs the mean velocity. ....	253
Figure 8-23 THC emissions for S <sub>1</sub> – S <sub>10</sub> vs the mean velocity. ....	253
Figure 8-24 CO emissions for S <sub>1</sub> -S <sub>10</sub> vs the mean velocity. ....	254
Figure 8-25 NO <sub>x</sub> emissions for S <sub>1</sub> – S <sub>10</sub> v. the mean velocity. ....	254
Figure 8-26 NO <sub>2</sub> emissions for S <sub>1</sub> -S <sub>10</sub> vs the mean velocity. ....	254
Figure 8-27 NH <sub>3</sub> emissions for S <sub>1</sub> – S <sub>10</sub> vs the mean velocity. ....	255
Figure 8-28 CH <sub>4</sub> emissions as a function of the average velocity. ...	262
Figure 8-29 N <sub>2</sub> O emissions as a function of the average velocity. ...	262
Figure 8-30 Benzene emissions as a function of the average velocity. ....	263
Figure 8-31 Toluene emissions as a function of the average velocity. ....	263

Figure 8-32 1, 3Butadiene emissions as a function of the average velocity.....	264
Figure 8-33 Formaldehyde emissions as a function of the average velocity.....	264
Figure 8-34 Acrolein emissions as a function of the average velocity.....	265
Figure 8-35 HCN emissions as a function of the average velocity..	265
Figure 8-36 Idle percentage as a function of the average velocity..	270
Figure 8-37 CO <sub>2</sub> as a function of the average velocity without idle.	270
Figure 8-38 Fuel consumption at idle as a function of idle percentage. ....	271
Figure 8-39 Additional fuel consumption as a function of idle percentage. ....	271

## **Abbreviations**

A/F: Air Fuel ratio by mass  
ATR: Auto Thermal Reformer  
AQMA: Air Quality Management Areas  
CFD: Computational fluid dynamics  
CFC: Chlorofluorocarbon  
CH<sub>4</sub>: Methane  
CHO: Aldehydes  
CI: Compression Ignition  
CO<sub>2</sub>: Carbon dioxide  
CO: Carbon monoxide  
CVCP: Continuously Varying Cam Phasing  
CVS: Constant Volume Sampling  
DI: Direct Injection  
DU: Dobson unit  
ECE: Economic Commission for Europe  
ECU: Electronic Control Unit  
EGR: Exhaust Gas Recirculation  
EHC: Electrically Heated pre Converter  
EI: Emissions Index  
EUDC: Extra Urban Driving Cycle  
FTIR: Fourier Transform Infrared.  
FTP: Federal Test Procedure  
GDI: Gasoline Direct Injection

GHG: Green House Gas  
GPS: Global Positioning System  
GWP: Global Warming Potential  
HBr: Hydrogen Bromide  
HC, UHC: Unburned Hydrocarbon  
HDSCC: High Dilution Stoichiometric Combustion Concept  
HNO<sub>3</sub>: Nitric acid  
H<sub>2</sub>O: Water  
H<sub>2</sub>SO<sub>4</sub>: Sulfuric acid  
IC: Internal Combustion  
IMEP: Indicated Mean Effective Pressure  
LHC: Leeds Headingley Cycle  
MBT: Minimum advance for Best Torque  
NEDC: New European Driving Cycle  
NO: Nitric Oxide  
NO<sub>x</sub>: Oxides of nitrogen  
NO<sub>2</sub>: Nitric dioxide  
OBS: On Board Emissions Measurement System  
O<sub>3</sub>: Ozone  
PAN: Peroxyethanol Nitrate  
PCV: Positive Crankcase Ventilation  
PEMS: Portable Emissions Measurement System  
PFI: Port Fuel Injection  
PM: particulate Matter  
POX: Partial Oxidation Reformer  
RDE: Real Driving Emissions  
RNA: Ribose Nucleic Acid  
REPO: Rapid Exhaust Port Oxidation  
SCR: Selective Catalytic Reduction  
SI: Spark Ignition  
STR: Steam Reformer  
SO<sub>2</sub>: Sulphur dioxide  
TAPs: Toxic Air Pollutants  
TC: Turbo Charged



TWC: Three Way Catalyst.

UDC: Urban Drive Cycle

UN: United Nations

UV: Ultraviolet

VOC: Volatile Organic Compounds

WLTC: World Light-duty Test Cycle.

# 1 Chapter One: Introduction

## 1.1 Air quality and real world driving

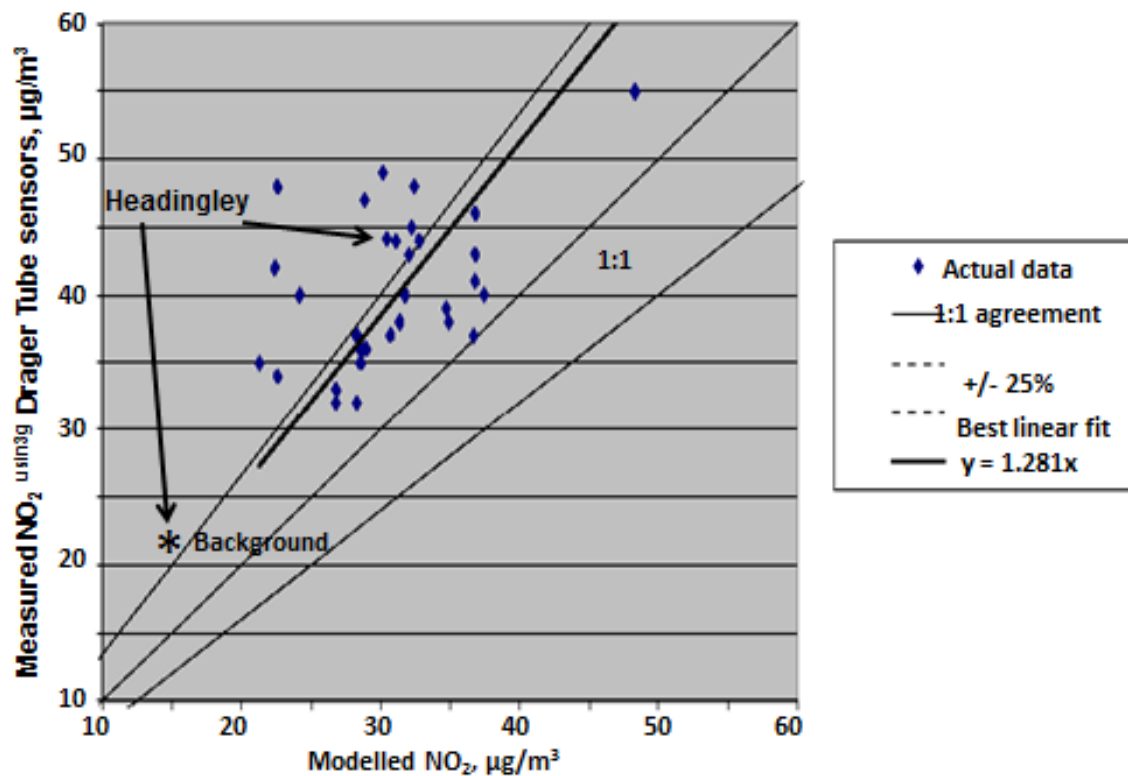
The road in the present work has been studied by Leeds City Council [1-3] in terms of its traffic density and travel times of the section studied in this work, together with associated air quality measurements using a roadside monitor alongside the test section. The studied road has many traffic lights, pedestrian crossings and 90% congestion occurs near the roadside air quality monitor during morning and evening commutes, which have the highest traffic load. This is typical of modern high population density cities with high daily commutes into the city's central areas. Leeds is the largest of three very close cities in an area with a population of 2.5 million; there are 100,000 jobs in central Leeds and 500,000 total jobs in the city. [1-3]. The road studied is one of the main radial roads into Leeds from the north and travels through a high-density population of houses and linked road junctions. It has a single lane of traffic in the inward and outward directions and is 80% congested from the outer ring road to the city centre at peak commuting times [2, 3], a distance of about 5 km.

For cities with higher populations the same condition is experienced in multi-lane highways and the total pollution will be higher than in the present work because of the multiple number of lanes. For example, in Hefei, China, which has a population of 5 million, one of the radial 8 lane highways is 90% congested (5kph average speed) on all four lanes at peak commuting times (personal experience of G.E. Andrews). Hefei has poor air quality with peak values during the evening commute that exceed EU air quality standards [4], mainly due to traffic pollution from its highly congested inner city roads.

In Europe, all of the cities have to meet defined European air quality standards and must declare Air Quality Management Areas (AQMA) if they exceed these standards. In an AQMA the city has to take action to determine the cause of the exceedance and has the power to introduce measures to reduce these emissions. In the UK, in nearly all cases where an AQMA had been declared, including Leeds, traffic pollution is the cause of the exceedance [1]. For the road studied in the present work (A660 from the Leeds Ring Road to Hyde

Park) the air quality at the roadside by the most congested part of the journey (Headingley) was monitored using a 24/7 air quality monitoring station.

The annually averaged air compositions measured at various sites in Leeds were compared with the traffic emission modelling results [1] in Figure 1-1. Air quality was modelled using the Leeds traffic model [2, 3] and vehicle NEDC emissions data together with national data on the age of the vehicles registered to drivers in Leeds, which gives the proportion of Euro 1-4 vehicles registered in Leeds. All roads were assumed to have this proportion of vehicle age. The Leeds air quality and traffic flow studies [1-3] were carried out in 2009 so only Euro 1-4 vehicles were in use.



**Figure 1-1 Comparison of measured and predicted annual averaged air quality data for various sites in Leeds. The Headingley roadside and background site measurements for midpoint of the studied route are indicated [1].**

No account was taken of traffic congestion or a cold start in the Leeds Air quality model, as the NEDC data used excluded the cold start first km, a procedure approved by government guidelines [1-3]. Other sources of NO<sub>x</sub>

are taken into account in the model, such as domestic gas central heating boilers [1-3]. Figure 1-1 shows poor agreement between the measurements and the model. On average, the Leeds air quality model was 28% too low in its prediction of NO<sub>2</sub> at the monitored sites across Leeds. At the Headingley roadside air quality measurement site, the modelled NO<sub>2</sub> concentration was 47% lower than the measured results at the roadside air quality monitoring station and 28% lower for the city centre site, which forms part of the national air quality monitoring system.

Away from the roadside, the Headingley background NO<sub>2</sub> measurement was 22 µg/m<sup>3</sup> compared with a predicted value of 15 µg/m<sup>3</sup>. Regulations for NO<sub>2</sub> are an annual averaged limit of 40 µg/m<sup>3</sup> annual limit and a 100µg/m<sup>3</sup> one hour limit. The annual averaged NO<sub>2</sub> measurements in Figure 1-1 for several sites in Leeds showed 16 sites above the EU annual limit where the model only predicted one site in exceedance. The high NO<sub>2</sub> for most of Leeds was attributed to traffic congestion [1-3].

The reduction of the legislated exhaust pollutants from the transportation industry for CO, NO<sub>x</sub> and HC has been over 90% since Euro 0. However, there has not been a proportionate reduction in the urban air concentrations of these pollutants. Although there has been an increase in the number of vehicles on UK roads, there is concern that the legislated test cycles may not be representative of how vehicles are driven in the real world. Many other parameters, such as ambient temperature and pressure, traffic conditions (level of congestion), topography, the number of junctions and traffic lights and driver behaviour also influence real world emissions [5-15] [16-29].

There is also concern that fuel consumption figures and CO<sub>2</sub> emissions on legislated test cycles do not agree with real world driving performance [8, 10-12, 14, 15, 24-29]. Figliozzi [27] analysed the CO<sub>2</sub> emissions from commercial freight vehicles for different levels of congestion and found significant impacts of congestion or speed limits on commercial vehicle emissions. The research concluded that public agencies and highway operators must carefully consider the implications of transport policies, such as travel speed limits on CO<sub>2</sub>

emissions and fuel economy. Lenaers [28] investigated fuel consumption and tailpipe CO<sub>2</sub> emissions from four family cars, including gasoline, diesel and hybrid cars, driving on various urban, rural and motorway routes. The results showed that fuel consumption and CO<sub>2</sub> emissions were the greatest on urban roads. Barth [29] investigated the impacts of traffic congestions on CO<sub>2</sub> emissions in Southern California and found that the CO<sub>2</sub> was reduced by up to ~20% via three strategies: congestion mitigation, which reduced severe congestion, thus allowing free flow; traffic speed management techniques, which reduced excessively high free flow speeds to more moderate conditions; and shock wave suppression techniques that eliminated acceleration and deceleration events, which are associated with the stop start events seen during congested traffic.

## **1.2 Introduction**

The current appalling press regarding modern low emission engines, which do not have the same low emissions in real world driving as seen on test cycles, shows a lack of understanding of the issue and an industry that has not conveyed its voice to the public. Irrespective of any engine calibration differences between test cycles and real world driving, which are illegal, real world driving uses different powers, average speeds, traffic congestion, road gradients, maximum acceleration rates, cold start conditions, numbers of stop/start events, occur at different ambient temperatures and pressures than on test cycles, and will inevitably have different emissions, as all these factors influence the emissions. This applies equally to spark ignition and diesel engines [5-14]. However, the most important influence on real world emissions is the driver and in a 20-driver study using A Euro 2 SI TWC vehicle Daham et al. [15] have shown a wide variation between 'aggressive' and 'conservative' drivers. This study was of a road loop that had no other traffic and the drivers were free to accelerate from junctions as they chose but were instructed not to exceed the speed limit of 48 kph.

In the present work with a spark ignition engine powered vehicle, the issue of traffic congestion was studied. Zero congestion is defined as travelling at the

maximum legal speed limit for the whole journey, e.g. travelling at a speed of 48kph (30 mph) on an urban road with a speed limit of 30 mph. Traffic congestion is then defined by Equation (1-1)

$$\text{Congestion \%} = [1 - \text{mean velocity}/48 \text{ kph}] 100 \quad (1-1)$$

If the study were for a road with a different speed limit then the speed limit value would be changed in Equation (1-1). The increased number of city regions that have introduced a lower speed limit of 32 kph in the UK will make road transport pollution worse, as vehicles have higher pollution at lower speeds, although for NO<sub>x</sub> there are also increases at high speed and high engine powers. In terms of Equation (1-1), 32 kph is a congestion of 33% for a road with a speed limit of maximum 48kph, but it will be shown in the present work that, for roads with a high traffic density in cities, 48 kph cannot be achieved and that congestion is much higher than 33%.

### **1.3 Objectives**

The main objective of this work was to determine SI vehicle exhaust emissions in congested traffic conditions using specifically designed real world driving cycles, which were located in the Leeds Headingley area where the A660 roadside air quality monitoring station is. This is one of the air pollution hotspots in Leeds and does not meet European air quality standards for NO<sub>2</sub> and PM. In the present work a 5km return journey that went past the monitoring station in the outward and return direction was used. Liu et al. [23] showed from a major survey of North American driving patterns that 50% of the trips were <4km so the present 5km journey is representative of the real world. This journey was repeated twenty nine times with a hot start, using the same driver but at different times of the day so that different congestion conditions were encountered. Eight cold start journeys were also tested [30] and the results will be compared with the hot start results as a function of the journey's mean velocity or congestion. The objective of this comparison was to show the increase in emissions that occurred when the cold start occurred in congested traffic. This is a common occurrence in cities with a high

population density, such as Leeds, with residences alongside the roads that have congested traffic.

A further objective was to measure and summarise the traffic flow characteristics responsible for poor roadside air quality in large cities. This would then provide information on the type of driving that should be included in Real Driving Emissions (RDE) legislation, if the objective of RDE was to reduce the vehicle emissions under conditions that give rise to the current poor air quality in cities. The current RDE proposals, which exclude congested driving and cold starts [23, 31, 32], will not produce data that is relevant to understanding the role of traffic emissions in generating poor air quality in urban areas. Nor will they require engine calibrations to be optimised to minimise emissions in the stop/start low speed conditions of congested traffic.

In JRC tests for light duty (LD) passenger car vehicles of Euro 3-6 [33], the gasoline vehicles in RDE were all within the NEDC emissions limits. However, this was because the RDE journeys excluded cold starts and congested traffic, which are shown in this work to have very significant real world driving influences on emissions for a Euro 4 SI vehicle. These deficiencies in the current RDE requirements are recognised and the second RDE package [34] approved by the EU TCMV (Technical Committee on Motor Vehicles) on 28<sup>th</sup> October 2015 recognises that urban NO<sub>x</sub> is a priority and should be more highly weighted than the present urban/rural/motorway equal weighting with a specific NO<sub>x</sub> limit for urban driving that must be met.

The RDE requirements include urban driving speeds of 15-40 kph with the maximum speed <60 kph (which is illegal in urban driving in the UK). In the present work in congested urban traffic the average speed is 5-26 kph, but excluding all these average speeds would be a legal RDE and most urban RDEs have average speeds of 30-40 kph, as the emissions and fuel consumption are lower at these speeds. This is how congested traffic is ignored in the RDE journey requirements. Cold start is ignored in RDE by ignoring emissions before the coolant is <70°C and the engine has been operating for >5 minutes [34]. However, in future, RDE will require tests to go

down to 3°C before 2020 and 0°C from 2020, but at present the above two criteria will still apply and the impact of cold ambient temperatures on cold start will still be ignored [41]. The package of EU RDE proposals [34] recognises that current PEMS procedures do measure cold start emissions, but exclude them when they are >70°C and five minutes from the vehicle start criteria. Procedures to include cold start in the RDE tests are being developed. However, unless cold start into congested traffic is included, the impact on air quality in congested traffic in urban areas will be underestimated. As congested traffic is currently excluded from RDE there is little chance that cold start into congested traffic will be included.

The portable emissions measurement system (PEMS) could start procedures under discussion (May 2016) under this third EU PEMS package [34]. This included cold soak at the outside ambient temperature and the inclusion of cold start in the urban phase of the RDE, where the mean velocity cannot exceed 60 kph, but mean velocities will still be 15-40 kph. Under discussion is the duration of the cold start, the impact of the cold start traffic conditions and the weighting given to the cold start emissions. The time spent under idle conditions at cold start is likely to be limited, as is the severity of driving during cold start RDE [34] (i.e. congested traffic will be excluded and the speed of driving after cold start is likely to be limited). The present work will show the importance of cold start emissions, particularly in relation to congested traffic and low speed driving.

The congested traffic route used in this work has also previously been used for real world emissions evaluations for a diesel vehicle [11-13, 35] and the present SI engine vehicle results may be compared with the diesel results for the same congestion. Although the present work and the diesel work were undertaken on Euro 4 and Euro 3 vehicles, respectively, the differences in the emissions standards from the current Euro 6 are small relative to the real world effects, which are dominated by traffic movement issues, where vehicles are operated outside the conditions of NEDC and FTP test cycles.



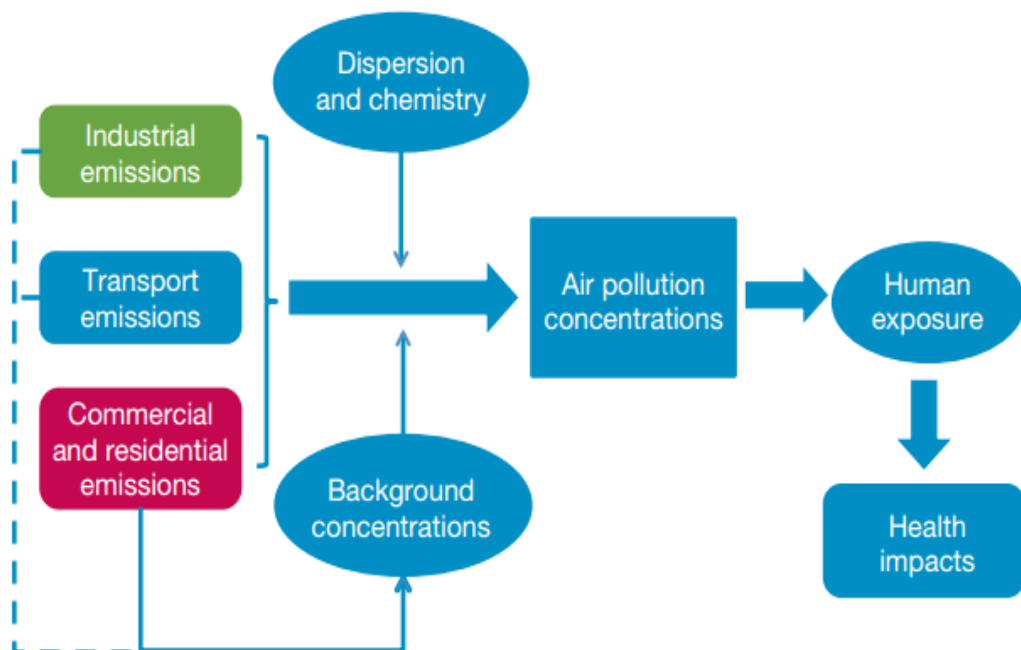
## **1.4 Structure of the thesis**

The thesis is comprised of nine chapters. Chapter one introduces the background of the research and describes the objectives and structure of the thesis. Chapter two is a literature review and chapter three is the research methodologies. Chapters four to eight are the results and chapter nine is the conclusions and suggestions. Chapter four contains traffic flow analysis for the road where the tests were conducted, a driving parameter analysis of testing journeys and GHG emissions. Chapter five deals with an analysis of nitrogen species from tailpipe emissions. Chapter six covers cold start emissions. Chapter seven is focused on comparisons between cold and hot starts. Chapter eight aims to investigate micro trip analysis of emissions under real world congested driving. Chapter nine conclusion and future work.

## 2 Chapter Two: Literature review

### 2.1 Introduction

Emissions (GHG and toxic pollutants) from combustion sources are mainly derived from three sectors: industrial, transport and commercial/residential. For toxic pollutants, they are formed during the combustion process and then undergo dispersion and further chemical reactions in the atmosphere to form secondary pollutants such as ozone. The existing relationship between the source of pollutants, their dispersion in the environment and their health impact is illustrated below in Figure 2-1. The scheme shows which industrial emissions, transport emissions and emissions coming from commercial and residential areas are among the main sources which contribute to the wider window pollution level [10, 36, 37].



**Figure 2-1 The relation between pollutant source, dispersion, chemistry and health impact [37].**

The transportation, from the 1970s onwards, and the combustion of gasoline and diesel in vehicles, have established increasing consideration as

significant sources of air pollution for local areas and global levels. According to Woodcock et al. (2007) [38] more than 95% of motorised transport depends on petroleum, which is about 30% of the world's petroleum demand. The numbers of cars has increased rapidly. For instance, within the countries of the OECD (Organisation of Economic Cooperation and Development), the average ownership of car records is over 45%, about 450 cars per 1000 persons and, in some industrialised countries, one person will often own more than one car. This trend is still increasing. Accordingly, fuel consumption has been increasing rapidly, and this has mainly been caused by increasing amounts of vehicle use, the growth of heavy duty fleet use, and a shift from personal passenger cars to personal light-duty trucks, sport utility vehicles and vans.

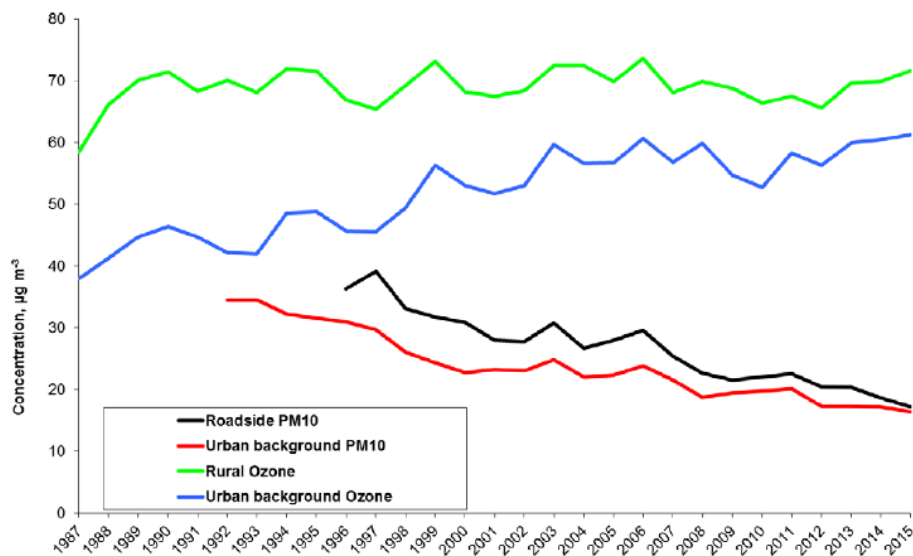
Suresh et al. (2009) demonstrated that steady expansion in vehicular populations had placed huge environmental stress on local and global scales in various forms, essentially causing poor air quality as a large amount of vehicle exhausts produce emissions. These exhaust emissions contain a variety of toxic components, such as CO, NO, HC, PAHs and PM. However, the chemical transformation process varies, as some compounds may cause higher concentrations of ozone (this will be discussed later) especially during the period of higher temperature. In addition, small aerosol particles are likely to be injurious to death during human respiration, as indicated by Corsmeier et al. (2005) [39]. Carbon dioxide (CO<sub>2</sub>) is considered to contribute to global warming and an increasing of the total anthropogenic greenhouse effect [40].

Though some alternative renewable fuels have been introduced into the transport sector, fuel efficiency or reduced fuel consumption is still one of the major pillars for CO<sub>2</sub> and pollutant reduction.

## **2.2 Air Pollution in the UK**

The UK has made several attempts to improve air quality in the last 60 years, when London suffered its 'great smog'. In the 60s, efforts to control emissions

of pollutants drove the UK to develop technology based on burning cleaner fuels (short chain hydrocarbons or natural gas). On account of that and relocated power stations in areas outside the main cities it was possible to achieve a decline of around 90% in the emission levels of ozone and SO<sub>2</sub>. As can be seen in Figure 2-2 [41], it is clear that a significant improvement in the air quality has been accomplished over the last few decades, specifically in relation to greenhouse gases such as NO<sub>x</sub> and SO<sub>x</sub> [41-43].



**Figure 2-2 Exhaust gases trend from the 1980's to 2015 in the UK [41].**

### 2.3 Measurements of air quality

As has been previously mentioned, the air quality is an international problem caused by the emission of pollutants which in turns these gasses can produce several reactions creating a negative impact in natural ecosystem and human health as well. In consequence, the continuous emissions and the changes in pollutant concentration in the air promote a constant monitoring of air quality in UK and in all around the world. An example of why is imperative collect daily measurements of air quality is the shift in concentration between a day when the dispersion is lower (low air flow) and a day with high wind speed. The process to monitoring the concentrations of pollutants is always accompanied

by a modelling of data collected and subsequently, these information is processed for the annual report visualized in the database of each country [44, 45].

## **2.4 Effects of vehicle exhaust emissions on global and local scales**

The pollution of air is present temporarily or permanently via air contaminants that negatively change the environment by interfering with health, comfort or the food chain or by interfering with people's characteristic values. Contaminating substances are classified as solid, liquid, gas or sub molecular particles that are generated from natural or anthropogenic sources or both.

It is a well-known fact that vehicle emissions have diverse and negative effects on communal health and the environment. For a more comprehensive understanding of the impact of vehicle exhausts, these problems are classified into two major areas: the global scale and the local scale (see Table 2-1).

Local effects of car emissions in urban areas represent one of the largest sources of primary air pollutants. Many vehicle exhaust emissions will have seriously adverse effects on human health, which is a major concern worldwide. Additionally, worldwide epidemiological research findings show a consistent increase in cardiac and respiratory morbidity and mortality from exposure to vehicle exhaust pollution [46, 47]. Both in urban and residential regions, these have become the main areas of toxic compound emissions as derived from the uncontrolled use of vehicles burning fossil fuels [48]. In these areas, the population is very sensitive to vehicular pollution [49, 50].

On the global scale, people are concerned about the global climate and the changes contributed by vehicle exhausts. Several researches have demonstrated that combustion engines contribute to greenhouse gas accumulation in the atmosphere [51]. Most climate researchers support the view that emissions of heat trapping gases into the atmosphere, particularly CO<sub>2</sub> from the combustion of fossil fuel, cause global warming. The

concentrations of CO<sub>2</sub> are currently rising by 2 ppm (parts per million) annually, as indicated by Patrick and Damon [52].

**Table 2-1 Primary sources of air pollutants and their effects on human health [53].**

Emission	Description	Sources	Harmful Effects	Scale
Carbon dioxide (CO <sub>2</sub> )	A product of combustion	Fuel production and tailpipes.	Climate change	Global
Carbon monoxide (CO)	A toxic gas caused by incomplete combustion	Tailpipes	Human health, climate change	Very local
CFCs and HCFC	A class of durable chemicals	Air conditioners and industrial activities	Ozone depletion, climate change	Global
Fine particulates (PM <sub>10</sub> ; PM <sub>2.5</sub> )	Inhalable particles	Tailpipes, brake lining, road dust, etc.	Human health, aesthetics	Local and regional
Road dust (non-tailpipe particulates)	Dust particles created by vehicle movement	Vehicle use, brake linings, tire wear	Human health, aesthetics	Local
Lead	Element used in older fuel additives	Fuel additives and batteries	Human health, ecological damage	Local
Methane (CH <sub>4</sub> )	A flammable gas	Fuel production and tailpipes	Climate change	Global
Nitrogen oxides (NO <sub>x</sub> ) and nitrous oxide (N <sub>2</sub> O)	Various compounds, some are toxic, all contribute to ozone damage	Tailpipes	Human health, ozone precursor, ecological damage	Local and regional
Ozone (O <sub>3</sub> )	Major urban air pollutant caused by NO <sub>x</sub> and VOCs combined in sunlight	NO <sub>x</sub> and VOC	Human health, plants, aesthetics	Regional
Sulphur oxides (SO <sub>x</sub> )	Lung irritant and acid rain	Diesel vehicle tailpipes	Human health and ecological damage	Local and regional
VOC (volatile organic compounds)	Various hydrocarbon (HC) gasses	Fuel production, storage and tailpipes	Human health, ozone precursor	Local and regional
Toxics (e.g. benzene)	Toxic and carcinogenic VOCs	Fuel production and tailpipes	Human health risks	Very local

## **2.4.1 Global scale-GHG and global warming**

### **2.4.1.1 GHG**

Earth's atmosphere consists of about 78.1% nitrogen, 20.9% oxygen and 0.9% argon by volume, in addition to carbon dioxide, methane and others. However, traces of greenhouse gases trap some of the heat and reflect back as radiation from earth as part of the effect. Thus, the region below where the heat is trapped warms up.

The major greenhouse gases are:

- A. Carbon dioxide: CO<sub>2</sub>
- B. Methane: CH<sub>4</sub>
- C. Nitrous oxide: N<sub>2</sub>O
- D. Water: H<sub>2</sub>O
- E. Chlorofluorocarbons: CFC-11 and CFC-12
- F. Ozone: O<sub>3</sub>

However, researches have shown that the methane molecule is 23 times powerful than the CO<sub>2</sub> molecule, and CFC is 10,000 times powerful than the CO<sub>2</sub> molecule. In addition, the de-nitrification and nitrification in the environment releases N<sub>2</sub>O, while the fossil fuel combustion amounts to only 4% of the total CO<sub>2</sub> released by nature [54]. The GWP of a particular GHG over a chosen time scenario is calculated by the GWP of that GHG multiplied by the amount of the gas emitted [55].

### **2.4.1.2 GWP (Global warming potential)**

In the 19<sup>th</sup> century, Arrhenius introduced the term 'greenhouse effect' and predicted that exhausting the fossil fuel increases the amount of CO<sub>2</sub>, which in turn leads to global warming [54]. In general terms, global warming can be defined as the increase of the average temperature on the earth. As a consequence of this increase, several phenomena can take place with more

frequency such as a hotter surface and increases in the amount of natural disasters (hurricanes, droughts and floods). In the last century, several studies have confirmed the increase of the average air temperature by 1.3 degrees Fahrenheit (less than 1°C). According to the findings coming from these diverse investigations, deforestation, ocean capture capacity and burning fossil fuels (oil, coal, natural gas, etc.) are huge contributors to the drastic increase of carbon dioxide in the atmosphere (Figure 2-3). The increase of this greenhouse gas into the atmosphere will strongly affect the global temperature, thus causing climate change. The increase of the average temperature can be explained by an analysis of the greenhouse effect, which will be illustrated in the subsequent section [7].

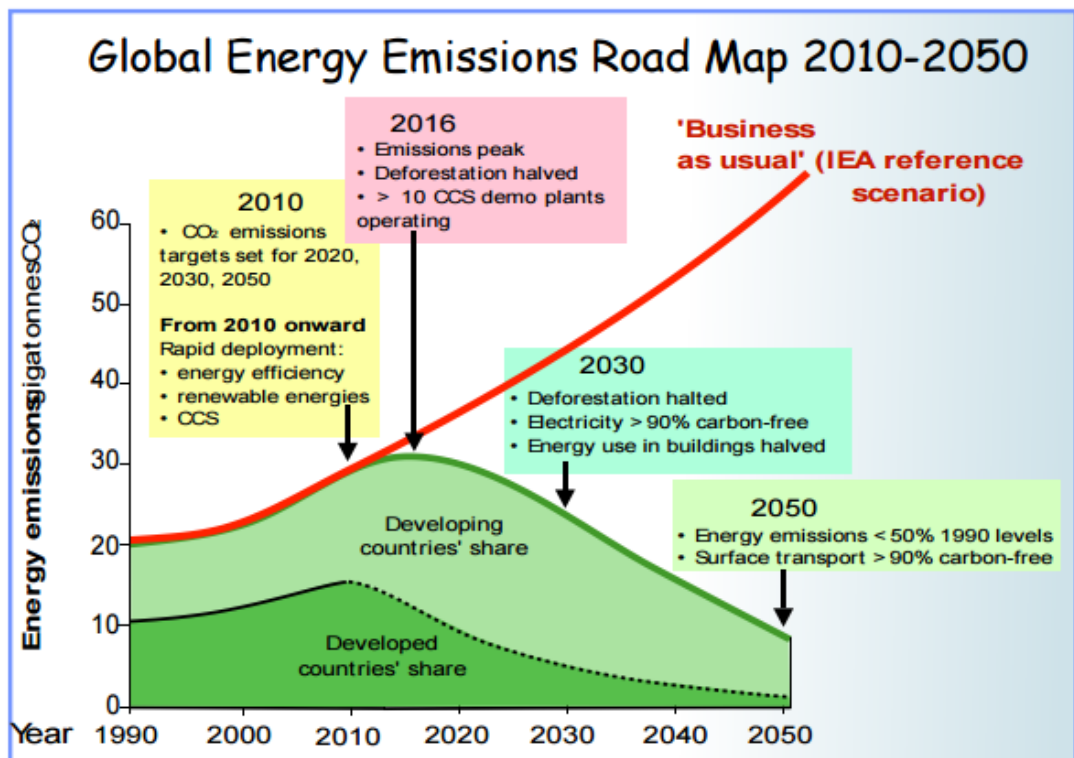


Figure 2-3 Global CO<sub>2</sub> emissions caused by several source.

It is believed that global warming leads to rapid climatic changes all over the world [56]. A theory states that global warming will increase the temperature to by 5 degrees, which would melt the glaciers in the polar regions. This melting would increase the sea level by 50 cm, covering up most of the land



areas. If the greenhouse cloud exists, it would certainly affect the flora and fauna and thus the entire food chain system.

Scientists also predict that by 2030 the global temperature will increase by 1 degree Celsius, thus affecting most of the agricultural patterns. Although there has been an obvious increase in CO<sub>2</sub>, some professionals still deny that the effects of greenhouse gases are caused by human activities [16, 55].

#### **2.4.2 Local scale photochemical smog and its effects**

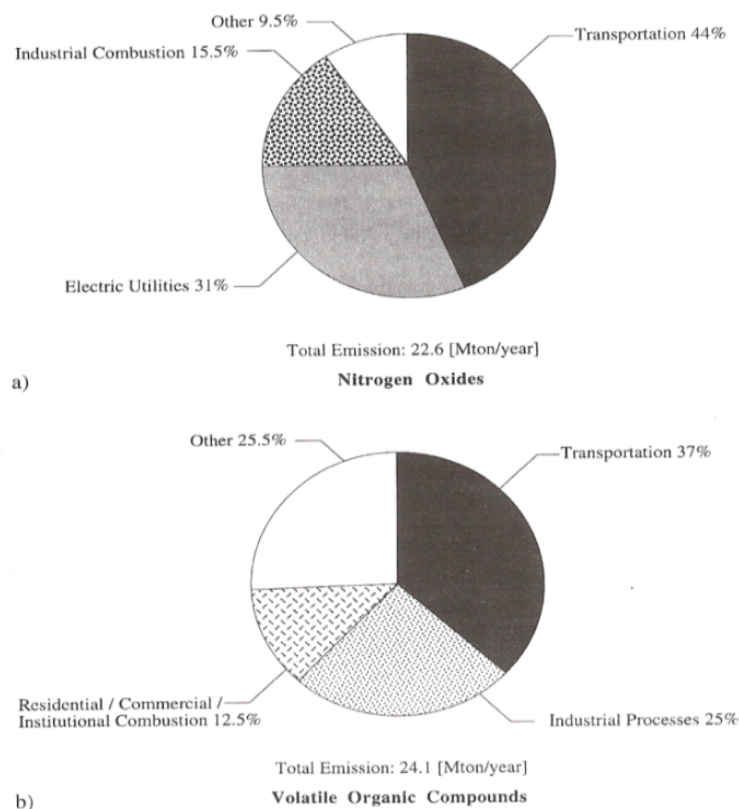
Photochemical smog is a pollutant mixture that consists of particulates, oxides of nitrogen, ozone, aldehydes, peroxy acetyl nitrates (PAN), hydrocarbons, etc. Because of the presence of oxides of nitrogen the smog often has a brown haze. Several researches have revealed that smog's effects, which cause headaches, eye, nose and throat irritations, also may impair the lung function, cause coughing and wheezing. In addition it can deteriorate rubbers and fabrics. Health-wise it can damage plants and conversely affect human beings.

Due to the presence of gaseous components, photochemical smog always gives off an unpleasant odour. The photochemical smog initiation appears to be the result of nitrogen oxide emitted into the air as pollutants mainly from IC engines. Although the nitric oxide splits to release an oxygen atom with UV energy, this single oxygen atom combines with the oxygen molecule to form ozone. Photochemical smog is the result of a variety of chemical reactions that take place in the presence of hydrocarbons and other organic compounds [57-59].

Urban air contains volatile organic compounds (VOC), which contain a C=C bond that is most reactive. Photochemical smog's major undesirable components are nitrogen dioxide, ozone, peroxyacetyl nitrate (PAN) and aldehydes (CHO), as indicated in Figure 2-4.

## 2.5 Formation of pollutants in engines and their impacts on human health

In most developed countries, cars, trucks and off-road vehicles are currently estimated to be responsible for about 40-50 percent of the hydrocarbon (HC) or volatile organic compounds (VOC) emissions, 50 percent of the oxides of nitrogen ( $\text{NO}_x$ ) emissions, in addition to 80 to 90 percent of the carbon monoxide (CO) emissions in urban areas. Other developed countries like Japan and others in Europe produce similar amounts of pollution. A large fraction of these emissions come from spark-ignited engines. In the past two decades, the emission of CO and VOC from automobiles has reduced by about 40 percent and  $\text{NO}_x$  by 25 percent.



**Figure 2-4 Sources of  $\text{NO}_x$  and VOCs in our atmosphere [54].**

As discussed previously, photochemical smog is also an attention-gaining problem, which is thought to mainly affect urban areas. However, research shows that even in rural areas the concentration of ozone has risen by half

the level of that of urban areas. The photochemical smog is further helped by the prevailing winds, which transport the smog to different places. Air quality measurements in the United States have shown that urban ozone has decreased by 12% in the past decade; also, incidents where national ambient air quality standards exceeded acceptable limits have reduced by 60 percent. Concentration of CO has reduced by 40 percent in the same period. All of these events have been made possible due to the latest developments in engine technology, as demanded by the emission regulations [54].

Vehicle exhausts emit many toxic compounds (such as gasoline containing aromatics, which are individually toxic or carcinogenic). Acute health responses that have been associated with air pollution include changes in respiratory mechanics, changes in respiratory symptoms, such as coughing or asthma attacks, cardiac symptoms, such as angina attacks, disabilities, stroke, absences from work or school, hospitalisation and premature mortality [60, 61].

### **2.5.1 Combustion in IC engines**

The internal combustion carried out in gasoline engines works by using the air available in the atmosphere and hydrocarbon fuel, which in general terms can be gasoline or diesel. The power produced is obtained by the chemical energy derived from the fuel. Nowadays, technology has enabled us to develop more efficient gasoline and diesel engines in comparison with those from the 60s. However, emissions control continues to be an issue in terms of pollution because the release of exhaust gases is active.

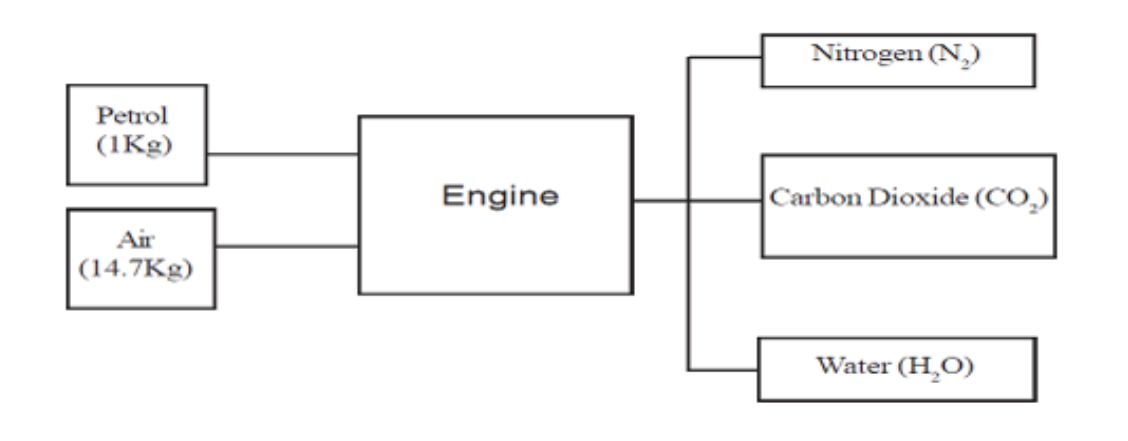
In order to understand the combustion chemistry that takes place in an engine it is necessary to explain in detail the chemical process that is generated. A certain sort of fuel (diesel or gasoline) interacts with air, and as a result of this mixture the fuel starts being burned. It is well known that air roughly contains 78% nitrogen, 21% oxygen with the balance belonging to inert gasses. The combustion reaction is carried out only with the oxygen from the air and the products of this reaction are water vapour and CO<sub>2</sub>. Nevertheless, undesirable

molecules such as nitrogen oxides ( $\text{NO}_x$ ) can be formed between  $\text{N}_2$  and  $\text{O}_2$  under favourable conditions of temperature and pressure within the cylinder.

According to several investigations it is imperative to mention which fuel/air ratio is a variable with high relevance, which plays a key role in increasing the efficiency and performance of engines and which has the most suitable emissions content (air/fuel ratio: 1/14.7 1kg of fuel per 14.7Kg of air). The air/fuel ratios are chosen according to the stoichiometry of the reaction; therefore, lower ratios will impact on the emissions content as well as on the economic aspect whereas higher ratios will increase the power of the engine but the emissions will reach their maximum as well [13].

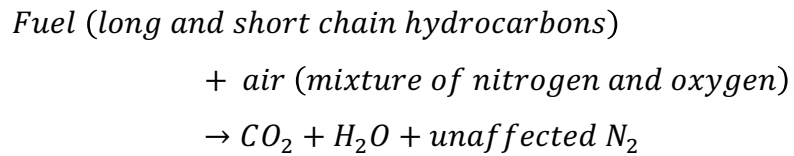
#### **2.5.1.1 Complete combustions**

Vehicle engines convert the chemical energy in the fuel into the mechanical or work energy that powers the vehicle, which generates a great deal of waste products. The created waste products occur due to fuel chemical formation and because of the combustion chamber burning inside the engine. The majority of the harmful gases created as a consequence of that internal combustion engine are the result of an inefficient device. A perfect engine with today's technology is not technically possible. A perfect mixture of air to fuel, burning with the ratio of 1kg of petrol to 14.7kg of air, produces carbon dioxide ( $\text{CO}_2$ ), water ( $\text{H}_2\text{O}$ ) and nitrogen ( $\text{N}_2$ ), which are classified as harmless chemicals. Nitrogen concentration is approximately 78% of the air we breathe daily. Carbon dioxide is not toxic to humans; it is an essential plant energy source. Plant photosynthesis is impossible without carbon dioxide, as demonstrated in (Figure 2-5) [13].

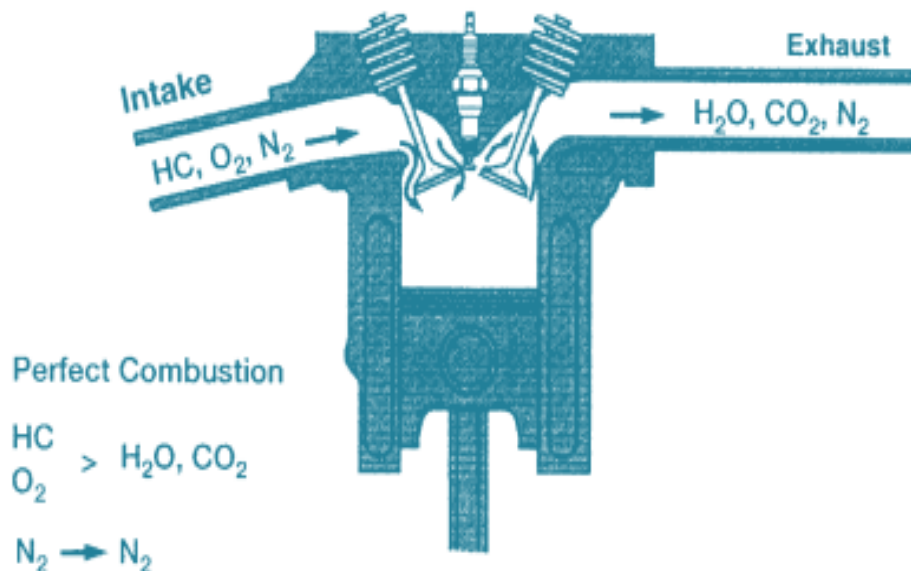


**Figure 2-5 Combustion of air fuel mixture[13].**

The ideal combustion carried out in an engine must operate as in the following reaction:

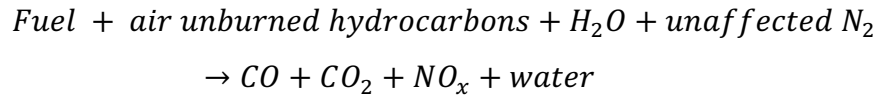


A perfect combustion process where the fuel (hydrocarbons) is oxidised can be visualised in (Figure 2-6) below:



**Figure 2-6 Complete combustion without undesirable species (not NO<sub>x</sub> formation [13]).**

However, the combustion has a typical reaction:



### 2.5.1.2 Incomplete combustions

The issue of incomplete combustion starts with the fuel itself. Pure distilled fuel for today's engine is totally unsuitable; this is something which was fine in the early days of motoring when there was less demand for engines, roads and drivers.

The inefficiencies of engines has created the majority of the harmful emissions. Incomplete combustion covers most of the problems, which is caused by many factors including volumetric, thermal and mechanical/frictional efficiency of vehicle engines that is completely generated by losses within the engine. Lack of air or rich mixtures during combustion causes the biggest two pollutants: the first pollutant is carbon monoxide (CO) and the second one is hydrocarbon (HC), whereas nitrogen oxide (NO<sub>x</sub>) pollution is produced at high combustion chamber temperature and also during the rapid cooling of exhaust gases Table 2-2 [13].

		<i>Conventional Gasoline Engine</i>	<i>Diesel Engine</i>	<i>Lean Engine</i>
<i>O<sub>2</sub></i>	%vol.	0.2-2	5-15	4-8
<i>CO<sub>2</sub></i>	%vol.	10-13.5	2-12	2-12
<i>H<sub>2</sub>O</i>	%vol.	10-12	2-10	2-12
<i>N<sub>2</sub></i>	%vol.	70-75	70-75	70-75
<i>CO</i>	%vol.	0.1-6	0.1-0.1	0.04-0.08
<i>H<sub>x</sub>C<sub>y</sub></i>	%vol.	0.5-6	0.005-0.05	0.002-0.015
<i>NO<sub>x</sub></i>	%vol.	0.04-0.4	0.003-0.06	0.01-0.05
<i>SO<sub>x</sub></i>	Related to the percentage of S in the fuel.			

**Table 2-2 Content of exhaust gases according to the engine used during the combustion process [62].**

## **2.5.2 CO (Carbon monoxide)**

### **2.5.2.1 CO formation mechanism**

Carbon monoxide (CO) is one of the main pollutants in the exhaust gases produced during the combustion of carbonaceous material. This gas is basically the result of an incomplete combustion reaction due to the amount of oxygen not being enough to burn the raw material introduced into the system where the combustion process will take place. In consequence, partial reactions become evident with the formation of undesired exhaust products, which means the incomplete oxidation molecules of any fuel not converted will remain in the exhaust stream.

Carbon monoxide is produced from diesel and gasoline engines but the content of this gas changes between both systems. In the particular case of diesel engines, the amount of CO produced is considerably low in comparison with gasoline engines. As a result of the great circulation of oxygen, complete combustion can almost be reached whereas in the gasoline systems the heterogeneity of the fuel feeds into the engine shift with the combustion reaction moving toward lower conversion. In addition, the chamber is another crucial factor in the CO formation in gasoline engines. There is a deficiency of oxygen in specific areas, which promotes a partial oxidation of the fuel. However, the requirements of drivers create a dependence on oxygen-deficiency due to acceleration on the engine. In general terms, the above points mentioned are intrinsically related to the air to fuel ratio, so it is obvious this relation is complex during transient operations, which imply gear changes, acceleration and deceleration.

Secondary oxidation can take place due to the effect of temperature. CO produced by the partial oxidation of fuel can interact with oxygen molecules in the zones of the cylinder. Additionally, the secondary reactions can be produced in the exhaust stroke due to appropriate temperature conditions, but if this parameter varies, this particular reaction becomes inactive (changes in the burning process conditions).

There are two main routes that occur in CO emissions. The first one is a rich mixture and the second one is inefficient combustion, which happens if all of a hydrocarbon fuel is not completely burnt; for example, if the mixture does not reach equilibrium then this increases CO emissions through partially burnt fuel and incomplete oxidation. Usually this is due to many reasons. The first reason is an insufficient residence period whereby that equilibrium is not achieved. The second reason is to poor mixing for fuel/air, which gives rise to rich local regions that have high equilibrium CO and that leads to lack of oxygen in the mixing zone being burned out, e.g. GDI. The third reason is flame quenching due to heat extraction (cooling at the cold walls) before combustion is completed to equilibrium.

Diesel engines emit low quantities of CO, since, generally, there is an abundance of oxygen in the charge. Nevertheless, some CO is still produced in localised areas with oxygen deficiency within the combustion chamber, given that the charge has an extremely heterogeneous nature. In petrol engines, CO is a considerably greater problem. Based on the standard design of such engines, they are supposed to run on a homogeneous charge, with a sufficient quantity of oxygen that will enable the entire fuel supply to be burnt; yet, in reality, this is often not the case. A late mixing process or poor vaporisation of fuel can be one of the reasons for the possible existence of localised areas with oxygen deficiency. When starting a cold engine, it is necessary that the mixture has oxygen deficiency for the initial few minutes; if not, a bumpy run and possible stalling of engine will be the result. A mixture deficient in oxygen is normally needed, if the driver demands high power; or, a slow acceleration response will be result. Finally, but still important, the preservation of a sufficiently accurate ratio of air and fuel in the transient process (acceleration, deceleration, changes of gear) is difficult. The CO levels are 1% at  $\phi=1$  and increase to over 10% if the mixture is very rich.

The CO produced in the combustion procedure itself will not all escape from the cylinder. It is possible for the expansion stroke process to witness a considerable burn-up, should the molecules of CO subsequently contact molecules of oxygen within the area of burnt gas, and should the temperature



degree continue to be sufficiently high. The temperature of the burnt gas varies, and so does the significance of the secondary oxidation depending on its location within the cylinder and the dynamics of gas mixing. Although secondary oxidation can occur in the course of the exhaust stroke, and even to a certain extent within the exhaust manifold, it is quickly extinguished by the decrease in temperature [63, 64].

### **2.5.3 NO<sub>x</sub> (nitrogen oxides)**

#### **2.5.3.1 Formation mechanisms of NO<sub>x</sub>**

NO<sub>x</sub> refers to NO and NO<sub>2</sub>. Heywood (1988) has provided a thorough description of the mechanisms of NO<sub>x</sub> formation in internal combustion engines. The formation of NO<sub>x</sub> occurs at the rear of the flame inside the area where the gas has been burnt; formation also occurs within the actual flame itself but to a smaller extent. The NO<sub>x</sub> is produced through a high temperature (over 1600<sup>0</sup>C) chain reaction, commencing with the nitrogen and the oxygen within the atmosphere. Given its compression to greater degrees of temperature, an early burning mixture often produces a greater quantity of NO<sub>x</sub> than a late burning mixture does.

As the required conditions for the production of NO<sub>x</sub> are quickly lost in the early stage of the expansion stroke, the relevant equilibria become essentially frozen. This permits the persistence of NO<sub>x</sub> at considerably greater concentrations than would be otherwise possible. This is also the reason for the small ratio of NO<sub>2</sub>/NO - below two percent - which is the case with petrol engines [64, 65].

#### **2.5.3.2 Environmental implications of NO<sub>x</sub>**

Epidemiological evidence shows an increased incidence of acute respiratory infections, especially in infants and children, resulting from exposure to NO, possibly augmented by NO<sub>2</sub>. These gases tend to combine with moisture to

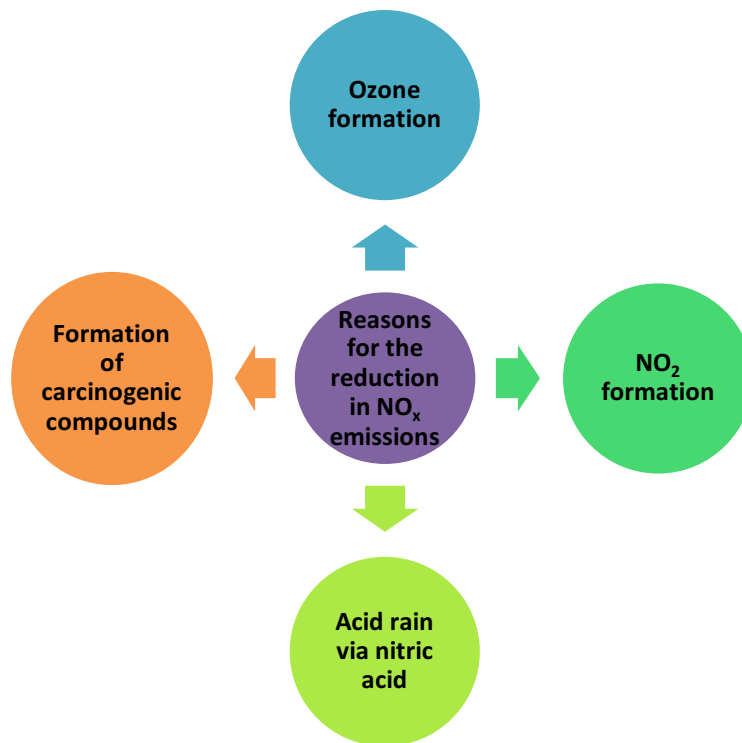
form acids. The exact mechanism of toxicity is the oxidation of fatty acids to produce highly reactive free radicals, which can impair the chemical and functional properties of membranes and alter structural proteins. Both NO and NO<sub>2</sub> also combine with haemoglobin in the blood's methaemoglobin which reduces the oxygen carrying capacity of the blood [66]. Respiratory illness was observed in adults and children chronically exposed to mean levels of near 1 ppm clinical studies indicate that normal and asthmatic subjects can experience detrimental respiratory effects when exposed for brief periods to high levels of NO<sub>2</sub>[67].

NO<sub>x</sub> (NO + NO<sub>2</sub>) is one of the main reactants for ground ozone formation. NO<sub>2</sub> is harmful to humans as it reduces lung function. Furthermore NO<sub>x</sub> forms nitric acid in the atmosphere and this forms acid rain. NO<sub>x</sub> is also a secondary greenhouse gas through its role in the formation of ozone, which is 2000 times more active as a greenhouse gas than CO<sub>2</sub>.

It cannot be said that both NO and NO<sub>2</sub> have an equal impact on the environment. NO is odourless, colourless and somewhat non-toxic, whilst NO<sub>2</sub> has a reddish-brown colour and is pungent and also poisonous. In low levels of concentrations such as only one ppm, known to exist in areas with high pollution, NO<sub>2</sub> is harmful to health. NO<sub>2</sub> harms the respiratory tract, strengthens airway resistance and causes damage to lung tissue. Several effects have been reported such as coughing, running noses, sore throats, bronchitis, emphysema and pulmonary oedema (Battigelli, 1971). A particularly at-risk group are asthma sufferers. NO<sub>2</sub> may impair the supply of oxygen within the bloodstream, by interacting with haemoglobin, and may reduce resistance to contagious illnesses (Figure 2-7) shows the impact of NO<sub>x</sub> emissions..

Whilst NO and NO<sub>2</sub> are the focus of attention today, N<sub>2</sub>O is a pollutant that will become the focus of lawmakers in the future. Although levels of engine-out are very little, under some conditions a small increase in tailpipe concentration can be caused by catalytic converters, especially during the warming-up process. Additionally, it is generated by microbial action within the soil,

through fertiliser-stimulated processes. Although, in toxicological terms, it is quite harmless, it is a strong greenhouse gas [64, 68].



**Figure 2-7 Impact of NO<sub>x</sub> emissions.**

#### **2.5.4 Volatile organic compounds (VOC)**

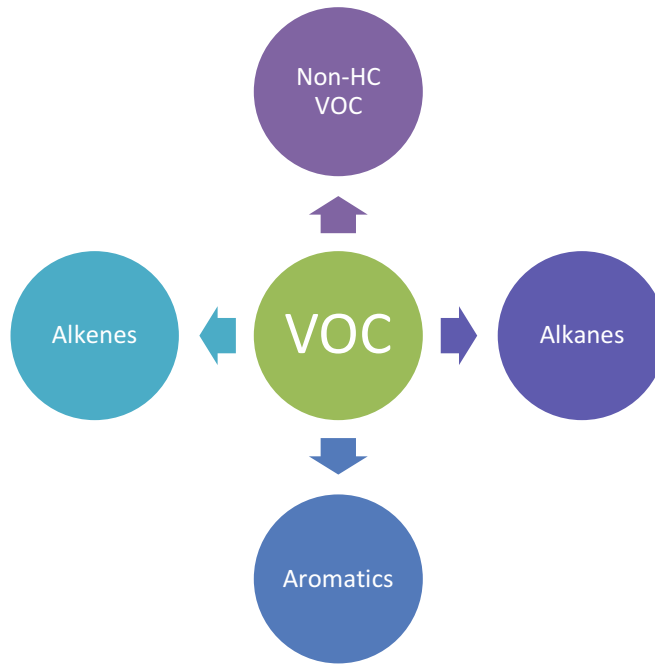
Volatile compounds can be generalised as those gaseous compounds which contain carbon in their chemical structure at conditions of ambient temperature. The number of molecules that encompass this classification is enormous considering the wide window of sources capable of producing or emitting VOC. A considerable number of sources derived from the human (anthropogenic) are hydrocarbons, which come from the combustion of raw materials such as are fossil fuels and solvents produced by polymer industries. Moreover, natural sources of VOC also exist, among them plants that produce ketones and marshland, which forms methane.

The chemical structure of HC is based on hydrogen, which is linked to carbon atoms. Nowadays, several systems are powered by using fuels from

hydrocarbons, a common example of which are diesel and petrol. However, the energy released by the combustion process involves reactions with conversion below 100%, which means that the incomplete reaction performed in the engine releases unburned hydrocarbon; accordingly, exhaust gases are released into the atmosphere creating secondary effects such as those previously mentioned (effects caused by global warming). In addition, hydrocarbons can react with nitrogen oxide species by forming ozone molecules, a reaction that is catalysed in the presence of sunlight. The effect of HC emission on human health is evident; for instance, some HCs promote cancer or another adverse diseases. The main sources of HC emissions are industries (particles in the shape of gases, tiny particles, droplets, etc.), cars and buses (urban areas), and other motor mobiles in rural areas [36, 45, 69].

In (Figure 2-8) we can see the four main groups who are representative of the VOC. It is imperative to mention that this classification is based on the chemical properties of the molecules. For example, the alkanes are formed by single bounds (hydrogen-carbon) and are usually named as saturated. Likewise, alkenes and alkynes are composed of double and triple bounds, respectively (unsaturated compounds). Moreover, the aromatic molecules have a poly(cyclic) hydrocarbon chain. In the same manner as CO, CO<sub>2</sub>, NO and NO<sub>2</sub>, the VOC are found in the exhaust stream after the combustion process is performed in a diesel or gasoline engine. For instance, methane is one of the primary compounds in the combustion carried out in diesel systems whereas which another kind of hydrocarbons is present as a constituent in the burning of fuel in gasoline engines (molecules with 2 to 12 carbons in the chain).

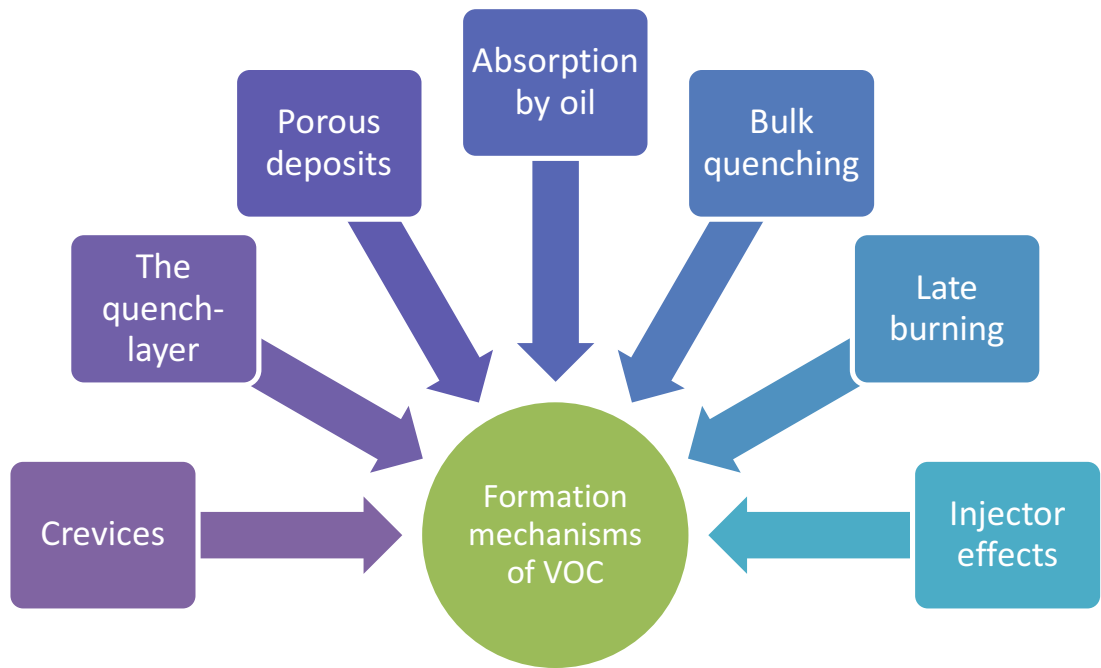
On the other hand, another group of molecules, despite the fact they are emitted in a small proportion, in contrast with hydrocarbons, is important due to their secondary effects as denominated oxygenates (non-hydrocarbon VOC). Among the typical compounds of this classification are acrolein, acetaldehyde and formaldehyde.



**Figure 2-8 Classification of hydrocarbons that belong to the category of volatile organic compounds (VOC).**

#### **2.5.4.1 Formation mechanism of volatile organic molecules**

As mentioned above, the formation of hydrocarbon particles is intrinsically related to the content of oxygen during the combustion (air-fuel ratio). However, not only in diesel and gasoline engines can be emitted, there are several ways that can be sources of VOC, such as those depicted in (Figure 2-9). Several studies have demonstrated that a considerable amount of hydrocarbons is released by the primary combustion which takes place in the flame. The second process involved is an oxidation that can be performed during the exhaust stroke and expansion of the gaseous mixture. It is the result of desorption from hot oil or from the crevices. On the exhaust manifold, the emission of hydrocarbons can be encouraged, but this process is strongly dependent of the operation parameters such as temperature.



**Figure 2-9 Formation mechanisms of VOC from several sources [70].**

Hydrocarbons with a short carbon chain and a low density are released in gasoline engines usually by the effect of defects on the seals in a vehicle fed with fuel. As result of this escape of gas, the empty space is filled by the presence of vapour above the feedstock (in the tank) used by generating the combustion reaction. These kinds of emissions are classified into three groups: a) diurnal emissions that most of the time are produced in daily cycles, b) hot soak emissions are the second groups, and they can emerge as a consequence of an engine shut-down and c) running emissions during engine start which comes from the operation of the engine. Usually, the temperature of the environment is known as the primary promotor of evaporative emissions as well as the driving patterns, according to Kishan et al. (1993). Not only engines are sources of hydrocarbon emissions but re-filling processes are also strong points of emission, as is the case with petrol pumps. Nowadays, many countries around the globe have adopted new measures to control emissions of these three groups, including control related to hardware and policies.

The oxygen present in the process of combustion powerfully drives the hydrocarbon emissions. This explains the HC's inclination to take a route

similar to that of CO and the reasons. Additionally, apart from the role of the air-fuel ratio itself, it is possible for HC to emanate in many other ways, as listed below (Heywood, 1988).

**(i) Crevices.** High cylinder pressures force the mixture of unburnt air-fuel into crevices, for example, the piston top land, or the threads surrounding the spark plug. It is not possible for the flame to gain access to a crevice; therefore, it is quenched when it reaches the entrance.

**(ii) The quench-layer.** The flame is extinguished just before it arrives at the walls of the cylinder, because the temperature in this area is cooler. It is believed that this is an inconsiderable contributor to emissions of hydrocarbon, if the walls are both smooth and clean. However, it can lead to contributing to such emissions, if the walls are worn or rough.

**(iii) Porous deposits.** Hydrocarbons are screened by these deposits from the combustion process, for reasons that are similar to those of the crevice impact.

**(iv) Absorption by oil.** Because the lubricating oil absorbs hydrocarbons, they are shielded from the flame; following this, they desorb in the process of the expansion stroke. The vapour pressure of a hydrocarbon and its solubility, as well as the diffusion rate within the oil, control this mechanism.

**(v) Bulk quenching.** Areas of the charge with excessive oxygen deficiency cannot enable the combustion, the consequence of this being bulk extinguishing of the flame. This rarely results in a problem if an engine has gone through appropriate calibration at steady-state; but it can occur in the process of transient operation in cases where the EGR, timing or fuel metering are not at an optimal level.

**(vi) Late burning.** When a mixture is persistently too late in the cycle, it may escape the combustion process, if a decreasing temperature quenches the flame.

**(vii) Injector effects.** There is a possibility that fuel will remain in the injector's nozzle sac. In a diesel engine, vaporisation rather than injection can be the means by which hydrocarbons enter the cylinder. If the impacts of the pressure wave cause the reopening of the nozzle, then secondary injections which are not desired may follow the main injection. When hydrocarbons enter in these ways, they are able to leave the key combustion event.

The large proportions of hydrocarbons which exit the initial combustion in the flame are known to consequently undergo oxidation in the expansion stroke and the exhaust stroke. This occurs when these hydrocarbons emanate from the crevices or when they desorb from the oil to penetrate into the hot, combusted gas. Further oxidation occurs when the spent charge goes into the manifold of the exhaust; however, such reactions are quickly extinguished as the temperature decreases rapidly. The point of operation is the determining factor in the level of burn-up within the secondary oxidation.

At this point, it is useful to mention another hydrocarbon emission source because it is considerably significant. Fuels which are more volatile and lighter, particularly petrol, are able to escape through the seals in the fuelling system of a vehicle by evaporation. The vapour-occupied space above the level of the liquid in the fuel tank is particularly relevant here. There are three types of classification of this kind of emission: (i) diurnal emissions (which occur in daily cycles), such as if a vehicle remains parked for a long period and its temperature consequently becomes the ambient temperature; (ii) hot soak emissions, which occur immediately after an engine shuts down and (iii) running emissions, being when a vehicle is operating. Ambient temperature is the factor which dominates with regard to evaporative emissions; however, patterns of driving also have a relevance (Kishan et al., 1993). The process of refuelling at the petrol pumps is another emissions' source which is very similar. In many countries, motor vehicles are now subject to mandatory evaporative control hardware, and also the procedure for refuelling is closely scrutinised by policymakers [64].



#### 2.5.4.2 Environmental Implications of VOC (Hydrocarbons)

Some VOCs are carcinogenic, such as benzene, but the main problem of hydrocarbon is the formation of ozone by reaction with  $\text{NO}_x$  in the presence of sunlight. The mucous membranes are irritated by several hydrocarbons; drowsiness, coughing and sneezing are examples of stronger effects. Some are in fact related to narcotic effects. Alkanes are odourless, but alkenes and alkynes emit a slightly sweet odour. The distinctive noxious smell emitted from diesel engines is due to hydrocarbons.

It is possible for some hydrocarbons to directly impact plants, with such an impact being phytotoxic. Benzene, which is a basic element of aromatics, is known for its toxic property and its carcinogenic effect; it is thought that the high percentage of benzene within the atmosphere emanates from motor cars. There is regulation on its concentration within fuel. Aldehydes cause eye irritation, and are also irritants for the throat and nose. The formaldehyde, which is present in urban regions, is a result of a large contribution by motor cars; however, it is not easy to quantify this, as aldehydes may also be generated from reactions of a secondary nature between nitrogen dioxide, hydrocarbons and water, within the atmosphere. Polycyclic aromatic hydrocarbons (PAH) have major health implications, some of which are known to be carcinogens. It is thought that motor traffic is responsible for the highest percentage of PAH; yet, there is a dispute about this PAH are also present in many additional kinds of combustion, particularly those which involve the burning of plants or wood, and they even exist within barbecued meat. Nitro-PAH are derivatives of PAH which have an even broader harmful effect. It is uncertain regarding the quantity of nitro-PAH that is generated by reactions of a secondary nature within the atmosphere or the quantity that emanates from tailpipes.

Apart from its primary pollutant property, hydrocarbon forms a reaction with  $\text{NO}_x$  within the atmosphere to generate secondary pollutants, for instance tropospheric ozone and photochemical smog. However, here methane is a rather special case. In some locations (such as California), legislation is in place concerning Non-Methane Hydrocarbons (NMHC). This is an indication

of the more considerable concern regarding tropospheric ozone in these regions' methane, being a comparatively stable hydrocarbon, is not involved in such atmospheric reactions. Nevertheless, it is a greenhouse gas, and therefore ought to be still examined because of its capacity to pollute on a worldwide scale [64, 68].

#### **2.5.4.3 Aldehydes**

Formaldehyde, acetaldehyde, and acrolein are the more prevalent aldehydes in exhaust. They act as eye, nose, throat and skin irritants, can produce nausea, kidney damage, chronic respiratory disease, inhibit the immune system, and have been shown to be mutagenic or carcinogenic, or both. Major effect is function of the eyes, nose and throat. Significant increase in symptoms of irritation are observed at levels of formaldehyde greater than 1 ppm (periods of 1.5 to 30 minutes). In the best conducted studies, formaldehyde irritation does not occur at levels less than 0.6 ppm.

Acrolein is one of the most irritating aldehydes, with most people reporting eye irritation at levels less than 1 mg/m<sup>3</sup>. Severe irritation results from exposure to 0.8 ppm [71].

Irritation of the upper respiratory tract is the primary symptom of acrolein inhalation, but lung edema can occur after exposure to high concentrations. Additionally, skin contact causes skin burns and severe injury to the cornea. Acetaldehyde is considerably less irritating where symptoms of irritation are felt at levels of 25 ppm.

#### **2.5.4.4 Aromatics**

Benzene, styrene, toluene, and the O-, -and p-xylenes are known to irritate eyes, nose and throat, and cause drowsiness, dizziness, headaches, vomiting, nausea, fatigue, abdominal pain, confusion, insomnia, and euphoria. The xylene isomers are clear, flammable liquids with an aromatic hydrocarbon odour. Some studies also report gastrointestinal disturbances, in addition to

kidney, heart, liver, and neurological damage. Styrene monomer is a colourless, oily liquid with an aromatic odour. Styrene is an instant, a narcotic, and a neuropathic agent and is classified as a possible human carcinogen. The principal effects due to styrene exposure involve the central nervous system. These effects include difficulty in concentrating, feeling of intoxication, liver injury, peripheral nervous system dysfunction, abnormal pulmonary function, chromosomal changes, reproductive effects, in addition to the list of subjective complaints give previous. Toluene is a flammable, colourless liquid with an aromatic hydrocarbon odour. Exposure to toluene has been considered to be a cause of headaches, nausea, bad taste in mouth, lassitude, temporary amnesia, impaired coordination, and anorexia. In longer term exposures, aromatics may be carcinogenic.

#### **2.5.4.5 Olefins (alkenes)**

1,3 Butadiene has been found to present a more potent cancer risk than benzene and formaldehyde. 1,3 Butadiene is a mild irritant to eyes, nose and throat, and causes drowsiness and light headedness [71].

#### **2.5.4.6 Paraffin**

Generally, the saturated paraffin hydrocarbons are considered to be inert. However, all of them are potentially asphyxiant. Methane (CH<sub>4</sub>) in particular is an asphyxiant since it can potentially be released in large quantities and mixes well with air. The heavier paraffin tend to form heavier-than-air clouds when released in large quantities.

#### **2.5.4.7 Others**

Ozone is a powerful and irritating pollutant that affects the respiratory system and can cause lung disease. Sulphur dioxide (SO<sub>2</sub>) is an eye, nose, throat and skin irritant, causes bronchoconstriction, coughing, choking, rhinorrhoea, and mutagen, and is suspected of reproductive effects. It is a colourless, non-flammable gas or liquid with a suffocating odour. Exposure to sulphur dioxide

causes both acute and chronic effects. The chronic effects of exposure include permanent pulmonary impairment, which is caused by repeated episodes of bronchoconstriction. Acute effects of SO<sub>2</sub> exposure include upper respiratory tract irritation, rhinorrhoea, choking, and coughing. These symptoms are so disagreeable that most people will not tolerate exposure for longer than 15 minutes. Within 5 to 15 minutes of the onset of exposure, people develop a temporary reflex bronchoconstriction and increased airway resistance.

## 2.6 Emission standards

The vehicle exhaust emissions standard provides the limitation of vehicle exhausts which can be directly released into the atmosphere.

The European Union (EU) Emission Standards limit the amount of pollutants emitted from the tailpipe of new vehicles sold in EU member states. The EURO I, EURO II, EURO III, EURO IV, EURO V and EURO VI emission standards are progressively more stringent. Euro1 to Euro 6 legislations standard shown in (Table 2-3).

**Table 2-3 shows EU exhaust legislation for Euro 1-6 SI passenger cars [55].**

	<b>EURO1</b>	<b>EURO2</b>	<b>EURO3</b>	<b>EURO4</b>	<b>EURO5</b>	<b>EURO6</b>
<b>DATE</b>	<b>1992.07</b>	<b>1996.01</b>	<b>2000.01</b>	<b>2005.01</b>	<b>2009.09</b>	<b>2014.09</b>
<b>CO G/KM</b>	<b>2.7</b>	<b>2.2</b>	<b>2.3</b>	<b>1.0</b>	<b>1.0</b>	<b>1.0</b>
<b>HC+NOX G/KM</b>	<b>0.97</b>	<b>0.50</b>	<b>-</b>	<b>-</b>		
<b>HC G/KM</b>	<b>0.55*</b>	<b>0.29*</b>	<b>0.2</b>	<b>0.1</b>	<b>0.1</b>	<b>0.1</b>
<b>NOX G/KM</b>	<b>0.42*</b>	<b>0.21*</b>	<b>0.15</b>	<b>0.08</b>	<b>0.06</b>	<b>0.06</b>
<b>NMHC G/KM</b>					<b>0.068</b>	<b>0.068</b>
<b>PM G/KM</b>					<b>0.005**</b>	<b>0.005**</b>

\* Split based on the ratio of EURO 3 legislation

\*\* Applicable only to the vehicles using DI engines

## 2.7 Three-way catalytic converter (TWC)

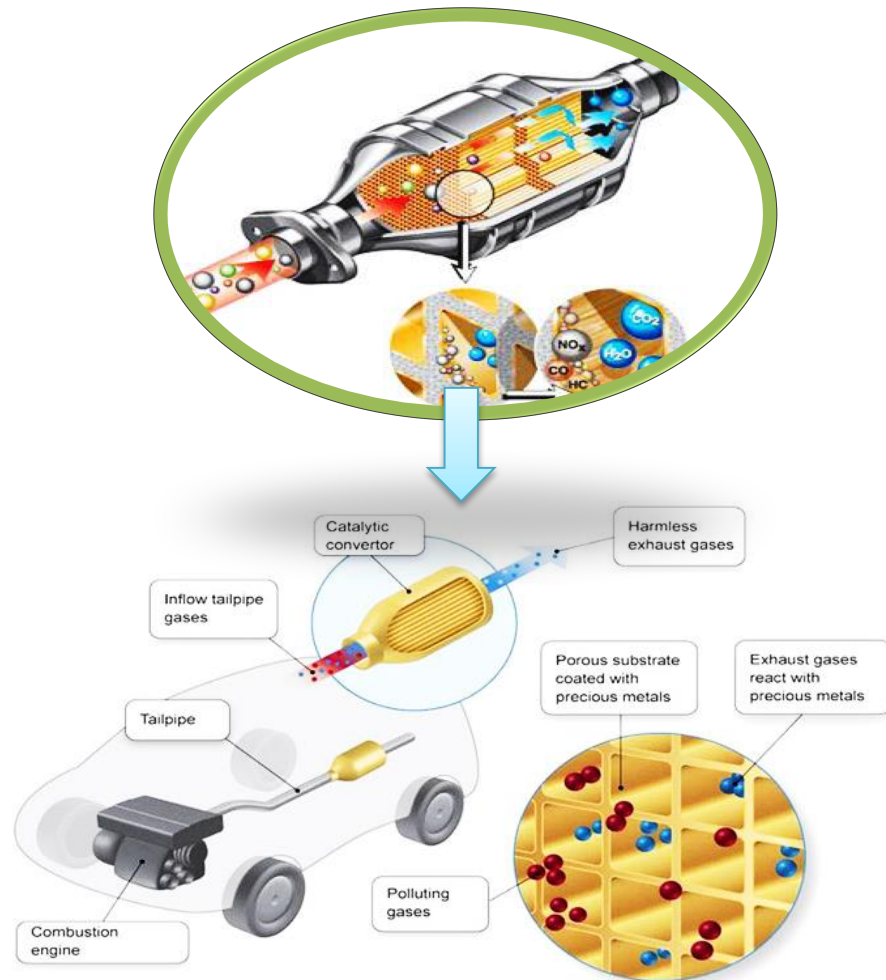
### 2.7.1 Fundamentals of TWC

Over the last three decades, enormous efforts have been made in order to control the negative impact of pollutants from vehicles. Scientists and industry professionals have proposed and developed novel technologies in order to mitigate the emissions of pollutants into the atmosphere, including improvement of engine design fuel pre-treatment, use of different kinds of fuels (hydrogen, biomass, among other kinds), fuel additives, exhaust treatment, as well as others. Although the new technology has offered good results in many fields, catalytic converters (CC) have been the best option to control the exhaust emissions of automobiles based on petrol (CO,  $H_xC_y$  and  $NO_x$ ) [72, 73].

Catalytic converters have been extensively applied in the last 30 years because of their efficiency and economic feasibility to mitigate the pollutants released by the combustion of engine. Throughout the use of catalytic converters the worldwide legislation about the limits of pollutant emissions has been satisfied though becomes stricter day by day. Although the automobile is covered by the legislation, it is not enough and numerous research groups try to find new ways to improve the efficiency and selectivity of CC in the automotive industry [72].

In automotive, catalytic converters are positioned inside the tailpipe where the gases coming from the incomplete combustion of fuel react with the catalyst, thereby decreasing the content of gaseous pollutants emitted. The three-way catalytic converter (TWC) performs the oxidation of carbon monoxide and hydrocarbons, as well as improves the reduction reaction of nitrogen oxides at the same time. This technology implies the use of a mixture of catalysts of noble metals as an active phase. Between the metals, Palladium (Pd) has been a focus of attention for chemical properties like selectivity for hydrocarbon compounds and catalytic activity as well as for the low price in comparison with other noble metals such as platinum (Pt). On the other hand, the reduction of NO to  $N_2$  has been performed using a rhodium-based catalyst. The performance of three-way catalytic converters may diminish by the effect

of the temperatures of the global process, generally  $> 600\text{ }^{\circ}\text{C}$ . Coming up next, we illustrate a catalytic converter, the location point in the car, the internal structure of the system and the precise place where the catalysts stand (Figure 2-10) [74-76].

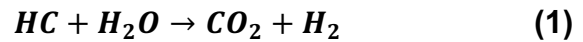


**Figure 2-10 Three-way catalytic converter located inside the tailpipe and their honeycomb internal structure [77].**

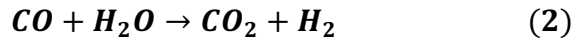
As noted above, catalytic converters involve an advanced technological development due to the complexity of the reactions which are carried out in the automotive exhaust catalysts. The primary reactions include reduction of  $\text{NO}_x$ , oxidation of  $\text{CO}$  and  $\text{H}_x\text{C}_y$ . Additionally, steam reforming reaction and water gas shift can also take place during the conversion or reactants to product. Due to the significant content of  $\text{NO}_x$ , a new concept was proposed and applied, named “ $\text{NO}_x$  storage”. This includes the incorporation of storage material blended with the TWC with the aim of storing this pollutant during the

lean conditions. To clarify the catalytic process into the CC, we will show the possible reactions. [12, 62, 78, 79]

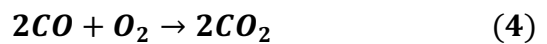
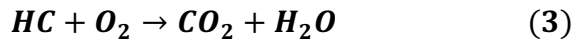
**Steam Reforming:**



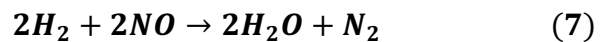
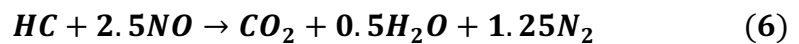
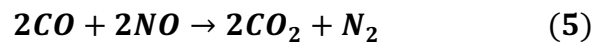
**Water gas shift:**



**Oxidation:**

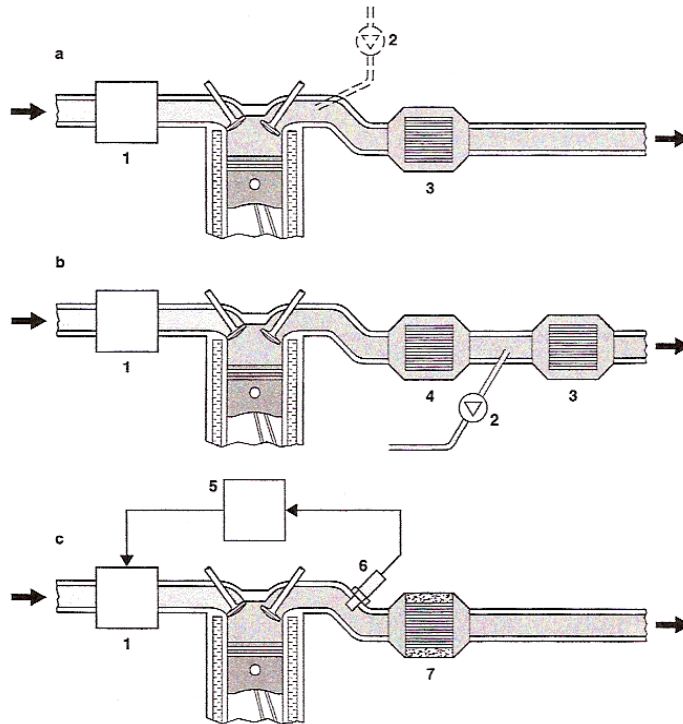


**Reduction:**



This type is also a single bed catalytic converter, but varies in the ability to convert huge amounts of all major pollutants. The three-way catalytic converter utilises information of the engine induction mixture and exhaust gas to maintain a stoichiometric ratio. The data that received from lambda sensor and processes them in a closed loop control to produce the required output of mixture. For this reason, this system is able to limit the pollutants under stringent legislation. When a three-way catalyst is used, it requires an engine induction mixture and exhaust gas an engine management system capable of very accurate air/fuel ratio control by lambda O<sub>2</sub> sensor, as shown in Figure 2-11.

a Single-bed oxidation catalytic converter, b Dual-bed catalytic converter, c Single-bed catalytic converter.  
 1 Mixture formation/injection system, 2 Secondary-air injection, 3 Oxidation catalytic converter for HC, CO,  
 4 NO<sub>x</sub> reduction catalytic converter, 5 Electronic control unit, 6 Lambda O<sub>2</sub> sensor,  
 7 3-way catalytic converter for NO<sub>x</sub>, HC, CO.



**Figure 2-11 Catalytic converter system [15].**

This is an effective method of monitoring the catalytic converter through the use of lambda sensor. For this purpose, an upstream sensor is supplemented with a downstream sensor. A correctly operating converter should store the oxygen, thus settling down the oscillations of the sensors as the catalytic converter deteriorates until the signal received from the upstream sensor approaches the downstream sensor. Then, it is time for a change, and a signal lamp will alert the driver for a replacement.

A catalytic converter consists of the following sections, as can be seen (**Figure 2-12**):

- metal housing
- substrate
- catalyst

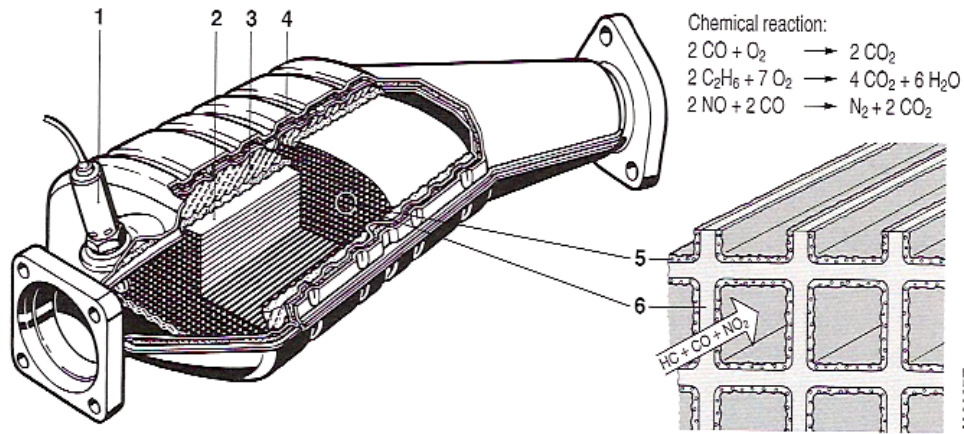
The substrate systems can be divided in two different types:

- 1) pellets
- 2) ceramic monoliths
- 3) metallic monoliths [23]



**Figure 2-12 Cross section of a 3 way catalytic converter [15].**

1 Lambda O<sub>2</sub> sensor, 2 Ceramic monolith, 3 Flexible metal screen, 4 Heat-insulated dual shell, 5 Platinum, rhodium coating, 6 Ceramic or metallic substrate.

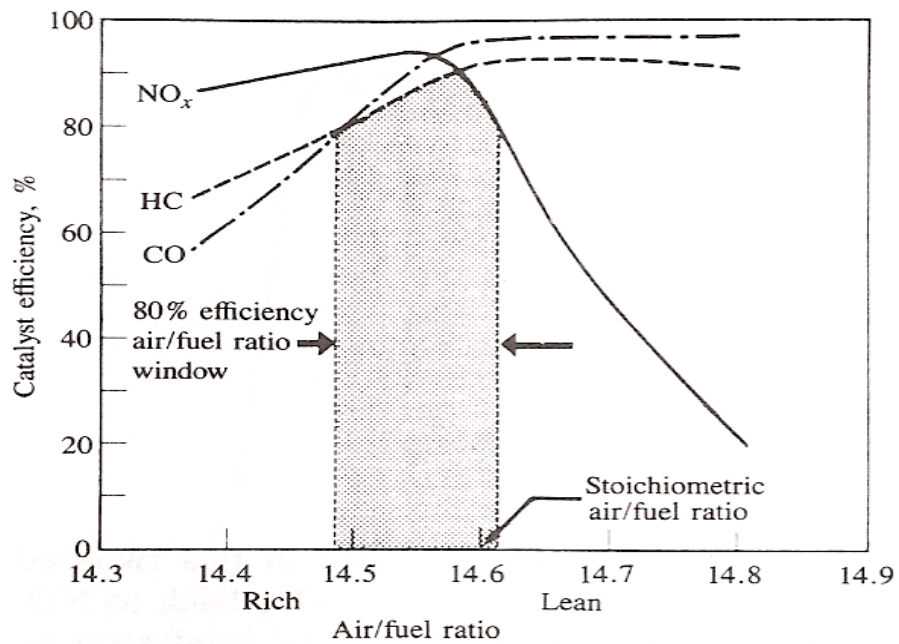


In a catalytic converter with an O<sub>2</sub> sensor, the temperature is very important factor. The unit must be warmed above 300 degrees to ensure an effective reading. The nominal temperature to ascertain a correct reading is "between" 400 to 800 degrees Celsius. These sensors have to be ruggedly built to ensure resistance against thermal ageing.

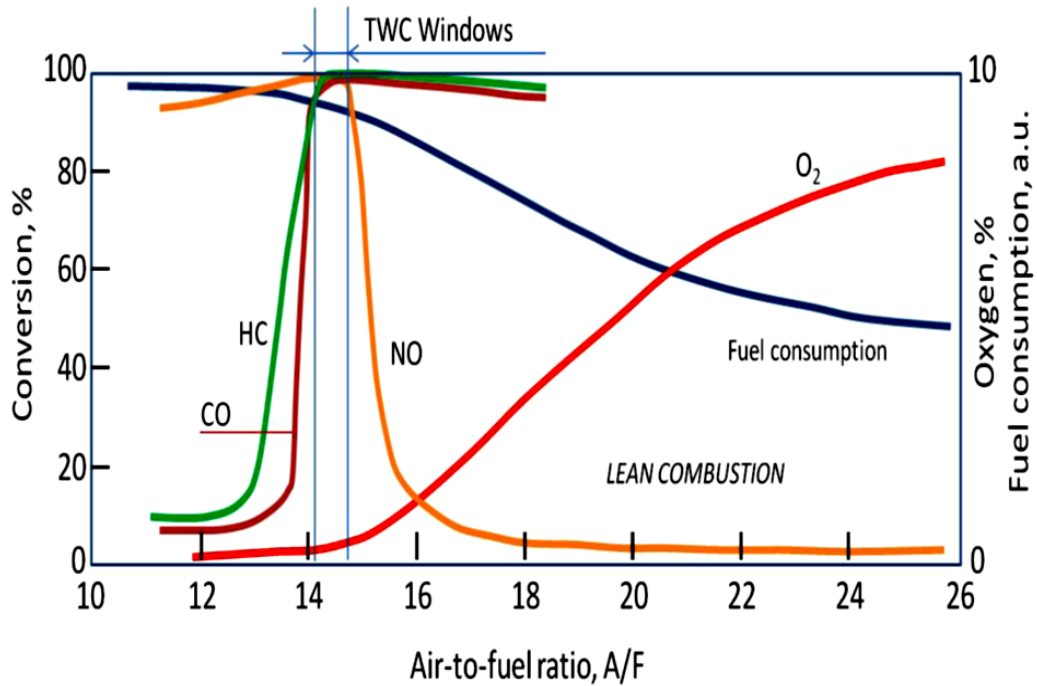
Running the Catalyst convertor on favourable conditions could raise the operation range up to 100,000 kilometres. Additionally, engine malfunctions, such as misfiring, could raise the temperature above 1400 degrees, melting the substrate and destroying the converter. Although the lead element deposits on the active substrate reduce the surface area for reaction.

Analysis of the results in(Figure 2-13), and (Figure 2-14) however, shows there is a narrow band as indicated in the in which high conversion efficiency can be achieved for all the three pollutants. It has also to be noticed that the narrow high efficiency band is achieved only near the stoichiometric range. The width of this narrow band is only about 0.1 air/fuel ratio range. This indicates that the catalytic converter must be operated under high mileage conditions and certain engine operating conditions. Consequently, any ordinary carburettor cannot perform the specified job within this range. Hence, the application of fuel injection becomes necessary. A closed loop sensor, that

is the oxygen sensor in the exhaust, could feed back the electronic control unit ECU, in turn adjusting the fuel system to achieve the desired air/fuel mixture. Experiments show that there is a fluctuation and the effect of fluctuation depends on the frequency; frequencies of about 0.5 to 1 hertz are the most effective and usable window. Benefits of fluctuations in equivalent ratios are achieved without any deliberate attempt to produce them, while in open loop the fluctuations are produced only during normal vehicle operation [70].



**Figure 2-13 Conversion efficiency for NO, CO and HC in 3 way catalyst [70].**



**Figure 2-14 Fuel conversion based on the air-to-fuel (A/F) ratio with classical three-way catalyst of stoichiometric petrol engines [62].**

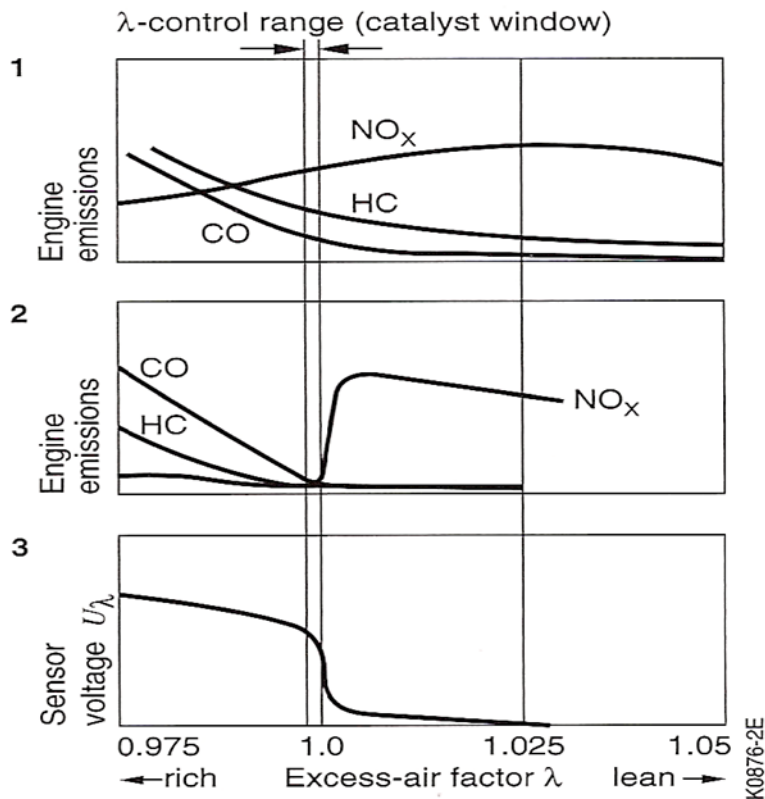
### 2.7.2 Lambda closed loop control

Among all the current methods available, the lambda closed loop control method fitted with the catalytic converter in spark ignition engine proved to be the most effective. No other alternatives are as efficient as this system. The present available ignition and fuel injection system can achieve extremely low emission levels. Moreover, the catalytic converter reduces all the major pollutant emission levels.

The three-way catalytic converter narrows the hydrocarbon emissions, carbon monoxide and oxides of nitrogen by 98%, if only the engine runs 1% around the stoichiometric range ( $\lambda=1$ ). Suggested that, to maintain the operating conditions under this range, even the best known injection system needs assistance. The answer is to simply install “a lambda closed loop control system which relies on a closed loop control circuit to consistently maintain the air-fuel ratio entering the engine with optimal range called “catalyst window”, as shown (Figure 2-15).

**Catalytic efficiency and lambda-sensor voltage relative to excess-air factor  $\lambda$**

- 1 Without catalytic post-combustion treatment,
- 2 With catalytic post-combustion treatment,
- 3 Voltage curve with 2-threshold  $\lambda$  sensor.



**Figure 2-15 Catalytic efficiency and lambda sensor voltage relative to excess air factor [15].**

Additionally, the stoichiometric air-fuel ratio is the mass ratio of 14.7 kg of air to 1 kg of gasoline, which is theoretically essential to complete the combustion. The excess air factor or air ratio  $\lambda$  indicates the actual air fuel ration deviation from the theoretical ratio [80, 81].

This system basically works on continuously checking the exhaust gas composition as the basis for making immediate feedback and to correct the air fuel mixture ratio. The monitoring tool is basically the oxygen or lambda sensor. If there is a voltage jump, it means that the sensor is working under the stoichiometric range. The voltage fluctuation shows whether the mixture inhaled by the engine is leaner or richer than 1 [15].

### **2.7.3 Development of TWC substrates for high conversion efficiency and fast light off.**

The Three-Way Catalyst (TWC) is used for the reduction of NO<sub>x</sub>, oxidise CO and HC. The regulations of spark ignition engine emissions in the USA and Europe cannot be met by engine design modifications, and the development of lean burn engines for NO<sub>x</sub> control and to improve specific fuel consumption (SFC) did not produce sufficient reduction in NO<sub>x</sub>, CO and HC. Consequently, the emissions were removed mainly by using an exhaust catalyst. The development decision related to these was taken in the USA in the 1980s and about a decade later in Europe. The first of the modern emission legislation in Europe (Euro 1) was in 1993, and nearly every SI vehicle manufactured since then has had a TWC for emission control. Lead ultimately poisons the TWC, and the anti-knock additive lead has to be removed from the fuels to allow TWC to be applied.

The TWC only works at exactly  $\lambda=1 \pm 1\%$ , and to achieve this requirement, new engines were developed with electronic control. The carburettor use was wholly inadequate. It was replaced by inlet port fuel injection with the inlet air mass flow metered and the computer controlling the time of opening of the fuel injector solenoid valve to give the precise amount of fuel. To improve the  $\lambda$  control, the oxygen out of the engine was monitored using a zirconium oxide electro ceramic sensor, which gives a higher output the lower the oxygen level. The accuracy of the  $\lambda$  control is crucial to the achievement of high conversion efficiencies by the TWC, and this efficiency has increased from Euro 1 to Euro 4.

### **2.7.4 Lean warm up concept**

The normal methods followed for the reduction of pollutants are based on using a catalytic converter which is an external process. The external process does not affect the combustion process in any way, but there are methods which directly influence the combustion process. Such methods involve combustion chamber design, exhaust gas recirculation, ignition advance or

retardation and A/F ratios. However, these methods have not produced any considerable results, compared with that of the external process. Modifications of the internal processes are applied in the lean burn concept.

The primary benefits of leaner mixtures are the reduction in HC, CO and increase in fuel economy, but at the price of higher NO<sub>x</sub>. Lean burn engine is combined with the combustion chamber design and the feedback from the exhaust [82, 83]. The lean burn concept has maintained the excess air ratio to 1.4 ranges. Although the concept itself reduces pollutants to a high extent, it still needs help from the catalytic converter to solve the severe emission norms [15].

### **2.7.5 NH<sub>3</sub> and HCN RDE emissions for TWC**

Undesirable emissions from TWCs are NH<sub>3</sub> and HCN, which occur in TWC through the reactions in Equations (2-1) and (2-2):



Both reactions occur in rich mixtures, as these generate equilibrium hydrogen and will also have high HC owing to inefficient combustion. For SI engine vehicles, neither species is regulated [84]. The higher accelerations used in real-world driving may generate locally richer mixtures, and it is possible that NH<sub>3</sub> and HCN could be higher in real-world driving than on test cycles. There is also interest in NO<sub>2</sub> emissions from vehicles as this is the air pollutant that is harmful to humans. For SI vehicles, NO<sub>2</sub> is normally assumed to be very low and is only of concern for diesel engines. In this work, it will be shown that NO<sub>2</sub> emissions are low but significant at about 5% of the NO levels. The final nitrogen species of interest is N<sub>2</sub>O, as this is a powerful greenhouse gas. Full nitrogen speciation in real-world congested traffic driving is reported in this work using an Fourier transform infrared (FTIR) as a portable emissions measurement system (PEMS).

Heeb [85-87] and Bielaczyc et al. [88] investigated  $\text{NH}_3$  emissions from TWC and their correlation with NO emissions. They concluded that catalyst temperatures and air/fuel ratios are the key parameters affecting the formation of  $\text{NH}_3$  in EURO 3 and 4 gasoline passenger cars. They also reported a conversion ratio of 2% to 45% for NO converting to  $\text{NH}_3$  when operating a Pd/Rh-based TWC vehicle under transient driving conditions. As  $\text{NO}_x$  regulations are lowered, higher conversion efficiencies of  $\text{NO}_x$  at the TWC are required, and this often involves biasing the controlled  $\lambda$  about 1 or 2% rich and this promotes  $\text{NH}_3$  formation by Equation (2-2) The authors [89, 90] have also measured significant emissions of  $\text{NH}_3$  from TWC under real-world driving with associated hydrogen cyanide (HCN) emissions. Li et al [48] investigated GWP of  $\text{CO}_2$ ,  $\text{N}_2\text{O}$  and  $\text{CH}_4$  tailpipe emissions for several urban driving cycles and reported ~10% of the total GWP coming from  $\text{N}_2\text{O}$ . Methane was always a negligible (<1%) contribution to total GHG emissions.

## **2.8 Emission test cycles and measurement**

### **2.8.1 Test cycles**

Different countries/regions in the world use different test procedures to compare the efficiency of different engines and the emissions; these test procedures are called driving cycles. A driving cycle refers to a standardised driving pattern, which is described by a velocity-time. The track to be covered is divided in several time steps mostly in seconds. It is assumed that the acceleration during a time step is constant, implying that the velocity during a time step is a linear function of time. Since acceleration and velocity at each time point is known, the mechanical power as a function of time can be determined by applying known formulae. Integration of this function over the duration of the driving cycle produces the mechanical energy required for that driving cycle. A dynamometer was used to execute the off-road driving cycle.

The following section discusses the prevailing driving cycles in the world; namely, European driving cycles, US driving cycles and Japanese driving cycle [91].

Road vehicle emit various atmospheric pollutants as a result burning fossil fuel during combustion. The emission tests for new light-duty vehicle models is require as a type approval. The procedures of pollutant collection and analyzing is specified in legislation. A power-absorbing chassis dynamometer used for the emission tests of Light duty vehicles. In the chassis dynamometer car set on rollers to simulate driving resistance. The exhaust emissions sampling performed as a car progresses to the specific driving cycle. A fixed schedule of vehicle operation used during the driving cycle, which specified as a function of time with vehicle speed and gear selection.

In tests conducted using a chassis dynamometer the vehicle drive wheels are placed in contact with rollers which can be adjusted to simulate frictional and aerodynamic resistance. The sampling of exhaust emissions is then performed as the vehicle progresses through a pre-defined driving cycle.

A driving cycle is a fixed schedule of vehicle operation, and is usually characterized in terms of vehicle speed and gear selection as a function of time. The defined cycle applied on car by employing a trained driver on the chassis dynamometer follow the driving cycle his aid is to provide and ensure that he following the pattern of defined driving cycle[1].

#### **2.8.1.1 USA passenger car and light commercial vehicles (FTP) test cycle**

Federal Test Procedure (FTP) is the name of USA test cycle, which consists of the actual speed cycle recorded in the Los Angeles commuter traffic, as indicated in (Figure 2-16).

##### **2.8.1.1.1 Test condition**

The vehicle is subjected to 20 to 30 degrees Celsius (°C) as an ambient temperature for a period from 6 to 36 hours.



#### **2.8.1.1.2 Pollutants collection**

Starting and driving the vehicle on a specific speed cycle. The collection of pollutants emitted from the vehicle is in separate bags during defined phases.

#### **2.8.1.1.3 Cold Transient (CT phase)**

Exhaust gas collection during the phase of cold test is between 0 to 505 seconds see the test cycle in (Figure 2-16).

#### **2.8.1.1.4 Cold stabilised (CS phase)**

Stabilised phase starts from 506 seconds after the start. The collection of the exhaust gas is without interrupting the driving cycle. Upon cold stabilised (CS phase) termination and after 1372 total seconds, the engine is switched off for 600 seconds hot soak period.

#### **2.8.1.1.5 Hot Transient (HT phase)**

Engine for the hot test is restarted. The speed is identical to the cold transient (CT phase).

#### **2.8.1.1.6 Hot stabilised (HS phase)**

Further hot stabilised (HS phase) is driven for a hybrid vehicle; for other vehicles, the emission values are assumed to be identical to the cold stabilised (CS phase).

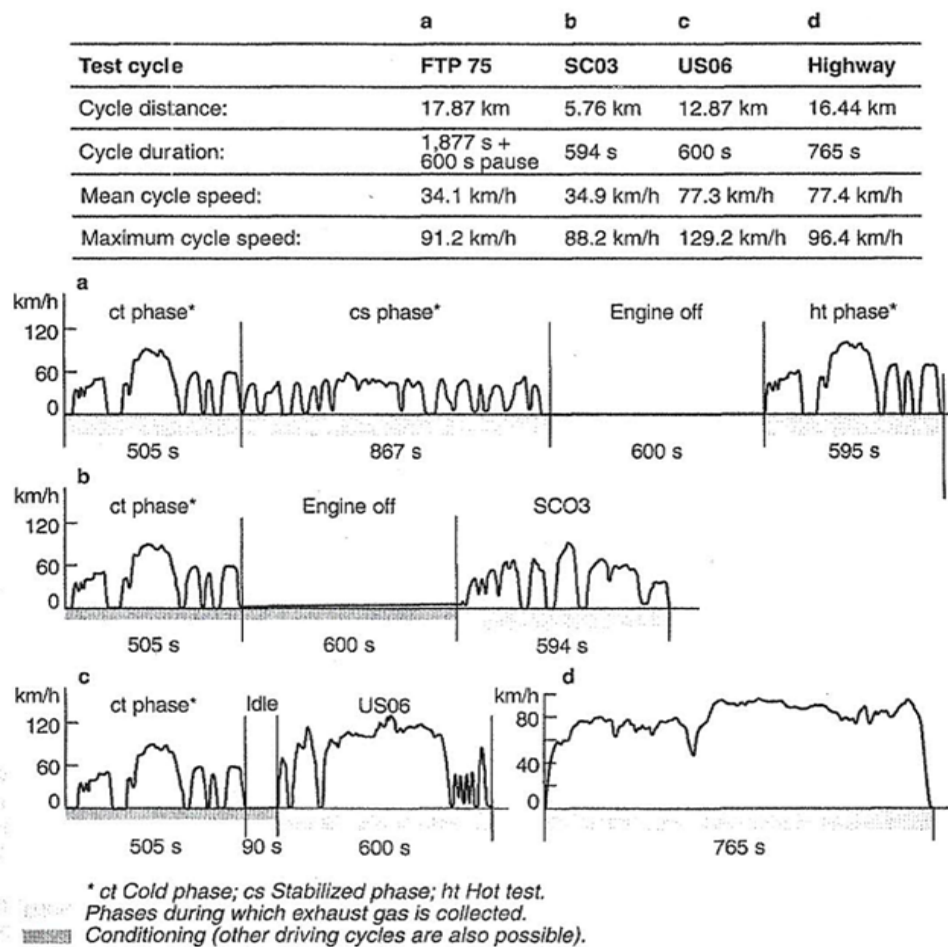
#### **2.8.1.1.7 Assessment**

The samples of bags are analysed from the first two phases before the hot test during the pause because samples may not stay in for a period exceeding 20 minutes. Also, the third sample bag of the exhaust gases analysed after the driving cycle completion. The total result from the three emission phases are rated at different weightings. The masses of pollutants from the cold transient (CT phase) and the cold stabilised (CS phase) are aggregated and assigned to the two phases' total distance. After that, the result is weighted at 0.43 as a factor.

The process applied is the same for the aggregated pollutant masses from the hot transient (HT phase) and the cold stabilised (CS phase) related to these total two distance phases and weighted at 0.57 .

### 2.8.1.1.8 The schedules of SFTP

Standard Federal Test Procedure test according to SFTP standard that was phased in between 2001 and 2004 which, two driving cycles are composed the SC03 cycle and the US06 cycle as shown in (Figure 2-16).



**Figure 2-16 US Test cycles for passenger cars and light commercial vehicles [91].**

The tests are extended which, represented examinations of the additional driving conditions as follow:

1. Aggressive driving.
2. Vehicle speed radical changes.
3. Start of engine and acceleration from standing start.

4. Frequent minor variations in speed for vehicle operation.
5. Vehicle parked periods.
6. Air conditioner on during vehicle operation.

The SC03 and US06 cycles for reconditioning proceed through the CT phase from FTP without the collection of exhaust gas. However, there are possibilities for other conditioning procedures. The vehicle with air conditioning SC03 cycle, which carried out at 35 degree Celsius (°C) temperature and 40% relative humidity. The schedules of driving are weighted individually as follows:

- Vehicles systems with air condition A/C: 35%FTP 75+37%SC03+28%US06.
- Vehicles systems without air condition A/C:72%FTP 75+28%US06.

The test cycle of SFTP and FTP 75 must be successfully completed individually.

The gasoline vehicle cold-start enrichment is necessary when the engine starts at low temperatures that produce high emissions that cannot be measured with current emissions testing conducted between 20 and 30 degrees Celsius (°C) as ambient temperatures. In order to limit these pollutants, an additional test for exhaust gas was performed at -7 degrees Celsius (°C) on vehicles. However, prescribe only a carbon monoxide limit with previous test which, introduced in 2010/2013 for NMHC [91].

#### **2.8.1.1.9 Determining fleet consumption test cycles**

Providing data on corporate average fuel economy is required from every vehicle manufacturer. Any manufacturer failing to comply with the target value will be required to pay a penalty. The produced exhaust gas emissions are used to determine fuel consumption during two test cycles: the FTP 75 test cycle, weighted at 55%, and the test of highway cycle, weighted at 45%. (Figure 2-16 d)represents an unmeasured test of highway cycle is conducted once after preconditioning which, allowed to the vehicle to stand with engine off at temperatures between 20 and 30 degrees Celsius (°C) for half a day (12

hours). Then, the second test run exhaust emissions are collected. Calculation of fuel consumption is performed by using CO<sub>2</sub> emissions [91].

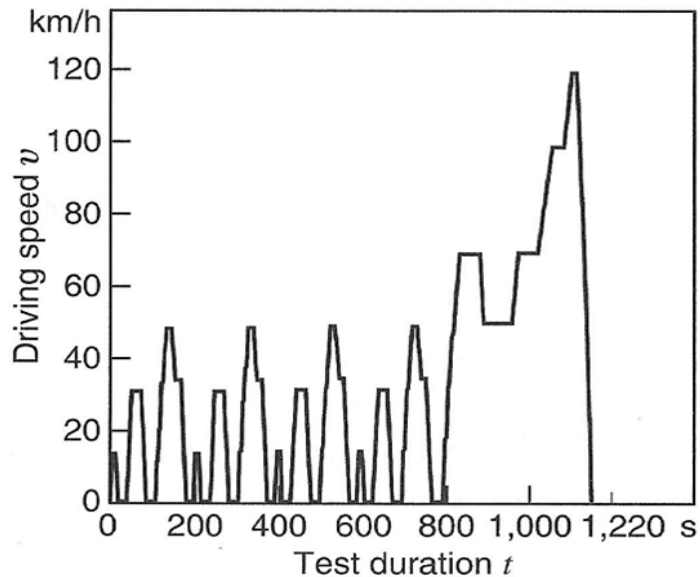
### 2.8.1.2 Additional test cycle

#### 2.8.1.2.1 (FTP 72 test)

Additional test cycles are FTP 72 test routine, which is also known as Urban Dynamometer Driving Schedule (UDDS) that corresponds to the test of FTP 75, but the hot test component HT is not included. This gasoline engine cycle, which driven during running loss test.

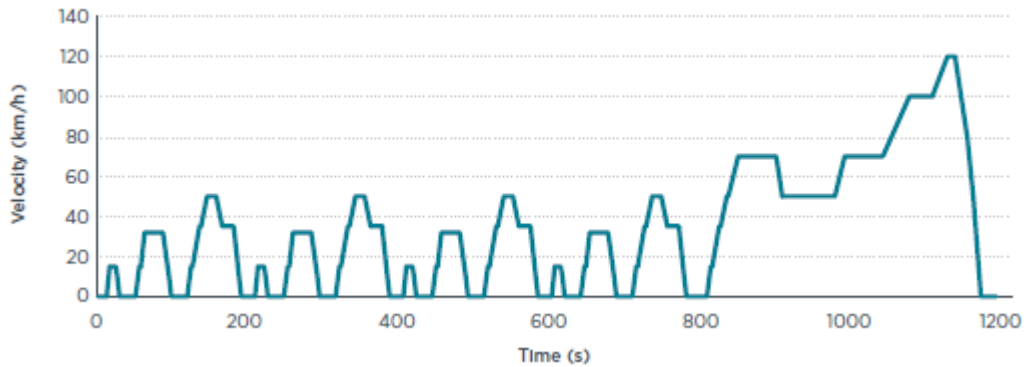
### 2.8.1.3 European test cycle for passenger car and light commercial vehicles new European driving cycle (NEDC)

NEDC New European Driving Cycle shown in (Figure 2-17) has been in force since Euro 3. Unlike its predecessor (Euro 2) where emissions measurement began after 40 seconds of vehicle start, NEDC includes, a cold start phase.



**Figure 2-17 NEDC for passenger cars and light commercial vehicles.**

Cycle Distance: 11Km; Average Speed: 33.6 Km/h; Maximum Speed: 120 Km/h [91].



**Figure 2-18 Driving schedule of the NEDC cycle [92].**

#### **2.8.1.4 NEDC conditioning**

The ambient temperature the vehicle is subject to is between 20 and 30 degrees Celsius ( $^{\circ}\text{C}$ ) for 6 hours as a minimum period. The starting temperature has been lowered to -7 degrees Celsius ( $^{\circ}\text{C}$ ) in gasoline vehicles for the Type VI test since 2002.

#### **2.8.1.5 NEDC pollutant collection**

There are two bags for the exhaust gas collection in two phases. The first one is during the Urban Driving cycle (UDC) which is at 50 km/h as a maximum speed. The second one is during the Extra Urban Driving cycle (EUDC) which is at 120 km/h as a maximum speed.

#### **2.8.1.6 NEDC Assessment**

The mass of pollutants is measured by analysing the contents of the bag which refers to the covered distance.

### 2.8.1.7 World Harmonised Light Duty Test Procedure (WLTP)

The NEDC in the medium term will be replaced by the new test cycle World Harmonised Light Duty Test Procedure (WLTP) which is more realistic. The European Union, the USA, China, India, Korea and Japan are working with others towards this goal on the UN/ECE level.

### 2.8.1.8 Japanese test cycle for passenger car and light commercial vehicles

The test is based on two different driving cycles as indicated in (Figure 2-19) and (Table 2-4).

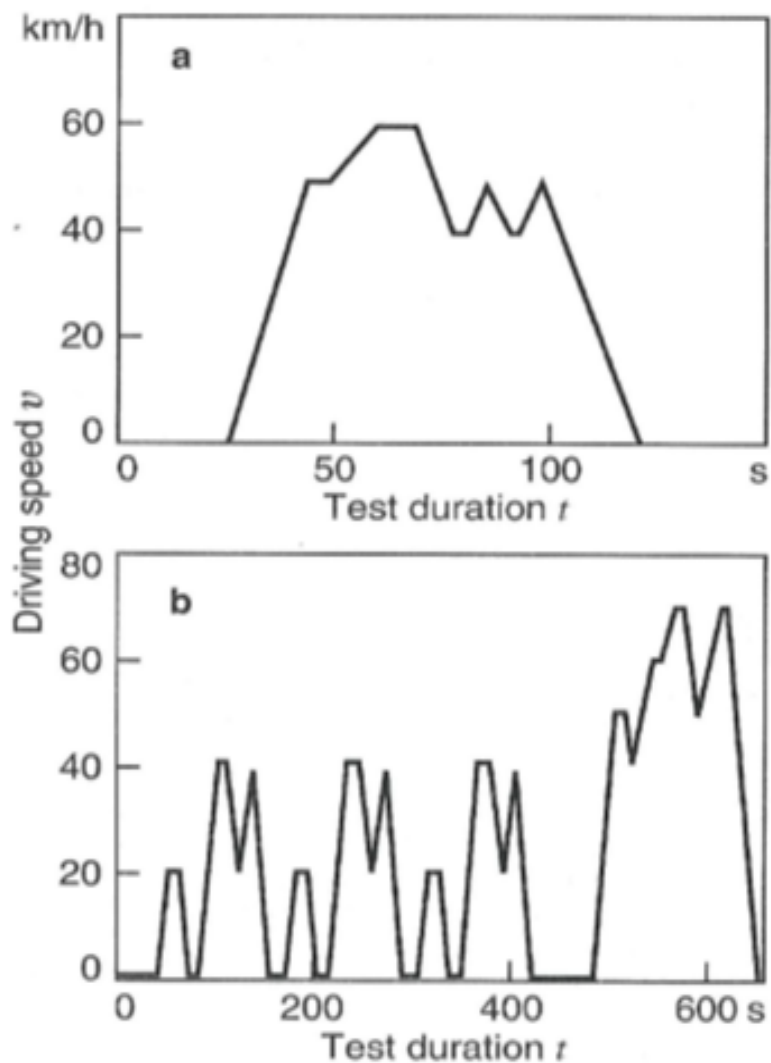


Figure 2-19 Japanese test cycles for passenger cars and light commercial vehicles [91].

**Table 2-4 Test based on two different driving cycles as indicated [91].**

	<b>11-MODE CYCLE (COLD TEST) (FIGURE A)</b>	<b>10 . 15- MODE CYCLE (HOT TEST) (FIGURE B)</b>
<b>CYCLE DISTANCE</b>	1.021 Km	4.16 Km
<b>CYCLES PER TEST</b>	4	1
<b>AVERAGE SPEED</b>	30.6 km/h	22.7 Km/h
<b>MAXIMUM SPEED</b>	60 Km/h	70 Km/h
<b>START-UP TESTING CONDITION</b>	Cold Start	Hot Start

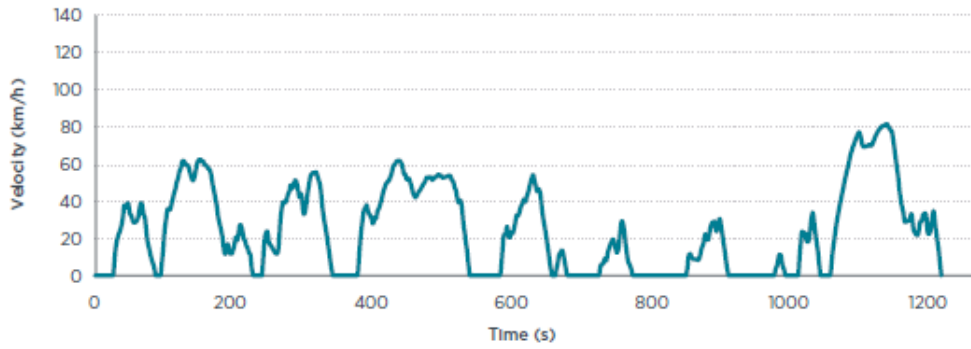
The hot test preconditioning procedures include the prescribed exhaust gas test at idle which, is as follows:

- The hydrocarbon (HC), carbon monoxide (CO), carbon dioxide (CO<sub>2</sub>), are measured at idle after the vehicle is allowed to warm up for a period of about 15 minutes at 60 km/h.
- The hot test of 10/15-mode begins after a second warm-up, which consists of 5 minutes at 60 km/h.

The pollutants examination in grams per test during the cold test, the results of hot test defined relative to distance which indicated in e JC08 form, initially as a cold test replaced the 11-mode test. The JC08 has continued to be used for a cold-start test and a hot-start test since 2011. Japan exhaust gas regulations include limits on evaporated emissions in gasoline vehicles measured by using the SHED method.

#### **2.8.1.8.1 JAPAN: JC08**

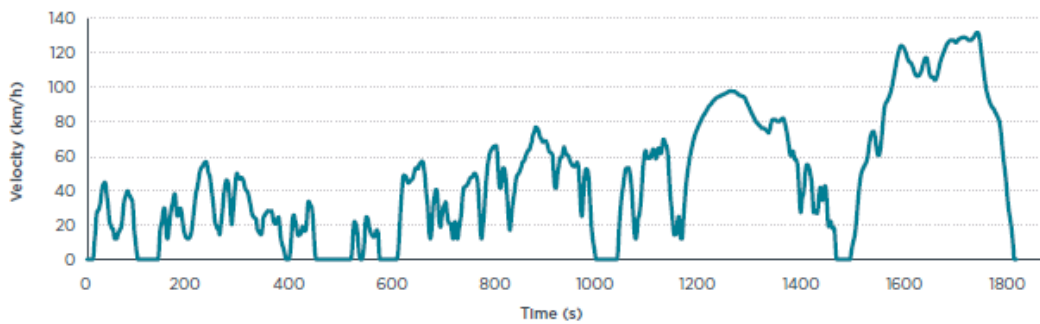
The JC08 introduced in 2005 into Japanese emission regulation and fuel economy determination as shown in Figure 2-20. The JC08 test fully phased-in by October 2011. The measurement were made twice, cold start being weighted by 25% and a hot start weighted by 75%.



**Figure 2-20 Driving schedule of the JC08 cycle [92].**

### 2.8.1.9 Worldwide harmonization (WLTC)

The Worldwide harmonized Light-duty Test Cycle (WLTC) as shown in Figure 2-21 developed by the UN ECE GRPE (Working Party on Pollution and Energy) group within the framework of the Worldwide harmonized Light Vehicles Test Procedure (WLTP), which expected to replace the European NEDC procedure for type approval testing of light duty vehicles with the transition to the Euro 6c emission standards in September 2017.



**Figure 2-21 Driving schedule of the WLTC cycle [92].**



**Table 2-5 Descriptive parameters of the driving cycles [92].**

	Units	FTP75 weighted	HWFET	CAFE	NEDC	JC08	WLTC
Start condition		43% cold / 57% hot	hot		cold	25% cold / 75% hot	cold
Duration	s	1369	765		1180	1204	1800
Distance	km	11.99	16.51		11.03	8.17	23.27
Mean velocity	km/h	31.5	77.7	52.3	33.6	24.4	46.5
Max. velocity	km/h	91.2	96.4		120.0	81.6	131.3
Stop phases		18	2		14	12	9
<b>Durations</b>							
Stop	s	241	4		280	346	226
Constant driving	s	109	126		475	21	66
Acceleration	s	544	338		247	432	789
Deceleration	s	475	297		178	405	719
<b>Shares</b>							
Stop		17.6%	0.5%	9.9%	23.7%	28.7%	12.6%
Constant driving		8.0%	16.5%	11.8%	40.3%	1.7%	3.7%
Acceleration		39.7%	44.2%	41.7%	20.9%	35.9%	43.8%
Deceleration		34.7%	38.8%	36.6%	15.1%	33.6%	39.9%
Mean positive acceleration	m/s <sup>2</sup>	0.50	0.19	0.36	0.59	0.42	0.41
Max. positive acceleration	m/s <sup>2</sup>	1.48	1.43		1.04	1.69	1.67
Mean positive 'vel * acc' (acceleration phases)	m <sup>2</sup> /s <sup>3</sup>	3.86	3.45	3.67	4.97	3.34	4.54
Mean positive 'vel * acc' (whole cycle)	m <sup>2</sup> /s <sup>3</sup>	1.53	1.52	1.53	1.04	1.20	1.99
Max. positive 'vel * acc'	m <sup>2</sup> /s <sup>3</sup>	19.19	15.17		9.22	11.60	21.01
Mean deceleration	m/s <sup>2</sup>	-0.58	-0.22	-0.42	-0.82	-0.45	-0.45
Min. deceleration	m/s <sup>2</sup>	-1.48	-1.48		-1.39	-1.19	-1.50

## 2.8.2 Emission measurement methods

Exhaust emissions measurement (EEM) has a significant role in air pollutant control from internal combustion (IC) engines. Infrared absorption is used to measure carbon monoxide (CO) concentrations, while flame ionization detector is used to measure unburned hydrocarbons (HC) concentrations and chemiluminescence for nitrogen oxides (NO<sub>x</sub>) concentrations [2].

### 2.8.2.1 Non-dispersive infra-red (NDIR) analyser

Carbon monoxide (CO) and carbon dioxide (CO<sub>2</sub>) concentration is measured by the NDIR Analysers, which is based on the principle that certain chemical groups (and hence compounds) absorb the infrared energy of a particular

wavelength, for example carbon monoxide (CO) wavelength absorption between 4.5 and 5 microns ( $\mu\text{m}$ ), and carbon dioxide ( $\text{CO}_2$ ) wavelength absorption between 4 and 4.5 microns ( $\mu\text{m}$ ) [2].

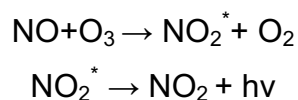
### 2.8.2.2 Flame-ionization Detector (FID)

The absorption of some hydrocarbons (HC) is 3.4 microns ( $\mu\text{m}$ ) while some others could not be absorbed, notably, for example, aromatics. The NDIR measured only about 50 percent of the exhaust hydrocarbons (HC) concentrations; consequently, the NDIR is not suitable for measuring hydrocarbons (HC) concentrations.

Hydrocarbons (HC) concentrations in the exhaust gases are mainly measured by the flame-ionisation detector (FID) which is based on the principle of difference in ionisation production amounts. For instance, the pure hydrogen-air flames produce a small ionisation amount while a small amount of hydrocarbon molecules in the flames produces a large ionisation amount. It should be noted that the ionisation amount is proportional to the carbon atoms number available in hydrocarbon (HC) molecules [2].

### 2.8.2.3 Chemiluminescence analysers

The nitric oxide (NO) concentrations are measured by the chemiluminescence analysers. The principle of this technique is based on the reaction of nitric oxide (NO) to ozone ( $\text{O}_3$ ) to produce some  $\text{NO}_2$  in an electronically excited state. Molecules that are excited on decaying to the ground state emit red light (photons) from 0.6  $\mu\text{m}$  to 3  $\mu\text{m}$  wavelength region.



Where;  $h$  is Planck's constant,  $\nu$  is a photon of light.

The nitrogen oxides ( $\text{NO}_x$ ) emitted from the exhaust of the engine mainly consist of a mixture of nitric oxide (NO) and nitrous oxide ( $\text{NO}_2$ ). The thermos-

catalytic converter converts any exhaust  $\text{NO}_2$  to  $\text{NO}$  before supplying the exhaust gas to the analyser; the total nitrogen oxides ( $\text{NO}_x$ ) value can be obtained [2].

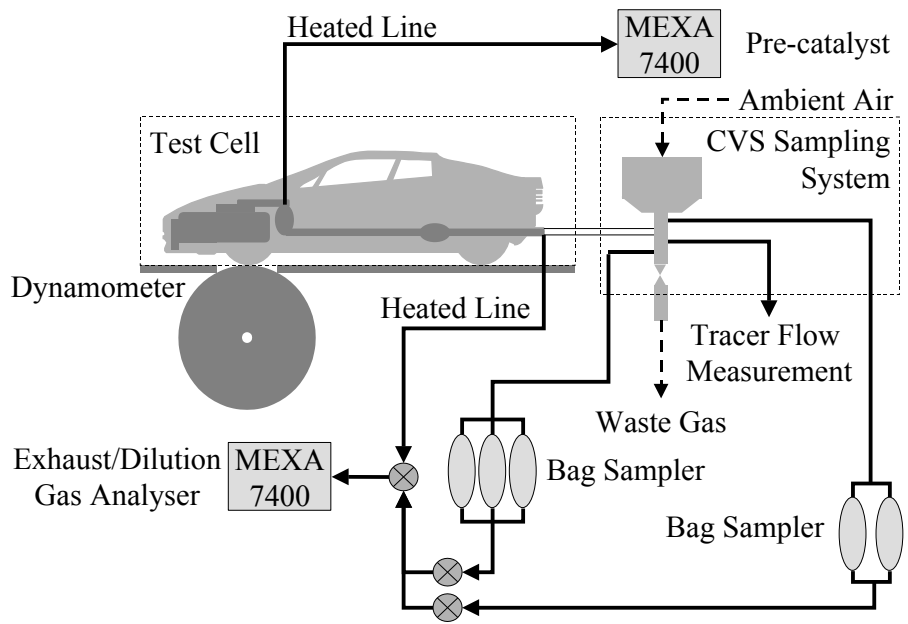
### **2.8.3 Chassis dynamometer test**

The exhaust tests on the chassis dynamometer are used for type approval to attain a general classification as well as for the development of engines and other components. Chassis dynamometers vary in exhaust-gas tests that are conducted for general and partial inspections use. Furthermore, the tests of exhaust gas are conducted on the engine test benches. However, the test of exhaust gas on chassis dynamometers is performed on vehicles. The simulated methods define, as far as possible, the actual vehicle operation on the road which offers some advantages as follows:

1. The environment condition can be kept constant which produces highly reproducible results.
2. Tests good comparability as a defined profile of speed-time can be driven independent of traffic flow.
3. Measuring stationary setup techniques required [91].

The test vehicle is parked on the chassis dynamometer with the drive wheels on the rollers.

Numerous forces such as rolling resistance, aerodynamic drag and inertia are applied on vehicle which must simulate actual driving conditions to ensure the chassis dynamometer emissions generation correspond as an actual high way operation [15] See (Figure 2-22). and (Figure 2-23).



**Figure 2-22 Chassis dynamometer [93].**



**Figure 2-23 Chassis dynamometer cell [93].**

## 2.9 Cold-start emissions

One of the major emissions problem is running the car during cold-start operation, which results in excess emissions from the cold start at low ambient temperatures owing to higher oil viscosity, friction and fuel dosing, which decrease combustion efficiency as shown in the cause and effect diagram (Figure 2-24). These cold-start effects are particularly significant for short journeys as the fraction of cold start within the whole journey is larger [20].

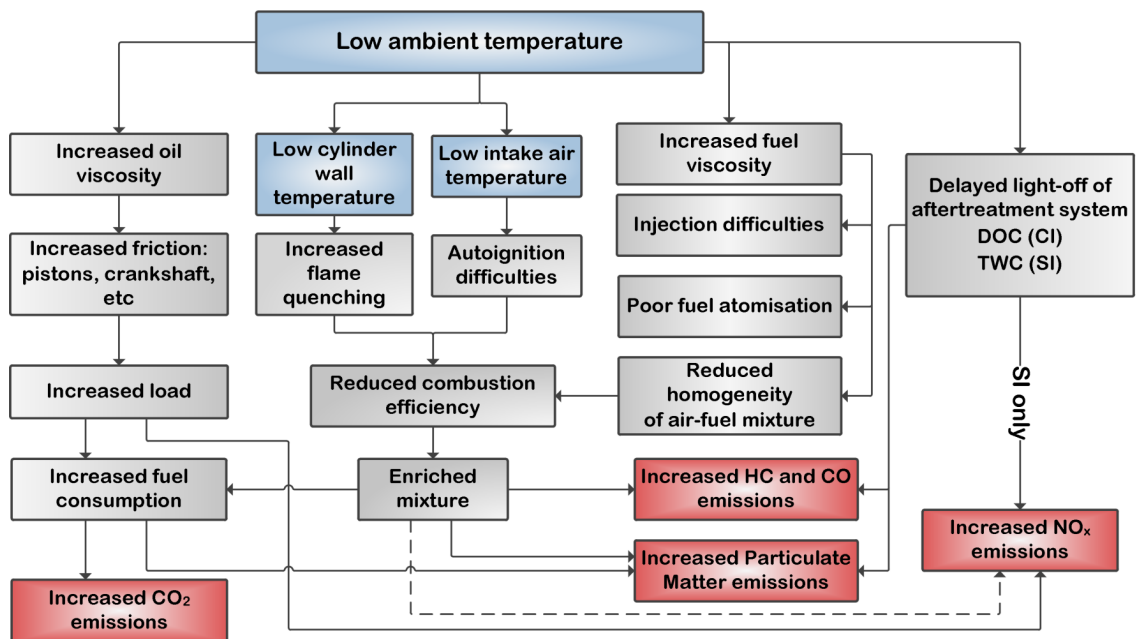


Figure 2-24 Cold starts cause and effect diagram [20].

When a vehicle stopped for several hours, the engine and exhaust system temperatures will be same to ambient temperature. After a start of the engine to begin a journey, the engine and exhaust system temperatures increase until they reach normal operational temperature levels. The coolant temperature is about 70°C to 90°C during normal operation. The exhaust system temperature will be about hundreds centigrade. The emissions amount and fuel consumption during warm up the car (cold start) is higher than normal operational temperature (hot start), especially with gasoline vehicles due to the following reasons:

1. Incomplete combustion: The petrol engine run near stoichiometric during low load and normal operation temperature as air to fuel ratio

in combustion chamber is balanced, which be ideal to complete combustion as all fuel vapor oxidize to form water vapor ( $H_2O$ ) and carbon dioxide ( $CO_2$ ). But during cold start operation (warm up stage) some fuel fraction condense on the cold surface of manifold inlet and cylinder that decrease the fuel amount in combustion chamber so more fuel need to be delivered to avoid misfire during driving, which lead to run the engine with rich mixture result to form more carbon monoxide ( $CO$ ) and unburned hydrocarbons ( $HC$ ).

2. Inefficiency of catalyst: The performance three way catalyst (TWC) in gasoline vehicles decrease during cold start (warm up stage). There are three reaction for three way catalyst (TWC) first one is oxidation of carbon monoxide ( $CO$ ) to form carbon dioxide ( $CO_2$ ). Second reaction is oxidation hydrocarbon ( $HC$ ) to form carbon dioxide ( $CO_2$ ) and water ( $H_2O$ ). Third reaction is reduction of oxides of nitrogen ( $NO_x$ ) to form to nitrogen ( $N_2$ ) and carbon dioxide ( $CO_2$ ). Most efficient reaction occur during running the engine at air to fuel ratio (14.7 parts air to 1 part fuel, by weight) stoichiometric point. The composition of the exhaust gas strongly dependent on mixture in combustion chamber. The mixture during cold start is rich so there is lack of oxygen to oxidize and convert hydrocarbon ( $HC$ ) to form carbon dioxide ( $CO_2$ ) and water ( $H_2O$ ). Also the exhaust gas from engine heat the catalyst convertor until reach about  $300\text{ }^\circ C$  minimum light off temperature in order work adequately as below this temperature the converting of pollutants is minimum.
3. Frictions increase: The fuel consumption during cold start increase due to higher viscosity of engine and transmission oil result to more friction furthermore the rolling friction of tyres is higher during cold start.

In modern cars the three way catalyst mount close to engine exhaust manifold close coupling this will minimize cold start effect [4].

↓ **Ambient temperature** = ↑ **Viscosity** , ↑ **Friction** , ↑ **Fuel dosing**, ↓  
**Combustion efficiency** = ↑ **Emissions** [20]

For SI engines with  $\lambda=1$  operation the temperature for high efficiency operation is 400°C [94] and potentially the cold start problem is greater than for diesels. However, the higher exhaust temperatures for SI  $\lambda =1$  engines makes the warm up period shorter. SI engine vehicles have the majority of their emissions during the cold start and the occurrence of longer cold start periods in real world driving, as shown by the authors [5, 6, 30, 90, 95, 96], leads to higher real world driving cold start emissions. For the same road used in the present work, the authors have published results for a Euro 4 Ford Mondeo for eight cold start journeys [30], which will be compared with the present twenty nine hot start journeys. These cold start tests were in congested traffic and had the time to 400°C at the TWC between 180s and 300s and the distance travelled during the warm-up period was 0.7 – 1.1km. The cold start distance in the test cycles is about 1km [23] but occurs in a shorter time as the time to the first significant acceleration is set by the test cycle, whereas in the real world it is set by the traffic congestion and the location of traffic light junctions. It is the longer time to catalyst light off that is important in real world emissions, as emissions remain close to the raw exhaust port levels during this period. In congested traffic the engine power used will be low and the engine out NO<sub>x</sub> emissions will be low, but the HC and CO emissions will be high.

## **2.10 Real driving emissions (RDE)**

NEDC has been used as a legislated test cycle for emission testing in Europe for more than a decade. However, it has been criticised for a long time, in that it cannot represent the real-world driving conditions. A new driving cycle WLTC (Worldwide light duty test cycle) is being developed. Changing driving cycles from NEDC to WLTC Increased driving cycle length which should be favourable for regulated emissions, since a greater proportion of the cycle is performed with the engine; however, harsh acceleration at high speed makes a challenge for emissions control.

## **2.11 Realistic real world driving emissions tests**

Threatening levels of polluted air are widespread in cities across Europe, mainly in areas close to the road side, leading to 400,000 unnecessarily early deaths yearly and comprising an overall expense of a staggering €1 trillion per year [95]. Although theoretically, air emission limitations have been imposed for cars, vans and trucks, the outdated tests implemented by manufacturers within the car industry have resulted in unsuccessful improvements within practice. It is noteworthy that, on balance, Euro 6 diesel cars can be expected to release seven times their authorised level of nitrogen oxides (NO<sub>x</sub>). To resolve this, the Commission suggested an innovative driving test (RDE) be utilised for new Euro 6 vehicles that would correspond to real life. Following significant contemplation, the initial stage of the process was consented to on 19 May 2015. The second RDE package is currently being considered by the member states, with the significant judgements regarding the timing of the initiation and the severity of the restrictions still to be decided.

The RDE test must finally be introduced in September 2017, having been committed to in 2012. The severity of the restrictions imposed regarding emission levels such as conformity factors must comply as far as possible with the agreed NO<sub>x</sub> measure of 80mg/km. To repair its reputation and to maintain having its cars on polluted European roads, ensuring that emission rates are genuinely diminished is a vital process for diesel to successfully achieve.

## **2.12 The crisis of air pollution in Europe**

Virtually the entireties of the individuals living in the EU have to endure rates of polluted air that the World Health Organisation has declared as being detrimental to health [97]. Roughly 33% of the EU's number live in areas that fail to comply with the less restrictive levels that the EU impose themselves this standard should have been fulfilled as far back as 2010. Resultantly, the European Commission has instigated disciplinary processes towards 18 member states for breaking the EU's regulations regarding particulate matter



(PM) and/or nitrogen dioxide (NO<sub>2</sub>). Due to the significant rate of air pollution, 400,000 individuals die prematurely each year; this is ten times the figure of those who die in traffic accidents. In addition, air pollution is responsible for limiting activity to the extent of 569 million days yearly and also resulting in 100 million working days going astray.

Europe air pollution costs approximately €1,000-2,000 for each individual annually. This is analogous to the entire community of Florence dying each year.

Details emerging indicate that the disturbing health consequences of air pollution are not fully realised as they merely incorporate the repercussions of fine particles and ozone and overlook the effect of NO<sub>2</sub>. Additionally, a research piece undertaken recently by King's College London has measured the other premature deaths not accounted for in London. This process more than doubled the figure from the initial suggestion of 4,300 to a renewed figure of 9,400. One anticipates that this would be equally true of many other major cities [84].

### **2.13 Real world tests**

To guarantee that Euro 6 diesels recorder reduced emissions, the RDE testing process is going to be implemented. This incorporates Portable Emissions Monitoring System (PEMS) to ascertain the level of diesel NO<sub>x</sub> emissions. For the first time, it will measure cars and vans on roads rather than in laboratories and will exploit the greatest quality of technology to measure real emission nowadays.

### **2.14 Car emissions testing facts**

These tests occur on authentic roads and reinforce lab experiments by judging when a car has reduced low pollutant emissions on the road.

RDE tests will determine the pollutants, including NO<sub>x</sub>, emitted by vehicle while they are being operated. RDE will be an addition to current tests,

including NEDC at present and WLTP in future, rather than being a direct replacement for them. RDE will guarantee that cars emit lower emissions on the road. Europe will be the first continent to instigate this method of testing, suggesting that this is a major innovative introduction for car emissions.

## **2.15 RDE test in practice**

In order to conduct the RDE test, a vehicle will be operated on public streets within a broad span of contrasting circumstances. Particular devices attached to the car prototype during the test will be used to corroborate that the regulations regarding limits, including NO<sub>x</sub>, are not breached. A list of conditions is mentioned below:

- A broad range of altitudes
- Temperatures encompassing the whole year
- Additional vehicle payload
- Driving up and down a hill
- Urban roads (reduced speed)
- Rural roads (normal speed)
- Motorways (increased speed)

## **2.16 Equipment needed for RDE test**

- Cars will have PEMS installed so as to measure the release of pollutants whilst it is being operated. This will provide live updates regarding to measurements of emissions released such as NO<sub>x</sub> and GHG.
- The PEMS utilised for controlling releases are very sophisticated devices that incorporate enhanced gas analysers, exhaust mass flow meters, weather station, Global Positioning System (GPS), and these technologies are connected to the vehicle networks.
- All bodies, including the approval authorities, must be encouraged to learn the operation principle of the PEMS system. There is no conventional PEMS equipment, and devices supplied by individual companies show minor differences on the results provided by the equipment. As a result, the

information compiled is scrutinised to verify that the RDE trip boundary conditions were fulfilled and that the extent of pollutants released corresponded to the rates permitted.

## **2.17 Implementation of RDE test**

- The EU has initiated a meticulous process in terms of initiating RDE, dividing the regulations into four individual and distinct 'packages'. Two of these have now been implemented, permitting companies the opportunity to plan for the initiation of this new form of test. Yet the other two packages have not yet been devised and thus the process is currently incomplete. The Commission intends to convey the third package to the relevant parties by October 2016, with the last package scheduled to be presented midway through 2017.
- The RDE test will be introduced in September 2017 for all new forms of car and will be applicable to all vehicles registered by September 2019.


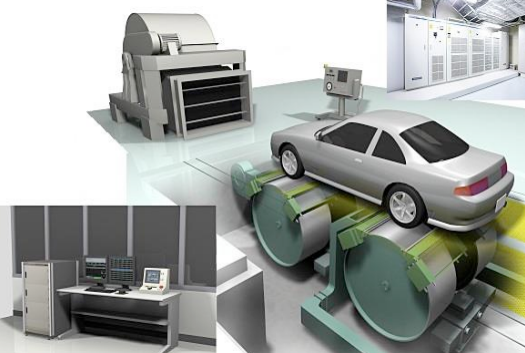
## **2.18 RDE conformity factors**

A conformity factor refers to a 'not to exceed limit' that provides the capacity to consider a range for error in terms of measurements. This occurs precisely because PEMS devices do not provide identical conclusions for every examination. PEMS, for instance, are less accurate than a comprehensive laboratory process and thus it will be more difficult to replicate the results precisely. Realistically, car companies would be well advised to declare their intentions within the design phase significantly below what the regulations permit to guarantee adhering to the legislation [94].

WLTC is more representative of real-world driving than NEDC, but it is not real-world driving. So the Real Driving Emissions (RDE) test procedure using portable emission measuring systems has been introduced and will be implemented in 2017 as a legal requirement for emission testing.(Table 2-6) below compares the WLTP and RDE.

Real world driving use different in driver user, powers, average speeds and different in maximum acceleration rates. Also the real world journeys are different from test cycles with different traffic congestion conditions, road gradients, cold start conditions, numbers of stop/start events and occurs at different ambient temperatures and pressures. All previous parameters will inevitably have different emissions, as all these factors influence the emissions. Thus it is only to be expected that vehicles have different emissions in real world driving than on test cycles [98].

**Table 2-6: comparison between WLTP test cycles and RDE [96].**

	
<b>RDE</b>	<b>WLTP</b>
Limited constant speeds	No constant speed
Variable idling time	Limited idling time
Variable acceleration rates	Variable acceleration rates
<p>Emissions related with real-life conditions, road profile, road surface quality, ambient conditions, traffic congestions and driver's behaviour (eco-driving, neutral ,aggressive) determine final parameters of the test (constant speeds, acceleration rates) and final emission levels.</p> <p>Relatively worse repeatability</p>	<p>Realized on the conditioned chassis test stand, less dependent on external factors.</p> <p>Relatively better repeatability</p>
Ideal flexibility (usage of all gears)	Customized gearshifts – good flexibility
Cold start excluded i.e. hot running real driving emissions	Commences from cold start

## **2.19 RDE implementation and its impact on current technology**

The furore over “Diesel gate” caused significant upheaval within the car industry because of the emission stipulations being breached. World Harmonised Light Vehicle Testing Procedure (WLTP) and Real Driving Emissions (RDE) processes were suggested at the start of 2008 and had not yet been approved by the official bodies. The controversy of the emission case provided the impetus for the theory becoming practice. In September 2016, The United Nations Economic Commission for Europe (UNECE) and World forum for harmonisation of vehicle regulations (WP29) established the WLTP that combines the circumstances of real life with other variables such as higher engine load, contrasting temperatures, increased acceleration and reduced stopping stages. OEMs including BMW, Daimler, PSA, Renault Nissan, VW, and GM played a significant role in finalising the conditions applicable to the test. Subsequent to the WLTP forum meeting, all OEMs will be provided with an outline of the proposed form of WLTP scrutiny and the date from which this is expected to apply. Following the occurrence of the Diesel Gate scandal, RDE were provided enhanced priority in comparison to WLTP. A range of engine techniques, including rightsizing/downsizing, swift transmission system, and a reduced weight, as well as advanced after treatment including selective catalytic reduction (SCR), lean NO<sub>x</sub> traps (LNT), exhaust gas recirculation (EGR), diesel particulate filters (DPF), and gasoline particulate filters (GPF) were granted an increased importance to ensure that the strict legislation was accepted by. The worldwide car industry is presently devising innovative testing processes.

## **2.20 Impact of RDE**

Following the Diesel gate furore, there has been a decline in the adoption of diesel. However, the prospect of diesel being made extinct will not occur as the RDE process will ensure that conventional engines remain within the guidelines identified for emissions. RDE will influence the present powertrain

and hybrid techniques, as the strategies being introduced will have to be integrated so as to ensure that the current rates of emission and high standards are retained. Assuming novel procedures (test cycles) such as those mentioned below (for gasoline and diesel engines), the real driving emissions will enhance their testing time and cost.

## **2.21 RDE testing for gasoline engines**

- Emphasise reduced CO<sub>2</sub>, NO<sub>x</sub>, and PN (particulate number) released at a high load operation and reduced temperature levels.
- Gasoline engine design and combustion processes that fulfil the RDE criteria will be constructed to ensure the optimum emission resoluteness with an emphasis on optimising lambda ( $\lambda$ ) = 1.
- Emission calibration maximisation with an emphasis on forceful and unconventional surrounding circumstances.
- Turbocharging, downsizing and scavenging have to be maximised to fulfil the RDE process.
- Gasoline particulate filters (GPF) three way catalyst provides an impetus for immersion for gasoline direct injection (GDI), incorporating soot loading model and regeneration on-board diagnostics (OBD) process.

## **2.22 RDE testing for diesel engines**

- At higher load of the engine being operated, the decrease of emitted NO<sub>x</sub> will be reduced as there are detrimental consequences to PMs and fuel consumption.
- Exhaust after treatment calibration for a range of different systems, including diesel oxidation catalyst (DOC), lean NO<sub>x</sub> trap (LNT), Selective Catalytic Reduction (SCR), diesel particulate filters (DPF), and SCR on DPF.
- SCR/LNT will benefit adherence to RDE and WLTP, because NO<sub>x</sub> and CO<sub>2</sub> will decline to respective figures of 98% and 100%.

- The DPF progression, coupled with temperature control and soot loading model.
- Consequently, the utilisation of SCR will compel all European diesel engines to adequately conform to RDE/WLTP [34].

The current appalling press coverage regarding RDE shows a lack of understanding of the issue and an industry that has not got its voice across to the public.

The VW issue in the press has been more about vehicles with higher emissions in RDE than on test cycles, which has been the situation since emission regulations came in and were applied equally well to SI engines as diesel.

Whether VW has cheated and made the RDE worse relative to the test cycle is a separate issue, but the RDE would have been higher on the test cycle, irrespective of any RDE calibrations that were different from those on the test cycle. It is my view that congested traffic is a key feature of RDE.

The RDE effect is closely related to longer cold start in RDE and higher acceleration rates and more stop/starts [99].

Legislated test cycles such as the NEDC and FTP75 were not designed to produce data for air quality modelling, but to compare cars A, B, C, and so on, with a reference standard on identical test cycle basis. It is important that the test cycle is representative of real-world driving with cold start, stop/starts, acceleration and deceleration, and transient operation comparable to real-world driving. This is why purely steady state testing ceased to be the only method of emissions testing for heavy duty vehicles in 2000 and was abandoned for fuel economy testing for passenger cars in 1993. However, if the test cycle conditions are well removed from current real-world driving, then there is concern that the emissions on the legislated test cycle may be too low and result in air quality not being improved as intended. This has led to the development of the WLTC test procedures and real-world emissions measurement using portable emissions measurement systems (PEMS) or real driving emissions test procedures (RDE) [31, 32]. compares some key



test parameters between the test cycles and typical RDE data, which are mainly taken from Hausberger et al [31]. Table 2-7 also includes the range of data reported in the present work.

**Table 2-7: Comparison of key parameters in test cycles and in real world driving.**

Test Cycle	NEDC	FTP	JC09	WLTC	RDE [35, 36]	This Work
Mean Vel. kph	33.6	31.5	24.4	46.5	30- 110	5–26
Congest.	30%	34%	49%	3%	0%	90-46%
Max. Acc. m/s <sup>2</sup>	1.0	1.5	1.7	1.7	1.5	2.2–2.8
Dist., km	11	12	8.2	23.3	80-90	5
No. Acc. /km	1.3	1.5	1.5	0.4	~0.2	1.4-7

RDE in congested traffic involves lower speeds, higher accelerations and many more accelerations from idle than on any legislated test cycle WLTC will have lower emissions than NEDC due to higher speeds and proposals for RDE ignore congested driving completely.

Key differences in the WLTC and RDE legislation and the existing NEDC, FTP and JC09 are the higher average speeds and the complete lack of congested driving. The longer distances of the cycles mean that the cold start portion, which lasts about 1km [23] , is a lower proportion of the whole cycle. This means that the cold-start emissions are divided by a longer distance to produce apparently lower emissions, but in fact the same emissions over the first km Liu et al. [23] analysed data for USA vehicle trips with 1851 trips using 292 passenger vehicles driving a total of 25,000km. A total of 50% of the trips were <4km, 25% were 4-8km and only 25% were for distances >8km. This justifies the use of the 5km trip distance in the present work and also shows the unrealistic trip distance in RDE test procedures.

The areas of concern for air quality in Europe are mainly measurement stations in cities by the roadside, and these are all strongly influenced by the emissions from congested traffic. Much of this congested traffic cold starts from a car park into congested traffic, resulting in a longer warm-up period

than on the test cycles, as shown in the present work and in previous work by the authors and others [6, 12, 13, 19-22, 100].

Direct comparison of the NEDC and WLTC was conducted by Marotta et al. [31]. For three Euro 4 and five Euro 5 passenger vehicles, the WLTC had higher  $\text{NO}_x$  emissions, owing to the higher powers used in this test cycle. However, for one Euro 6 vehicle with SCR  $\text{NO}_x$  control, there were the same emissions for the NEDC and WLTC, but these were three times the EURO 6  $\text{NO}_x$  legislated level and had higher  $\text{NO}_x$  than four of the five Euro 5 diesel vehicles. The SCR light off temperature is only a factor for Euro 6 diesel vehicles (there is an equivalent problem for  $\text{NO}_x$  storage catalysts or lean  $\text{NO}_x$  traps, LNTs) as  $\text{deNO}_x$  catalysts were not in widespread use prior to Euro 6. There is the same problem with diesel oxidation catalysts, DOCs, which were used to reduce the volatile fraction of the particulate matter, PM. However, the PM emissions were not as dependent on the oxidation catalyst as  $\text{NO}_x$  is on the  $\text{deNO}_x$  catalyst at Euro 6 emission levels. For Euro 6 passenger cars real world driving studies using prototype RDE journeys SI vehicles had no issues of exceeding the NEDC emissions. However, the exclusion of congested traffic and cold start from this work is the reason why this conclusion is at variance with the present work and previous work by the authors. It will be shown in the present work that it is only at the low average speeds of congested traffic that SI vehicles have gaseous emissions above the NEDC standard and that the real-world emissions will meet the NEDC standard or will even be better than it, if the mean velocity in the real-world congested traffic journey equals that on the NEDC. In the present work, none of the thirty-seven journeys had a mean velocity as high as in the NEDC, but in the Euro 6 SI vehicle tests, none of the journeys had a mean velocity below that in the NEDC. In contrast to the SI Euro 6 vehicle data, the Diesel Euro 6 vehicles on RDE test cycles all showed a problem in exceeding the NEDC  $\text{NO}_x$  emissions [34, 92]. This was a problem with SCR  $\text{NO}_x$  control at high powers and low catalytic efficiency at low exhaust temperatures and low power conditions [34, 92, 98].

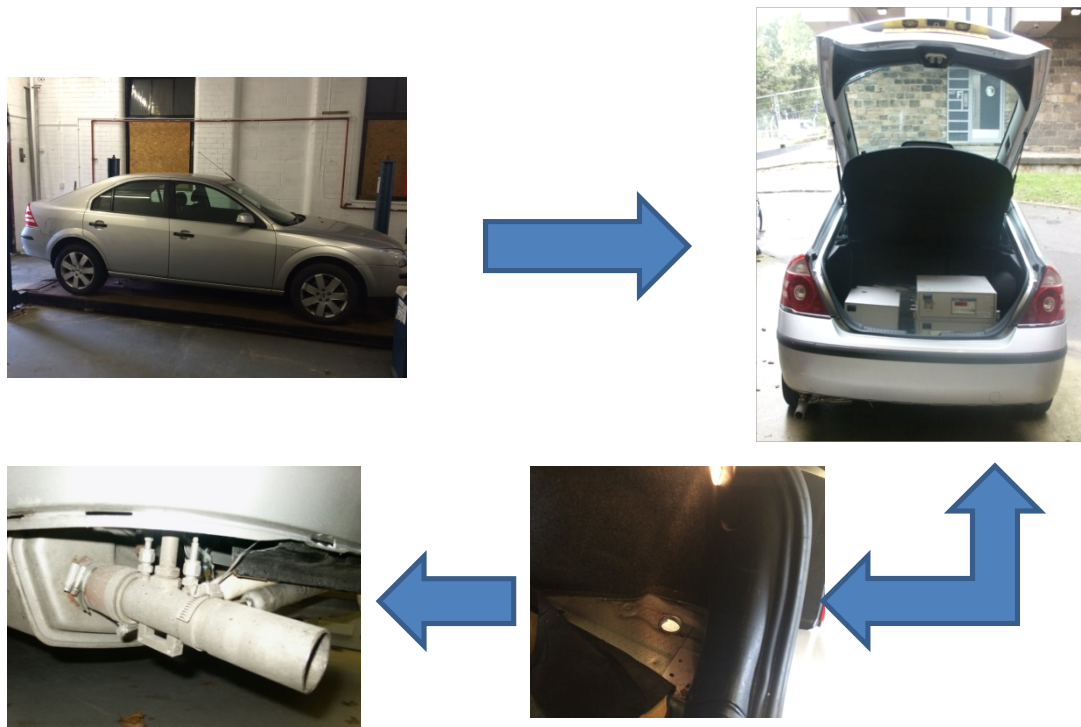
## **3 Chapter Three: Research methodologies**

### **3.1 Introduction**

This thesis aims to measure and analyse exhaust emissions under realistic urban driving conditions using a set of in-vehicle FTIR emission measurement systems capable of measuring 51 emission components simultaneously at a rate of 0.5 Hz. However, the objective for this research is to develop further understanding of the processes involved in exhaust emissions measurements, particularly nitrogen compounds, and also how driving parameters such as velocity and acceleration influence fuel consumption and volatile emissions. Additionally, online emission measuring techniques and sampling at the exhaust which have been employed in this research are described in this chapter.

### **3.2 Experimental test car and thermal measurements**

A EURO4 emission compliant Ford Mondeo manual transmission petrol car was used, which was fitted with a port fuel injected 1.8 litre 16V spark ignition engine with 4 cylinders and 16 valves. The odometer reading on the car was 4,400 miles prior to the tests. The vehicle was equipped with a Three-Way Catalyst (TWC). The curb weight of the car is 1374 kg. The car was instrumented with three thermocouples, which measured the temperature of the lubricating oil in the sump, and also exhaust gas temperatures upstream and downstream of the TWC. All temperatures were measured using a grounded junction mineral insulated Type K thermocouples with a response time of  $\sim 0.25$  ms. see (Figure 3-1).



**Figure 3-1 Scheme of the measurement system integration in a probe car Ford Mondeo.**

### **3.3 Measurements of fuel flow, air/fuel ratio and GPS**

#### **3.3.1 Fuel consumption measurement**

A MAX710 fuel flow measurement system was employed to measure realistic fuel consumption which intercepted the vehicle fuel system and was connected with the fuel tank and engine. This measured the fuel mass flow rate by using a level controlled recirculation tank, a transfer pump and a high-resolution flow meter. The pump maintained a constant pressure to the recirculation tank that fed fuel to the engine. This recirculation tank collected return fuel from the engine and recirculated this fuel back to the engine instead of returning it to the fuel tank. This recirculation loop allowed the use of a single meter to measure make-up fuel as it replaced the fuel consumed by the engine. Total fuel consumption was determined to be better than 1% accuracy. The rate of fuel consumption was determined at a 1-second

resolution. The device had an analogue output, which was logged into the second laptop computer. Commercially available standard ultra-low sulphur RON95 petrol fuel was used throughout the tests.

### **3.3.2 Air/fuel ratio**

The air/fuel ratio was measured using a Horiba “Lambda Checker LD-700” in terms of lambda with a response time of 0.08 ~ 0.15 seconds. The LD-700 was connected to an NTK brand wide-band oxygen sensor (ZrO<sub>2</sub> type), which was inserted into the exhaust gas upstream of the TWC. The unit is calibrated for a fuel with a hydrogen/carbon ratio of 1.85 and an oxygen/carbon ratio of 0. The accuracy of the unit is  $\pm 0.04\lambda$  for  $0.91 \sim 1.19 \lambda$  and  $\pm 0.08 \lambda$  outside this range. The LD-700 had a DC output of 0-5 volts, which was directly proportional to lambda. The DC voltage output was logged into a data logger and then into a laptop.

### **3.3.3 Exhaust flow measurement using OBS**

The vehicle was instrumented with the Data Integration Unit (DIU) component of a Horiba on Board Emissions Measurement System (OBS 1300). This measures the exhaust mass flow rate together with  $\lambda$  and enables the mass emissions to be computed from the volumetric measurements. The DIU comprises a zirconia type NO<sub>x</sub> and Air/Fuel ratio analyser (NO<sub>x</sub>/A/F), and an Annubar (modified Pitot style) flow meter, additional in the vehicle and ambient air monitoring, data logger (laptop) and software, global positioning system (GPS) and power supply unit. All exhaust monitoring was conducted via a purpose-built exhaust attachment fitted to the end of the vehicle exhaust pipe. NO<sub>x</sub> concentrations and A/F were measured by an NO<sub>x</sub> A/F probe. Exhaust flow rate was measured by Annubar. Exhaust temperature was monitored by thermocouple probe. All of these were mounted on the exhaust attachment. Exhaust pressure was measured by an open-line connection and a DIU mounted pressure sensor.

Vehicle speed and engine revolutions were also logged from external (vehicle) inputs. In addition, ambient conditions (local temperature, pressure and humidity) were monitored using dedicated vehicle mounted sensors. For further details of this system, see the development work of Nakamura et al. [101] In this research the OBS 1300 was used only for exhaust mass flow rate. The other OBS1300 data is not reported in this study.

### **3.3.4 Geographical positioning system (GPS)**

A Racelogic VBOX II differential GPS system was used to provide geographical position, speed and acceleration data. The VBOX II is a GPS data-logging system developed by Racelogic specifically for automotive applications. It is normally used for race track testing and other performance testing where accurate speed, position and acceleration data is required for driver performance evaluation. Data was logged at 1 Hz and stored on a compact flash memory card, and subsequently transferred to a PC. The analogue output from the VBOX II was a 0-5V DC signal corresponding to road speed, and was fed to the data logger and then to a laptop.

## **3.4 Emission measurements system (EMS)**

### **3.4.1 Fourier transform infrared spectroscopy FTIR**

A portable Fourier Transform Infrared (FTIR) spectrometer was used to measure on road realistic emissions. The model used was the Temet Gasmet CR 2000 which was capable of measuring concentrations as low as 0.5~3 ppm, depending on the species and applications. It has been specifically calibrated by the manufacturer to an accuracy of 2% within the calibrated measurement range, which was 20,000 ppm for CO, 30% for CO<sub>2</sub> and 7000 ppm for NO<sub>x</sub> respectively.

An FTIR emission measurement system was selected because of its ability to speciate VOC, NO/NO<sub>2</sub>/N<sub>2</sub>O and measure ammonia, in addition to CO, NO<sub>x</sub>, and THC emissions. The FTIR measurement for regulated emissions was

calibrated against standard CVS measurement by authors using a chassis dynamometer facility and various driving cycles. It was discovered that the FTIR measurement had excellent agreement (2% deviation) with the CVS measurement for CO<sub>2</sub> emissions. The N<sub>2</sub>O and CH<sub>4</sub> were checked in the laboratory using bottled gases and also found good.

The Temet instrument comprised a FTIR analyser, a portable sample handling unit (filtering and controlling sample flow), heated sample lines and a laptop. The system weighed approximately 30 kg. The entire on-board measurement instrumentation including the FTIR system, the fuel consumption measurement system, two batteries and a DC-AC converter weighed approximately 150 kg.

The software of the FTIR system has the additional capability of accepting analogue inputs, which can be logged, together with the emissions' spectra and the analysis data. One of these analogue input channels was employed to log one or two external analogue signals for time alignment between the FTIR laptop and the second laptop. The voltage output from the VBox was used as the external signal and exported to two laptops; one for the FTIR that logs emission spectra and external analogue signals, and the other for temperature measurement and fuel meter logging. The throttle position and VBox Voltage output were used for time alignment between the two laptops as both signals were sent to these laptops. As shown in (Figure 3-2)

### **3.4.2 Power for instruments**

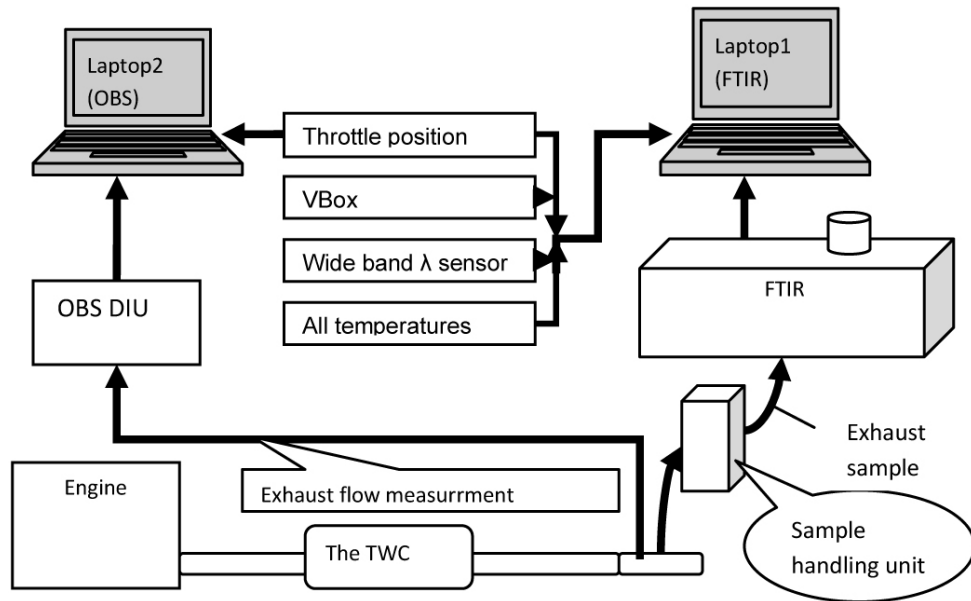
The power needed for the on-board measuring system was around 1200 watts and this would have necessitated drawing up to 100 A at 12V from the car's electrical system. This would have required an upgraded alternator and would have increased the load on the engine, consequently affecting the emissions characteristics. Another possibility was to use a small dedicated generator, but this option is only feasible in large heavy duty vehicles. Therefore, a dedicated power supply, two 12V battery packs and an on-board DC-AC converter, were employed to provide the 240V AC necessary for instrument

operation. The two batteries used weighed a total of 70 kg. They provided approximately 2-3 hours of operation before needing to be recharged.

### **3.4.3 Sample conditioning**

In order to measure wet concentration, the raw undiluted sample gas extracted from the exhaust system had to be maintained at about 180°C, otherwise low boiling point pollutants would drop out due to condensation. Furthermore, the extracted exhaust sample had to be hot-filtered so that the sample cell remained free of particulates which would contaminate it and shorten its lifetime. A sample handling unit was acquired to perform these functions. The sample handling unit uses a pump to extract sample continuously from the vehicle's exhaust system at a constant flow rate (2~3 l/min) via a heated line. This is then filtered using a 0.2 µm filter and introduced via another heated line into the sample cell of the FTIR. Both heated lines were maintained to 180°C by the sample handling unit. The sample handling unit consumed the greatest quantity of power since it performed heating and pumping functions. It was installed in the boot of the car along with the FTIR, as shown in (Figure 3-2). The gas sample was taken downstream of the catalyst, and the heated sample line was passed through a small hole in the car's floor pan. There was no possibility of dilution of the sample by pressure pulsations from the tailpipe.





**Figure 3-2 Schematic diagram of sampling and data logging system.**

### **3.5 Mass emission and VSP calculations**

#### **3.5.1 Mass emission calculation**

The FTIR emission measurements were on a volumetric basis and were converted into a mass basis using the conventional method for the computation of emissions index (EI: g/kg fuel).

Where:

$$EI = 1000 * K * C * (1 + A/F) \text{ g/kg fuel} \quad (3-1)$$

K is a conversion coefficient, which is the ratio of the molecular weight of a certain emission component to the molecular weight of the whole sample gas. The molecular weight of the exhaust sample gas is close to that of air and does not vary within more than 1% for H/C ratios of about 2 (i.e. gasoline), irrespective of the air/fuel ratio. For this reason, K is treated here as a constant.

C is concentration of the component. If this is measured in ppm or % then the equation has to be multiplied by  $10^6$  and  $10^2$  respectively.

A/F is the air/fuel ratio on a mass basis measured by a lambda sensor.

The EI was then converted into mass emission rate g/s using fuel consumption measured for the sampling period. Then the distance based emissions can be calculated for any distance travelled.

### 3.5.2 Vehicle specific power (VSP)

The generic VSP estimation equation was applied with the typical coefficient values for a light-duty vehicle as shown in Equation (3-2).

$$\text{VSP} = v \cdot (1.1 \cdot a + 9.81 \cdot \sin(\text{atan}(\text{grade})) + 0.132) + 0.000302 \cdot (v)^3 \quad (3-2)$$

Where:

v is a vehicle speed (m/s)

a is vehicle acceleration ( $\text{m/s}^2$ )

grade is road grade, = vertical rise/horizontal distance (dimensionless)

VSP is defined as the instantaneous power per unit mass of the vehicle, with units of kilowatts per tonne (kW/tonne).

V= speed,  $1.1 \cdot a$  = acceleration,  $9.81 \cdot \sin(\text{atan}(\text{grade}))$  = road grade, 0.132 rolling resistance coefficient and  $0.000302 \cdot (v)^3$  drag coefficient.

VSP represents the power required from the engine to move a vehicle to overcome the aerodynamic drag, rolling resistance and the road grade effect.

### 3.6 Test and routes

The strategies adopted in this work during emission measurement are described using the test route and procedures 1-3.

#### (A) Journeys

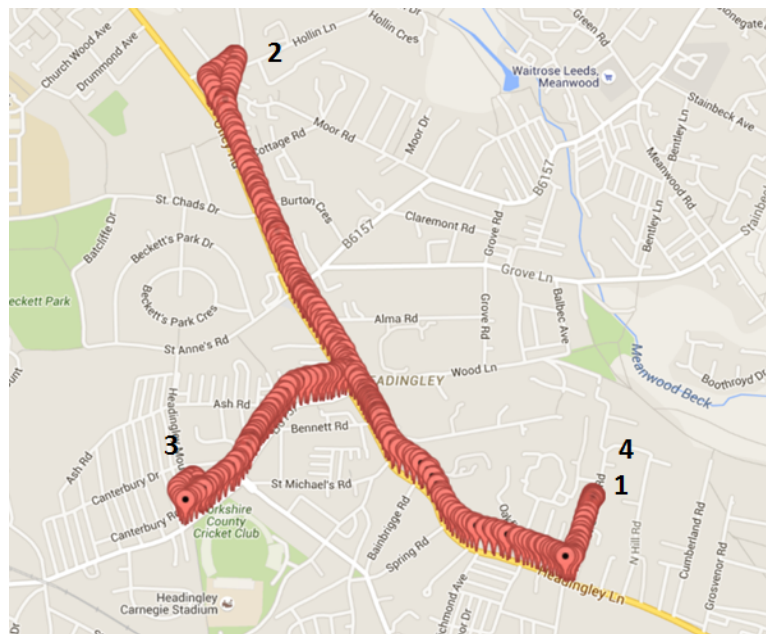
#### (A) Distance = 4.9 Km

#### 1-North Grange Road 2-Three Horses 3-Headingley Ave 4-North Grange Road.

- 1) Day 1\_EURO4\_1925\_A
- 2) Day 2\_EURO4\_1213\_A
- 3) Day 2\_EURO4\_1256\_A
- 4) Day 2\_EURO4\_1334\_A
- 5) Day 2\_EURO4\_1704\_A\_HL

- 6) Day 3\_EURO4\_0746\_A
- 7) Day 3\_EURO4\_0830\_A
- 8) Day 3\_EURO4\_1215\_A
- 9) Day 3\_EURO4\_1256\_A2
- 10) Day 4\_EURO4\_0753\_A
- 11) Day 4\_EURO4\_0852\_A
- 12) Day 5\_EURO4\_1222\_A
- 13) Day 5\_EURO4\_1311\_A\_HL
- 14) Day 5\_EURO4\_1701\_A

The journey (A) map shown in (Figure 3-3)



**Figure 3-3 Journey (A) map 1-2-3-4.**

**(B) Journeys**

**(B) Distance = 4.9 Km**

**1-North Grange Road 3-Headingley Ave 2- Three Horses 4- North Grange Road**

- 1) Day 1\_EURO4\_1908\_B
- 2) Day 1\_EURO4\_1941\_B
- 3) Day 2\_EURO4\_1234\_B
- 4) Day 2\_EURO4\_1316\_B
- 5) Day 2\_EURO4\_1740\_B

- 6) Day 3\_EURO4\_0807\_B
- 7) Day 3\_EURO4\_0853\_B
- 8) Day 3\_EURO4\_1235\_B
- 9) Day 3\_EURO4\_1318\_B
- 10) Day 4\_EURO4\_0825\_B\_HL
- 11) Day 5\_EURO4\_1247\_B\_HL
- 12) Day 5\_EURO4\_1337\_B
- 13) Day 5\_EURO4\_1734\_B
- 14) Day 6\_EURO4\_0849\_B\_HL
- 15) Day 6\_EURO4\_0913\_B\_HL

The journey (B) map shown (Figure 3-4)

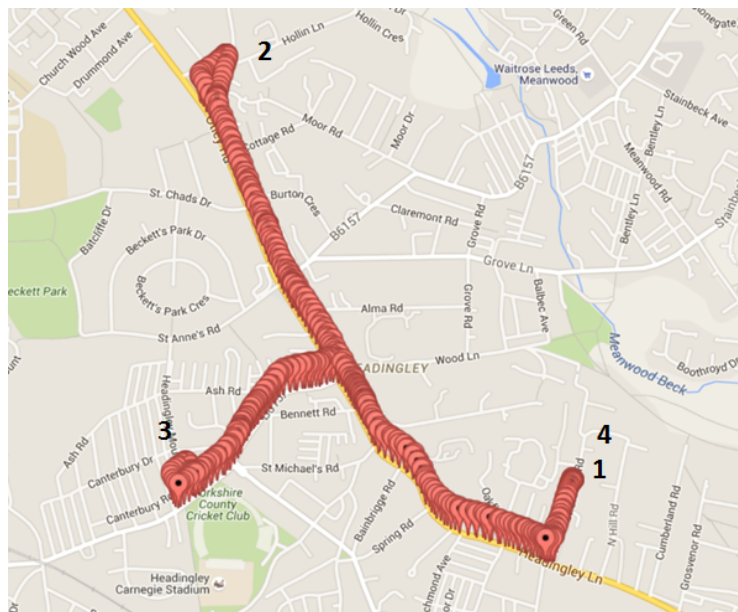


Figure 3-4 Journey (B) map 1-3-2-4.

**Cold Start Journeys (CSR) Journeys:**

**(CSR1) Distance = 5.4 Km**

**1-Lodge street 2-Three Horses 3-North Grange Road**

- 1) Day 1\_EURO4\_1850\_CSR1

**(CSR2) Distance = 6.6 Km**

**1- Lodge street 2-Headingley Ave 3- Three Horses 4- North Grange Road**

- 1) Day 2\_EURO4\_1150\_CSR2

- 2) Day 3\_EURO4\_0722\_CSR2

- 3) Day 3\_EURO4\_1153\_CSR2
- 4) Day 5\_EURO4\_1157\_CSR2
- 5) Day 5\_EURO4\_1624\_CSR2

**(CSR3) Distance = 4.65Km**

**1-Lodge Street 2-Headingley Ave 3-(opposite Three Horses)**

- 1) Day 2\_EURO4\_1620\_CSR3

**(CSR3s) Distance = 4.38 Km**

**1-Lodge Street 2-Headingley Ave 3-St. Chad's Drive**

- 1) Day 4\_EURO4\_1620\_CSR3s

### **3.6.1 Test route procedure 1**

Two urban driving cycles were designed to undertake emission tests as follows: Headingley route A and route B, hereafter referred to as route A and B (Figure 3-3) and (Figure 3-4) show the maps of the routes. Headingley is a dense residential area in Leeds and features as a typical urban road network, i.e. carrying numerous city social-economy activities and is also one of the main transportation carriers.

The test trips started from point 1 in (Figure 3-5), a side road, enabling the preparation of instruments and then turned right to join one of the city's major roads, the A660. The probe vehicle passed a pedestrian crossing and travelled towards point 2, where routes A and route B differed. (Figure 3-6) shows the different movement at point 2 for the two routes. For route A, the vehicle went directly through the junction and travelled to point 3 and then took a U-turn moving back towards point 2. At the junction, the vehicle took a right turn and moved towards point 4 and then took the second U-turn travelling back to point 2. The vehicle turned right at point 2 back to the A660 and travelled back to point 1. For route B, the vehicle coming from point 1 took a left turn at point 2 and travelled up to point 4 and then took a U-turn moving back to point 2. The vehicle turned left at point 2 and continued to travel to point 3, where a U-turn was taken and the vehicle travelled back to point 2

along the A660. The vehicle was then travelled directly across the junction at point 2 and moved back to point 1.

There are four pedestrian crossings and three sets of junction traffic lights in this urban road network. Although the testing routes were return trips, they did not pass all these crossing and traffic lights. The topography of the road is not flat and thus uphill and downhill travels are experienced. The real time elevations of the probe vehicle were logged by on-board GPS system and were validated by the ordnance map and the final corrected elevation data were plotted in all the diagrams.

The distance travelled for each trip is ~5 km and the speed limit on these urban streets is 48 km/h (30 mph)

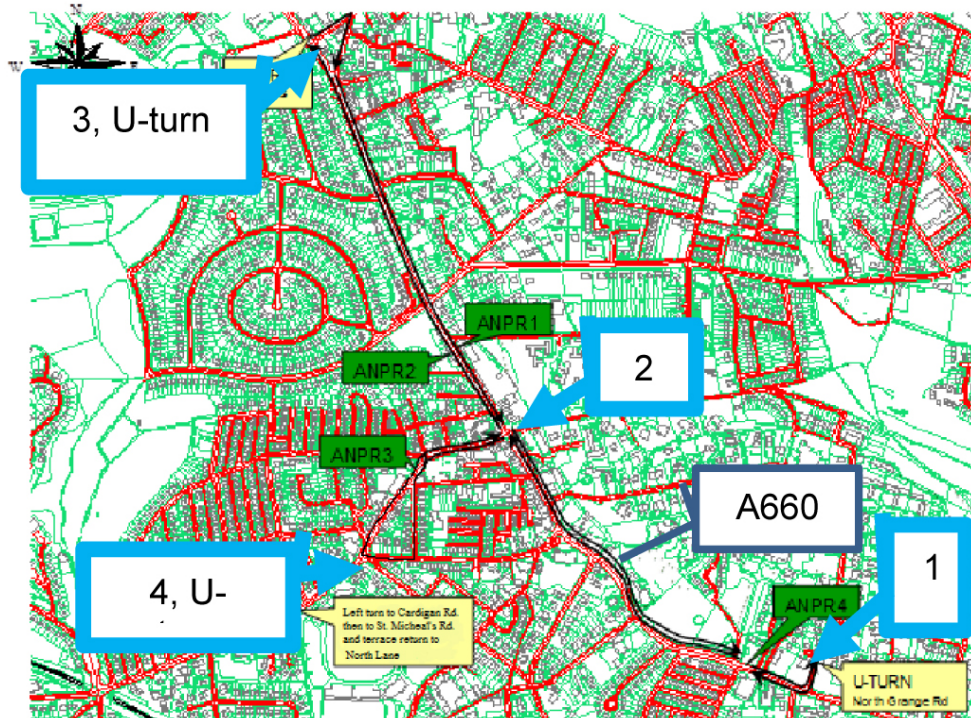


Figure 3-5 Map and notations of driving routes.



**Figure 3-6 Different manoeuvre at point 2 for route A (left) and B (right).**

Additionally, shows (Table 3-1) the list of file names and the starting and ending times of the eight testing trips. The file names are based on the estimated trip starting time, but the actual starting time was slightly later than the planned time.

**Table 3-1 Start and end time of all the testing trips**

Trip name	Start time	End time
Day 1_EURO4_1925_A	19:26	19:39
Day 1_EURO4_1941_B	19:42	19:55
Day 2_EURO4_1256_A	12:57	13:13
Day 2_EURO4_1316_B	13:17	13:31
Day 3_EURO4_0746_A	07:47	08:03
Day 3_EURO4_0807_B	08:07	08:26
Day 3_EURO4_0830_A	08:30	08:51
Day 3_EURO4_0853_B	08:53	09:13

### 3.6.2 Test route and procedure 2

An urban road network located in the Headingley area of Leeds city was designed to carry out emission tests as shown in (Figure 3-7). Headingley is a dense residential area in Leeds and features as a typical urban road network, i.e. carrying numerous city social-economy activities and is one of the main transportation carriers. Four different cycles were conducted: CSR1, CSR2, CSR3 and CSR3s. All the trips started from point 1, travelling uphill towards point 2 where the road becomes relatively flat. The trips continued towards point 3 with some uphill and downhill sections, and from point 3 the trips took different routes as shown in (Table 3-2).

**Table 3-2 Directions of different driving routes**

Driving cycle (route)	Direction
CSR1	1-2-3-5-6
CSR2	1-2-3-4-5-6
CSR3	1-2-3-4-3-5
CSR3s	1-2-3-4-3

Table 3-3 listed the file names and the starting and ending time of the eight testing trips. The file names are based on the estimated trip starting time but the actual starting time was slightly later than the planned time. The vehicle's travel profiles, fuel consumption, VSP and emissions for all these eight journeys were analysed for journey average. Two journeys were selected for detailed analysis (Day 2\_EURO4\_1150\_CSR2 and Day 5\_EURO4\_1624\_CSR2) and are presented. One was a congested journey with a longer journey time and the other one was much less congested with a much shorter journey time. Both took the same route.





**Figure 3-7 Map and notations of driving route.**

Trip name	Start time	End time
Day 1_EURO4_1850_CSR1	18:51:42	19:04:26
Day 2_EURO4_1150_CSR2	11:52:09	12:09:49
Day 3_EURO4_0722_CSR2	07:24:31	07:43:30
Day 3_EURO4_1153_CSR2	11:53:38	12:12:47
Day 5_EURO4_1157_CSR2	11:58:47	12:19:06
Day 5_EURO4_1624_CSR2	16:25:22	16:59:03
Day 2_EURO4_1620_CSR3	16:20:51	16:52:49
Day 4_EURO4_1620_CR3s	16:21:21	16:42:39

**Table 3-3 Start and end time of all the testing trips.**

### 3.6.3 Elevation calculation

One of greatest problems that was encountered was finding elevation, particularly in the case of journeys of about five kilometres or more, as with such journeys there are much data for longitude and latitude, some of which are about one thousand points. It is a major problem in going on the Internet

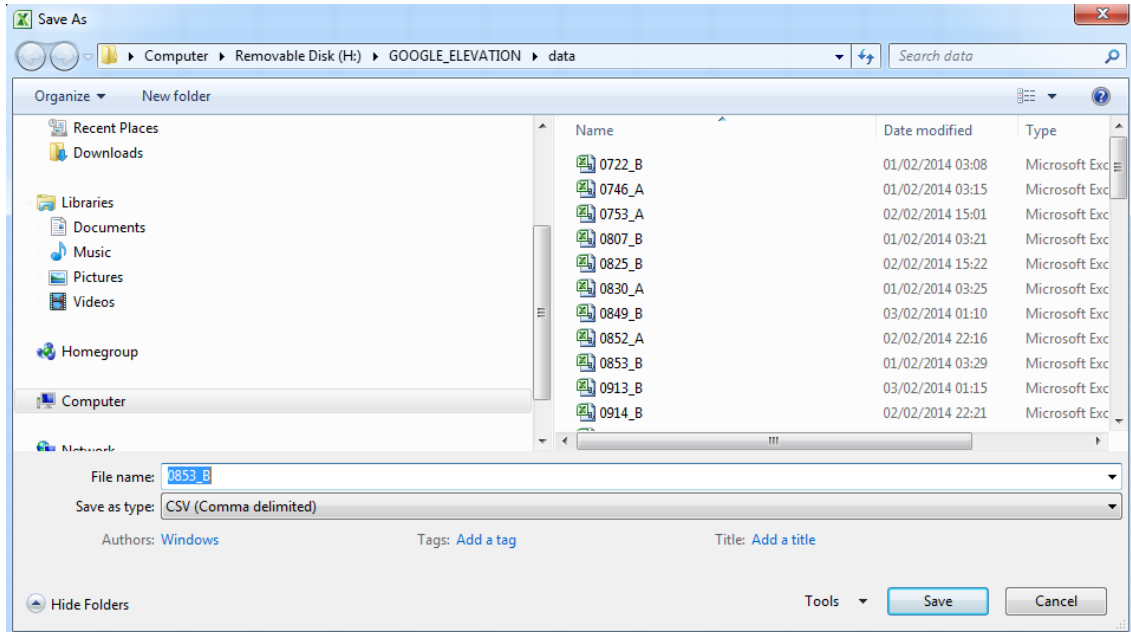
and inputting every single item of longitude and latitude data in order to find the elevation. Following much research, I found a solution to this problem by using a package of software for Google elevation. To find the elevation, there are many steps which must be followed.

Firstly, open the excel sheet and paste all longitude data for whole journey in column (A) then paste all longitude data for whole journey in column (B) and after that put : (colon) in column (C) next to the latitude column as shown in (Figure 3-8).

	A	B	C	D	E	F	G	H
1	3229.1	94.10511	:					
2	3229.1	94.10515	:					
3	3229.098	94.10706	:					
4	3229.093	94.11103	:					
5	3229.088	94.11119	:					
6	3229.081	94.11498	:					
7	3229.073	94.11851	:					
8	3229.065	94.12196	:					
9	3229.057	94.12552	:					
10	3229.053	94.12743	:					
11	3229.046	94.13077	:					
12	3229.039	94.13351	:					
13	3229.032	94.13575	:					
14	3229.026	94.13734	:					
15	3229.02	94.13976	:					
16	3229.019	94.14107	:					
17	3229.017	94.14299	:					
18	3229.015	94.14484	:					
19	3229.014	94.14542	:					
20	3229.014	94.14611	:					
21	3229.013	94.14668	:					
22	3229.013	94.14711	:					
23	3229.013	94.14735	:					
24	3229.013	94.14746	:					
25	3229.013	94.14746	:					
26	3229.013	94.14738	:					
27	3229.013	94.14733	:					
28	3229.013	94.14734	:					
29	3229.013	94.14734	:					
30	3229.013	94.14737	:					
31	3229.012	94.14846	:					
32	3229.01	94.15612	:					
33	3229.013	94.1697	:					
34	3229.017	94.1845	:					

**Figure 3-8 Longitude and latitude data in excel sheet.**

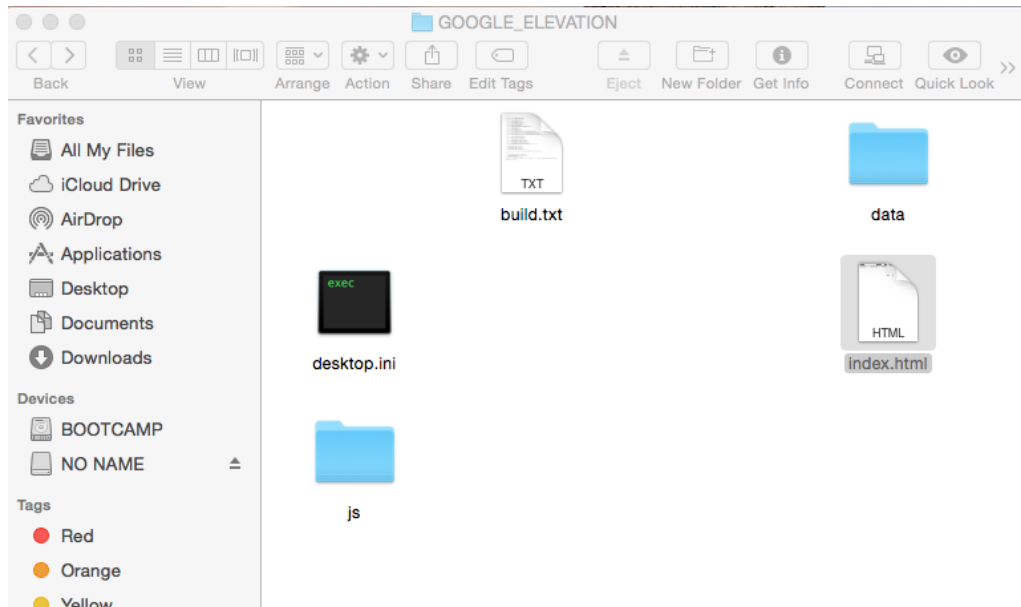
then save it as file name (journey name) and save as type CSV. (Comma delimited), must be save the file in data folder in google elevation folder as shown in (Figure 3-9).



**Figure 3-9 Saving file system in Google elevation.**

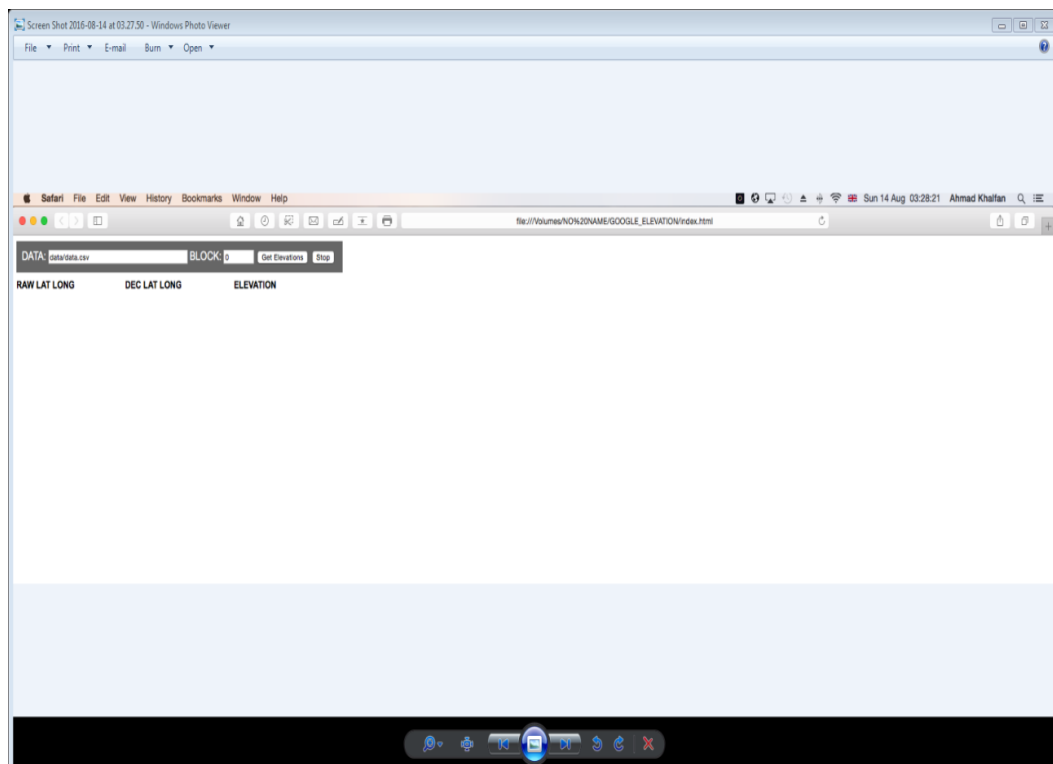
The next step finding the elevation of journey, which cannot be found by a Windows computer (Window PC) as the Google software package does not work in a Windows computer, so for this reason a MAC computer must be used to run the Google software package for finding the elevation of journey.

Open , on MAC computer, the Google elevation folder software as shown in (Figure 3-10).



**Figure 3-10 Finding the elevation of journey on MAC computers.**

Then open index.html it take you on Google elevation site as shown in (Figure 3-11).



**Figure 3-11 Index file in Google elevation.**

After that put the saved journey name in the data folder, for example data/0853\_B.csv as shown in (Figure 3-12).

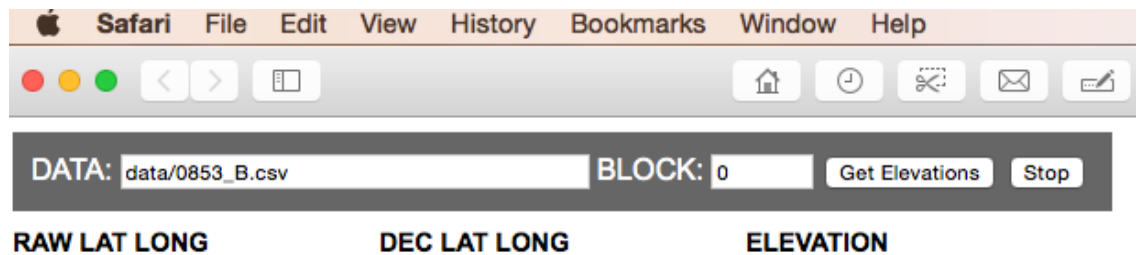


Figure 3-12 Data and name of the journey to find elevation.

Then click on ‘get elevation’ and it will give all the elevations data according to latitude and longitude as shown in (Figure 3-13).

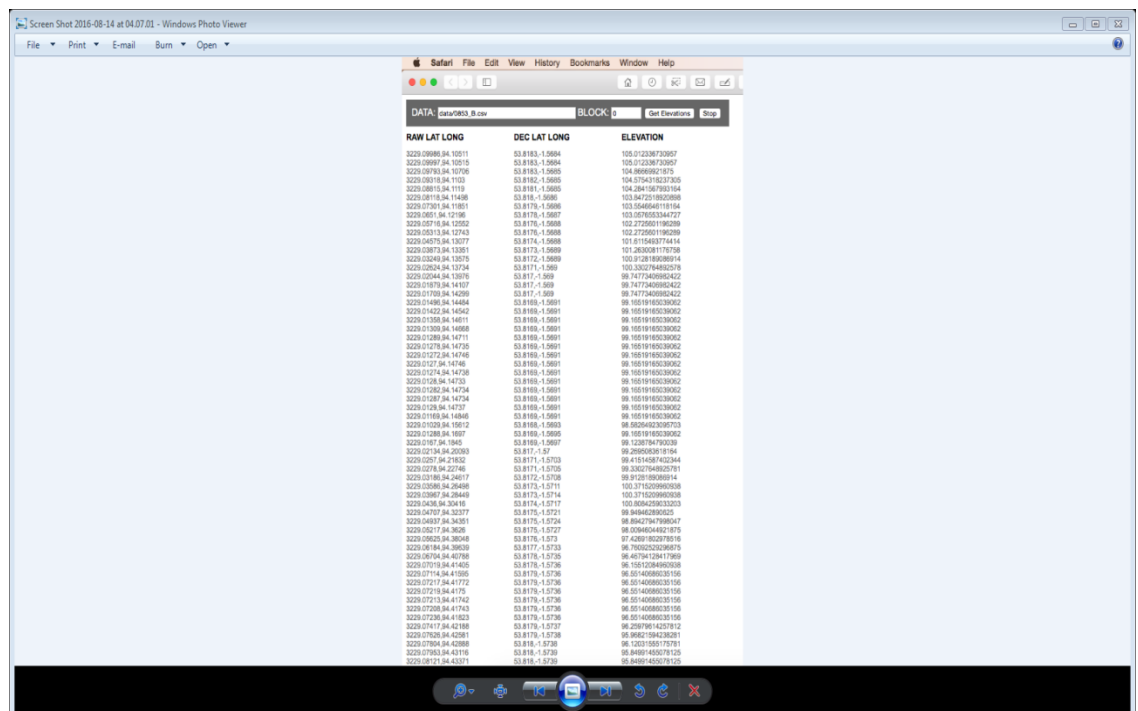


Figure 3-13 Elevations data according to latitude and longitude.

### 3.6.4 Journeys route finder and drawing

To find the routes of the journeys, we must change the units of the latitude and longitude from minute form to decimal degree form, so we divide the

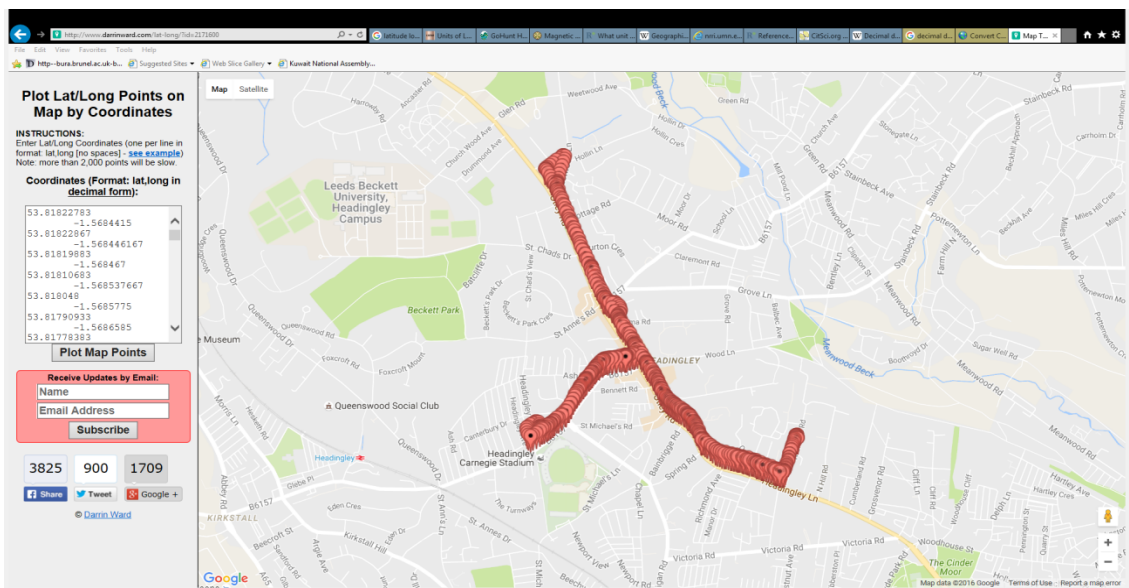
latitude by 60 and the longitude by -60 in the excel sheet for all the latitude and longitude data during whole journey as shown in (Figure 3-14).

	A	B	C	D
1	Latitude(minute)	Longitude(minute)	Latitude(decimal degree)	Longitude(decimal degree)
2	3229.09986	94.10511	53.818331	-1.5684185
3	3229.09997	94.10515	53.81833283	-1.568419167
4	3229.09793	94.10706	53.81829883	-1.568451
5	3229.09318	94.1103	53.81821967	-1.568505
6	3229.08815	94.1119	53.81813583	-1.568531667
7	3229.08118	94.11498	53.81801967	-1.568583
8	3229.07301	94.11851	53.8178835	-1.568641833
9	3229.0651	94.12196	53.81775167	-1.568699333
10	3229.05716	94.12552	53.81761933	-1.568758667
11	3229.05313	94.12743	53.81755217	-1.5687905
12	3229.04575	94.13077	53.81742917	-1.568846167
13	3229.03873	94.13351	53.81731217	-1.568891833
14	3229.03249	94.13575	53.81720817	-1.568929167
15	3229.02624	94.13734	53.817104	-1.568955667

**Figure 3-14 Excel sheet show the longitude and latitude conversion.**

Then open the link <http://www.darrinward.com/lat-long/> and paste the latitude and longitude values in decimal degree from C and D in excel sheet into the darrinward.

site in the square below\_Coordinates (Format: lat, long in decimal form): then click on plot map point and will draw whole the journey as shown in (Figure 3-15).



**Figure 3-15 Journey route on map.**

If required any single point during the journey just enter the value of latitude and longitude and it will show directly the pace position on map as shown in (Figure 3-16).

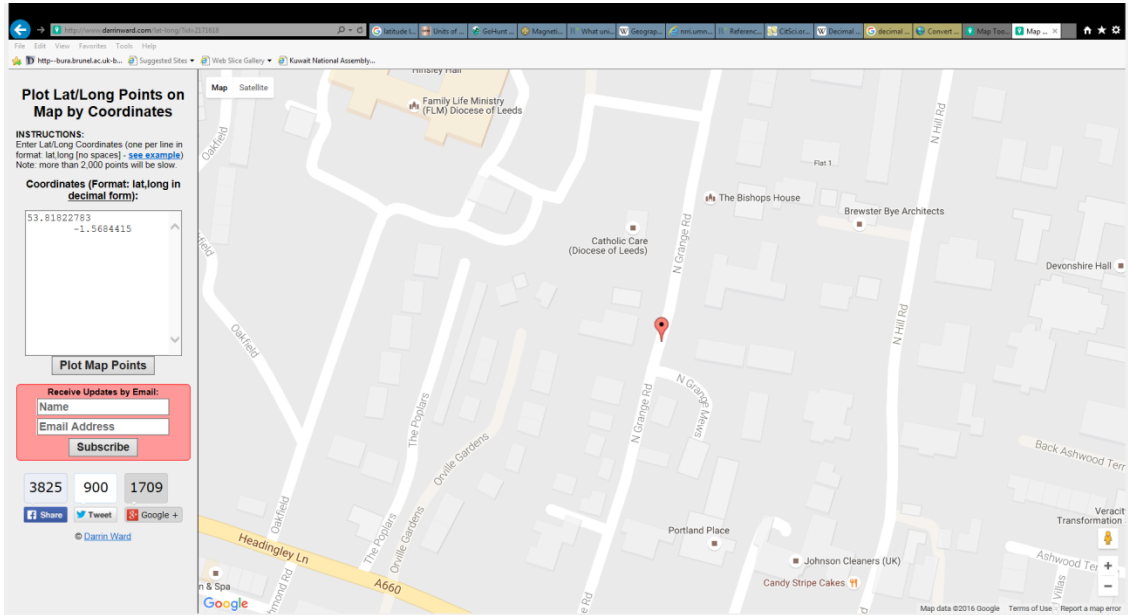


Figure 3-16 Single point of journey on map.

## **4 Chapter Four: Traffic flow analysis, determination of GHG emissions, fuel consumption and thermal efficiency**

### **4.1 Introduction**

Present-day methods designed for evaluating exhaust emissions from road transport vehicles, were mainly based on measurements from rolling road, and also constant volume sampling facilities using standard drive cycles. Emissions are characteristically well-defined as a function of average speed or distance for the complete cycle. In addition, the average values from standard cycles are subsequently used to estimate transport emissions [18]. However, numerous investigations demonstrated that many other parameters such as vehicle operating conditions, traffic conditions (such as free-flowing, congested), ambient temperatures, fuel compositions, topography and road geometry strongly influence realistic emissions [6, 8, 9, 14, 18, 24, 102-105].

Lenaers, 2009, [28] examined fuel consumption and tailpipe CO<sub>2</sub> emissions from four family cars, including gasoline, diesel and hybrid cars driving on various roads such as urban, rural and motorway routes. The results have shown that fuel consumption and CO<sub>2</sub> emissions were higher on urban roads than on rural and motorway routes. Fonseca, et al, 2011., [106] measured CO<sub>2</sub> emissions using two diesel vehicles in two urban driving circuits with one of the vehicles equipped with a fuel cut-off system at stoppage. Their results showed up to 20% reductions in CO<sub>2</sub> for the vehicle with the fuel cut-off system compared to the one without the fuel cut-off system due to zero idling emissions. This is consistent with the results in this research which have shown that idle fuel consumption could account for 12~24% of total fuel consumption. Additionally, Barth and Boriboonsomsin, 2008, [29] investigated the impacts of traffic congestion on CO<sub>2</sub> emissions in Southern California and found that CO<sub>2</sub> can be reduced up to ~20% via three strategies: congestion mitigation that reduces severe congestion allowing free-flowing traffic; speed management techniques to reduce excessively high speeds to more moderate conditions; and shock wave suppression techniques to eliminate acceleration and deceleration events which are associated with the stop/start events during congested traffic. Figliozzi, (2011, [27]) examined CO<sub>2</sub>



emissions from commercial freight vehicles for different levels of overcrowding and presented a significant impact of congestion or speed limits on commercial vehicle emissions but admitted that this is difficult to predict. The research concluded that the public agencies and highway operators must carefully consider the implications of transport policies such as travel speed limits on CO<sub>2</sub> emissions and fuel economy. The study also recommended that if the speed is set to optimal, CO<sub>2</sub> emissions can be reduced without compromise in fleet sizes and distances travelled.

In this research work, fuel consumption, brake thermal efficiency and GHG (Green House Gas) emissions generated under realistic urban driving conditions during a different time of day have been investigated. The routes used represented typical urban busy circuits including arterial and minor roads, turnings, pedestrian crossings and traffic lights. The impact of traffic conditions, road grade and vehicles' movements was investigated.

## **4.2 Traffic flow variations at different times of the day on the congested road**

The A660 road north from Leeds was used as the test road as it is one of the most congested roads in the UK. The road has single lane traffic in each direction with cycle lanes alongside. As with many UK cities, historic buildings along the route prevent the road from being widened. Leeds has a high population density and no open ground to build new radial roads into the city centre. The vehicle flow on the road is limited by the single lane, and the flow can be scaled up by a number of lanes to obtain equivalent congestion on two to four-lane highways. In large cities with populations of several million, even four-lane highways can be congested in a similar way to congestion on the present road, but with four times the implication for air quality. Four-lane highways which are as congested as the present single lane highway can be seen in many cities today, where there are populations of several million.



Figure 4-1 Congested traffic driving route.

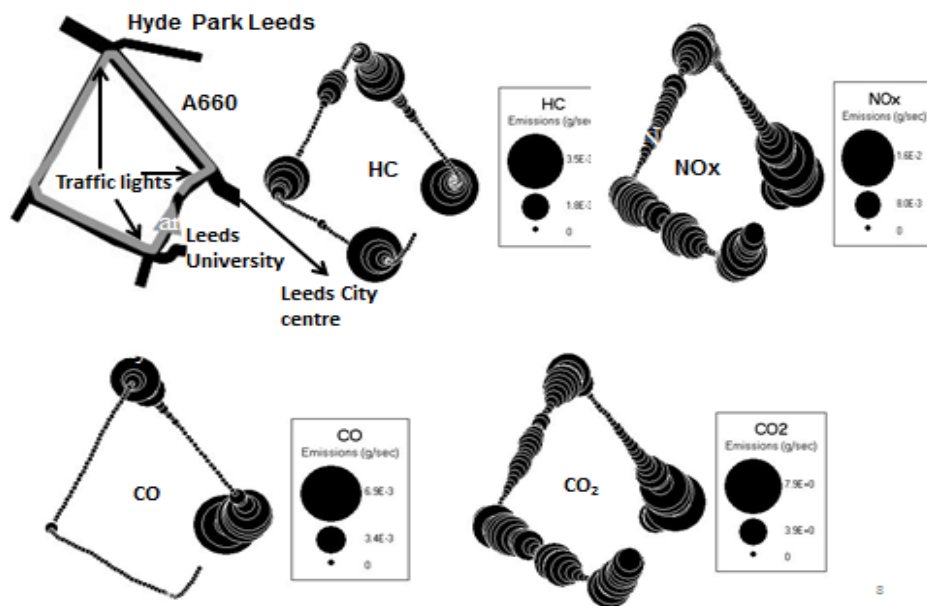
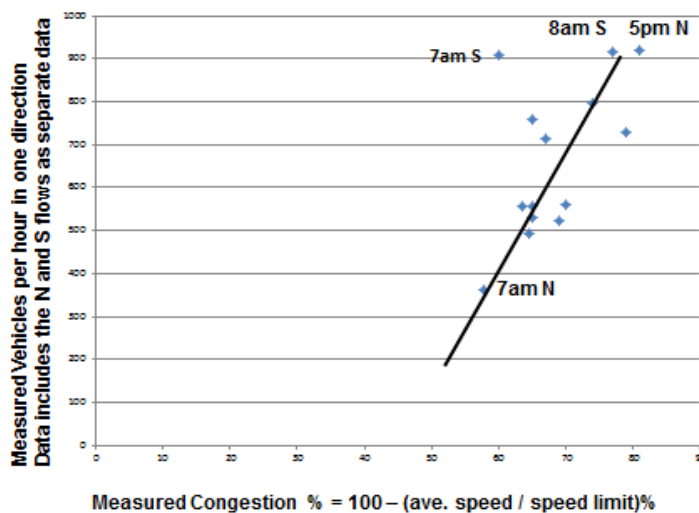
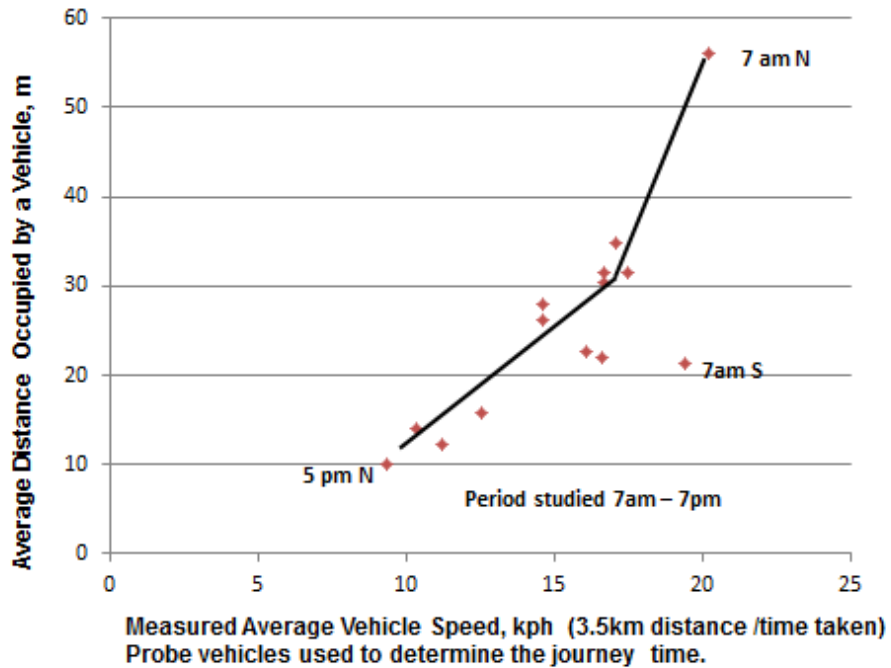


Figure 4-2 Mass emissions at junctions in real world driving [24-26].

The route studied in this work is shown in (Figure 4-1) and it passes the Headingley roadside air quality monitoring station, at which the annual average NO<sub>2</sub> concentrations exceeds the European standard of 40ppb, The height variation of the road across the route was monitored, but was only 20m, and one of the objectives of using a reverse route, with each journey starting and finishing at the same elevation, was to reduce any influence of the change in elevation along the route. In the return journey loop in (Figure 4-1) there were seven traffic light junctions and seven pedestrian crossings and these result in random variations in the number of stop/starts. Thirty-seven return loop journeys were taken at different times of the day in order to give a wide range of congestion conditions. The distance travelled for each trip was 5 km. The speed limit on these urban streets was 48 km/h (30 mph) and this was the reference speed in the congestion definition in Equation (1-1). The journey had two variants in terms of the numbered locations in (Figure 4-1). Journey A was 1-2-3-4 and journey B was 1-3-2-4. Journey A had five right hand turns and three left hand turns and journey B had three right hand turns and five left hand turns. Both the journeys had 14 pedestrian and traffic-light crossings where a stop could occur relatively randomly.



**Figure 4-3 Congestion as a function of traffic flow in vehicles per hour, vph. [107, 108].**



**Figure 4-4 Average road space per vehicle as a function of the average vehicle speed [107, 108].**

This is a potential red light stop every 0.36 km on average. In addition, there were twenty junctions in each loop where vehicles could leave the main flow or join it.

Every traffic movement into or out of the main flow causes disruption to the main flow, with another potential stop/start action. This gives a total of thirty-four events per 5km loop where the main traffic flow could be required to stop and start with one event every 150m. However, these thirty-four disruptive events would occur randomly but would increase with the flow. In terms of stop/start events per km, the above events give a maximum of seven stop/start events per km. It will be shown in the present work that this number of events was found in the most congested traffic situations.

The importance of junctions in realistic driving is illustrated in (Figure 4-2) [24-26], which shows in the size of the circles and the mass of emissions at specific locations. This is a simple loop circuit closer to the centre of Leeds than considered in the present work. This loop was designed to have minimal influence of other traffic, as the roads further from the A660 have low traffic flows. The A660 side of this loop is a dual carriageway and has relatively high-

speed uncongested driving, so that the whole loop is in relatively uncongested driving conditions.

The use of uncongested driving enables the influence of a junction to be evaluated in the absence of other traffic, influencing the driver behaviour of the instrumented car [24-26]. The results in (Figure 4-2) were for a Euro 2 TWC SI Ford Mondeo, but the trends are independent of the vehicle reference emissions level. (Figure 4-2) shows that for HC and CO, virtually all the emissions were generated at the junctions. For NO<sub>x</sub> and CO<sub>2</sub> the majority of the emissions were generated at the junctions, but there were significant emissions due to local accelerations between the junctions. In the present work, the eight right and left-hand turns in each circuit of the route in (Figure 4-1) will create an emissions footprint similar to those at the junctions in (Figure 4-2). The main A660 road in (Figure 4-1) was the subject of a Leeds City traffic monitoring study [1-3] which involved the use of probe cars to determine the time taken to travel 3.5km on the A660 with the section in (Figure 4-1) being in the middle of this journey. The study reported the travel times for the fixed distance, and these have been employed to derive the mean velocity and congestion from Equation (1-1). The results are shown in (Figure 4-3) as congestion as a function of the traffic flow density, vehicles per hour or vph. The number count is that for vehicles crossing the outer Leeds ring road which is approximately 1km north of the test section in (Figure 4-1) It is reasonable to take this traffic flow as the one through the test section of road in (Figure 4-1) and (Figure 4-3) shows that as the traffic density increases the congestion also increases linearly. The data scatter is significant as the data points are hourly averages taken over a number of days.

The highest traffic density and greatest congestion is when travelling south into Leeds at 8 am and north out of Leeds at 5pm.. The 7 am south data point is abnormal and this is because the majority of this traffic is not commuting into Leeds, but rather it is driving through onto the motorway travelling south towards London. Therefore, there is a much lower traffic flow at junctions, as at 7am the main commuting traffic from houses along the route have not yet

started their journeys. For this reason, the congestion is less than would be expected for the high traffic load.

Figure 4-4 shows the average space occupied by a vehicle as a function of the mean vehicle speed. The average space occupied by a vehicle is the average vehicle speed divided by the number of vehicles per hour, which has units of distance per vehicle. For the lowest velocity or highest congestion, the distance per vehicle is 10m and the mean velocity is 7 kph (85% congested). A car space <5m would be close to bumper to bumper vehicles, and would be the peak capacity of the road, which from Figure 4-3 would be about 1000 vph. This was the congestion recorded by the roadside air quality monitor in Figure 4-1.

### **4.3 Analysis of driving parameter, fuel consumption and thermal efficiency**

Two urban driving cycles were designed to perform emission tests: Headingley route A and route B, referred as route A and B, and also the mappings of the routes for the test area as depicted in chapter 3. Headingley is a dense residential area of Leeds and has features as a typical urban road network, i.e. carrying numerous city social-economy activities and being one of the main transportation carriers. The combustion parameters' measurements such as fuel consumption and air/fuel ratio, the vehicle movement (GPS) measurements and emission measurements are described in detail in Chapter 3.3.

#### **4.3.1 Velocity and acceleration**

Figure 4-5 to Figure 4-8 shows profiles for A trips, including vehicle velocity, acceleration, transient, and cumulative fuel consumption, transient VSP and cumulative power output, elevation of road, and also distance travelled, and lambda. The results also demonstrate transient and cumulative CO<sub>2</sub>, N<sub>2</sub>O and CH<sub>4</sub> mass emission rates. In addition, the junctions and pedestrian crossing along the route were marked on the elevation diagrams of, Figure 4-5 to

Figure 4-8 where R is for right turn, L is for left turn, P is for pedestrian crossing, T is for traffic light and U is for U-turn.

Trip A was divided into two directions: an outwards and an inwards section towards the city centre. The first 2.0 km was the outward trip. The inward trip towards the city centre is about 2.5 km. It is noticeable in Figure 4-9 to Figure 4-12 that the outbound journeys for two morning ones and for the lunch-time one took approximately 300 seconds whereas the one in the evening Figure 4-8 took ~250 second, indicating less traffic in the evening. The velocity and acceleration profiles show that outbound journeys were less congested than that of inbound journeys.

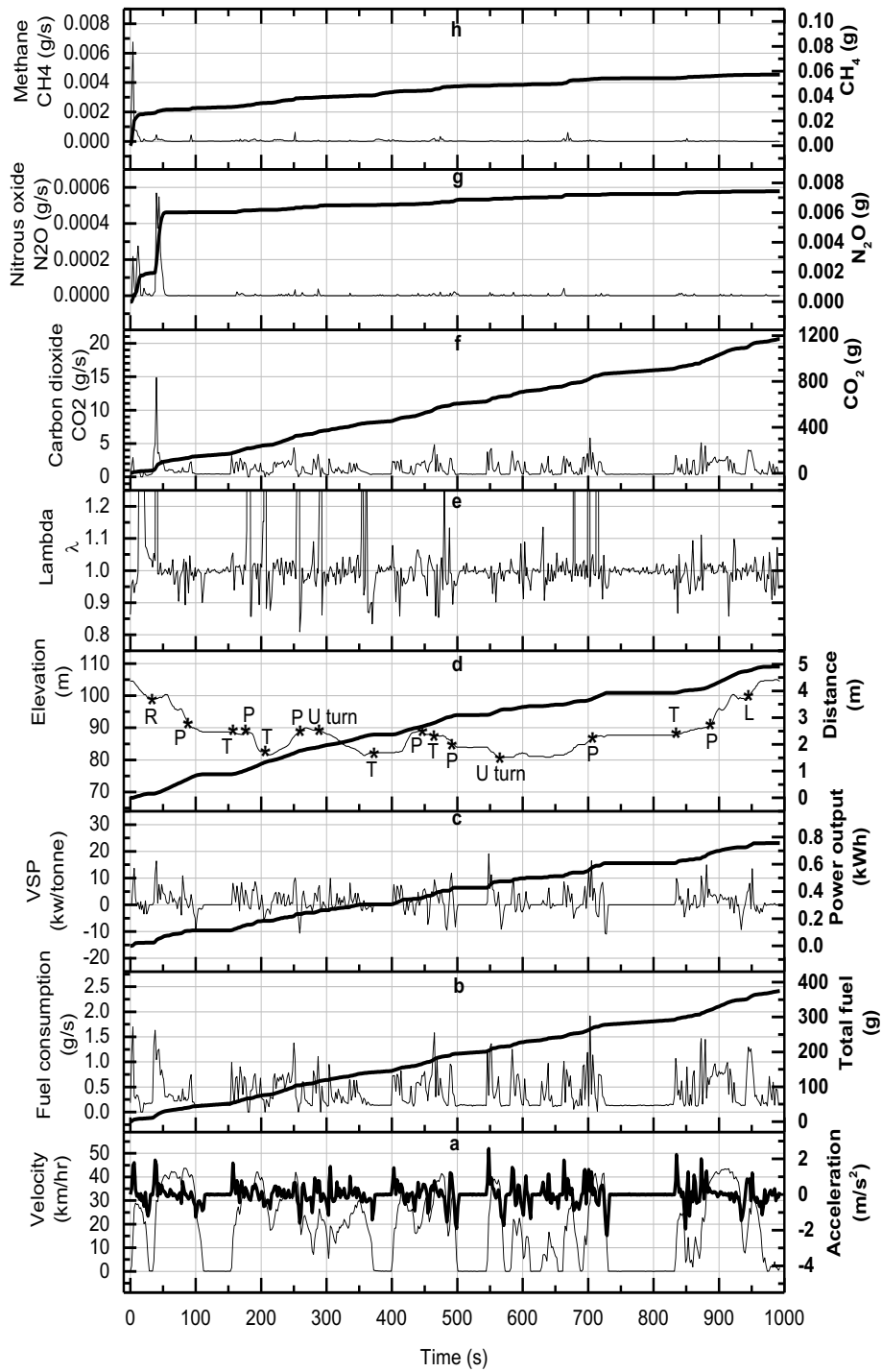


Figure 4-5 Profiles for the trip 7:46A.



19062007 EURO4 0830 A HL

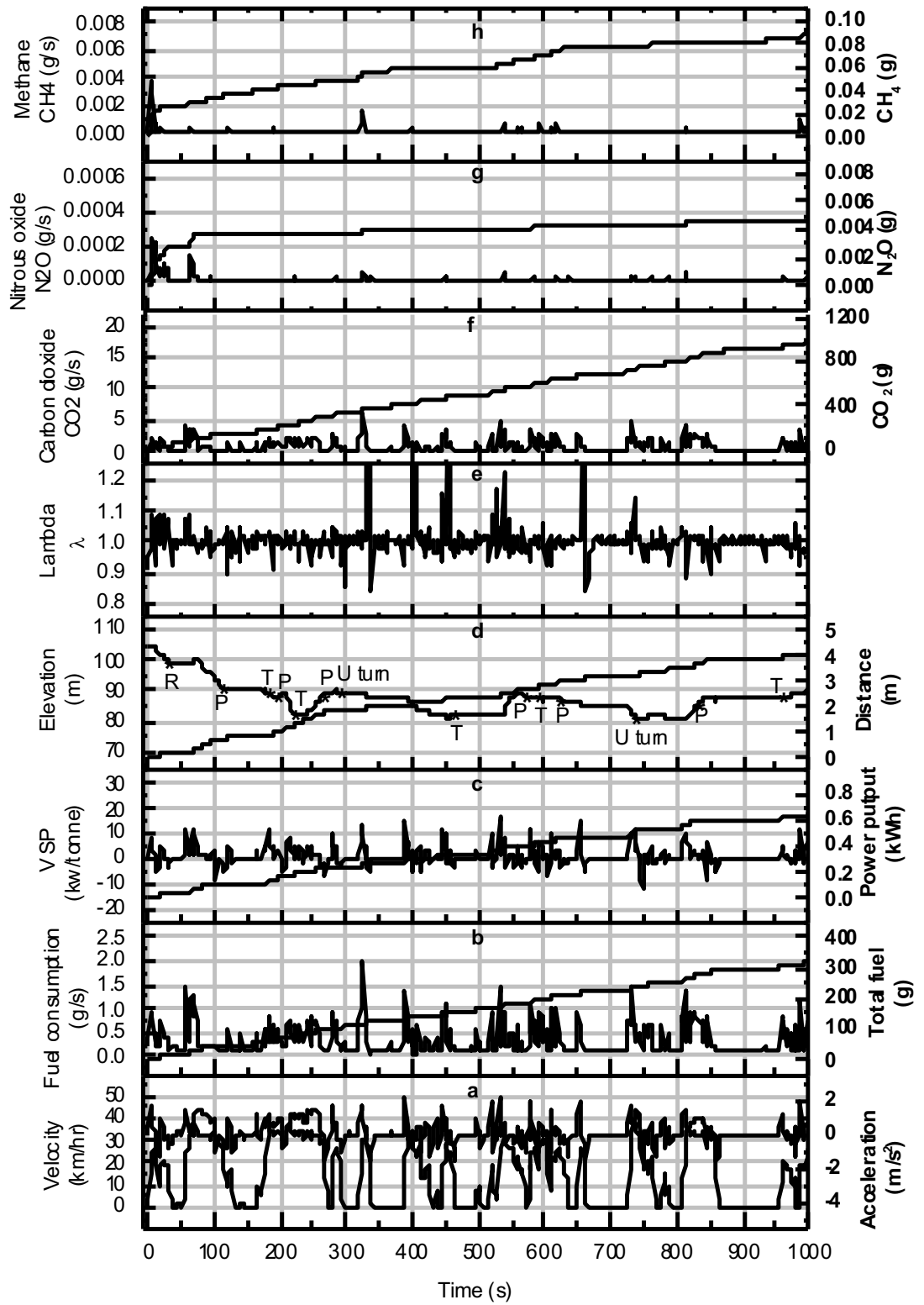


Figure 4-6 Profiles for the trip 8:30A.

There were one to two stops for the outbound journeys but in general there was a time period when the vehicle was in cruise mode. The inbound journeys

however, were considerably more congested, as indicated by more stops and longer idling times. This was particularly apparent for the two morning trips as they were in morning rush hours. The evening trip (Figure 4-8) was considerably less congested as this was off-peak time and therefore there traffic is minimal.

(Figure 4-9) to (Figure 4-12) show the profile of the B trips. The outbound section was approximately 3 km, leaving 2 km for the inbound section. The morning B trips show different traffic scenarios; 8:07 B trip in (Figure 4-9) show that this outbound journey took approximately 550 seconds and was relatively uncongested whereas the outbound journey in (Figure 4-10) (8:53 B trip) took about 750 seconds and was a very congested section.

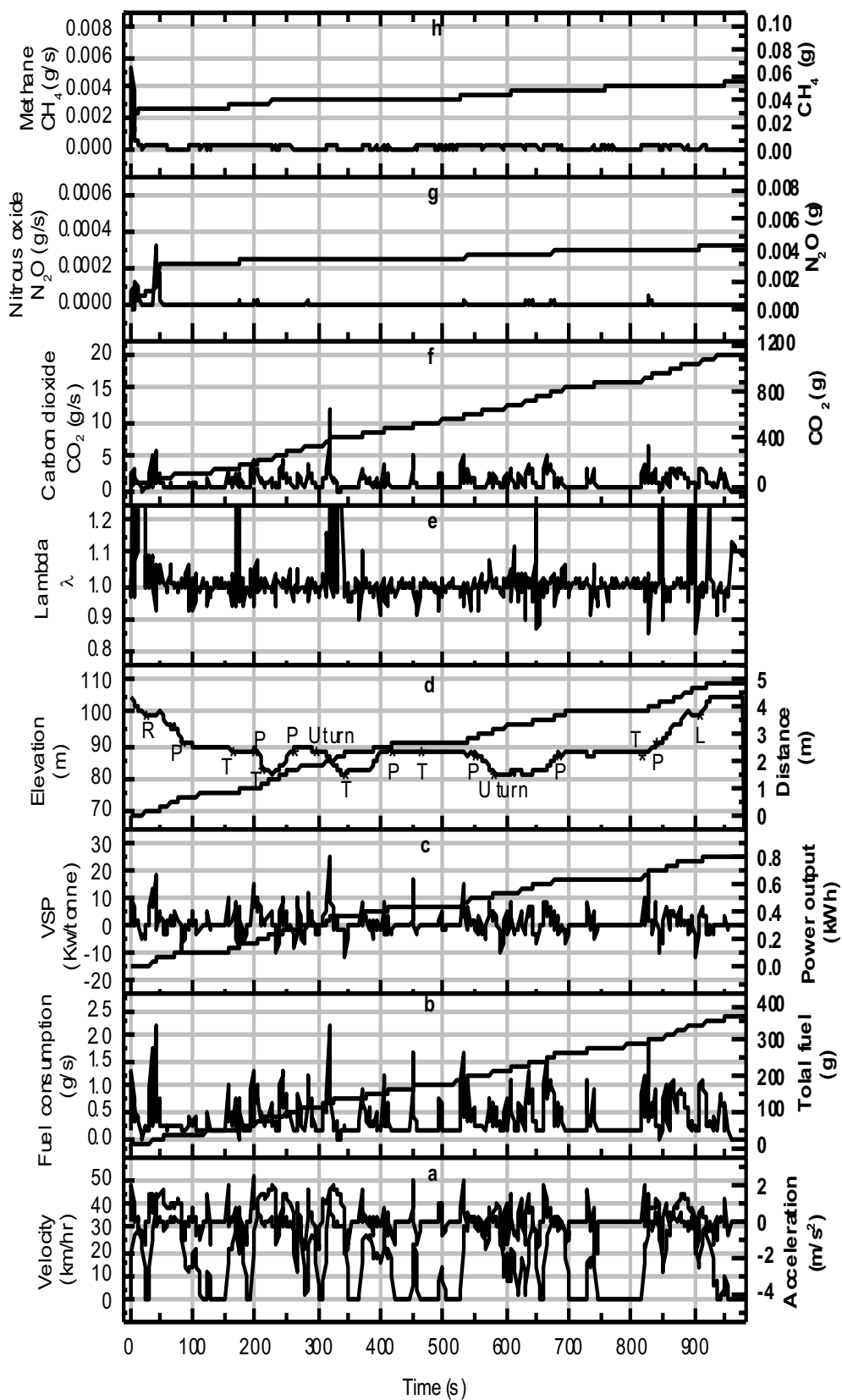


Figure 4-7 Profiles for the trip 12:56A.

11062007 EURO4 1925 A HL

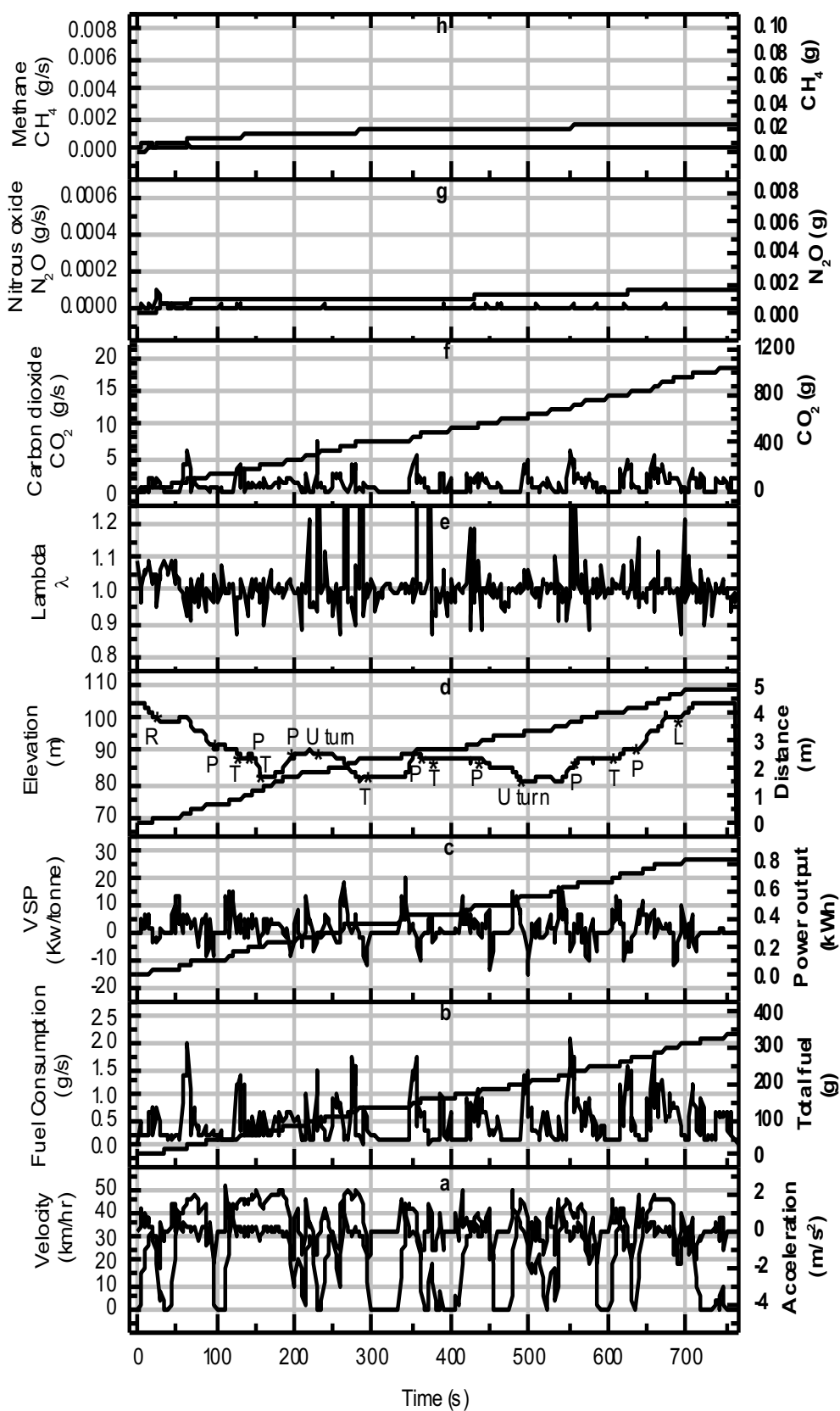


Figure 4-8 Profiles for the trip 19:25A.

In contrast, the inbound journey in Figure 4-9 and Figure 4-10 showed an opposite trend, although the one in Figure 4-9 was very congested compared to the one in Figure 4-10. This can be explained by the time, which means the journey in Figure 4-10 started at 8:53 and when the vehicle reached the U-turn point 3 and started travelling back towards city centre, it was approximately 9:05. The traffic was becoming calm by this time as most of the commuters needed to arrive at their work by 9 am. Figure 4-11 and 13:16 trip B reveals that there was some congestion in outbound direction during the middle of the day. This was common as this is a congested road (A660) for most times of the day. Figure 4-12 illustrates that at off-peak times, the journey (19:41 trip B) was much smoother with cruise mode in use for much of the time.

19062007 EURO4 0807 B HL

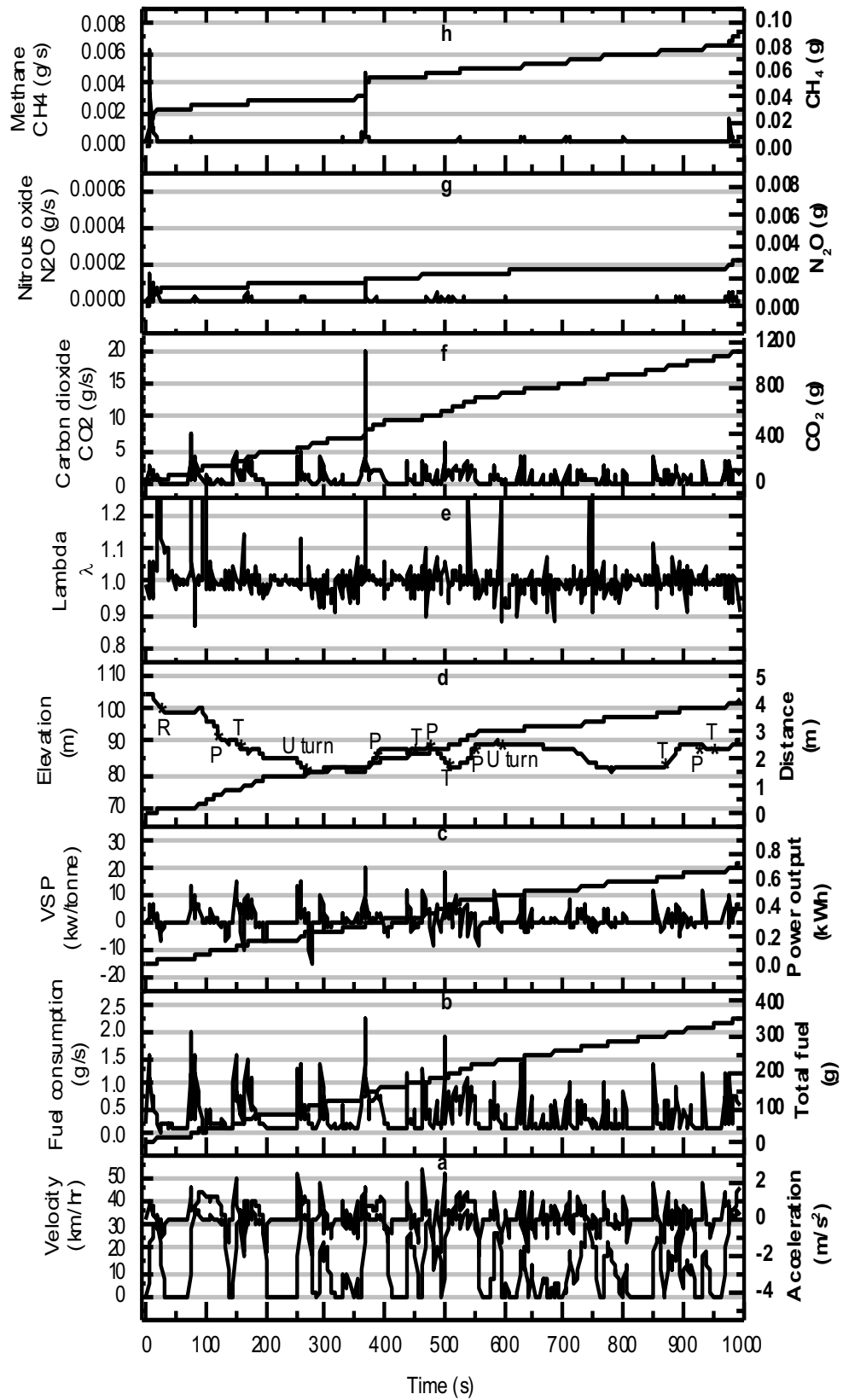


Figure 4-9 Profiles for the trip 8:07B.

19062007 EURO4 0853 B HL

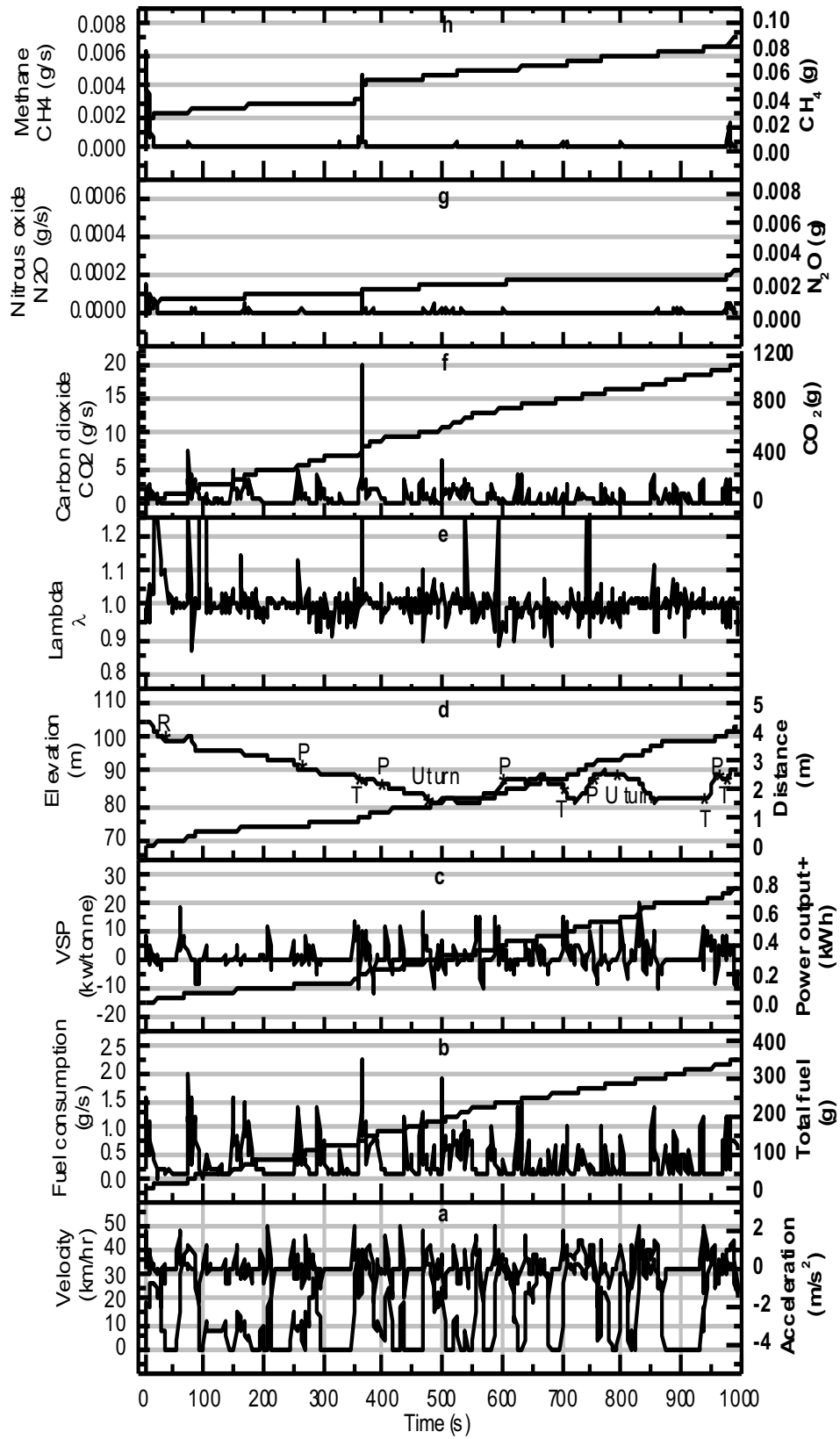


Figure 4-10 Profiles for the trip 8:53B.

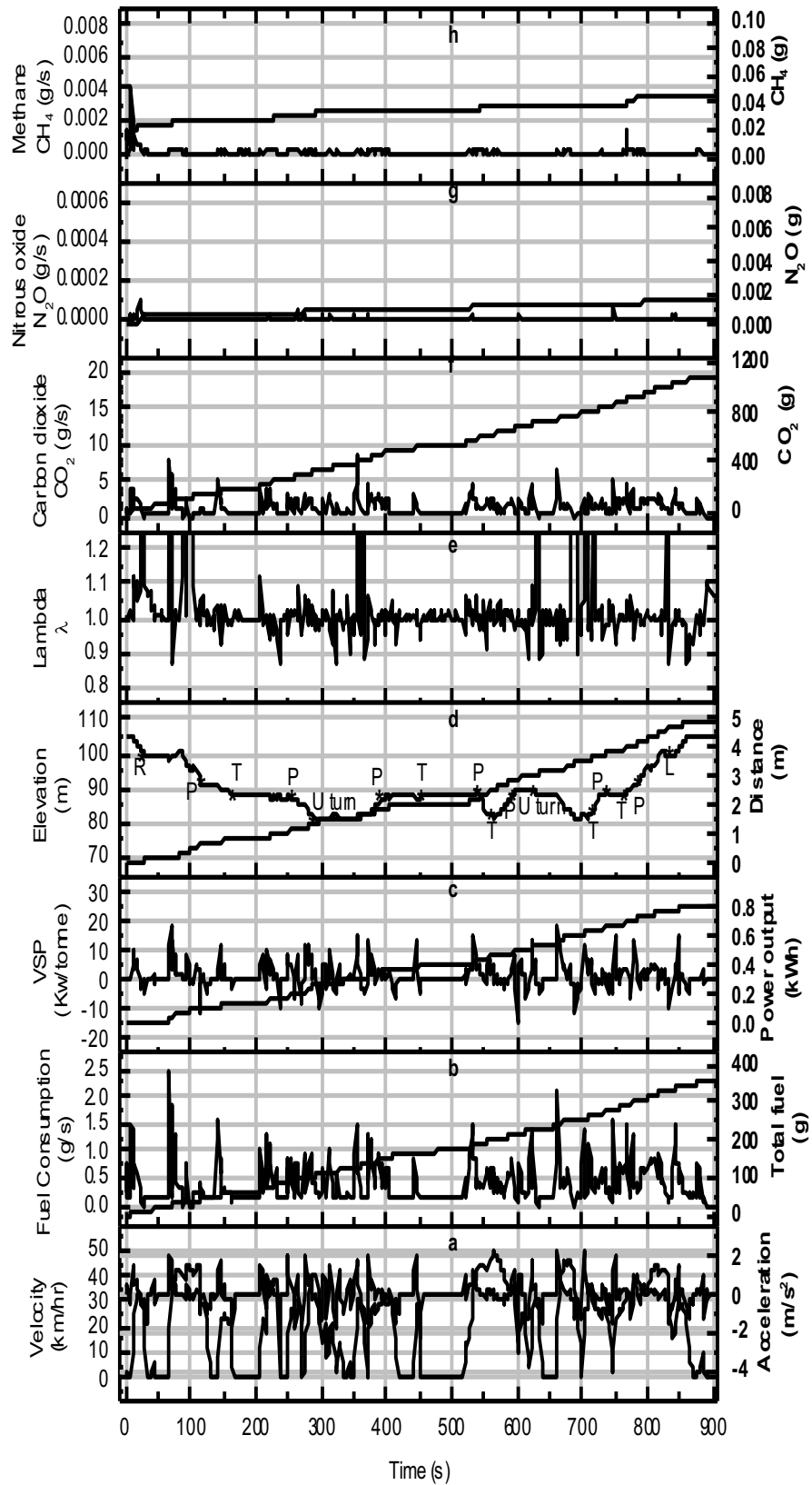


Figure 4-11 Profiles for the trip 13:16B.



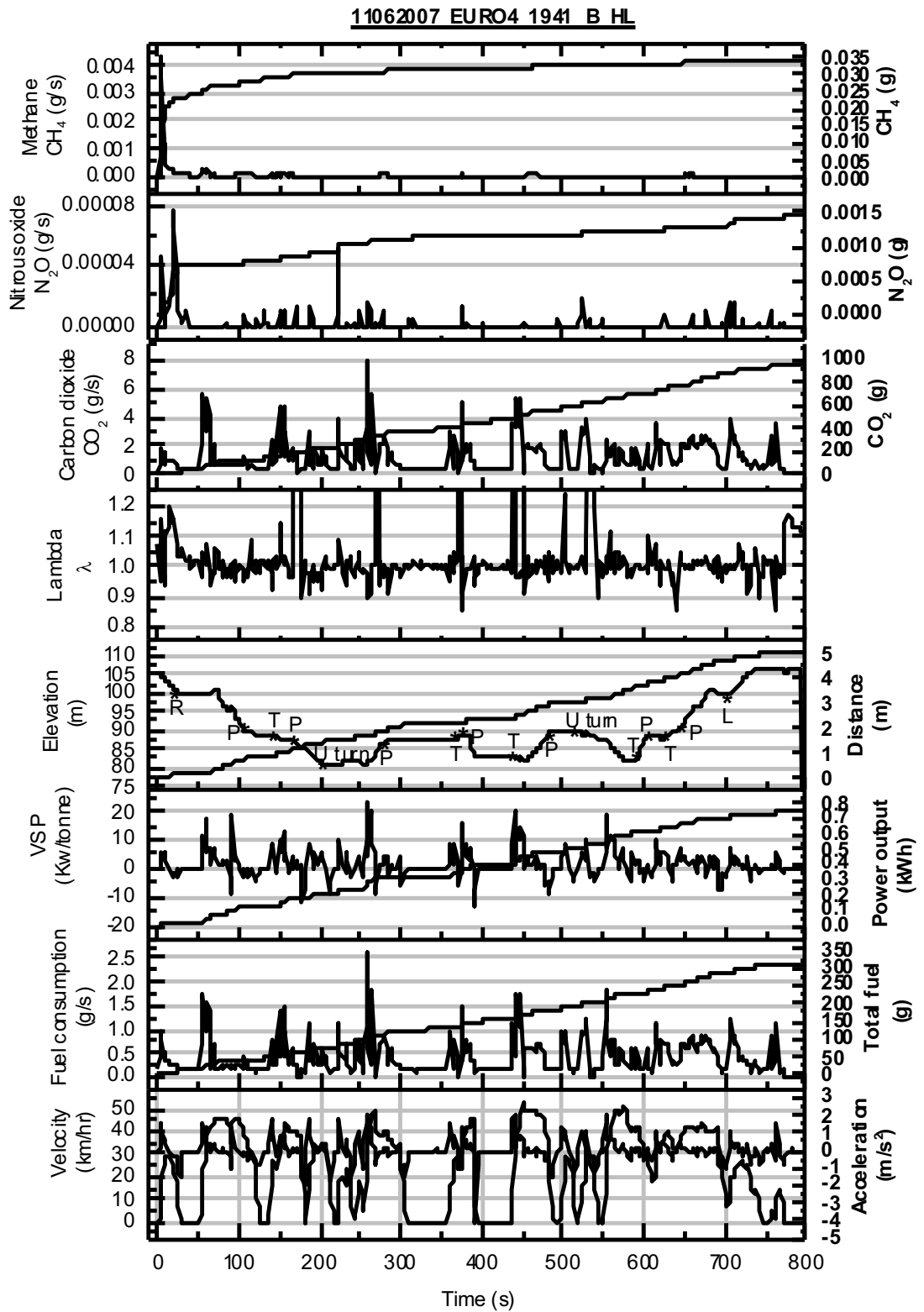


Figure 4-12 Profiles for the trip 19:41B.

### 4.3.2 Fuel consumption and VSP

Fuel consumption is generally associated with a vehicle's velocity, but this dependency is not linear. The results show that each time a vehicle was started from idle and accelerated to cruise speed, there was an initial peak in fuel consumption, then followed by a decrease in fuel consumption even when the vehicle was travelling at a constant speed. Although an exceptional case exists, for instance, when the vehicle is climbing the hills where a fairly constant fuel supply was needed, it is the accelerations that caused spikes of fuel consumption. Consequently, frequent stop/start events in congested traffic are major contributors to the increased fuel consumption on congested trips.

The fuel economy as revealed in Table 2-1 remains only 24-28 mpg in the morning rush hours whereas the evening trip in the off-peak time, this could increase to 32 mpg. The fuel consumption for this type of vehicle, measured on the NEDC urban part is 28 mpg, but that included the cold starts which have higher fuel consumption.

However, if the fuel consumption from the NEDC urban part excludes the cold start, the fuel economy will be better than 28 mpg, i.e. the fuel economy for a hot NEDC urban part for this type of vehicle will be greater than 28 mpg. Hence, for realistic driving in a congested traffic, fuel economy can hardly achieve certified values.

The value of VSP is mainly determined by acceleration and road grade. Nevertheless, there is uncertainty when the vehicle is travelling on a flat or downhill road at a constant speed because the value of VSP would be small due to the low power supply demand. This can be illustrated with examples 40-100 s in Figure 4-5 and 7:46 trip, 50-100 s in Figure 4-7 and Figure 4-12. The most dominant factor for VSP is acceleration, evidenced by the fact that most negative VSP spikes are linked with deceleration peaks.

The average of overall VSP and positive VSP for all trips have been presented in Table 4-1. This table indicates that the two evening trips had the higher

values as a result of more free-flowing driving, whereas the morning trips had lower values. This means that the average VSP could be used as an indication of congestion. From this study, an initial suggestion is that average VSP 1.4 or average positive VSP 3.1 could be used as an indication of a non-congested trip.

### 4.3.3 Overall thermal efficiency

The brake thermal efficiency, defined as a measure for the conversion efficiency of fuel energy to useful work output, is employed here to assess overall thermal efficiency and is defined as follows:

$$\eta_b = \frac{\text{brake work output}}{\text{fuel energy}} = \frac{\text{VSP} * \text{mass of vehicle} * 3600}{\text{fuel consumption} * \text{Cv of fuel}} \quad (4.1)$$

When the vehicle is at stoppage or deceleration, the VSP values become zero or negative. This means that the energy from fuel was wasted as there was no effective work output to drive the vehicle. Therefore, the brake thermal efficiency of the engine was compromised.

The positive VSP values were multiplied by the vehicle weight and then integrated. This results in the trip total brake power output (work done) from the engine as shown in c of all diagrams and in Table 4-1. The power output was then divided by the fuel energy, and thus the overall thermal efficiency of the trip was obtained. The overall thermal efficiency for all trips in Table 4-1 was in a range of 16~20%. This is remarkably lower than the typical SI engine thermal efficiency of ~30%. The reason for this is the stop/start driving pattern that seriously compromised the SI engine's thermal efficiency.

The efficiencies are the lowest for the three morning trips: 7:46, 8:07 and 8:30, with values of around 16.5%, which were linked to higher fractions of stoppage time and lower average velocity. The higher thermal efficiencies (~20%) for the two evening trips were correlated to the lowest stoppage time (percentage) and the highest average velocity. So if the engine was shut down during those idle periods as in some modern engine designs, the thermal efficiency would be increased to around 30%.

The total negative power output calculated from negative VSP as shown in Table 4-1 accounted for approximately 30~40% of the actual power output from the engine. Although not all of these negative power outputs are available for recovery as there are some accessory and transmission losses which are non-recoverable, which provides significant potential for energy recuperation for hybrid vehicles.

**Table 4-1 Summary of driving parameters and GHG emissions for all journeys.**

Journeys	0746 A HL	0830 A HL	1256 A HL	1925 A HL	0807 B HL	0853 B HL	1316 B HL	1941 B HL
Carbon dioxide CO2 (g/km)	238.329	240.346	229.972	213.412	270.444	269.667	221.656	191.356
Nitrous oxide N2O (g/km)	0.0015	0.0011	0.0009	0.0003	0.0007	0.0007	0.0003	0.0003
Methane CH4 (g/km)	0.012	0.021	0.011	0.005	0.021	0.021	0.009	0.007
Av. Velocity (km/hr)	17.772	14.835	18.051	23.127	14.976	14.963	19.348	22.499
Max Velocity (km/hr)	43.700	43.370	48.670	49.420	44.590	44.070	49.310	52.240
Min Velocity (km/hr)	0.000	0.000	0.000	0.000	0.000	0.000	0.000	0.000
Av. Acceleration (m/s <sup>2</sup> )	0.003	0.007	-0.003	-0.003	0.014	0.007	0.006	-0.007
Max Acceleration (m/s <sup>2</sup> )	2.567	2.168	2.418	2.397	2.650	2.292	2.349	2.114
Max Deceleration (m/s <sup>2</sup> )	-2.286	-1.768	-1.800	-2.149	-2.036	-2.001	-4.296	-4.026
Av. VSP (Kw/tonne)	1.088	0.990	1.171	1.461	1.120	1.105	1.358	1.394
Max VSP (Kw/tonne)	19.083	16.826	25.758	20.070	19.251	20.224	18.104	22.958
Min VSP (Kw/tonne)	-10.901	-12.021	-11.211	-15.482	-14.767	-11.158	-15.008	-13.542
Av. VSP+ (Kw/tonne)	2.569	2.244	2.791	3.686	2.442	1.884	2.916	3.088
Av. VSP- (Kw/tonne)	-2.177	-1.949	-0.738	-3.222	-1.870	-2.377	-2.442	-2.459
Power output+ (kWh)	0.756	0.652	0.805	0.832	0.721	0.782	0.802	0.748
Power output- (kWh)	-0.277	-0.223	-0.300	-0.325	-0.228	-0.289	-0.268	-0.252
Total stoppage time (s)	275.000	362.000	301.000	172.000	317.000	342.000	256.000	201.000
Stoppage time (%)	27.694	36.309	30.746	22.425	31.891	34.406	28.132	25.220
Cruise time (%)	32.125	24.273	34.423	44.980	26.157	27.666	35.385	40.652
Total fuel consumption (g)	374.853	319.066	364.947	338.302	353.028	353.028	354.103	313.257
Av. fuel consumption (g/s)	0.377	0.322	0.371	0.442	0.357	0.357	0.389	0.390
Idle fuel consumption (g)	62.319	77.908	61.925	39.987	73.578	73.578	50.617	42.656
Idle fuel consumption (%)	16.625	24.418	16.968	11.820	20.842	20.842	14.294	13.617
Journey Av. fuel consumption (g/km)	76.314	77.844	74.339	68.705	85.360	85.115	72.119	62.814
Fuel economy (mile/UKG)	26.717	26.192	27.427	29.676	23.886	23.955	28.271	32.459
Overall brake thermal efficiency (%)	16.355	16.574	17.894	19.930	16.568	17.949	18.373	19.359
Overall brake thermal efficiency with no stops %	38.7	43.2	42.5	44.6	41.2	44.7	42.2	44.2
Power output-/power output+	-36.6	-34.2	-37.3	-39.1	-31.6	-37.0	-33.4	-33.7

## 4.4 GHG emissions

Greenhouse gases are generally emitted from all energy systems and this in turn, contributes to an anthropogenic effect as well as climate forcing agents. These gases are widely recognised as emissions resulting from the use of particular energy technology, and this needs to be quantified at every process technology unit, as well as its fuel usage [109].

Numerous studies have demonstrated that GHG has active radiative properties. These GHGs emissions from different sources are associated via indexed according to global warming potentials (GWP) [110]. Additionally, global warming potential (GWP) has been defined as the ability of greenhouse gases GHG to adsorbed heat within the atmosphere relative to an equal quantity (volume) of CO<sub>2</sub>. Three GHGs: CO<sub>2</sub>, methane (CH<sub>4</sub>) and nitrous oxide (N<sub>2</sub>O) were measured in this research.

This section presents and analyses GHG emissions from realistic urban driving using a novel SI probe car. The vehicle was warmed up before the test journeys started, so there was no cold start. However, the vehicle had to stop at the start point of the journey to set up instruments which may take up to 10~15 minutes. Therefore, there was a drop in catalyst temperatures. This resulted in a spike in CH<sub>4</sub> and N<sub>2</sub>O emissions during the initial 20~50 seconds. The spike in N<sub>2</sub>O emissions indicated that the catalyst temperatures were in the range of 250~350°C.

The CO<sub>2</sub> emissions are directly responded to fuel consumptions by comparison of (a) and (d) in all figures and also a good reflection of VSP spikes. CH<sub>4</sub> and N<sub>2</sub>O emissions were very low after the engine was fully warmed up (after 25s) and only had occasional spikes, which were linked to sharp accelerations, spikes of fuel consumption, VSP, and lean spike in lambda values. Interestingly, not all of these spikes produced high CH<sub>4</sub> and N<sub>2</sub>O emissions. It appears that the spikes of CH<sub>4</sub> and N<sub>2</sub>O only occurred when the fuel consumption had a sharp rise with a peak value of 2 g/s and above.

By examination of all these trips, it can be found that most of the CO<sub>2</sub> peaks are linked to pedestrian crossings, traffic lights and turnings where the vehicle was forced to stop (red light or queue). There were a few CO<sub>2</sub> peaks which are related to uphill movements.

Figure 4-13 presents the correlation between trip CO<sub>2</sub> emissions in terms of g/km Vs trip average speed for all trips. A good linear correlation is observed. Similarly, a good linear correlation between CH<sub>4</sub> emissions and trip average speed is also observed as shown in Figure 4-14. However, there is no clear correlation between N<sub>2</sub>O and trip average speed as shown in Figure 4-15, due to the fact that N<sub>2</sub>O emissions are a function of the TWC.

The type approval CO<sub>2</sub> emission data for this make and model is 179 g/km based on NEDC driving cycle [111]. The CO<sub>2</sub> emissions from this study have a range of 190-270 g/km and yet the results did not include any cold start emissions. Authors reported that if the cold start is included, the realistic CO<sub>2</sub> emissions from this vehicle could reach 280-340 g/km [112]. It clearly indicated that realistic CO<sub>2</sub> emissions in densely populated areas are much higher than legislated cycle results, even the cold start is not considered.

N<sub>2</sub>O and CH<sub>4</sub> have a much higher global-warming potential (GWP) compared to CO<sub>2</sub> and their GWP index is about 300 and 35 relative to CO<sub>2</sub> respectively. However, due to the very low mass emissions, their contributions to GWP are only 0.1-0.4% and thus negligible .

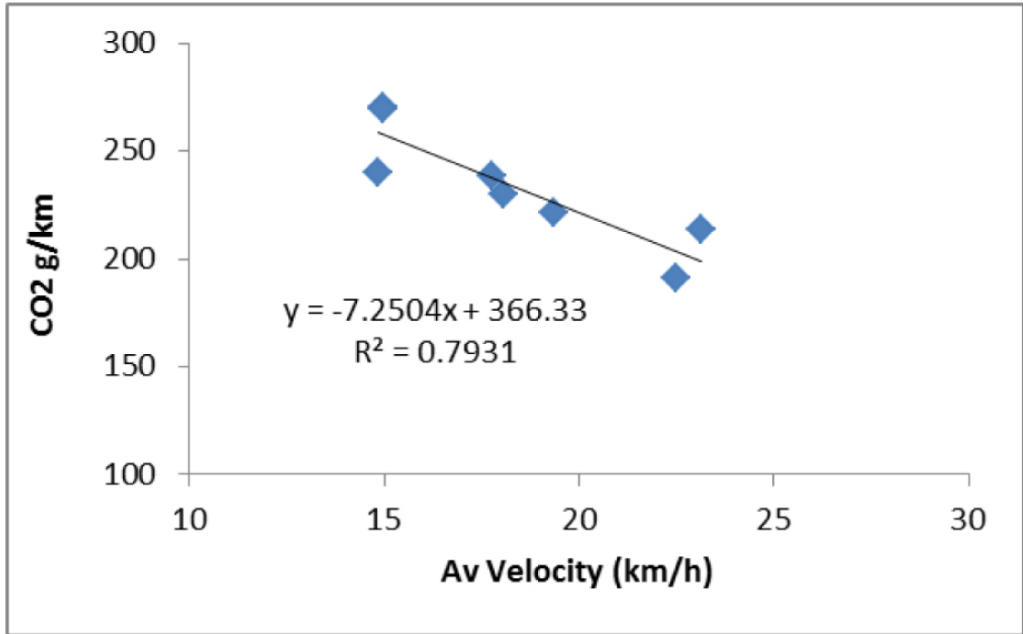


Figure 4-13 Trip mean CO<sub>2</sub> emissions vs vehicle's average trip velocity.

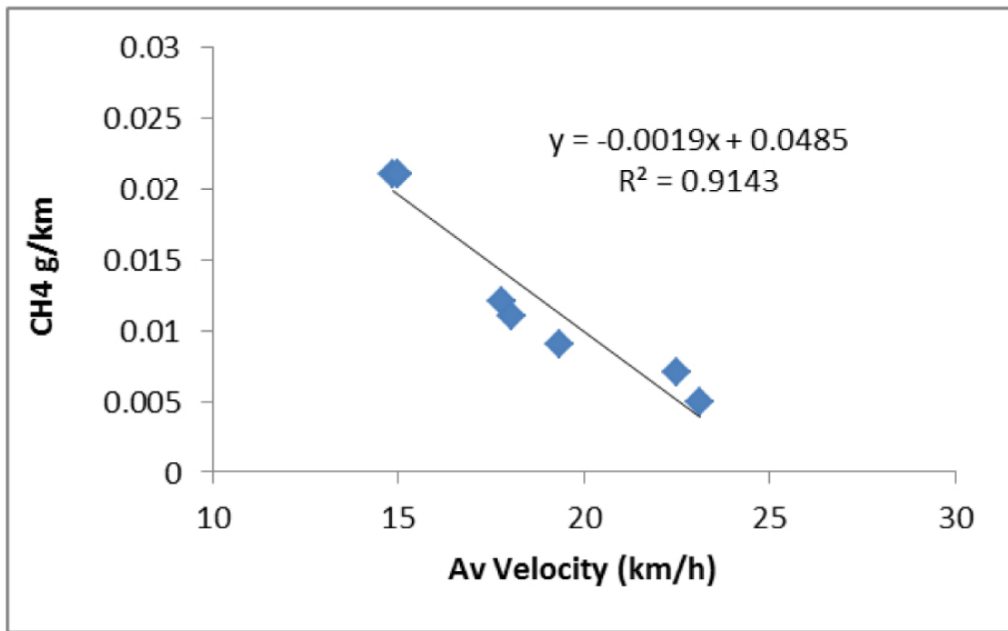


Figure 4-14 Trip mean CH<sub>4</sub> emissions vs vehicle's average trip velocity.



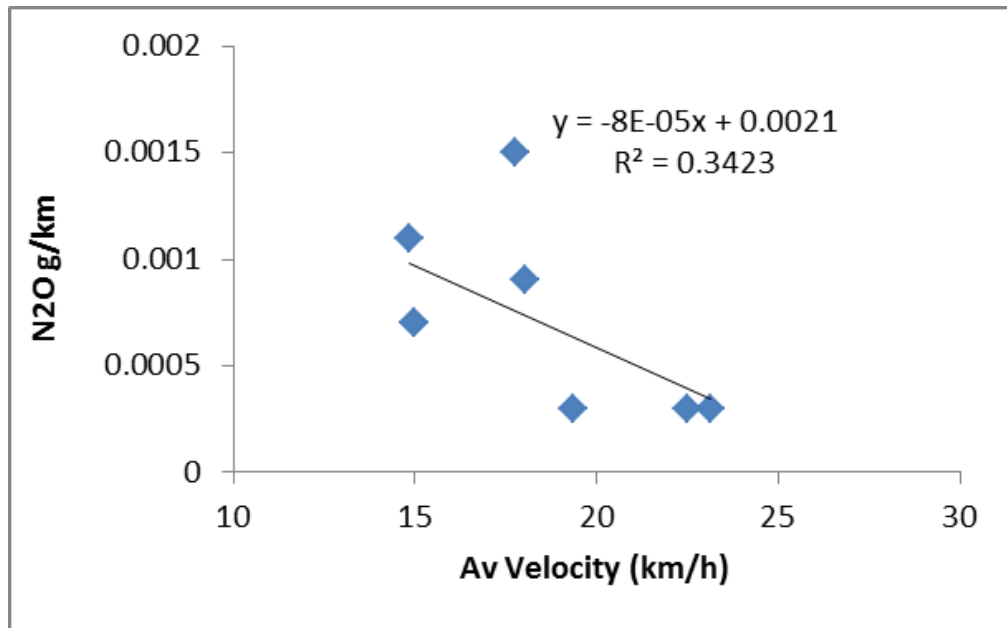


Figure 4-15 Trip mean N<sub>2</sub>O emissions vs vehicle's average trip velocity.

## 4.5 Conclusions

Two real world driving cycles (route A and B) using the routes located in a dense populated area of Leeds representing typical urban road network were developed and selected for a series of real world emission tests. These two cycles represented the congested road networks in cities. The emissions were measured in the morning rush hours, lunch time and off-peak time in the evening using a EURO 4 SI probe car. The results have shown that:

- Fuel consumption in congested traffic is much deteriorated. Fuel economy can hardly achieve the certified values in urban congested traffic. The idling fuel consumption accounted for 12~24% of total fuel consumption, which will give rise to 12~24% of increase in CO<sub>2</sub> emissions as well.
- VSP representing the power demand to move a vehicle is dominantly affected by the accelerations in urban driving conditions. The value of average VSP and average VSP+ can be used as indicators for traffic congestions. The minimum values for free flow VSP could be 1.4 for average VSP and 3.1 for average VSP+.
- The long stoppage time (idle) in a traffic queue can seriously deteriorate the engine thermal efficiency. In this study, the thermal efficiency of the engine was 16-20%, significantly lower than theoretical values.
- CO<sub>2</sub> emissions were 190-270 g/km from this study and could be higher if the engine cold start is to be included. The type approval CO<sub>2</sub> for this vehicle is 179 g/km based on NEDC cycle. This would result in an underestimation of CO<sub>2</sub> emissions for emission inventories.
- N<sub>2</sub>O and CH<sub>4</sub> emissions can be very low when the engine is hot, even in very congested traffic. Their impacts on GWP are thus negligible.

## 5 Chapter Five: Speciation of nitrogen compounds in the tailpipe emissions from a SI car under realistic driving conditions

### 5.1 Introduction

Nitrogen compounds from vehicle tailpipe such as NO, NO<sub>2</sub>, N<sub>2</sub>O, NH<sub>3</sub> and HCN are toxic air pollutants (TAPs). NO is a product of combustion inside the engine. NO<sub>2</sub> is mainly a secondary pollutant from the exhaust catalytic systems where extra oxygen is available to oxidize NO into NO<sub>2</sub>. NO and NO<sub>2</sub> are involved in the formation of ozone (O<sub>3</sub>) in the atmosphere and able to oxidise unburned hydrocarbons to form oxygenated irritants such as formaldehyde, peroxyacetyl nitrate etc. [113]. NO<sub>2</sub> itself is an irritant air pollutant regulated by EU air quality legislation. NH<sub>3</sub> is not a product of combustion and instead is formed across the TWC. NH<sub>3</sub> is not directly regulated by vehicle emission legislation but is required to be monitored for the sake of the air quality, soil and surface water concerns [114]. The United Nations Economic Commission for Europe (UN ECE) has set the limits for NH<sub>3</sub> for different European countries. However, there is no legislative requirement for NH<sub>3</sub> released from vehicle tailpipes. NH<sub>3</sub> can form NH<sub>4</sub>NO<sub>3</sub> and/or (NH<sub>4</sub>)<sub>2</sub>SO<sub>4</sub> and contribute to the formation of the secondary aerosols and is an important constituent of particulate matter (PM). NH<sub>3</sub> has the potential to be transported over long distances within the atmosphere, and thus could potentially have adverse impacts on soil and water because of the deposition of ammonium salts which lead to acidification and eutrophication of soils and surface waters.

Heeb et al. [112, 115, 116] investigated NH<sub>3</sub> emissions and their correlation with NO emissions and concluded that catalyst temperatures and air/fuel ratios are key parameters affecting the formation of NH<sub>3</sub> in EURO 3 and 4 gasoline passenger cars. They also reported a conversion ratio of 2% to 45% for NO converting to NH<sub>3</sub> when operating a Pd/Rh-based TWC vehicle under transient driving conditions. There is a kind of trade-off between NO<sub>x</sub> and NH<sub>3</sub>. As the NO<sub>x</sub> emission legislation is getting more stringent, more effective and

efficient  $\text{NO}_x$  reduction across the TWC is demanding. This may cause the rising of  $\text{NH}_3$  emissions.

Hydrogen cyanide (HCN) is a toxic air pollutant and a by-product formed during the  $\text{NO}_x$  reduction reactions across the catalyst [117, 118]. There are very limited data being reported on the HCN emissions from vehicle tailpipes[118].

Nitrous oxide ( $\text{N}_2\text{O}$ ) is a powerful GHG (~300 stronger than  $\text{CO}_2$ ) and has a long life span (>170 years). The transport sector is a minor contributor to the total  $\text{N}_2\text{O}$  flux in the atmosphere. However, its GWP (Global Warming Potential) could account for a significant contribution to the total GWP from vehicle tailpipe emissions. Li et al. [119] investigated GWP of  $\text{CO}_2$ ,  $\text{N}_2\text{O}$  and  $\text{CH}_4$  tailpipe emissions for five urban driving cycles and reported ~10% of the total GWP coming from  $\text{N}_2\text{O}$ .

This chapter investigates the tailpipe emissions of five nitrogen compounds ( $\text{NO}$ ,  $\text{NO}_2$ ,  $\text{NH}_3$ , HCN,  $\text{N}_2\text{O}$ ) under realistic urban driving conditions during the different times of day employing a EURO 4 SI passenger car. The routes used represented typical busy urban circuits including arterial and minor roads, turnings, pedestrian crossings and traffic lights. The impact of traffic conditions, road grade and vehicles' movements on these five nitrogen compounds was investigated.

## 5.2 Results and discussions

### 5.2.1 Driving parameter analysis - velocity and acceleration

Figure 5-1 to Figure 5-4 and Figure 5-5 to Figure 5-8 show the profiles of four A trips and four B trips respectively, including the vehicle's velocity, acceleration, transient and cumulative fuel consumption, transient VSP and cumulative power output, elevation of road, distance travelled, lambda and concentration of HCN, NH<sub>3</sub>, NO<sub>2</sub>, NO, N<sub>2</sub>O in ppm. The junctions and pedestrian crossings along the route are marked on the elevation diagrams of Figure 5-1 to Figure 5-8. The notes are R for right turn, L for left turn, P for pedestrian crossing and T for traffic lights.

### 5.2.2 Concentration of nitrogen compounds

The detection limits of the FTIR for these five nitrogen compounds are around 3 ppm. The results show that in the morning rush hour and at midday HCN and NO<sub>2</sub> concentrations were above detection limits Figure 5-1 to Figure 5-7 and Figure 5-4 and Figure 5-8 whereas for the two evening trips Figure 5-4 and Figure 5-8, HCN and NO<sub>2</sub> concentrations were generally below the detection limits. NH<sub>3</sub> and NO concentrations were higher than the detection limit for all the trips. N<sub>2</sub>O concentrations were overall below or close to its detection limit.

### 5.2.3 Time resolved mass emissions

Figure 5-9 to Figure 5-16 show the mass emission rate (g/s) and cumulated mass emissions for five nitrogen compounds as a function of time, along with some driving parameters. NH<sub>3</sub> is the most abundant nitrogen compound emitted from the exhaust gases and has a value of 0.05~0.09 g/km (see appendix A). Bielaczyc et al.[88] investigated NH<sub>3</sub> emissions from EURO5, 4 and 3 emission compliance SI passenger cars using the NEDC test cycle. They reported much lower NH<sub>3</sub> emissions from all three vehicles compared with NH<sub>3</sub> emissions from Bielaczyc work with this research. The make and

model of the EURO4 passenger car in Bielaczyc’s paper is unknown and therefore direction comparison may be difficult as the tailpipe NH<sub>3</sub> emissions may be related to the type of the TWC. However, the gap between their results from NEDC and the realistic driving cycle in this research is too large to be attributed to account for the possible difference in catalyst technology and type. The frequent stop/start, much harsher acceleration and deceleration, greater and more transient power demands for the engine under realistic driving conditions presented in this study are important parameters causing high tailpipe NH<sub>3</sub> emissions. Karlsson et al. [118] compared NH<sub>3</sub> emissions from NEDC and UDC (Urban Driving Cycle) of FTP-75 and observed much higher NH<sub>3</sub> emissions from UDC than from NEDC due to harsher accelerations in the UDC. This is consistent with this paper’s finding, i.e. rapid and harsh accelerations are the main causes of NH<sub>3</sub> emissions.

The peak NH<sub>3</sub> emission rate (g/s) from eight trips in Figure 5-9 to Figure 5-16 are generally in the range of 2~3 mg/s, well aligned with the reported data from Heeb et al. [112] using the German highway cycle (BAB).

**Table 5-1 Comparison of NH<sub>3</sub> emission (mg/km) from reference [88] and this research.**

	<b>EURO 5 (REF)</b>	<b>EURO4 (REF)</b>	<b>EURO3 (REF)</b>	<b>EURO4 (THIS STUDY)</b>
<b>NEDC</b>	5.27	2.91	16.52	
<b>UDC</b>	6.7	4.13	19.21	
<b>EUDC</b>	4.46	2.2	14.99	
<b>LEEDS- HEADINGLEY CYCLE</b>				50~90

The peak mass emission rate of HCN was generally around 2 mg/s. The distance-based HCN emissions were 5~15 mg/km between the eight trips. These values are significantly higher than those using Euro 1 and 2 SI cars and close to the values of a high-mileage pre-Euro SI car as reported by Karlsson et al. [118]. The high HCN emissions from the Euro4 SI car may be related to the high NH<sub>3</sub> emissions, as both are by-products of de-NO<sub>x</sub> reduction reactions across the TWC. However, the detailed mechanism on the formation of HCN through the TWC is not clear.

The NO<sub>2</sub> emissions are generally low for all the trips, but the fraction of NO<sub>2</sub> in NO<sub>x</sub> is higher than those generally recognised values [112], which were <1%. Possible reasons for this are that the journeys presented in this paper were mostly in congested road conditions and thus have more decelerations (lean spikes), which resulted in further oxidation of NO.

N<sub>2</sub>O is usually formed when the TWC temperature is at a particular range (250~350°C). The TWC temperature was not measured but the downstream of TWC gas temperature was measured in this research, which can be used as an indirect indication of the TWC temperature. The downstream of TWC temperatures was above 450C in seven out of eight of the journeys, except the journey in figure 9. The N<sub>2</sub>O emissions had an initial spike for all journeys after the engine started. However, there were hardly any obviously detectable N<sub>2</sub>O emissions during the trips. This indicated that when the catalyst temperature was higher than 450 C, N<sub>2</sub>O formation across the TWC was trivial. There is a clear N<sub>2</sub>O concentration spike in figure 9 at around 360 s, where the catalyst temperature is about ~400 C. This means that the ceiling of the temperature window for the formation of N<sub>2</sub>O could be approximately 400 C.

All the nitrogen compound emissions were related to the accelerations and positive VSP because of lambda deviation and more fuel pumped with each acceleration.

#### **5.2.4 Distance based cumulative mass emissions**

Figure 5-17 to Figure 5-24 show the cumulative mass emission gas as a function of the distance travelled for five nitrogen compounds. One of the main purposes of these diagrams is to illustrate the effect of pollutant accumulation on the congested traffic; the longer the vehicle stands still, the higher the accumulated emissions. Every main step increase in all the emissions are linked to stoppages of the vehicle. As the traffic lights, pedestrian crossings, left or right turns are marked in the diagrams, the accumulation of pollution can then be determined.

Day 3 EURO4 0746 A

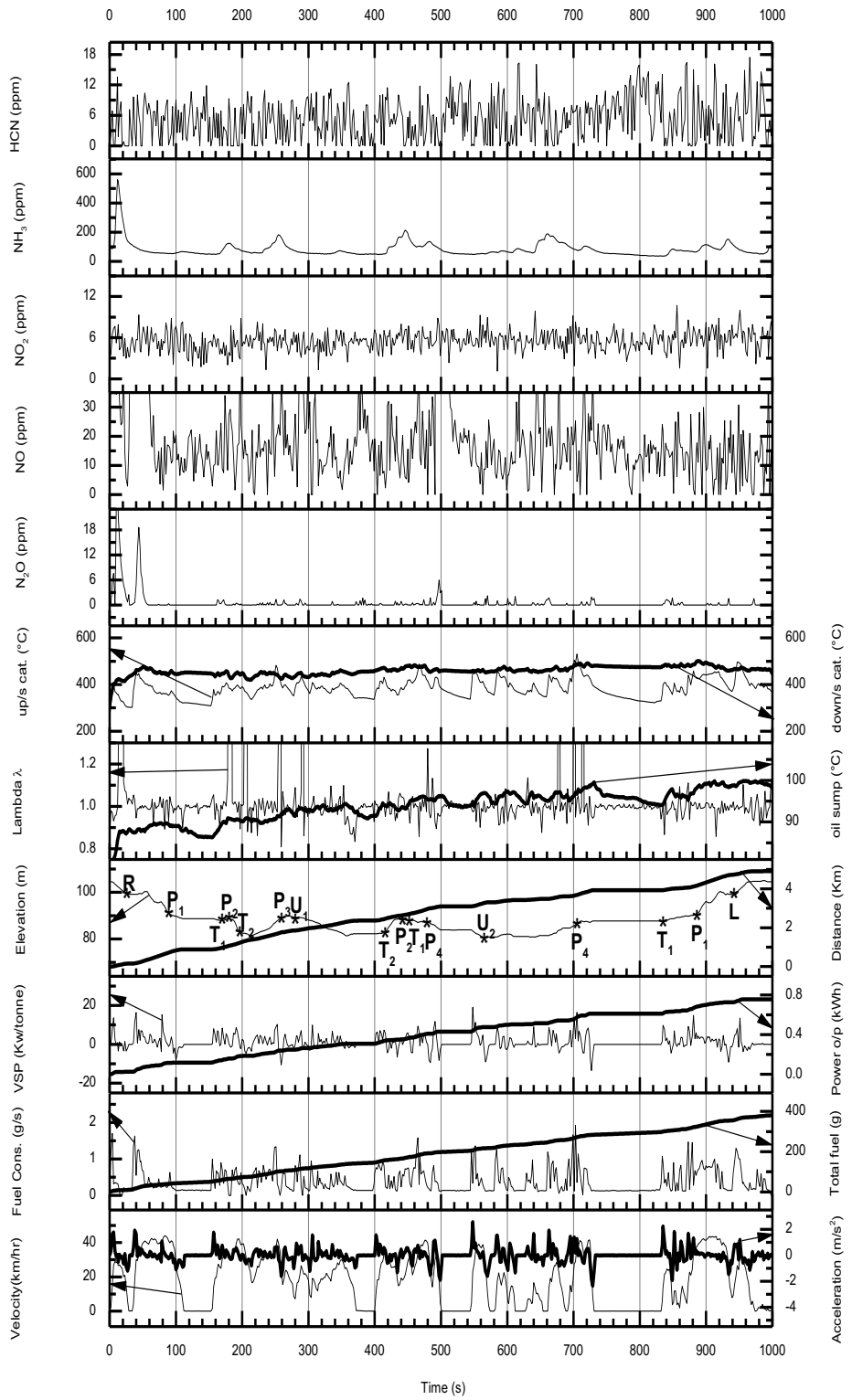


Figure 5-1 Profiles for the trip 7:46A-a.



Day 3 EURO4\_0830\_A

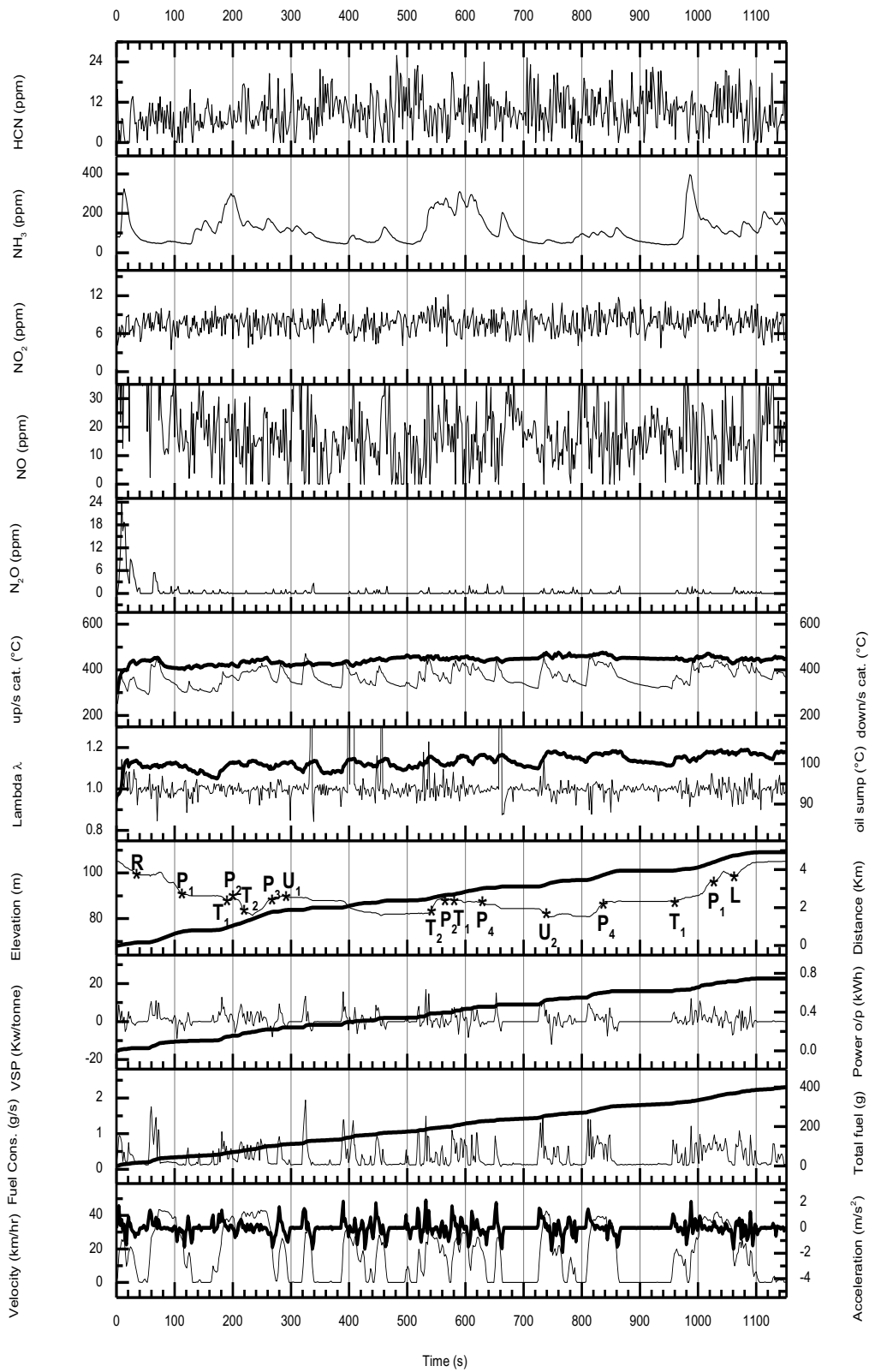


Figure 5-2 Profiles for the trip 8:30A.

Day 2 EURO4 1256 A

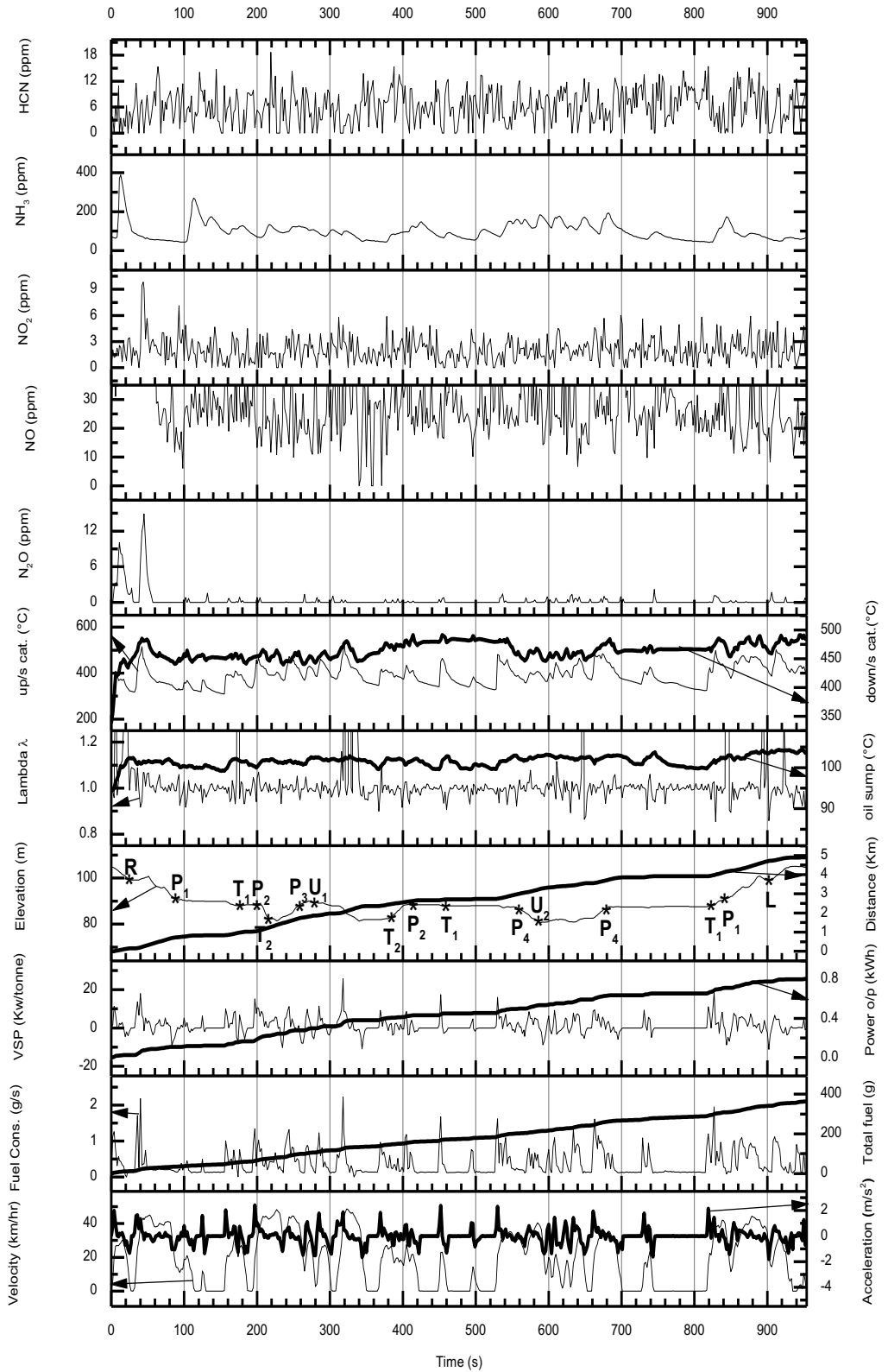
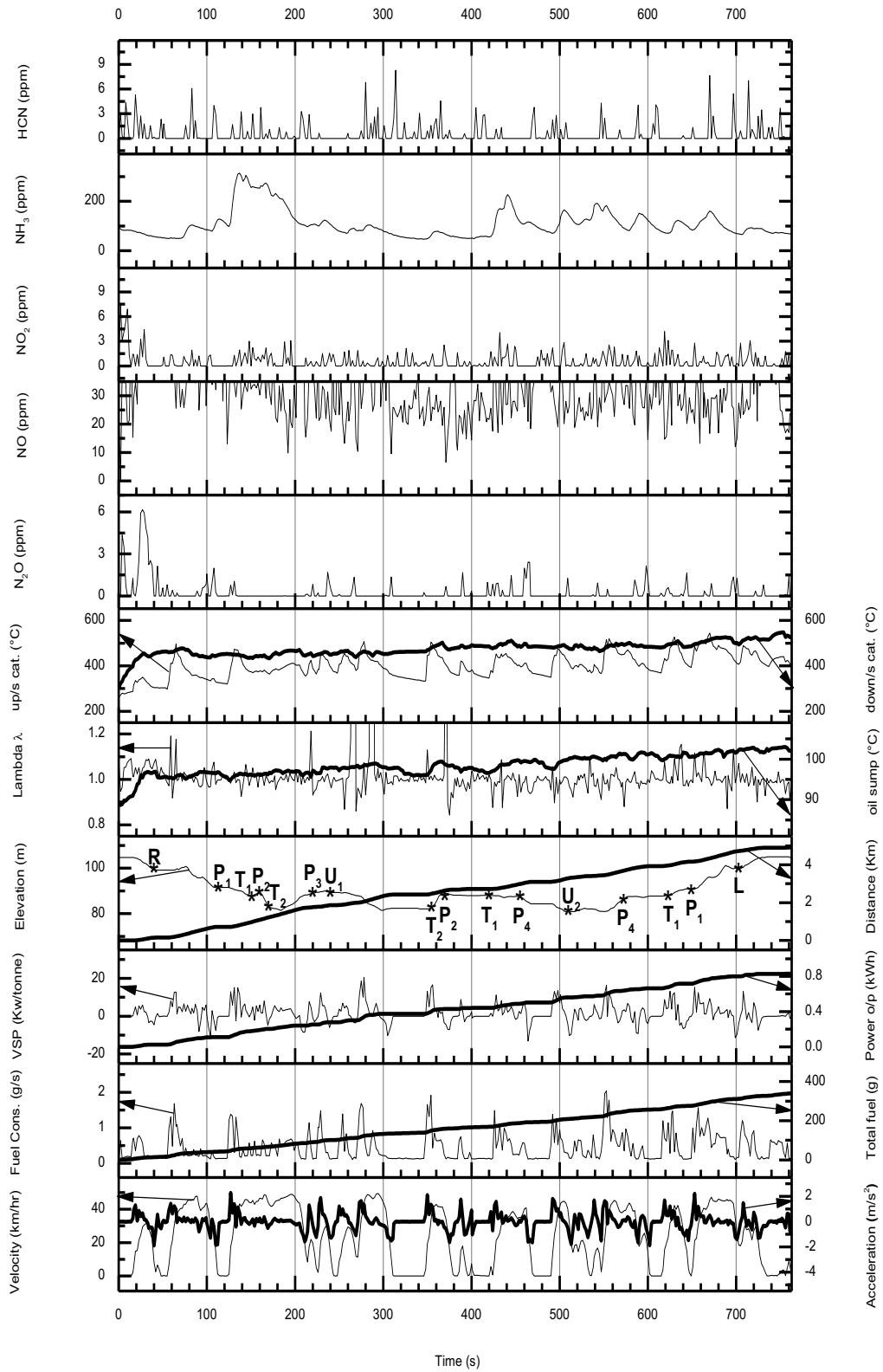


Figure 5-3 Profiles for the trip 12:56A-a.

### Day 1 EURO4 1925 A



**Figure 5-4 Profiles for the trip 19:25A-a.**

Day 3 EURO4\_0807\_B

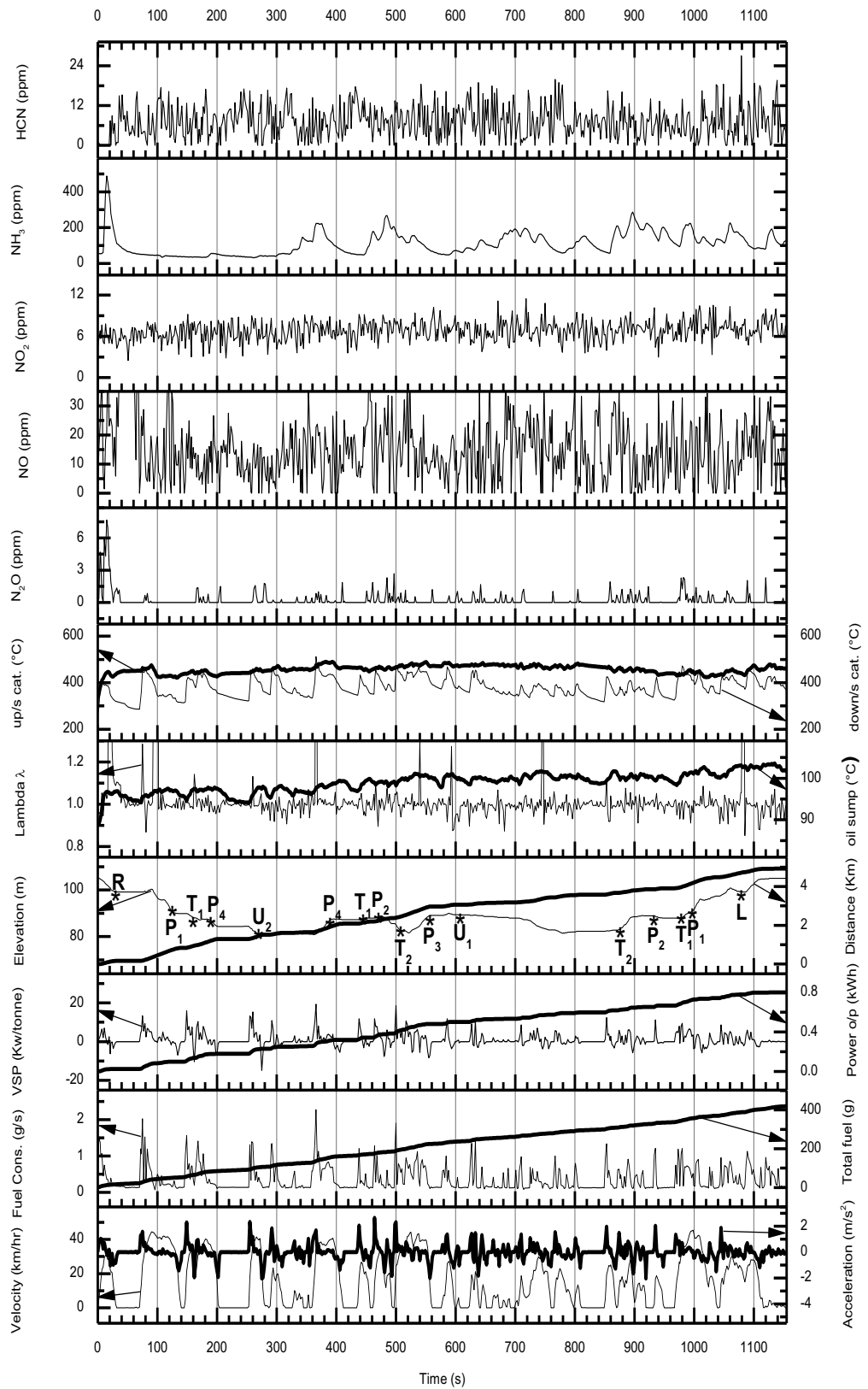


Figure 5-5 Profiles for the trip 8:07B-a.

Day 3 EURO4\_0853 B

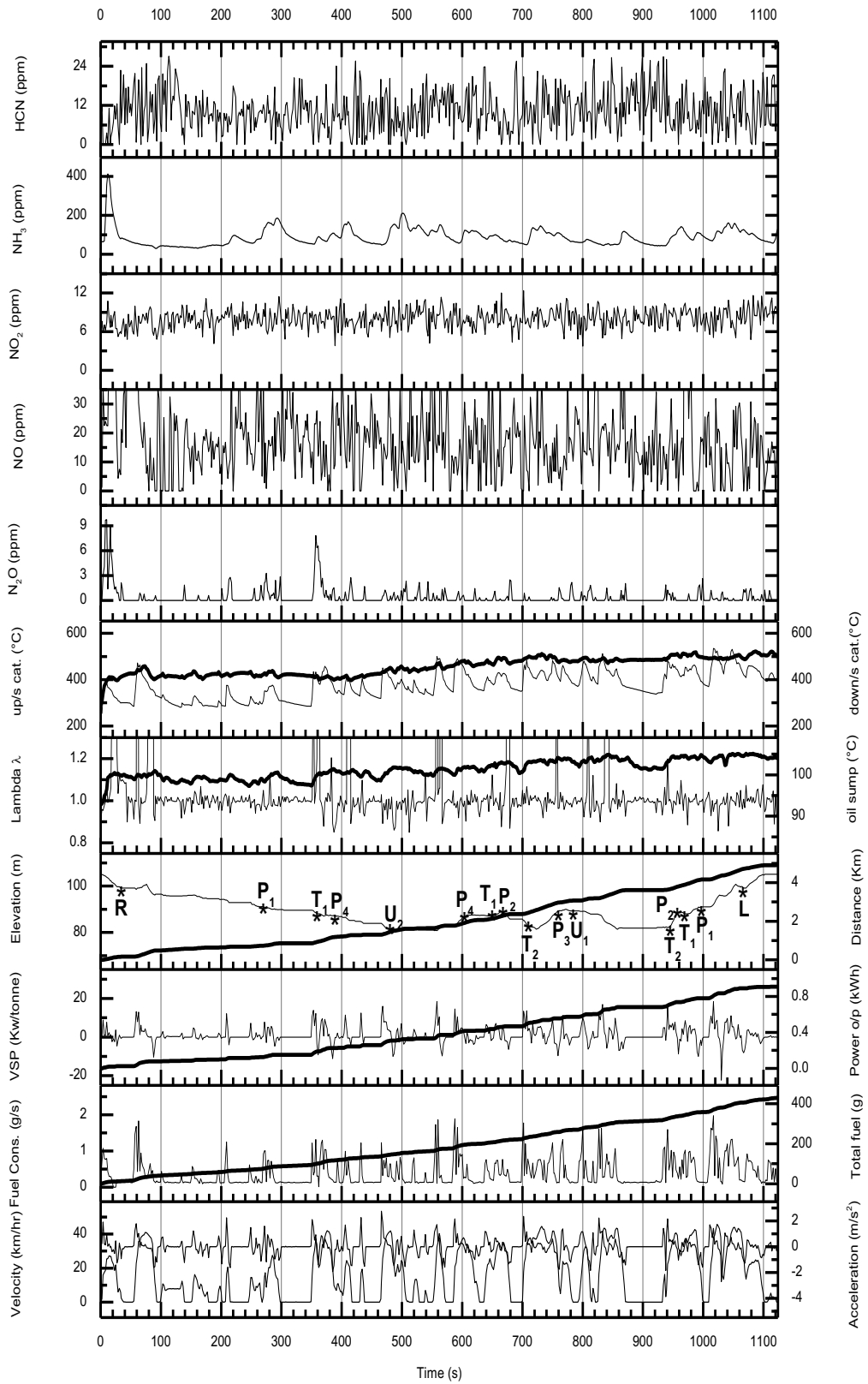


Figure 5-6 Profiles for the trip 8:53B-a.

Day 2 EURO4 1316 B

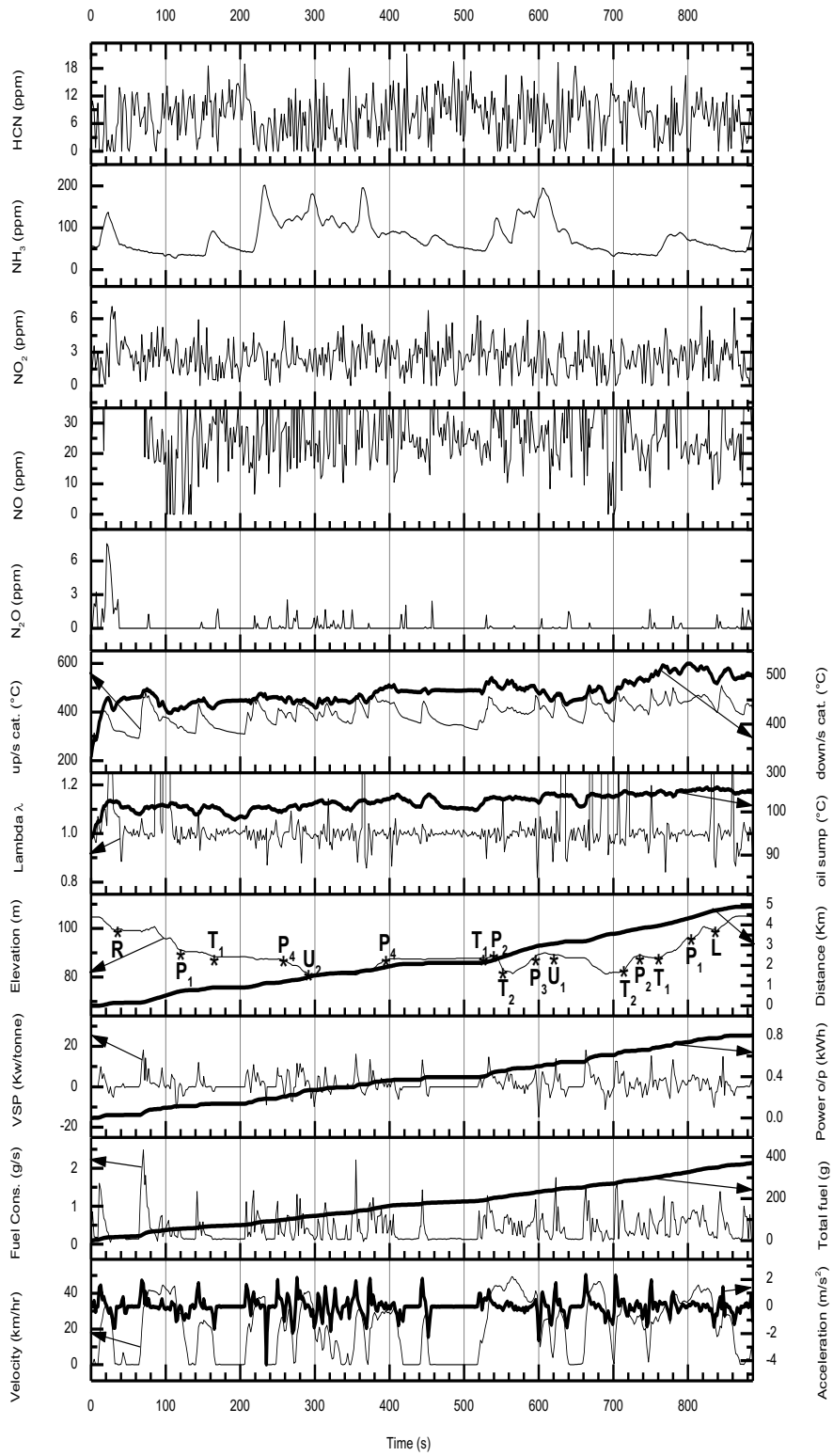


Figure 5-7 Profiles for the trip 13:16B-a.

Day 1 EURO4 1941 B

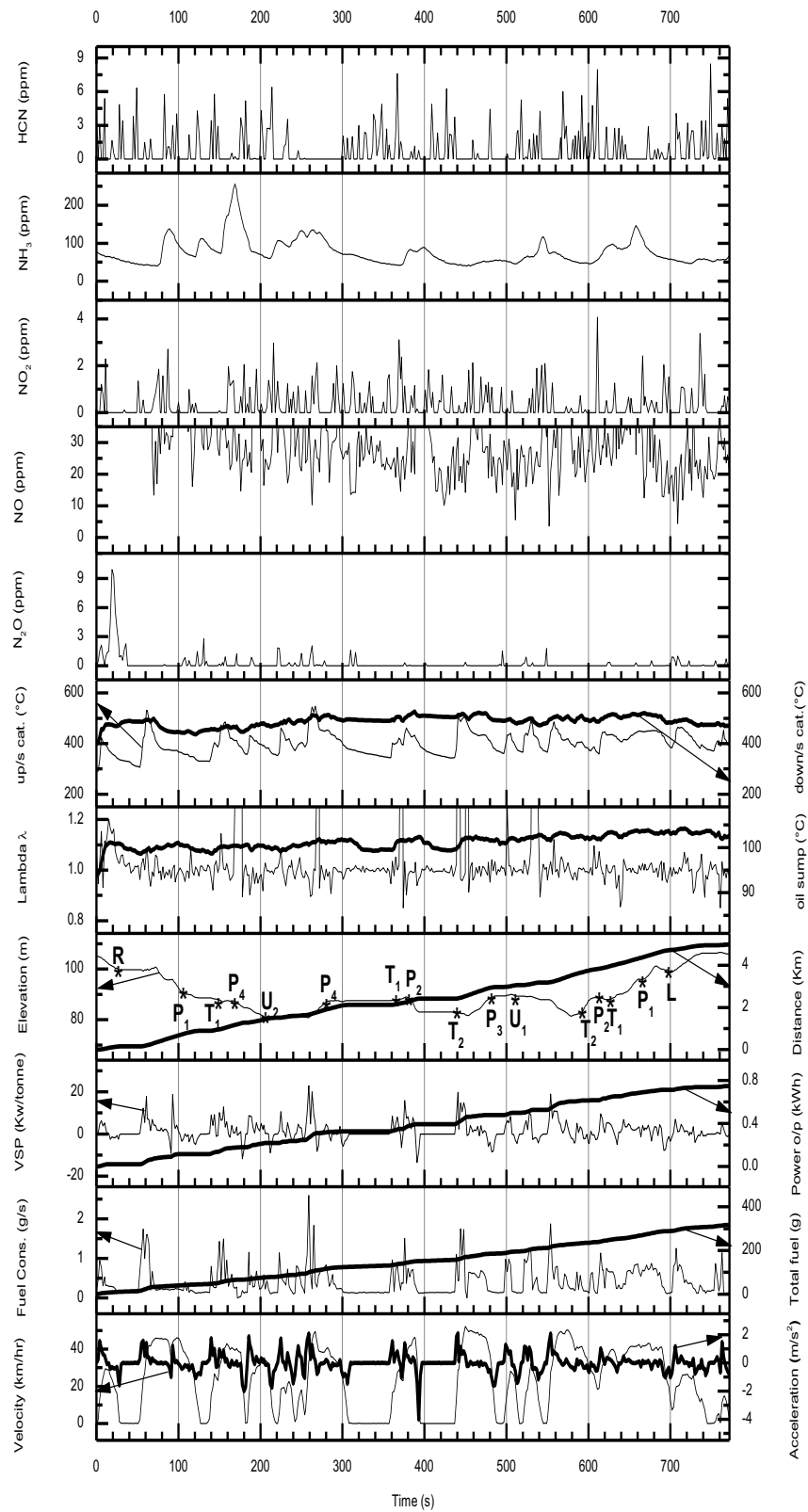


Figure 5-8 Profiles for the trip 19:41B-a.

Day 3 EURO4 0746 A

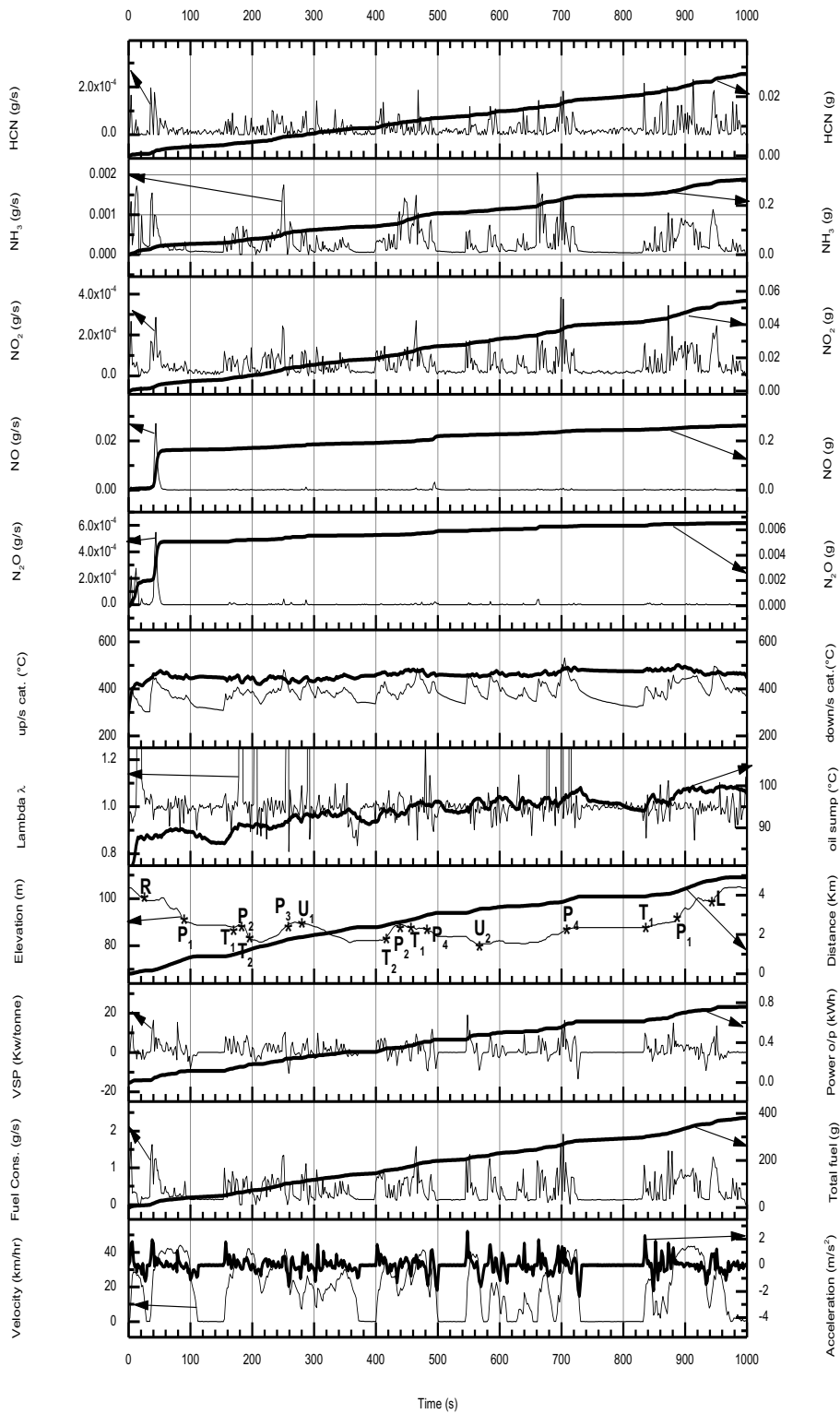


Figure 5-9 Profiles for the trip 7:46A-b.



Day 3 EURO4 0830 A

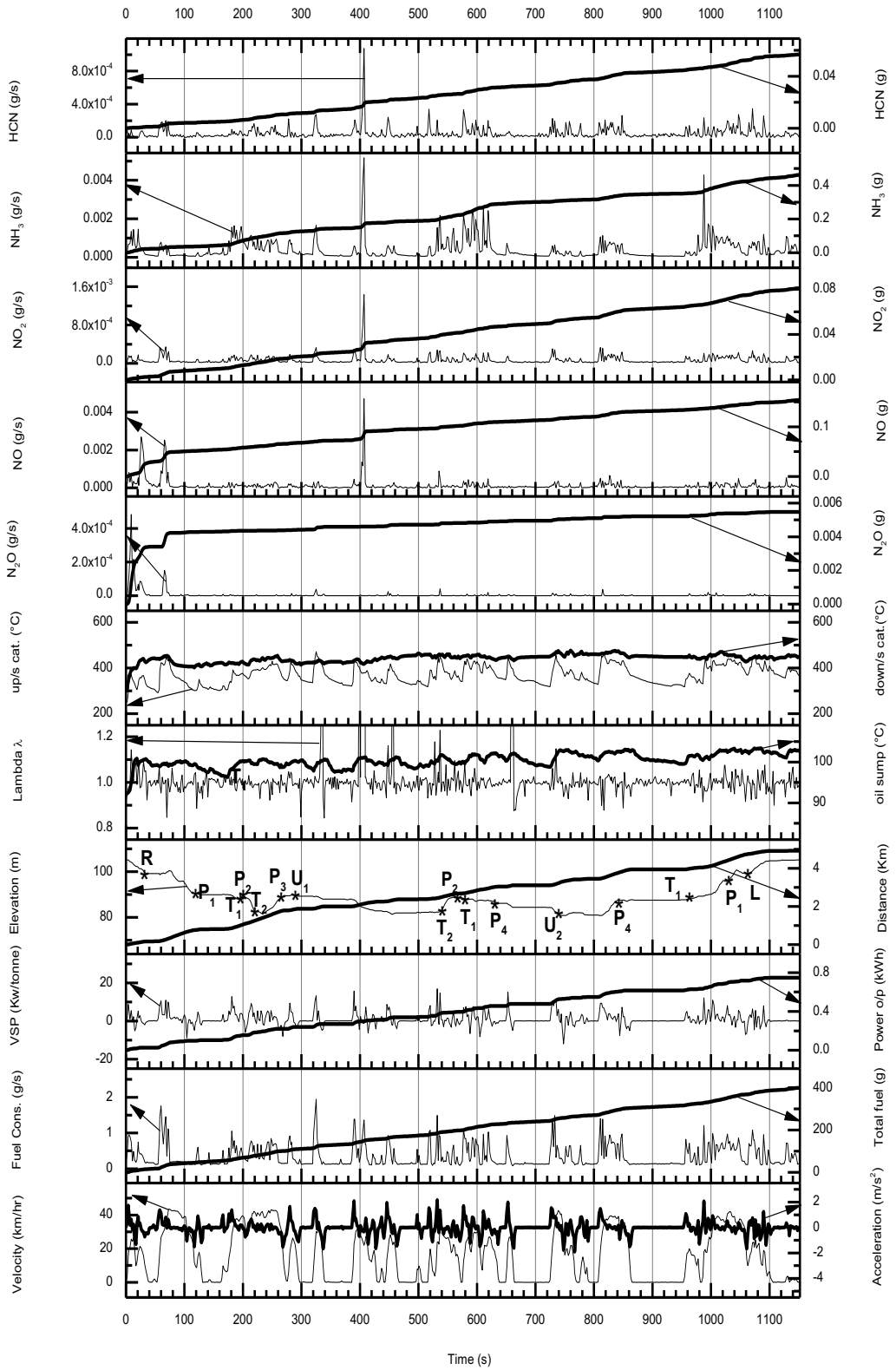


Figure 5-10 Profiles for the trip 8:30A-b.

Day 2 EURO4 1256 A

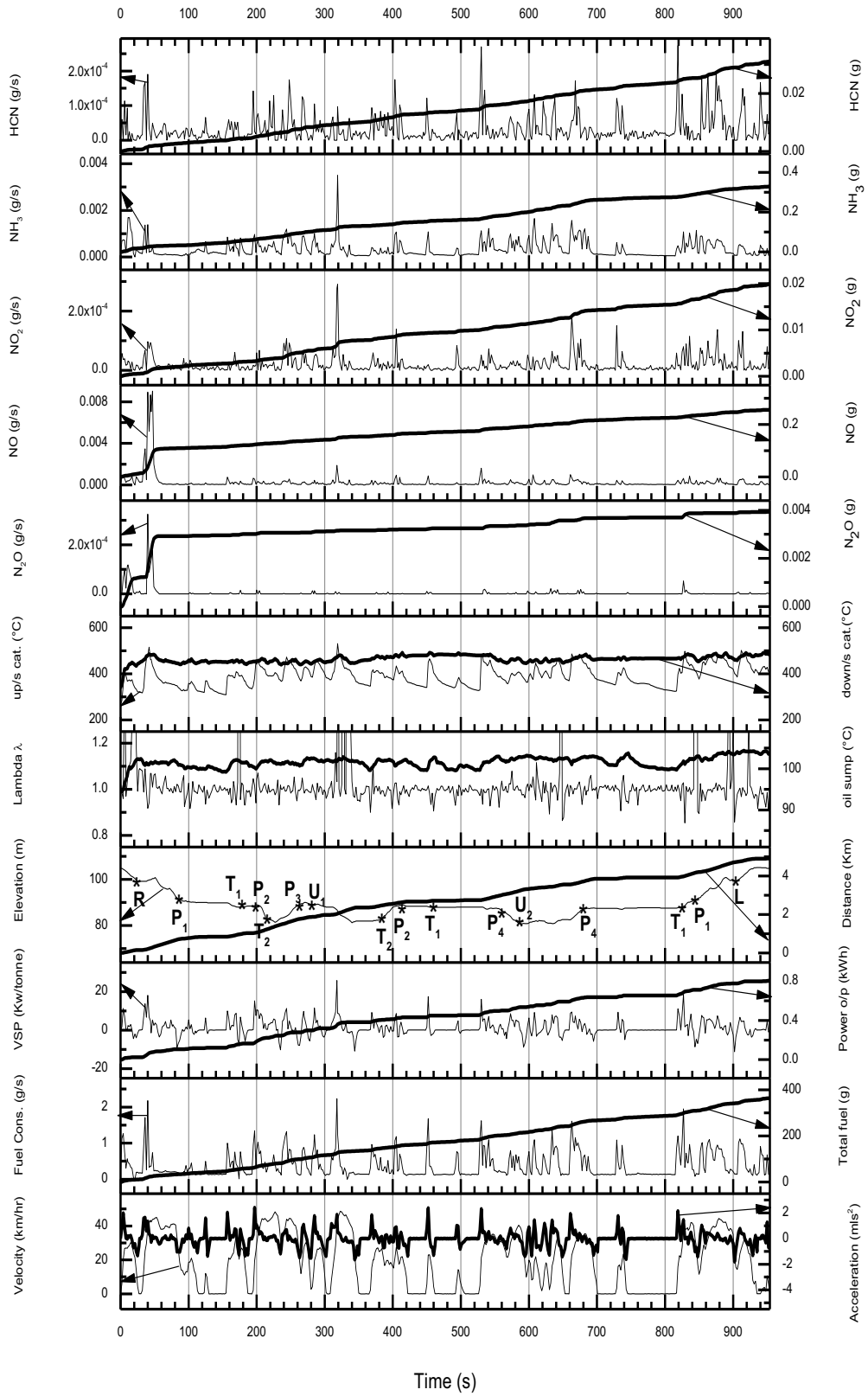


Figure 5-11 Profiles for the trip 12:56A-b.

Day 1 EURO4 1925\_A

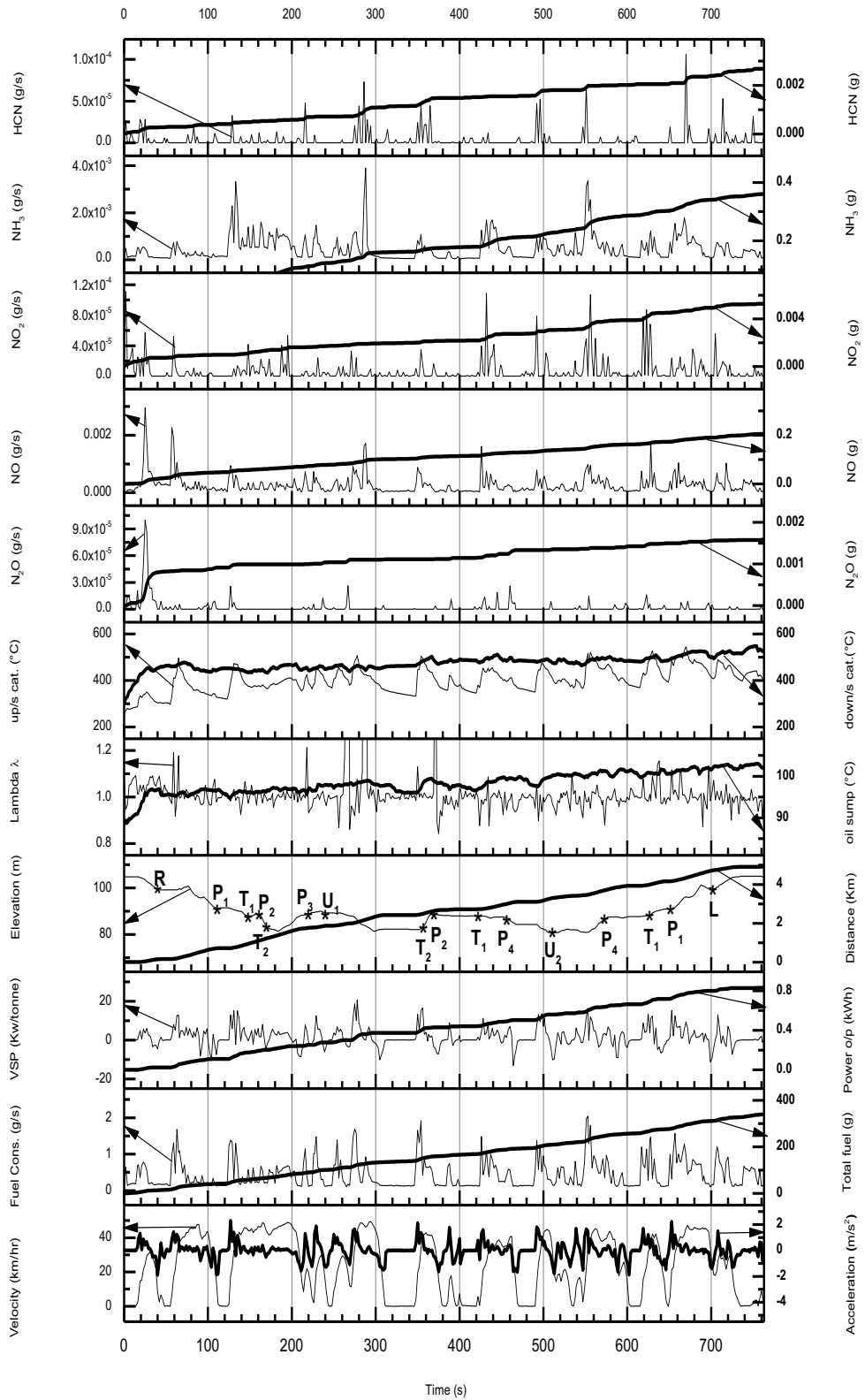


Figure 5-12 Profiles for the trip 19:25A-b.

Day 3 EURO4\_0807\_B

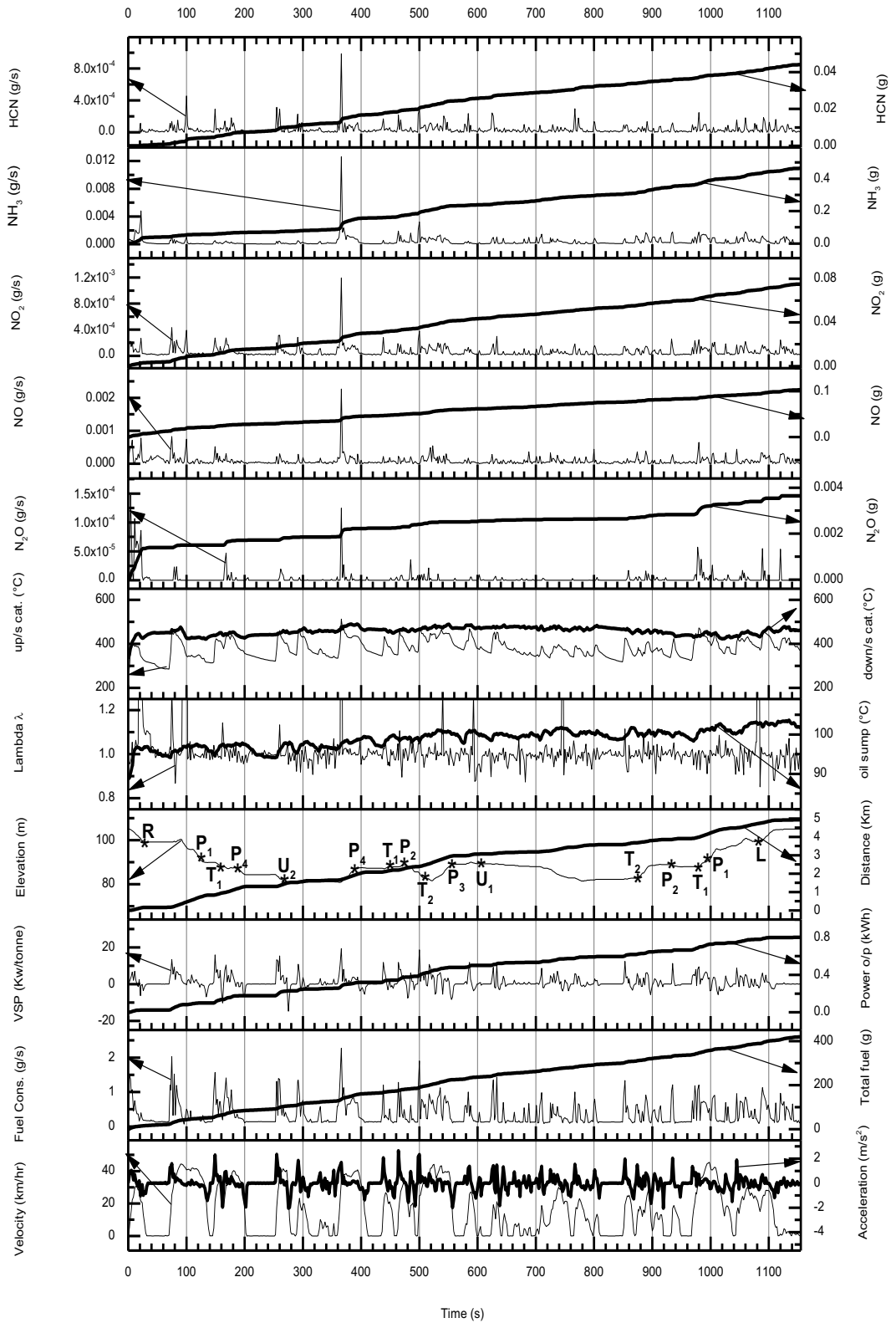


Figure 5-13 Profiles for the trip 8:07B-b.

Day 3 EURO4 0853 B

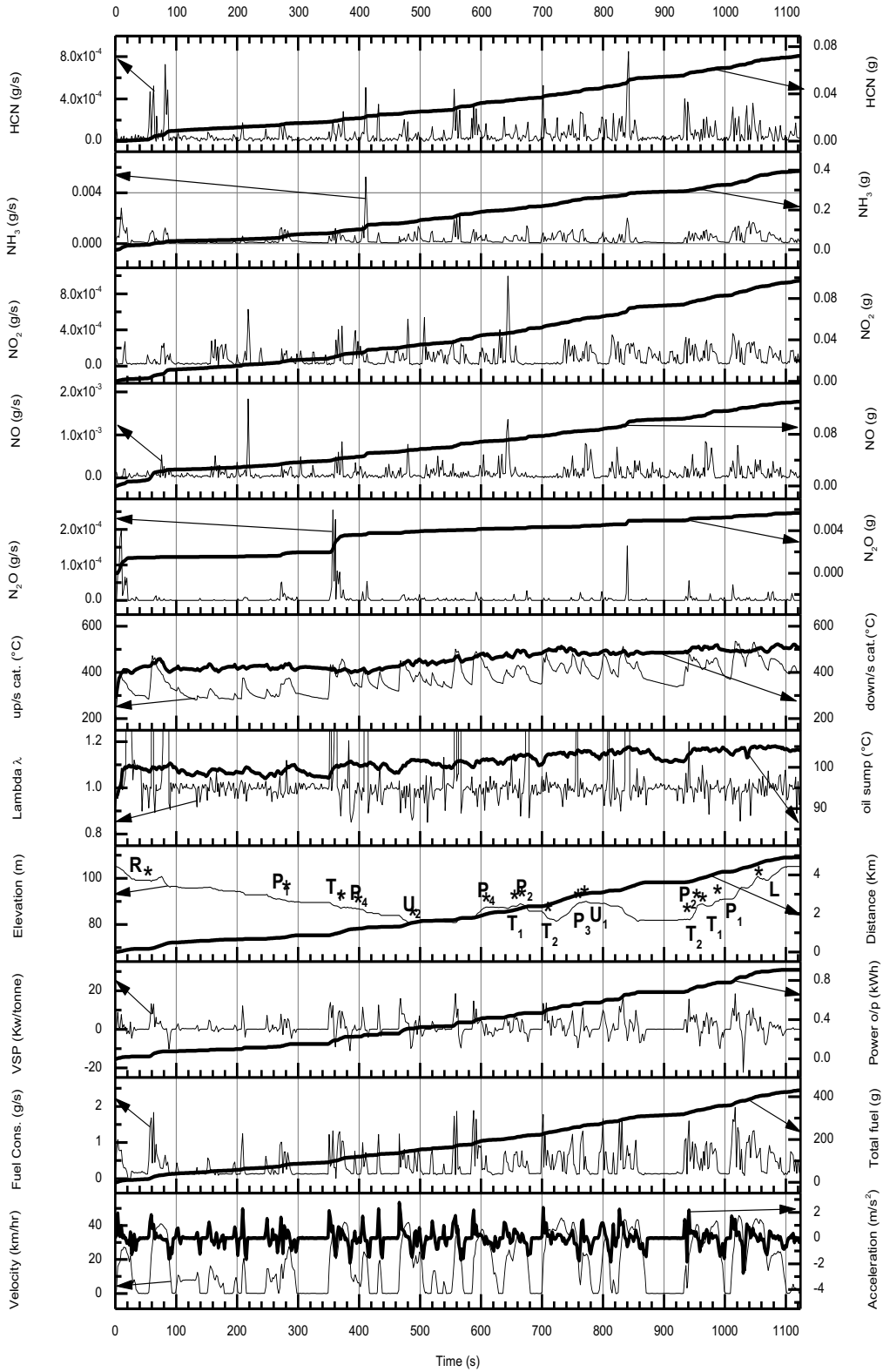


Figure 5-14 Profiles for the trip 8:53B-b.

Day 2 EURO4\_1316\_B

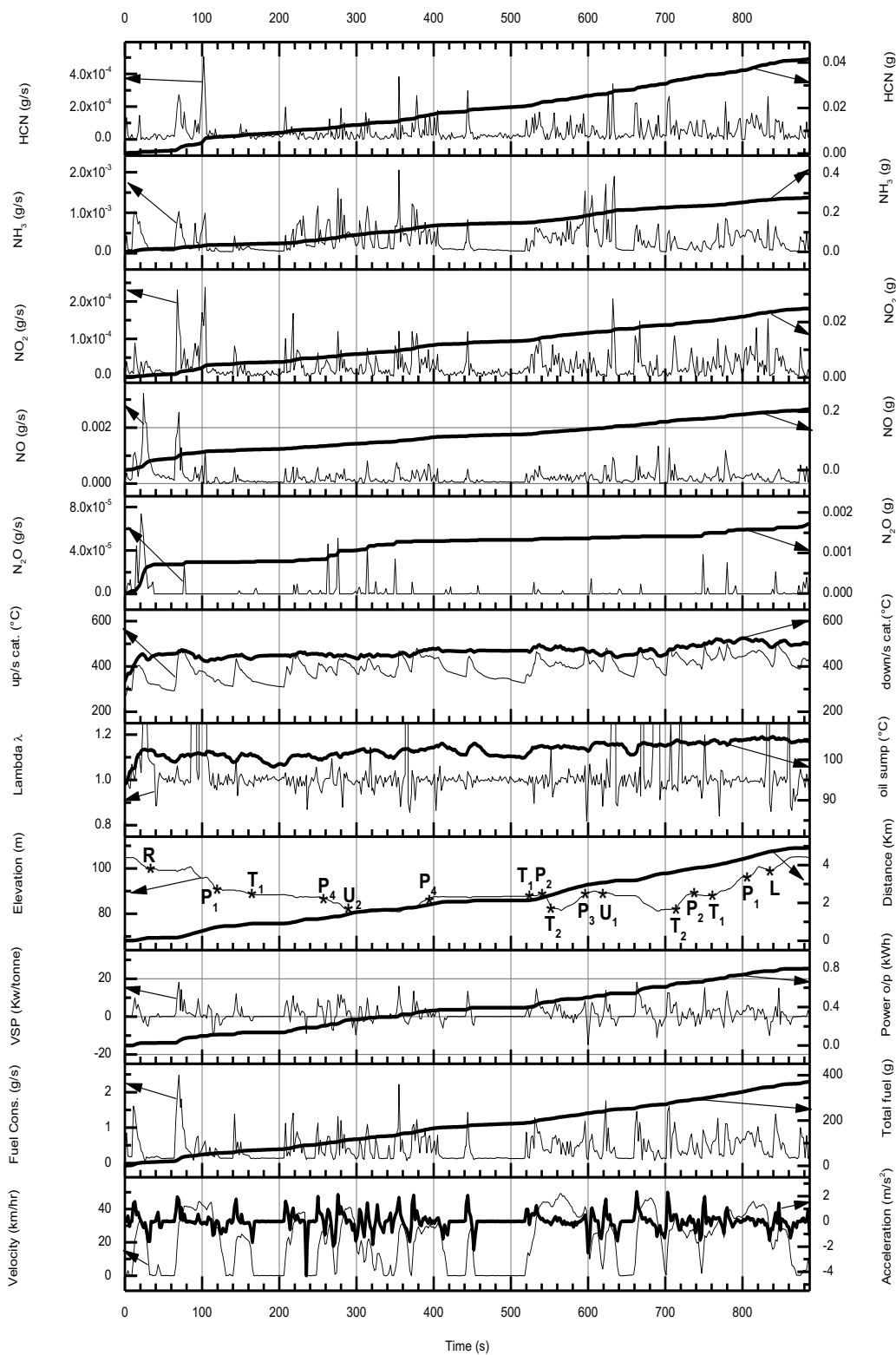


Figure 5-15 Profiles for the trip 13:16B-b.

Day 1 EURO4 1941\_B

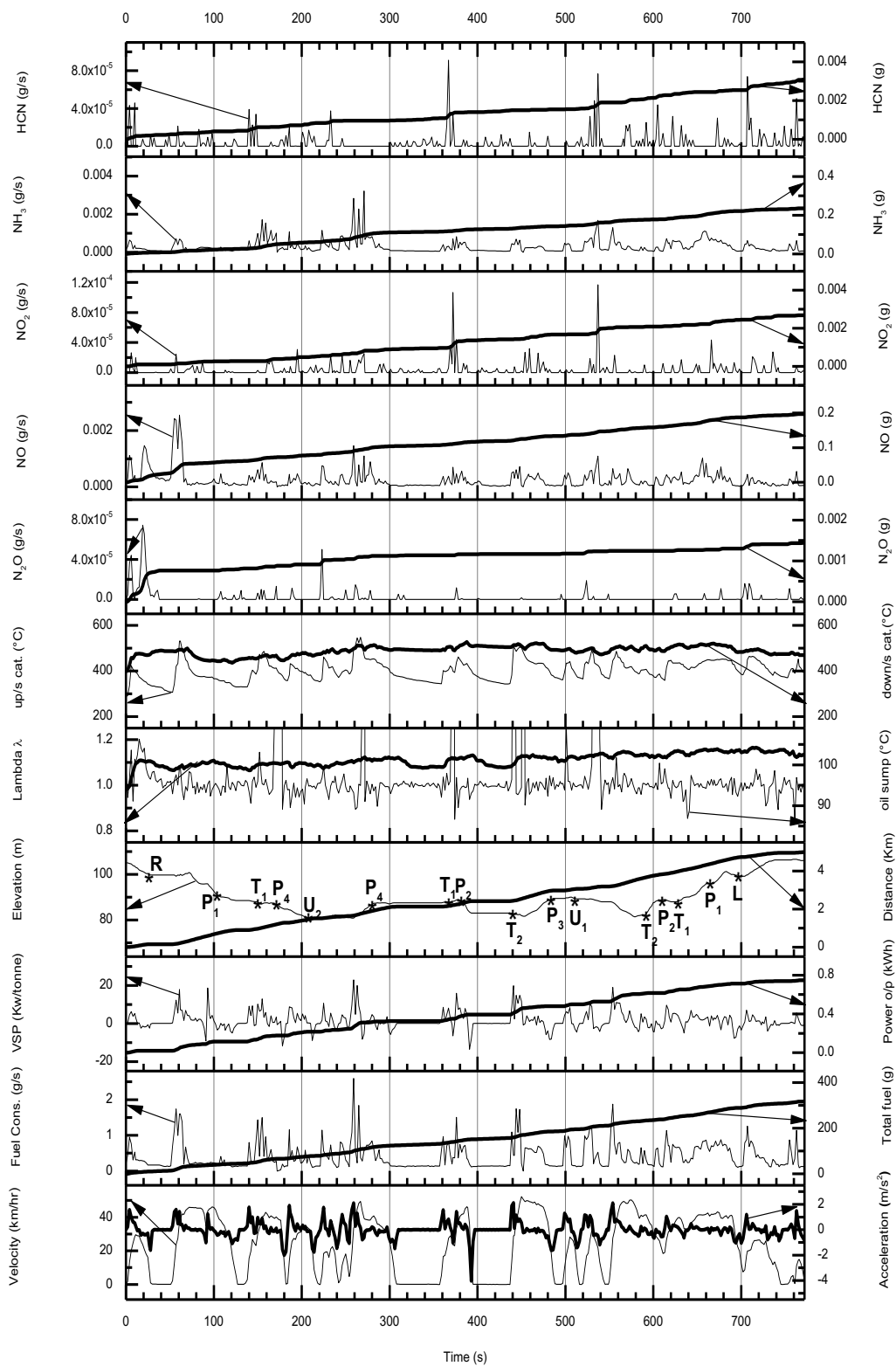


Figure 5-16 Profiles for the trip 19:41B-b.

Day 3 EURO4\_0746\_A

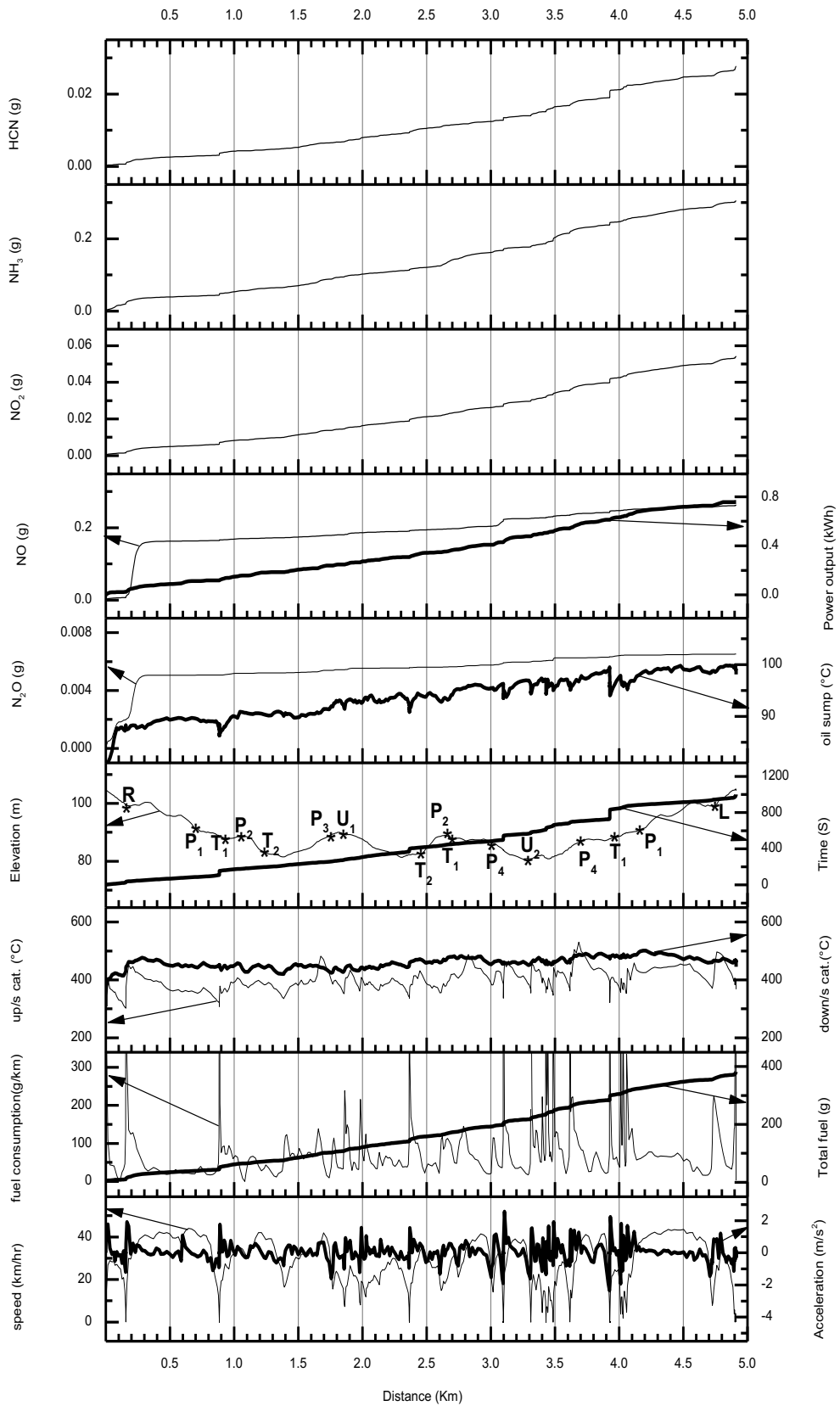


Figure 5-17 Profiles for the trip 7:46A-c



Day 3 EURO4 0830 A

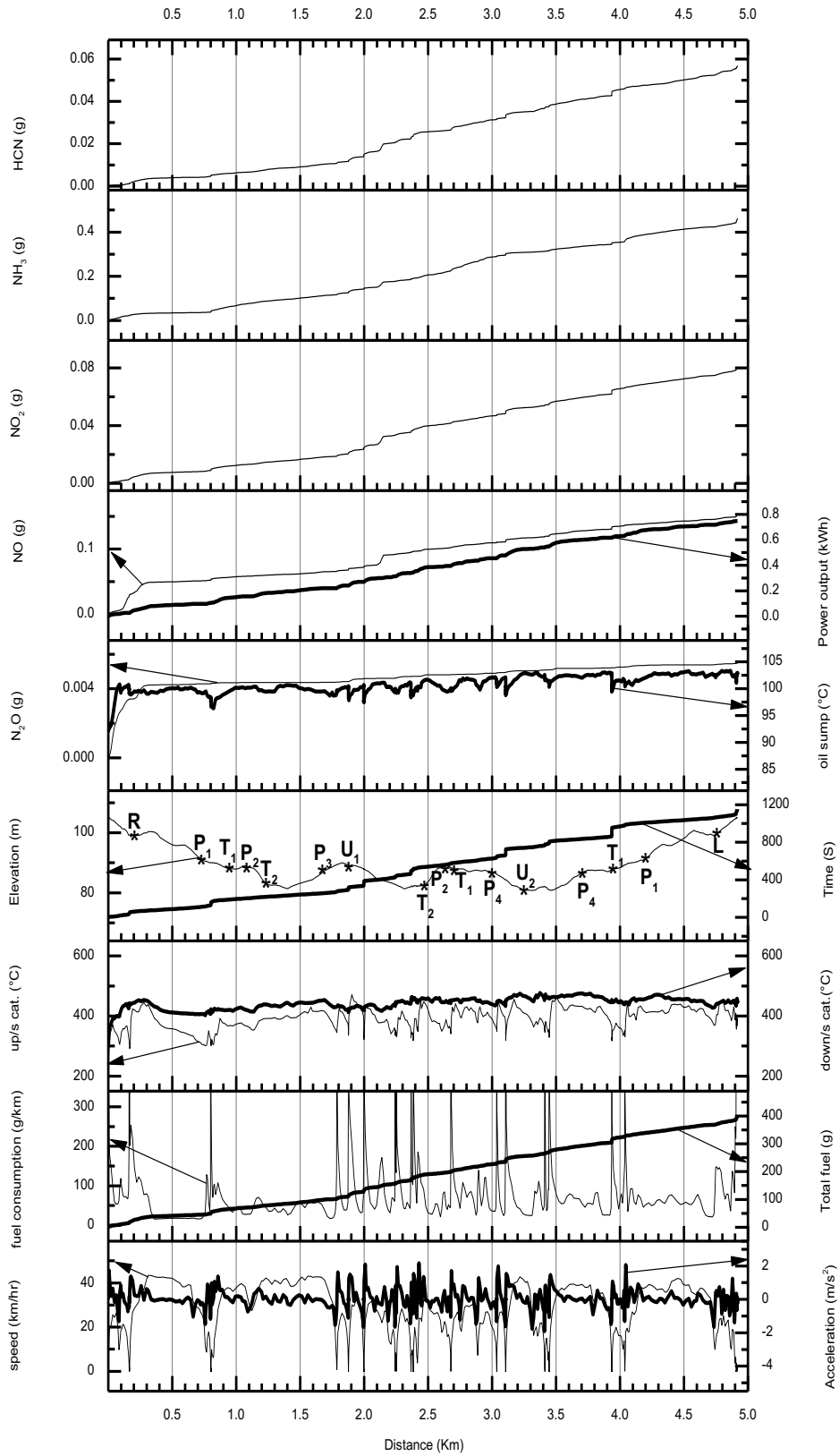


Figure 5-18 Profiles for the trip 8:30A-c.

Day 2 EURO4 1256 A

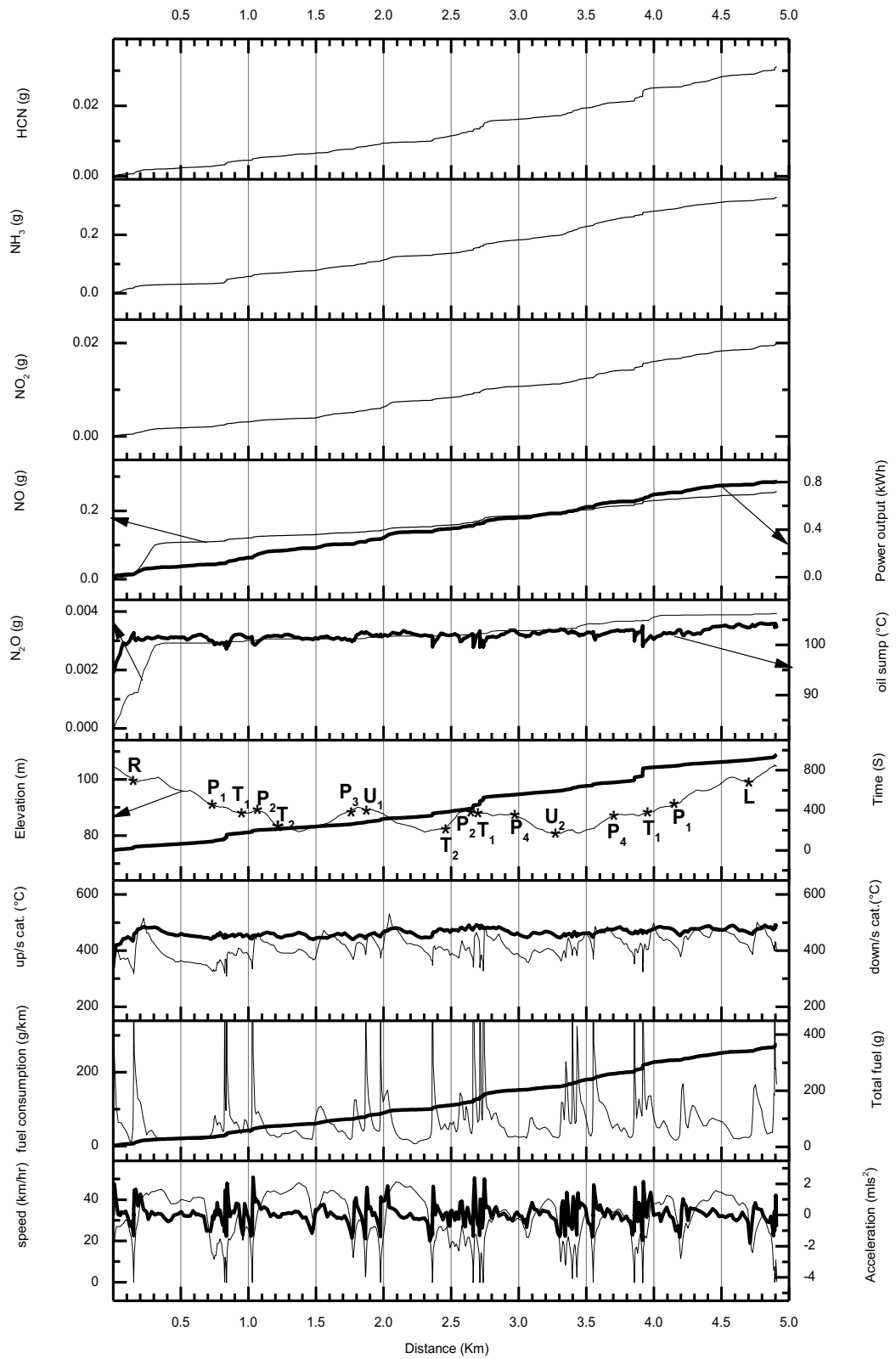


Figure 5-19 Profiles for the trip 12:56A-c.

Day 1 EURO4 1925 A

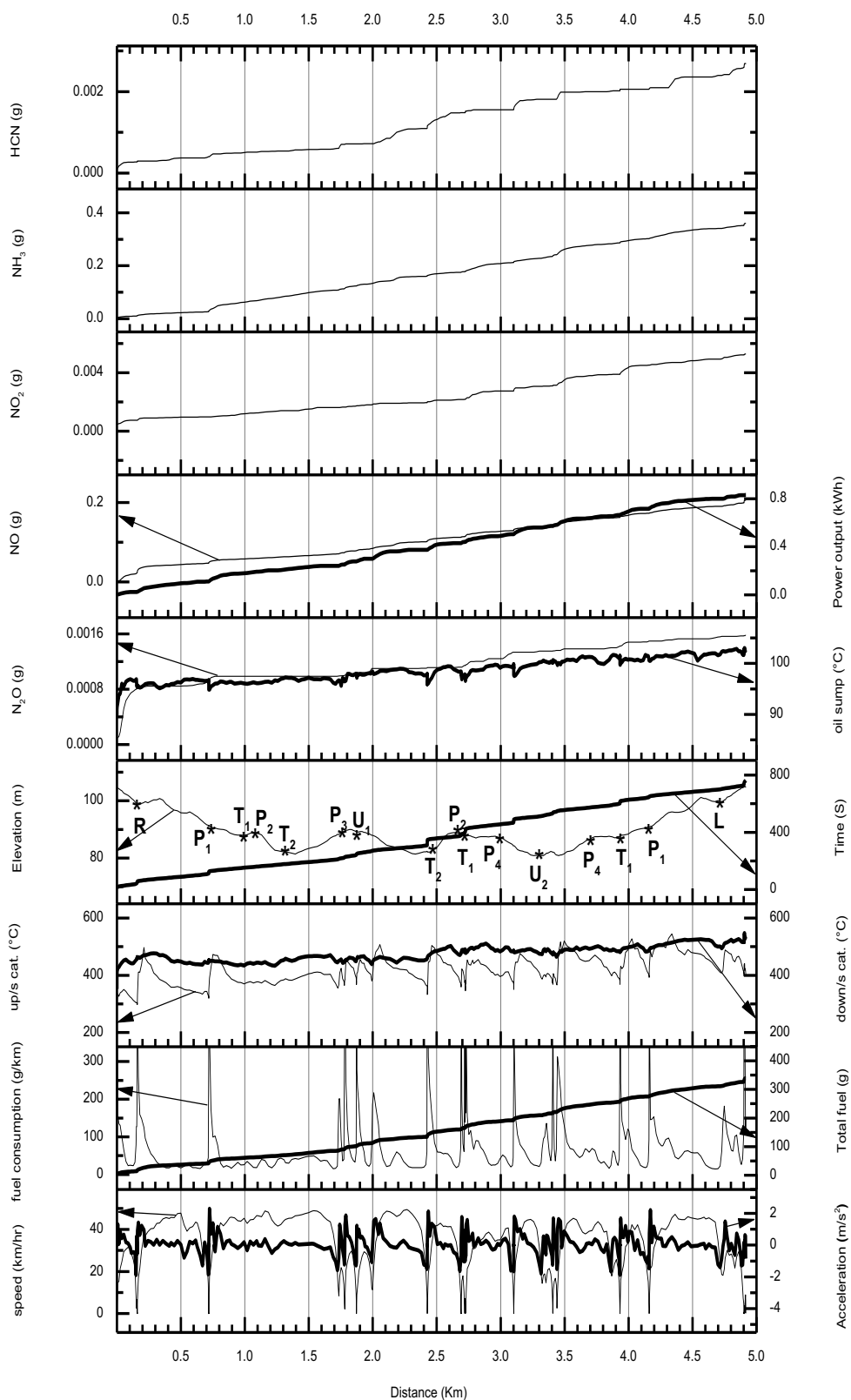


Figure 5-20 Profiles for the trip 19:25A-c.

Day 3 EURO4\_0807\_B

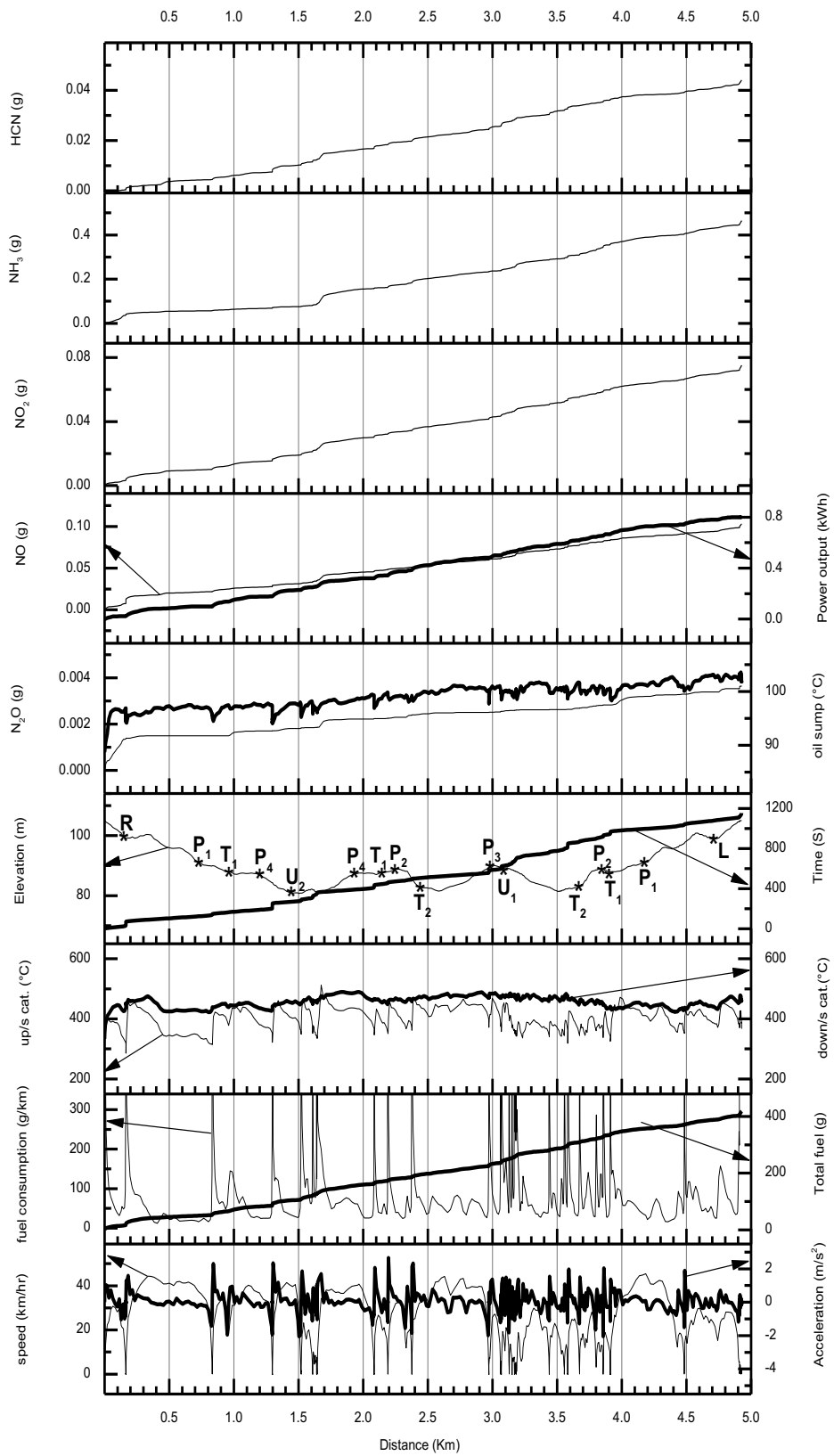


Figure 5-21 Profiles for the trip 8:07B-c.

Day 3 EURO4 0853 B

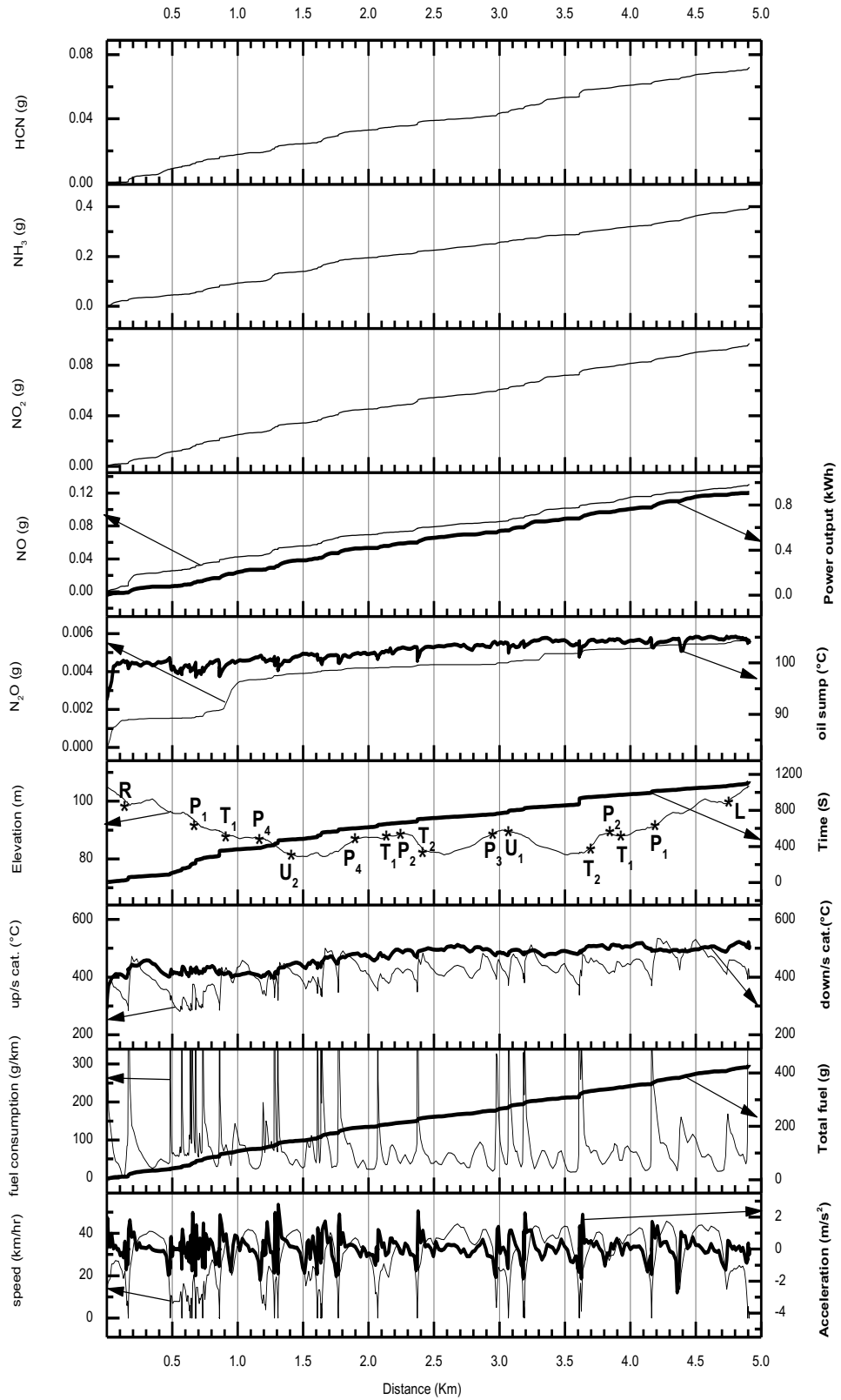


Figure 5-22 Profiles for the trip 8:53B-c.

Day 2 EURO4 1316\_B

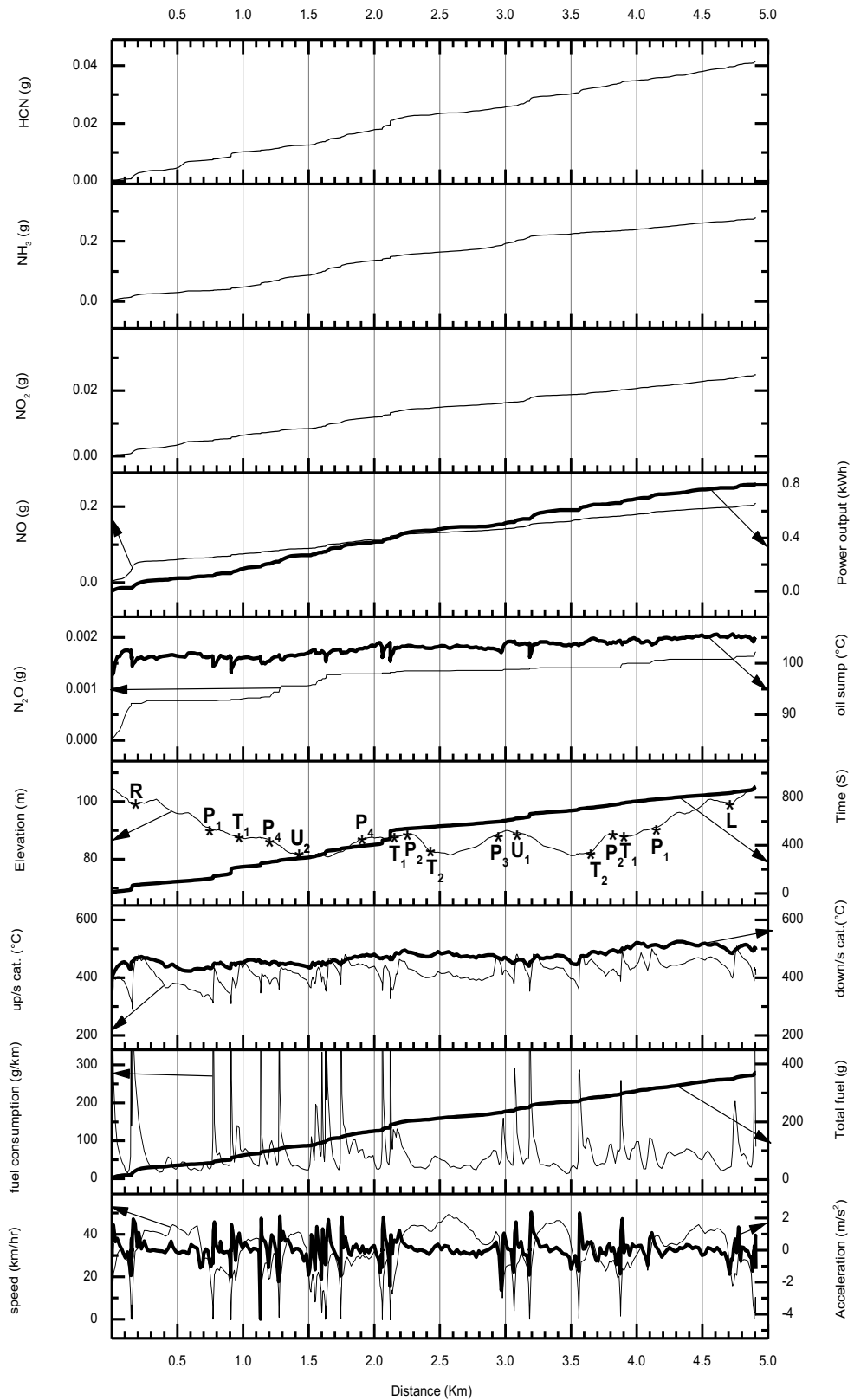


Figure 5-23 Profiles for the trip 13:16B-c.

Day 1 EURO4\_1941\_B

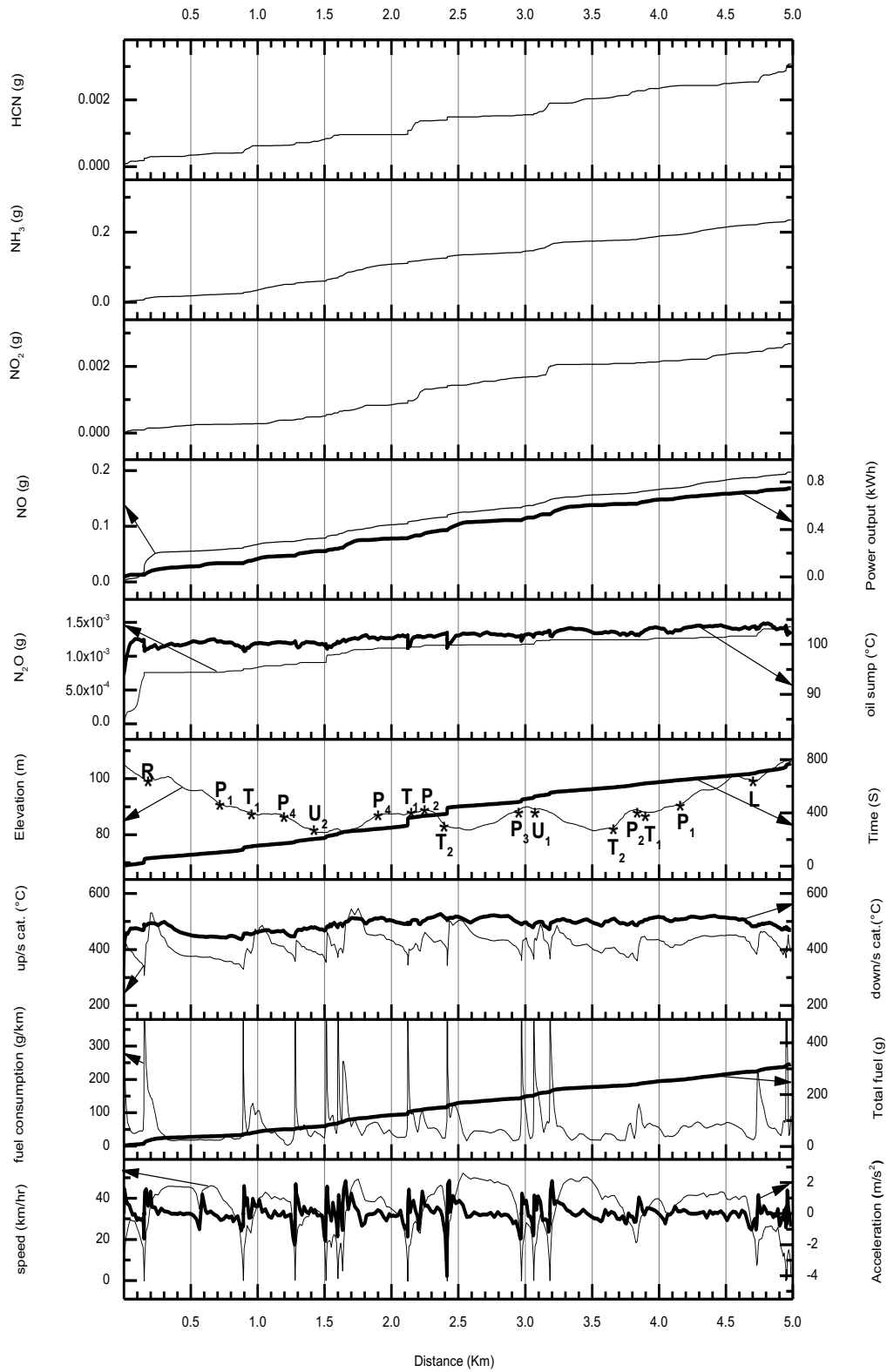


Figure 5-24 Profiles for the trip 19:41B-c.

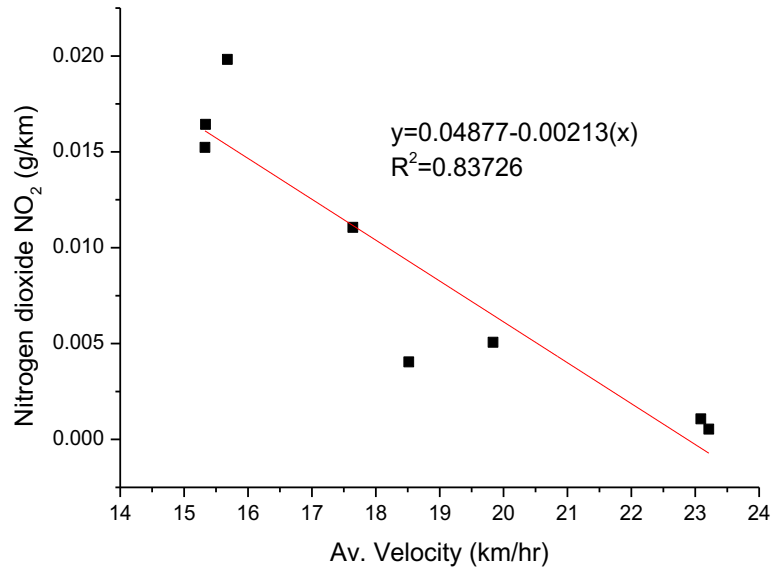
### 5.3 Correlations between emissions and driving parameters

Figure 5-25 to Figure 5-29 present the relationship between emissions of five nitrogen compounds and trip average velocity for eight trips.  $\text{NO}_2$  and HCN showed good negative linear correlation with trip average velocity; i.e. increasing the average velocity will decrease the emissions of  $\text{NO}_2$  and HCN.  $\text{NH}_3$  and  $\text{N}_2\text{O}$  showed a moderate negative correlation with the average velocity. There was no correlation observed for NO with average velocity. The reductions in  $\text{NO}_2$ , HCN and  $\text{NH}_3$ , with increased average velocity, might be due to reduced congestion and more free-flowing driving and thus fewer rich spikes in lambda. The reduction in  $\text{N}_2\text{O}$  with increased average velocity is probably due to the fact that the catalyst temperatures exceeded the  $\text{N}_2\text{O}$  formation window.

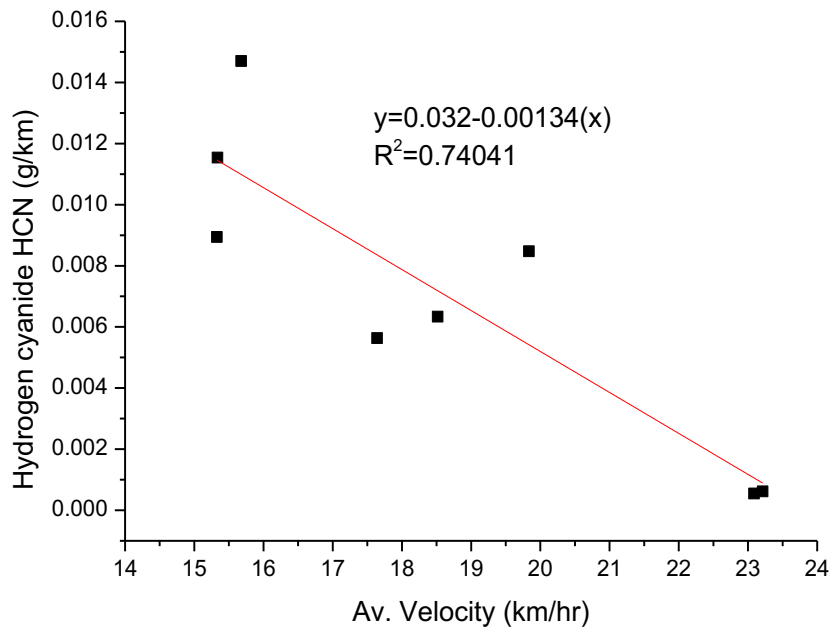
Figure 5-30 to Figure 5-34 present the relationship between emissions of five nitrogen compounds and trip average acceleration for eight trips. There were no correlations observed between the five nitrogen compounds and average accelerations. This is surprising as accelerations could directly affect the air/fuel ratio and lambda, especially harsh accelerations, tending to cause rich spikes, and thus produce more emissions. One of the reasons could be that average accelerations are not a good parameter for trip characterization, at least not on its own.

Figure 5-35 to Figure 5-39 present the relationship between emissions of five nitrogen compounds and trip average VSP for eight trips.  $\text{NO}_2$  and  $\text{N}_2\text{O}$  showed good negative linear correlation with average VSP.  $\text{NH}_3$  and HCN showed a moderate negative correlation with average VSP. There was no correlation observed between NO and average VSP. The correlations are similar to those between emissions and average velocity. This is because for a fixed vehicle and a fixed testing route, the values of VSP are determined by travel velocity.





**Figure 5-25 Trip mean NO<sub>2</sub> emissions vs vehicle's average trip velocity.**



**Figure 5-26 Trip mean HCN emissions vs vehicle's average trip velocity.**

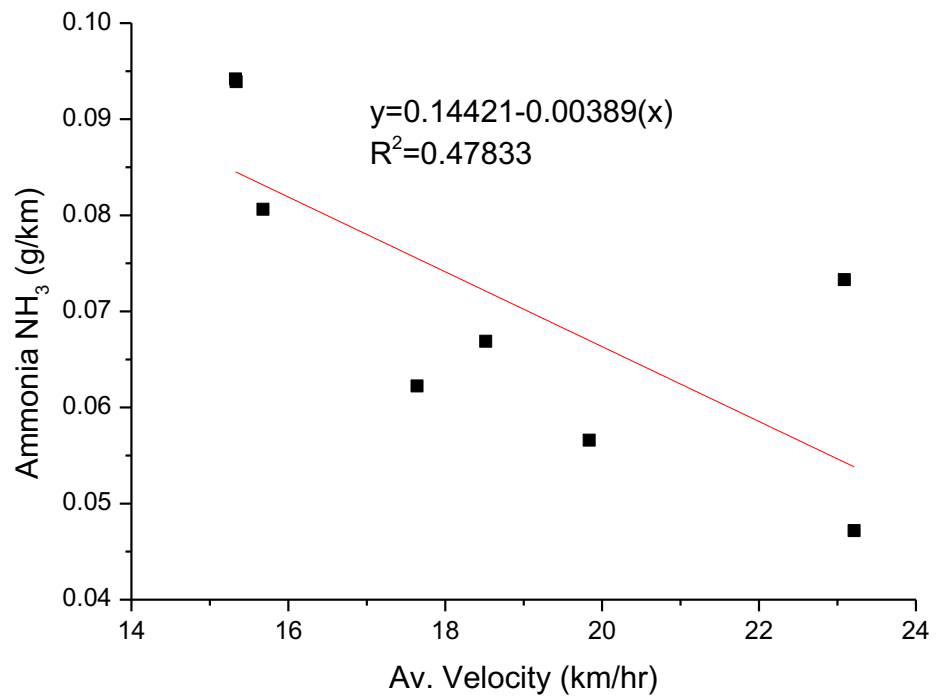


Figure 5-27 Trip mean NH<sub>3</sub> emissions vs vehicle's average trip velocity.

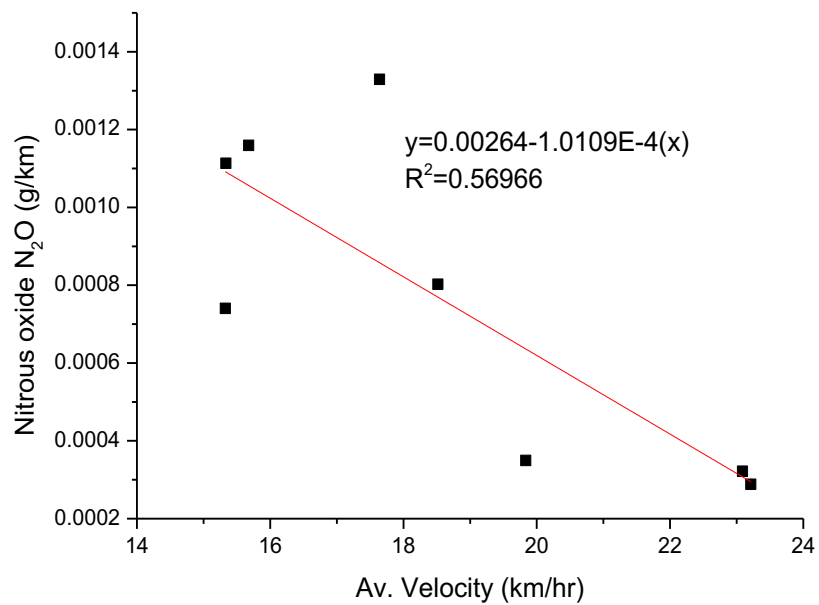
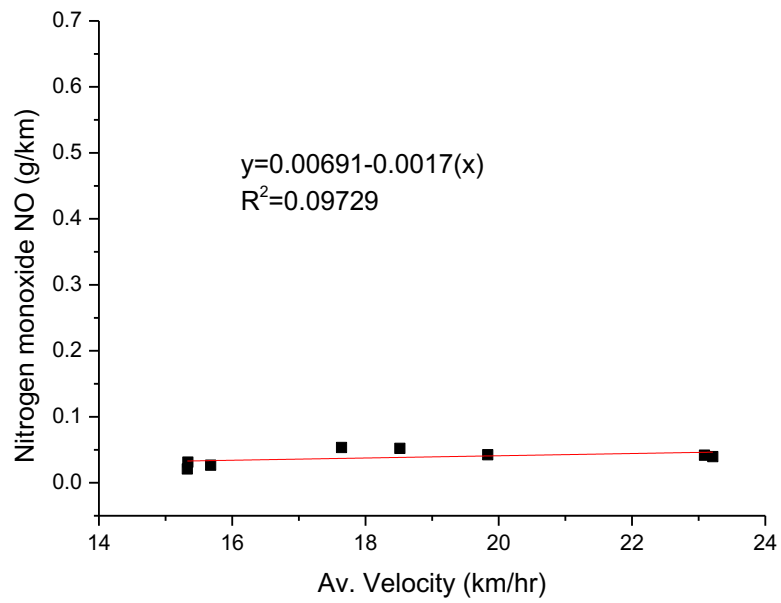
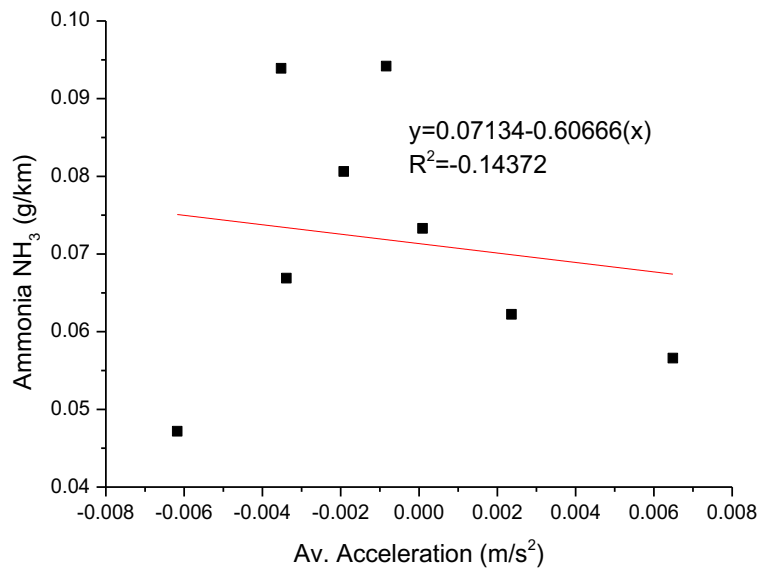


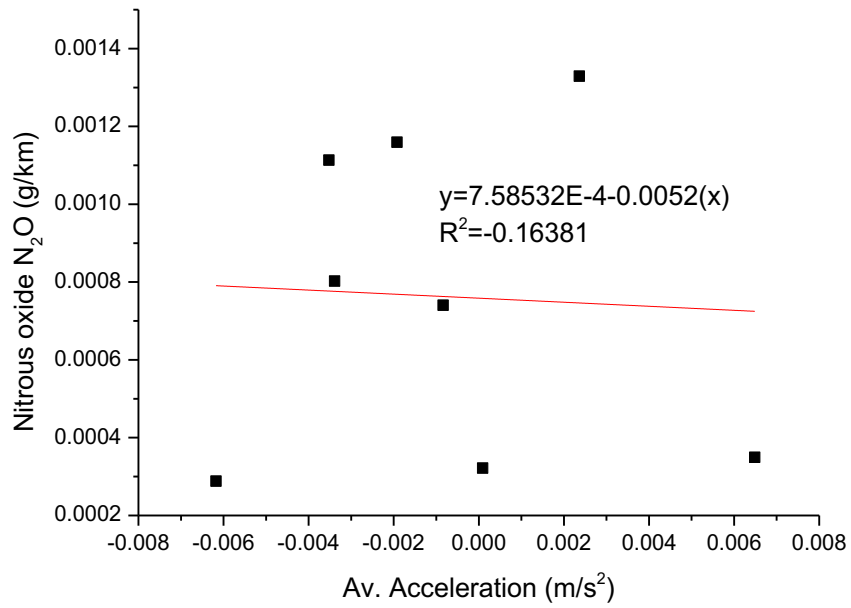
Figure 5-28 Trip mean N<sub>2</sub>O emissions vs vehicle's average trip velocity.



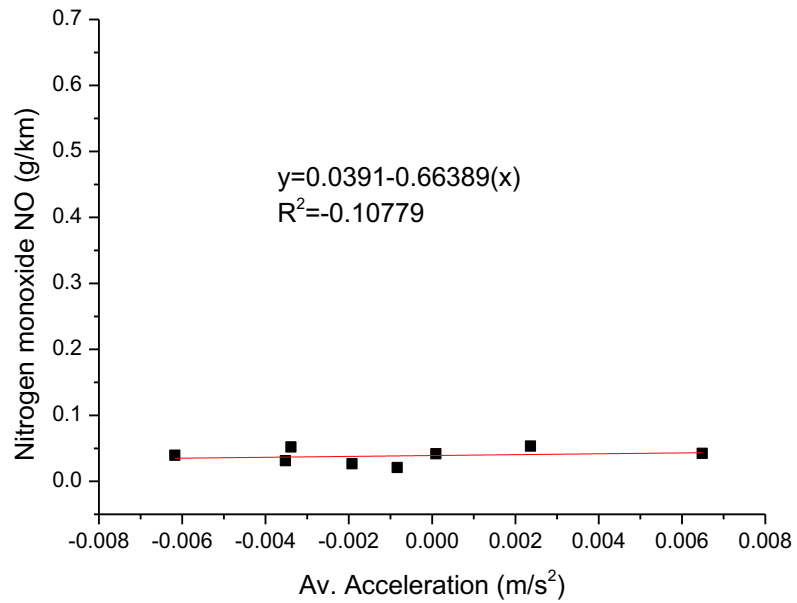
**Figure 5-29 Trip mean NO emissions vs vehicle's average trip velocity.**



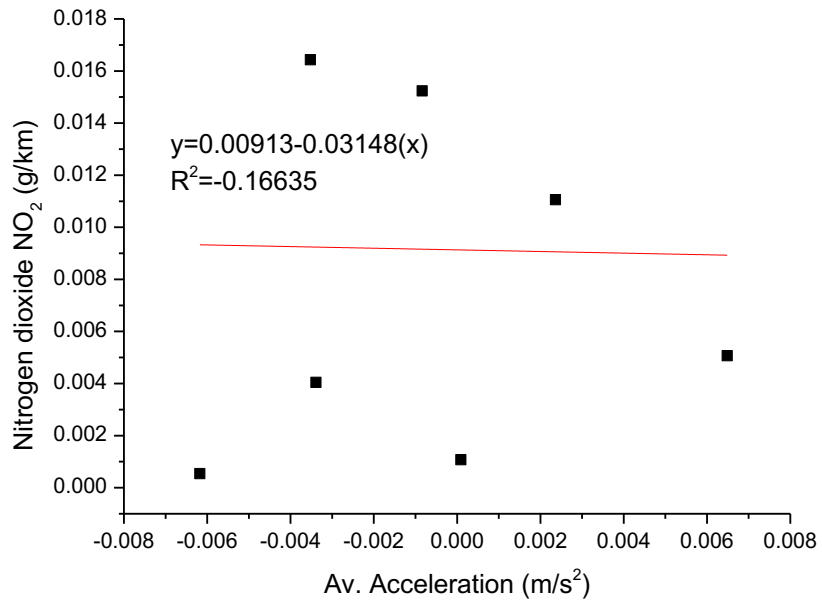
**Figure 5-30 Trip mean NH<sub>3</sub> emissions vs vehicle's average trip acceleration.**



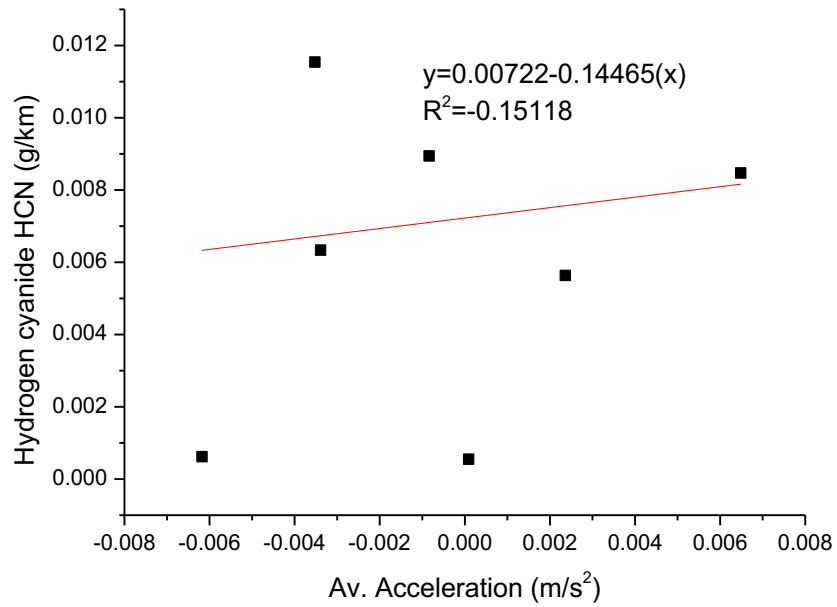
**Figure 5-31 Trip mean N<sub>2</sub>O emissions vs vehicle's average trip acceleration.**



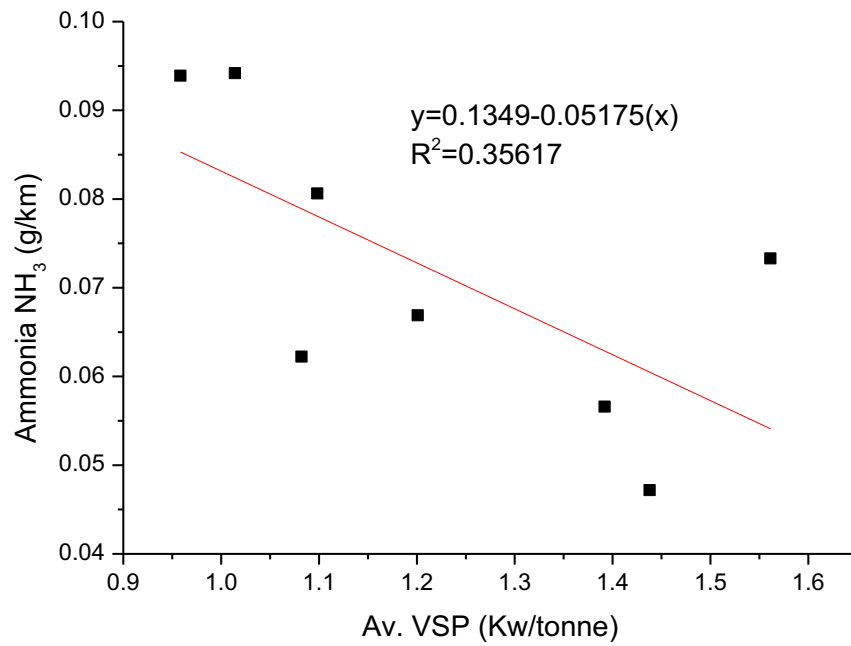
**Figure 5-32 Trip mean NO emissions vs vehicle's average trip acceleration.**



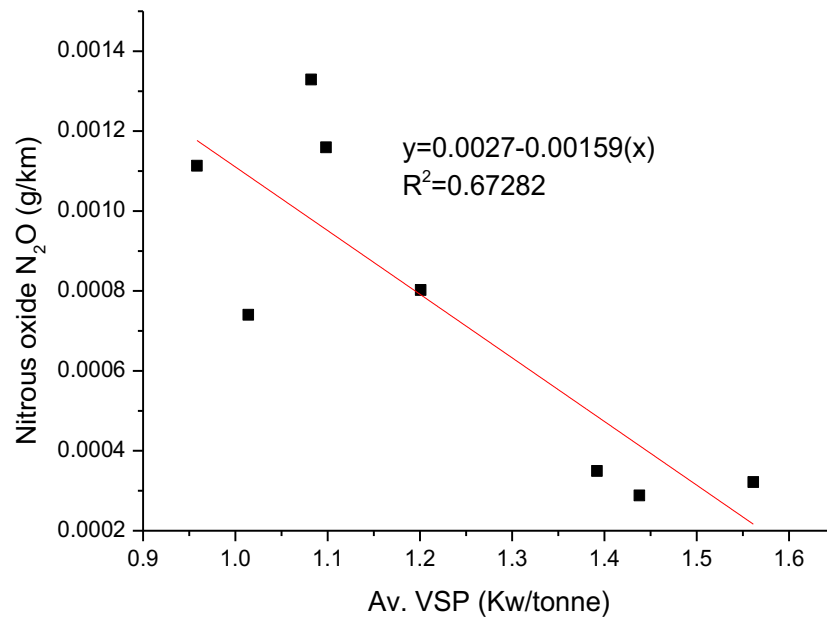
**Figure 5-33 Trip mean NO<sub>2</sub> emissions vs vehicle's average trip acceleration.**



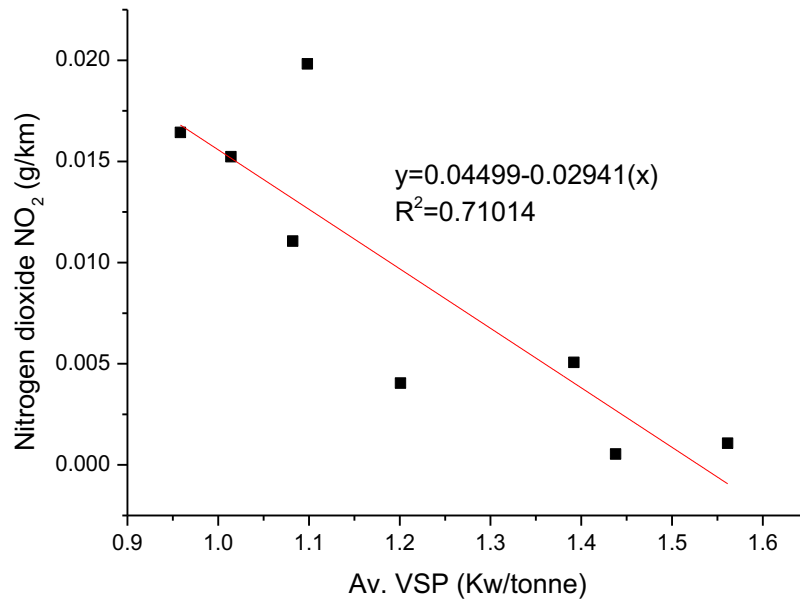
**Figure 5-34 Trip mean HCN emissions vs vehicle's average trip acceleration.**



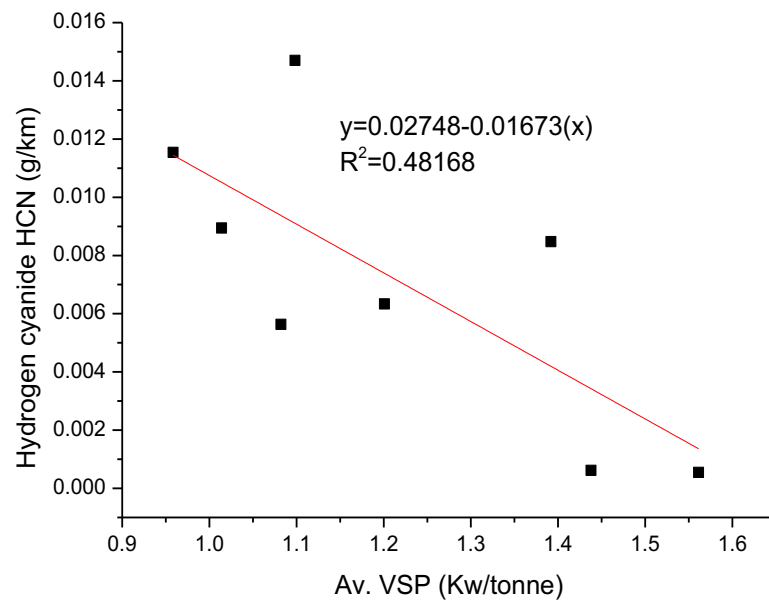
**Figure 5-35 Trip mean NH<sub>3</sub> emissions vs vehicle's average trip vehicle specific power.**



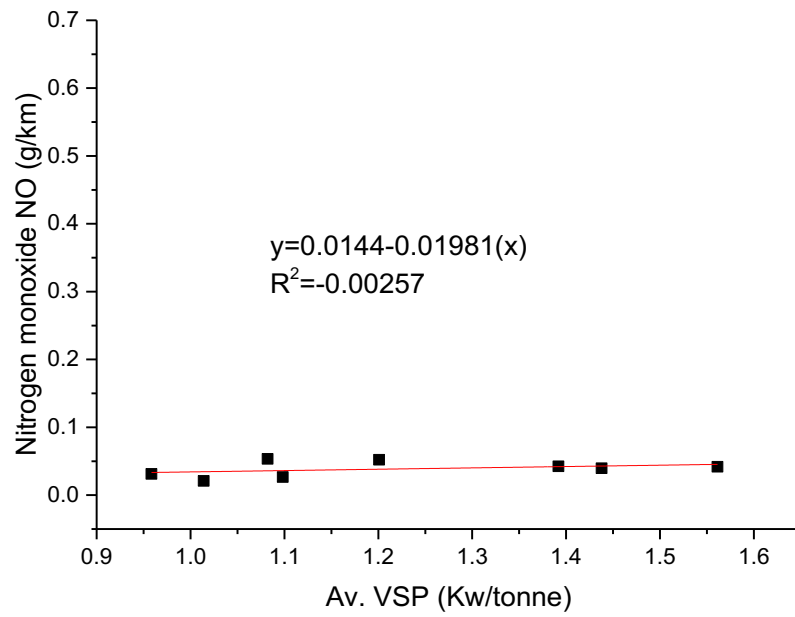
**Figure 5-36 Trip mean N<sub>2</sub>O emissions vs vehicle's average trip vehicle specific power.**



**Figure 5-37 Trip mean NO<sub>2</sub> emissions vs vehicle's average trip vehicle specific power.**



**Figure 5-38 Trip mean HCN emissions vs vehicle's average trip vehicle specific power.**



**Figure 5-39 Trip mean NO emissions vs vehicle's average trip vehicle specific power.**



## 5.4 Conclusions

Nitrogen compound emissions (HCN, NO, NO<sub>2</sub>, N<sub>2</sub>O and NH<sub>3</sub>) from a EURO4 SI passenger car were measured using a portable FTIR system. The first observed emissions in term of quantity in gram per km was ammonia (NH<sub>3</sub>) as its was from 0.05 g/km to 0.09 g/km. The second observed emission was nitrogen monoxide (NO) that was from 0.02 g/km to 0.05 g/km. The third observed emission was nitrogen dioxide (NO<sub>2</sub>) that was from 0.0005 g/km to 0.0198 g/km. The fourth observed emission was Hydrogen cyanide (HCN) that was from 0.0005 g/km to 0.015 g/km. And the least observed emission was Nitrous oxide (N<sub>2</sub>O) that was from 0.0003 g/km to 0.0013 g/km, which can be negligible. The vehicle was driven on two realistic driving cycles (routes A and B) taking the routes located in a densely populated area of Leeds representing a typical urban road network. Eight realistic emission tests were conducted at different times of day, such as the morning rush hours, lunch time and off-peak time in the evening. The emissions were presented in ppm, g/s and g/km. The correlations between five nitrogen compounds emissions and trip average velocity, acceleration and VSP were analysed. The results have shown that:

1. NO and NH<sub>3</sub> emissions are the most abundant nitrogen species in the tailpipe and can be detected from all the trips. NO<sub>2</sub> and HCN can be detected from six relatively congested trips but not from two evening free-flowing trips. This reflected that frequent stop and start and associated accelerations can increase nitrogen compound emissions.
2. NH<sub>3</sub> emissions from this research were significantly higher than some reported data from other Euro 4 SI cars using NEDC. One of the major reasons for this is that the real driving cycles used in this research had more frequent stop and start and harsher accelerations.
3. The results of mass emissions as a function of distance travelled showed clear evidence of the accumulation of emissions during the vehicle's stoppage periods at traffic lights and in the queues.
4. NO<sub>2</sub> and HCN showed good linear negative correlations with trip average velocity. NH<sub>3</sub> and N<sub>2</sub>O showed a moderate negative correlation with

the average velocity. There was no correlation observed for NO with the average velocity.

5. There were no correlations observed between the five nitrogen compounds and average accelerations.

NO<sub>2</sub> and N<sub>2</sub>O showed good negative linear correlations with average VSP.

NH<sub>3</sub> and HCN showed a moderate negative correlation with average VSP.

There was no correlation observed between NO and average VSP.

**Appendix A: Summary of driving parameters and nitrogen species emissions for all journeys.**

<b>Journeys</b>	<b>1925 A</b>	<b>1256 A</b>	<b>0746 A</b>	<b>0830 A</b>	<b>1941 B</b>	<b>1316 B</b>	<b>0807 B</b>	<b>0853 B</b>
<b>Av. Velocity (km/hr)</b>	23.09	18.52	17.64	15.34	23.21	19.84	15.33	15.68
<b>Max Velocity (km/hr)</b>	49.42	48.67	44.04	43.48	52.24	49.31	45.48	45.76
<b>Min Velocity (km/hr)</b>	0.00	0.00	0.00	0.00	0.00	0.00	0.00	0.00
<b>Av. Acceleration (m/s<sup>2</sup>)</b>	0.0001	-0.0034	0.0024	-0.0035	-0.0062	0.0065	0.00	0.00
<b>Max Acceleration (m/s<sup>2</sup>)</b>	2.29	2.42	2.57	2.17	2.11	2.35	2.65	2.76
<b>Max Deceleration (m/s<sup>2</sup>)</b>	-1.90	-1.80	-2.35	-1.91	-4.03	-4.30	-2.04	-2.71
<b>Av. VSP (Kw/tonne)</b>	1.56	1.20	1.08	0.96	1.44	1.39	1.01	1.10
<b>Max VSP (Kw/tonne)</b>	20.61	25.76	19.08	16.83	22.96	18.10	19.25	18.47
<b>Min VSP (Kw/tonne)</b>	-13.11	-11.21	-13.49	-12.02	-13.54	-15.01	-14.77	-22.33
<b>Av. VSP+ (Kw/tonne)</b>	3.65	2.89	2.59	2.21	3.21	2.99	2.39	2.02
<b>Av. VSP- (Kw/tonne)</b>	-3.01	-0.74	-2.13	-1.98	-2.48	-2.48	-1.81	-2.45
<b>Power output+ (kWh)</b>	0.83	0.81	0.76	0.75	0.75	0.80	0.80	0.91
<b>Power output- (kWh)</b>	-0.31	-0.30	-0.27	-0.26	-0.25	-0.27	-0.28	-0.35
<b>Total stoppage time (s)</b>	167.00	276.00	281.00	392.00	176.00	235.00	339.00	368.00
<b>Stoppage time (%)</b>	21.89	28.93	28.30	34.03	22.80	26.49	29.35	32.74
<b>Cruise%</b>	46.13	36.06	33.30	27.26	47.15	41.38	26.58	28.29
<b>Total fuel consumption (g)</b>	339.30	363.70	380.79	399.75	316.96	370.32	418.99	430.35
<b>Av. fuel consumption (g/s)</b>	0.44	0.38	0.38	0.35	0.41	0.42	0.36	0.38
<b>Idle fuel consumption (g)</b>	41.90	62.81	60.76	84.84	42.56	50.07	83.34	78.45
<b>Idle fuel consumption (%)</b>	12.35	17.27	15.95	21.22	13.43	13.52	19.89	18.23
<b>Journey Av. fuel consumption (g/km)</b>	69.00	74.09	77.53	81.27	63.57	75.46	85.03	87.67
<b>Fuel economy (mile/UKG)</b>	29.55	27.52	26.30	25.09	32.07	27.02	23.98	23.26
<b>Overall thermal efficiency (%)</b>	0.20	0.18	0.16	0.15	0.19	0.18	0.16	0.17
<b>Nitrous oxide N<sub>2</sub>O (g/km)</b>	0.0003	0.0008	0.0013	0.0011	0.0003	0.0003	0.0007	0.0012
<b>Nitrogen monoxide NO (g/km)</b>	0.04	0.05	0.05	0.03	0.04	0.04	0.02	0.03
<b>Nitrogen dioxide NO<sub>2</sub> (g/km)</b>	0.0011	0.0040	0.0111	0.0164	0.0005	0.0051	0.0152	0.0198
<b>Ammonia NH<sub>3</sub> (g/km)</b>	0.07	0.07	0.06	0.09	0.05	0.06	0.09	0.08
<b>Hydrogen cyanide HCN (g/km)</b>	0.0005	0.006	0.006	0.012	0.0006	0.008	0.009	0.015
<b>NOx (g/km)</b>	0.07	0.08	0.09	0.06	0.06	0.07	0.05	0.06

## **6 Chapter Six: Cold start SI passenger car emissions from realistic urban congested traffic**

### **6.1 Introduction**

In Europe, all cities are required to meet the defined European air quality standards and must declare Air Quality Management Areas (AQMA). If they exceed these air quality standards in an AQMA, then the city has to take action to determine the cause of the exceedance and has the power to introduce measures to reduce the emissions. Research conducted by Li, et al. (2009), show that in the UK that in nearly every case where an AQMA had been declared, traffic pollution was found to be the cause of the exceedance [119]. Additionally, the road on which the research was undertaken was the subject of a City of Leeds traffic and congestion study [16, 120].

Air quality, as a fundamental property of investigation, needs to be monitored while conducting research on traffic emission. Li et al, (2009) monitored the air quality in the same area and compared it with traffic emission modelling results. However, findings by Li show that the air quality model NO<sub>2</sub> concentrations were 47% lower than the actually measured results in the area and 28% lower for the city. Measurements of the NO<sub>2</sub> indicated fourteen sites in Leeds which were above the EU limit where the model only predicted four sites in exceedance, although, the high level of NO<sub>2</sub> in the area was attributed to traffic congestion as there are no other pollution sources.

Several research findings demonstrated that Spark Ignition (SI) engine in cold atmospheric conditions has much higher exhaust emissions than one that is fully warmed up [16-19, 21, 22, 121]. Additionally, the cold start has cold oil, water and all metal surfaces, as well as cold catalysts and the thermal energy that is required to heat these is the main thermal efficiency and CO<sub>2</sub> problem in cold starts. However, the warm up of the lubricating oil takes about fifteen minutes, but according to Li et al, (2008) the greenhouse gases methane, nitrous oxide and benzene as well as other hydrocarbons are predominantly emitted during the cold start period before 200 seconds has passed.

Present-day techniques for assessing exhaust emissions from road transport are mainly based on measurements from rolling road constant volume sampling facilities using standard drive cycles. Emissions are characteristically described as a function of average speed or distance for the complete cycle. The average values are subsequently used to estimate transport emissions. In comparison, studies have demonstrated that many other parameters such as vehicle operating conditions, traffic conditions (free-flowing, congested), ambient temperatures, fuel compositions, topography and the road geometry strongly affect realistic emissions.

In this work, cold start into congested traffic after leaving a car park adjacent to the road was investigated. The vehicle entering congested traffic, after a cold start, often has stop/start velocities of 10 kmph. It is often >100s before the first significant acceleration to 40 kmph and 200 s before the TWC is fully active. Under urban driving conditions, the cold start emissions often dominate the entire journey emissions, although as the journey length increases, the proportion of cold start emissions is reduced. The net result is that emissions are higher in cold start into congested traffic, and this is part of the reason why air quality in cities has not responded in proportion to emissions' reduction on the test cycle. Additionally, the stop/start frequency is greater in realistic driving than it is on the test cycles and this gives higher NO<sub>x</sub> emissions after the TWC has lit off; hence, this is now recognised as a problem. The continuing air-quality problems have resulted in the adoption of a new World Light-duty Test Cycle (WLTC), which is more realistically based and might be more representative of congested traffic. However, the proposed cycle has a time to first acceleration which is much shorter than in congested traffic.

The limit values for each EU exhaust emission standard are represented in Table 6-1 EU exhaust legislation of EURO SI passenger cars. Prior to EURO 3 THC and NO<sub>x</sub> were summated. They have been listed as separate targets here on the basis of their ratio in the EURO 3 legislation [112] .

**Table 6-1 EU exhaust legislation of EURO SI passenger cars.**

	<b>EURO1</b>	<b>EURO2</b>	<b>EURO3</b>	<b>EURO4</b>
<b>CO G/KM</b>	2.7	2.2	2.3	1.0
<b>THC+NO<sub>x</sub> G/KM</b>	0.97	0.50	-	-
<b>THC G/KM</b>	0.55*	0.29*	0.2	0.1
<b>NO<sub>x</sub> G/KM</b>	0.42*	0.21*	0.15	0.08

\*: EURO 3 THC/NO<sub>x</sub> ratios were used to calculate EURO1 and 2 THC and NO<sub>x</sub> limit values, the cold start procedure was altered for EURO 3. The routes used represented typical urban busy circuits including arterial and minor roads, turnings, pedestrian crossings and traffic lights. A Euro 4 vehicle was used as EURO 4 SI cars are still a significant proportion of the UK vehicle fleet. It takes about 16 years for 90% of vehicles sold in any one year to be no longer in use.

## **6.2 Aim and objectives**

### **6.2.1 Aim**

The aim of this research work section for this thesis was to investigate the impact of cold start and traffic on emissions.

### **6.2.2 Objectives**

The objective of this chapter is (1) to investigate the fuel consumption and brake thermal efficiency, and (2) to explore the legislated emissions, GHG (Green House Gas), as well as five nitrogen compounds (NO, NO<sub>2</sub>, NH<sub>3</sub>, HCN, N<sub>2</sub>O) emissions during cold start under realistic urban driving conditions, principally considering the impact of traffic congestion on emissions.

## **6.3 Experimental techniques**

The methods employed in this section of this thesis are indicated as follows:

An urban road network located in the Headingley area of Leeds city was designed to perform these emission tests. Additionally, four different cycles were conducted as follows: CSR1, CSR2, CSR3 and CSR3s. A EURO4 emission compliant Ford Mondeo manual transmission petrol car was used, which was fitted with a port fuel injected 1.8 litre 16V spark ignition engine with 4 cylinders and 16 valves. The odometer reading on the car was 4,400 miles prior to the tests. The vehicle was equipped with a Three Way Catalyst (TWC). The curb weight of the car is 1374 kg. The car was instrumented with 3 thermocouples which measured the lubricating oil in the sump temperature, exhaust gas temperatures upstream and downstream of the TWC. All temperatures were measured using grounded junction mineral insulated Type K thermocouples with a response time of ~0.25ms. This strategy was adopted successfully and the details of the procedure have been demonstrated in chapter 3 of this thesis.

## **6.4 Results and discussions**

### **6.4.1 Driving parameter analysis – velocity, acceleration and TWC light off during cold start**

From Table 6-2, it can be seen that the average velocity was from 8.8 to 25.5 km/h; however, the slowest trips were those during evening rush hours. The evening trip was in fact a free-flowing trip (Day 1\_EURO4\_1850\_CSR1). It can be seen that the maximum acceleration was from 2.39 to 2.68 m/s<sup>2</sup>. The Maximum acceleration was in fact a free-flowing trip in the morning (Day 3\_EURO4\_0722\_CSR2). The average acceleration was from -0.0076 to 0.0083 m/s<sup>2</sup>. The average was a negative value (deceleration) in all trips in the morning. It can be seen that the average VSP+ was from 1.43 to 3.24 kw/tonne. The lowest one was in fact a congested trip in the evening (Day 2\_EURO4\_1620\_CSR3). It can be seen that the stoppage time was from 160 to 952 s. The highest stoppage time was in fact a congested trip in the evening (Day 2\_EURO4\_1620\_CSR3). Also the number of stops was from 10 to 54. Although, the highest stoppage time was, in fact, a congested trip in the evening (Day 5\_EURO4\_1624\_CSR2). Table 6-1 revealed that the cruise

percentage was from 9.7 to 52.62 %, but the minimum value was in fact a congested trip in the evening (Day 2\_EURO4\_1620\_CSR3).

Figure 6-1 to Figure **6-12** present the profiles of the trips (Day 2\_EURO4\_1150\_CSR2 and Day 5\_EURO4\_1624\_CSR2) representing free-flowing and congested respectively, including the vehicle's velocity, acceleration, transient and cumulative fuel consumption, Transient VSP and cumulative work done, elevation of road, distance travelled, lambda and GHG emissions Vs time. Essentially, Figure 6-1 and Figure 6-2 compared GHG emissions Vs time while Figure 6-3 and Figure **6-4** compared GHG emissions Vs distance for two journeys. Additionally, Figure **6-5** and Figure **6-6** compared nitrogen species' emissions Vs time at the same time Figure **6-7** and Figure **6-8** and compared nitrogen species emissions Vs distance for two journeys. Figure **6-9** and Figure **6-10** indicated the comparison between legislated emissions and time, as well as, Figure **6-11** and Figure **6-12** compared legislated emissions Vs distance for two journeys.

The trips started from the garage in Lodge Street and were divided into two directions: inwards towards the city centre and outwards. The distance from point 1 to 2 was 0.4 km, 2.2 km from point 2 to 3, 0.6 km from point 3 to 4, 1.5 km from point 4 to 5 and 1.9 km from point 5 to 6. The inwards trip was 3.2 km from point 4 to 6. It can be found in the odd numbered Figure 6-1, Figure 6-3, Figure **6-5**, Figure **6-7**, Figure **6-9** and Figure **6-11** show that the journey took 1060 seconds indicating a free-flowing trip whereas the even numbers Figure 6-2, Figure **6-4**, Figure **6-6**, Figure **6-8**, Figure **6-10** and Figure **6-12** took 2021 seconds, indicated a congested traffic trip. However, the velocity and acceleration profiles demonstrate that outbound journeys were less congested than were inbound journeys for a free-flowing trip and opposite to a congested trip. There were eleven stops for a free-flowing trip with a duration of 212 seconds as the total stoppage time whereas there were fifty four stops on the congested journey with a duration of 905 seconds as total stoppage time. The free trips generally, included a period of time when the vehicle was in cruise mode. However, these were much more congested,



as indicated by more stops and longer idling times. This was particularly obvious for congested trips as they were during rush hours.

The catalyst temperatures, measured at upstream and downstream of TWC, were used for determining the catalyst light off, which is defined as when the downstream temperature is equal to or higher than the upstream temperature. Table 6-2 shows that the light-off time was 196-349 seconds, which was related to the severity of congestions.

**Table 6-2 Summary of driving parameters and emissions species for all journeys.**

Journeys	1850_CSR1	1150_CSR2	0722_CSR2	1153_CSR2	1157_CSR2	1624_CSR2	1620_CSR3	1620_CSR3s
Av. Velocity (km/hr)	25.490	22.36	20.90	20.70	19.64	11.82	8.80	12.44
Max Velocity (km/hr)	49.180	49.85	61.20	54.63	66.76	61.35	52.80	55.43
Min Velocity (km/hr)	0.00	0.00	0.00	0.00	0.00	0.00	0.00	0.00
Av. Acceleration (m/s <sup>2</sup> )	0.0083	-0.0076	-0.0010	-0.0016	-0.0029	0.0029	0.0051	-0.0012
Max Acceleration (m/s <sup>2</sup> )	2.493	2.52	2.68	2.67	2.60	2.57	2.46	2.39
Max Deceleration (m/s <sup>2</sup> )	-1.954	-2.41	-1.88	-2.60	-2.46	-3.21	-1.83	-2.69
Av. VSP (Kw/tonne)	1.563	1.29	1.27	1.41	1.25	0.96	0.67	0.98
Max VSP (Kw/tonne)	17.292	22.51	26.34	23.43	23.86	23.39	17.83	20.63
Min VSP (Kw/tonne)	-11.215	-16.17	-14.70	-18.55	-11.12	-22.67	-8.30	-14.88
Av. VSP+ (Kw/tonne)	3.06	2.97	2.75	3.24	2.73	2.09	1.43	1.99
Av. VSP- (Kw/tonne)	-2.34	-2.23	-2.58	-2.60	-2.39	-2.00	-1.30	-2.35
Power output+ (kWh)	0.73	0.93	0.96	1.10	1.04	1.30	0.81	0.83
Power output- (kWh)	-0.22	-0.31	-0.33	-0.38	-0.36	-0.46	-0.27	-0.29
Total stoppage time (s)	160.00	212.00	313.00	290.00	356.00	905.00	952.00	594.00
Stoppage time (%)	20.94	20.00	27.64	25.24	29.20	44.78	49.64	46.48
Cruise%	52.62	47.45	42.32	43.60	39.79	19.69	9.70	18.70
Total fuel consumption (g)	317.00	456.09	544.68	514.63	461.97	668.26	441.71	488.33
Av. fuel consumption (g/s)	0.42	0.43	0.48	0.45	0.38	0.33	0.23	0.38
Idle fuel consumption (g)	30.85	43.22	42.12	63.30	39.88	157.30	122.13	94.37
Idle fuel consumption (%)	9.73	9.48	7.73	12.30	8.63	23.54	27.65	19.33
Journey Av. fuel consumption (g/km)	58.40	69.00	82.25	77.57	69.49	100.65	94.85	111.39
Fuel economy (mile/UKG)	34.91	29.55	24.79	26.28	29.34	20.26	21.50	18.30
Overall thermal efficiency (%)	0.19	0.17	0.14	0.17	0.18	0.16	0.15	0.14
Total Distance (Km)	5.43	6.61	6.62	6.63	6.65	6.64	4.66	4.38
Carbon dioxide CO2 (g/km)	178.375	218.61	263.13	242.73	222.80	311.09	292.61	373.64
Nitrous oxide N2O (g/km)	0.0110	0.0073	0.0079	0.0142	0.0142	0.0161	0.0162	0.0152
Methane CH4 (g/km)	0.013	0.013	0.019	0.019	0.023	0.035	0.030	0.040
Nitrogen monoxide NO (g/km)	0.085	0.078	0.066	0.161	0.070	0.140	0.126	0.100
Nitrogen dioxide NO2 (g/km)	0.001	0.002	0.008	0.003	0.008	0.005	0.004	0.006
Ammonia NH3 (g/km)	0.065	0.060	0.065	0.079	0.065	0.108	0.097	0.097
Hydrogen cyanide HCN (g/km)	0.0008	0.0012	0.0022	0.0008	0.0010	0.0012	0.0010	0.0018
NOx (g/km)	0.13	0.12	0.11	0.25	0.12	0.22	0.20	0.16
Total HydrocarbonTHC (g/km)	0.29	0.31	0.33	0.36	0.32	0.49	0.48	0.57
Carbon monoxide CO (g/km)	1.57	1.45	1.85	1.94	2.25	2.58	1.88	2.66
Number of stops	10	11	17	17	15	54	50	39
Journey duration (s)	764.00	1060.00	1139.00	1149.00	1219.00	2021.00	1918.00	1278.00
Light off time (s)	227.0	196.0	295.0	257.0	231.0	262.0	263.0	349.0
Light off distance (km)	1.18	1.06	0.97	1.11	1.08	0.87	1.11	0.93
Oil temperature when TWC lit off (°C)	56.3	39.2	43.4	67.0	36.0	38.1	69.0	52.8

## 6.4.2 Fuel consumption and VSP

Vehicle speed and acceleration is related directly to fuel consumption. The results show the spikes for fuel consumption were in the case of every speed and acceleration spike followed by a decrease in fuel consumption during deceleration and when the vehicle was travelling at a constant speed. Vehicle fuel consumption is increased during uphill travels, which required more fuel supply. The traffic and pedestrian lights were a major reason for frequent stop start events in a congested traffic, which caused a considerable increase in fuel consumption on congested trips. The fuel economy for congested trip was only 18.3 mile/UKG whereas for the free-flowing trip in the off-peak time, this could be increased to 34.9 miles/UKG as shown in Table 6-2. The fuel consumption for this type of vehicle measured on the NEDC urban part is 28 miles/UKG including cold start. It can be seen that the congested trips had a much higher fuel consumption than the certified values by NEDC.

VSP represents the power required from the engine to move a vehicle to overcome the aerodynamic drag, rolling resistance and road grade effect. The value of VSP is mainly determined by acceleration and road grade. If the vehicle is travelling on a flat or downhill road at a constant speed, the value of VSP would be small, as the power demand will be low. This can be illustrated with examples in the odd figures numbers from Figure 6-1 to Figure 6-11, with low VSP less spikes whereas high VSP has more spikes in even figures numbers from Figure 6-2 to Figure 6-12. The most dominant factor for VSP is acceleration, evidenced by the fact that most of the negative VSP spikes are linked with deceleration peaks and the number of stops.

The average of overall VSP and positive VSP for all trips presented in Table 6-2 generally shows that the free-flow trips had the higher values as results of more free-flowing driving. The congested trips had lower values. This means that the average VSP could be used as a congestion indication. From this study, an initial suggestion- is that average VSP 1.41 or average positive VSP 3.24 could be used as indication for a non-congested trip.

### 6.4.3 Greenhouse gases emissions (GHG)

Figure 6-1 and Figure 6-2 shows the mass emission rate (g/s) and cumulated mass emissions for greenhouse gases emissions (GHG) as a function of time along with some driving parameters. As indicated in there are more GHG spikes than in Figure 6-1, which is a free-flowing trip. Also Figure 6-2 shows more spikes for lambda, VSP, fuel consumption, velocity and acceleration as it is a congested trip.

Figure 6-3 and Figure 6-4 show the cumulative mass emission (g) as a function of the distance travelled for GHG. Figure 6-3 shows the mass of CH<sub>4</sub>, N<sub>2</sub>O and CO<sub>2</sub> were 0.09, 0.05 and 1500 g respectively. Total fuel was 450 g and cumulative work done was 0.95 kWh. Whereas a higher value shows in Figure 6-4, which is a congested trip, the mass of CH<sub>4</sub>, N<sub>2</sub>O and CO<sub>2</sub> were 0.23, 0.11 and 2100 g respectively. Total fuel was 680 g and cumulative work done was 1.3 kWh.

The vehicle started from cold. This resulted in a spike in CH<sub>4</sub> and N<sub>2</sub>O emissions during the initial 250 seconds. These spike in N<sub>2</sub>O emissions indicated that the catalyst is not lit off. The three-way catalyst took longer to light off in congested traffic compared to free-flowing traffic.

The CO<sub>2</sub> emissions directly respond to fuel consumptions in all Figures and are also a good reflection of VSP spikes. CH<sub>4</sub> and N<sub>2</sub>O emissions were very low after the engine was fully warmed up (after 300s) and only had occasional spikes, which were linked to sharp accelerations, spikes of fuel consumption and VSP, and also a lean spike in lambda values. Interestingly, not all of these spikes produce high CH<sub>4</sub> and N<sub>2</sub>O emissions. It appears that the spikes of CH<sub>4</sub> and N<sub>2</sub>O only occurred when the fuel consumption had a sharp rise with a peak value of 2 g/s or above.

By analysing all these trips, it is discovered that most of the CO<sub>2</sub> peaks are linked to pedestrian crossings, traffic lights and turnings where the vehicle was forced to stop (red light or queue). There were a few CO<sub>2</sub> peaks related to uphill movements.

Day 2 EURO4\_1150\_CSR2

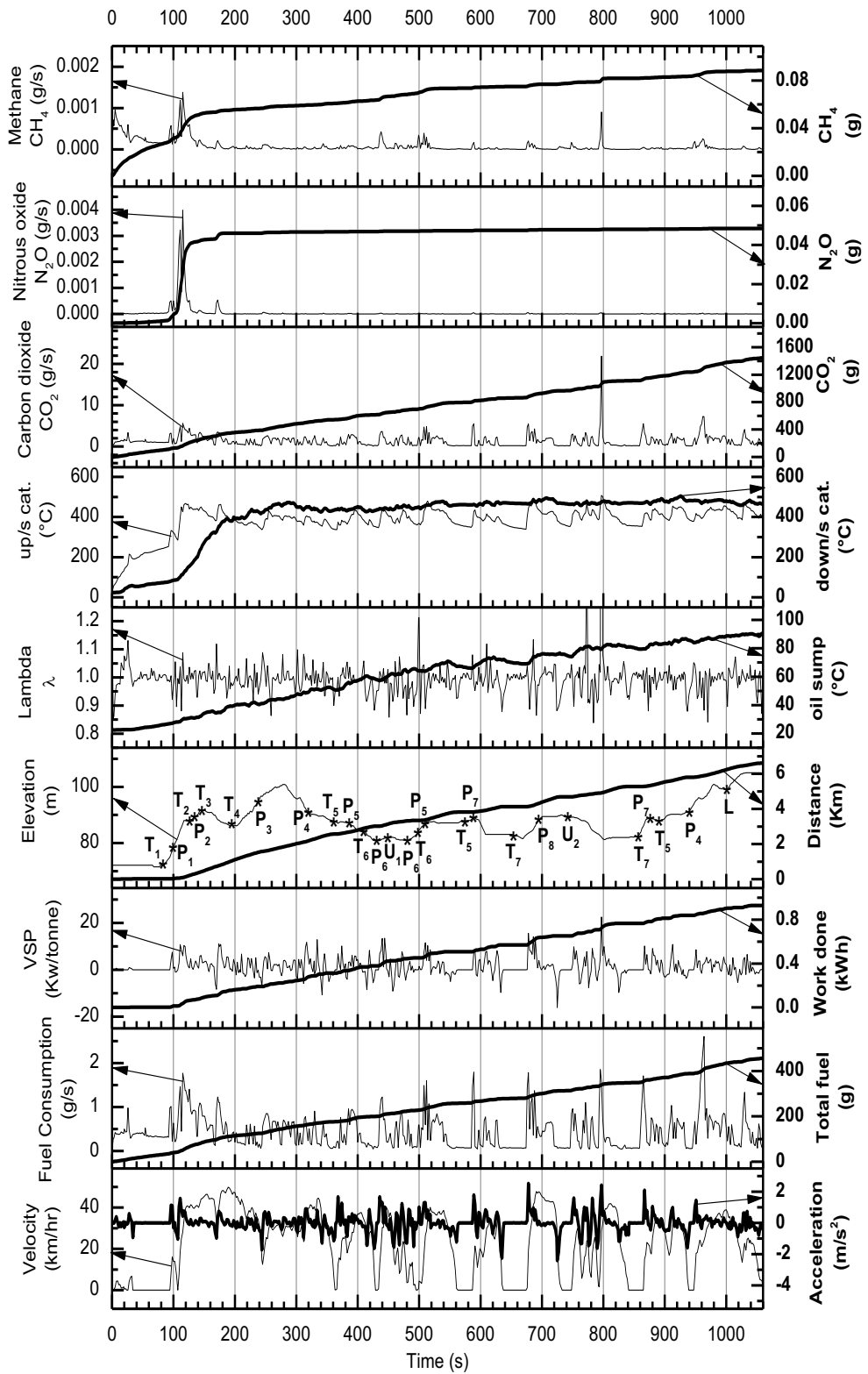


Figure 6-1 GHG Vs time profiles for the free flow trip 11:50.

Day 5 EURO4 1624\_CSR2

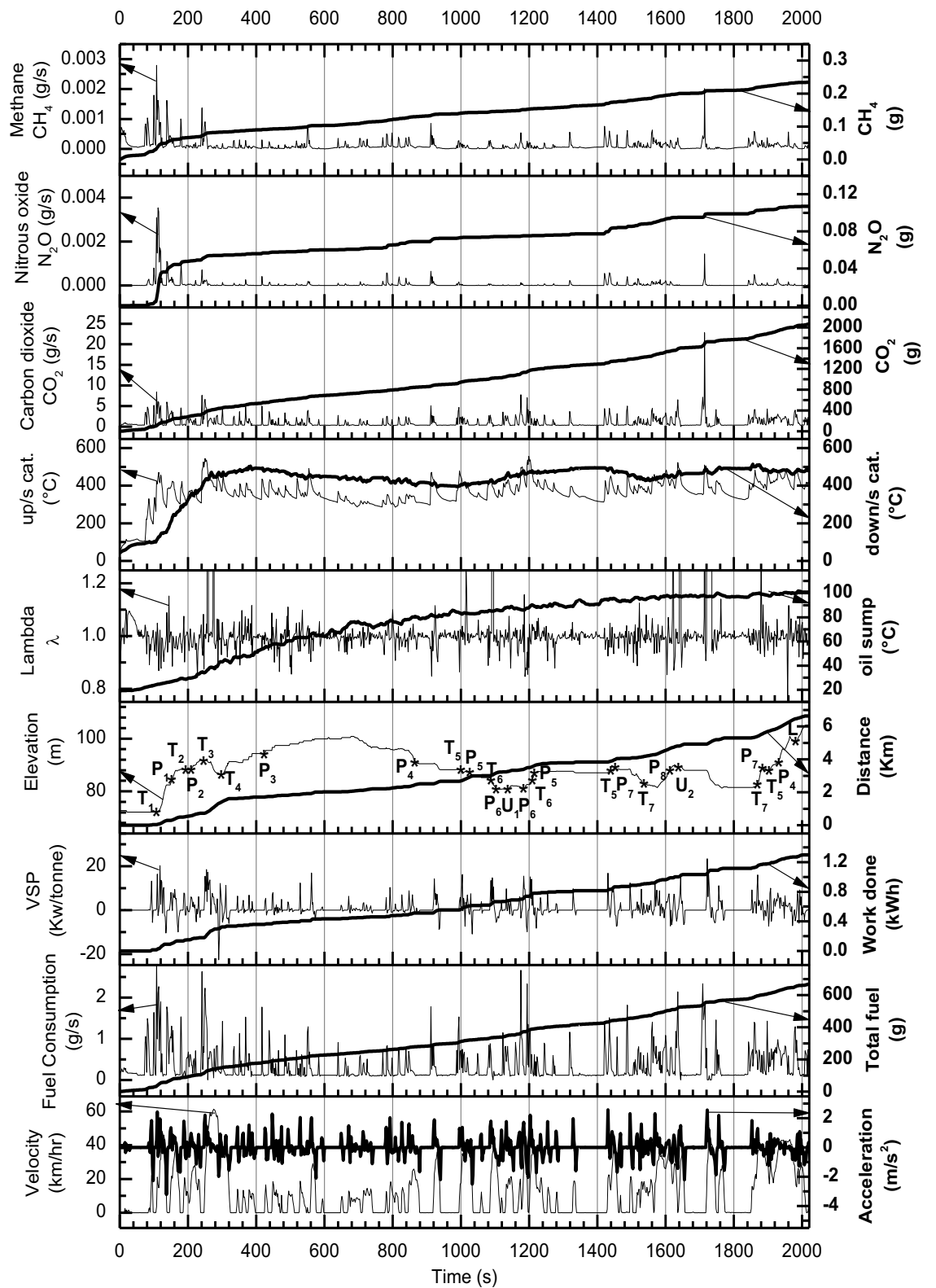
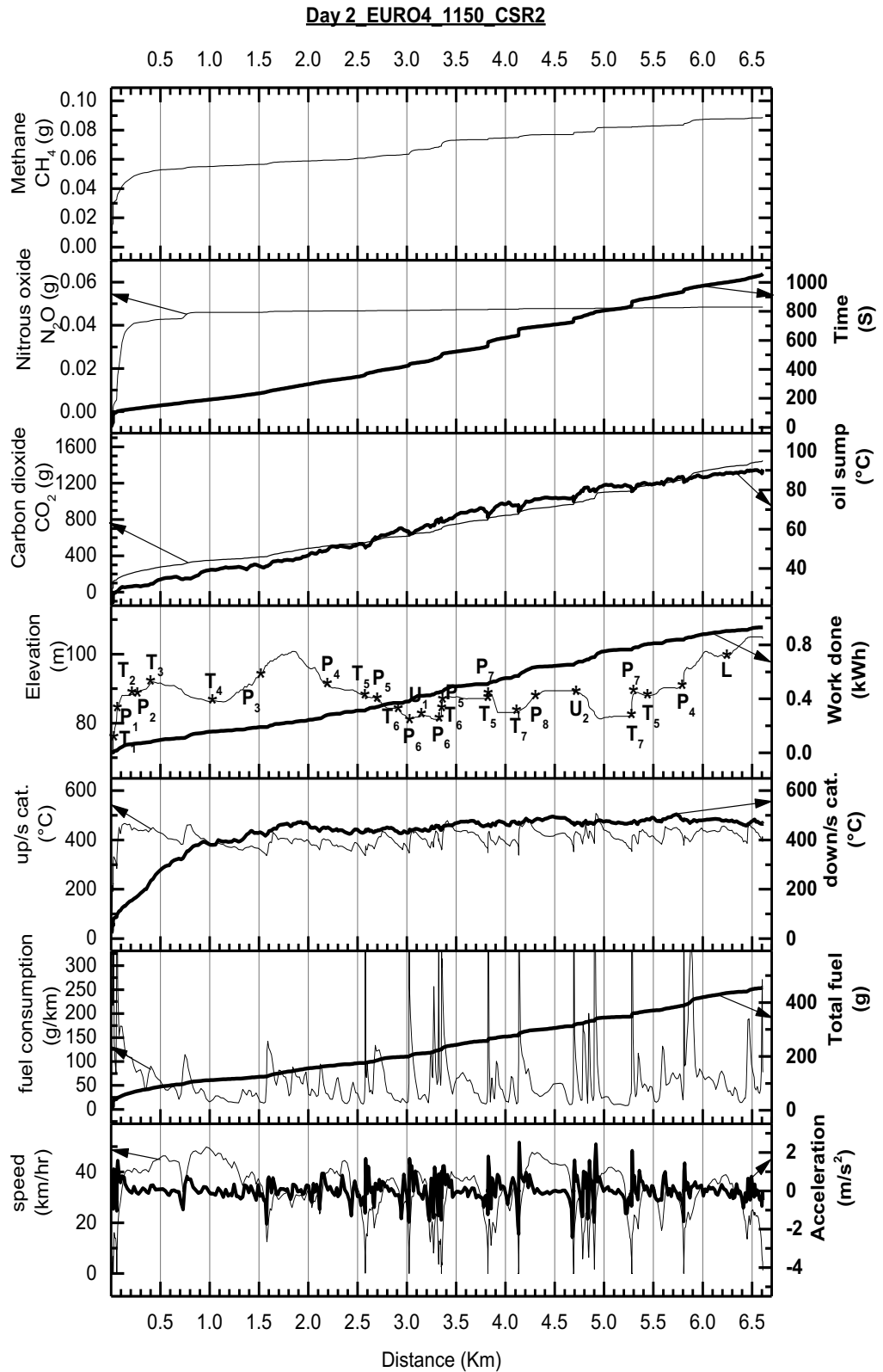
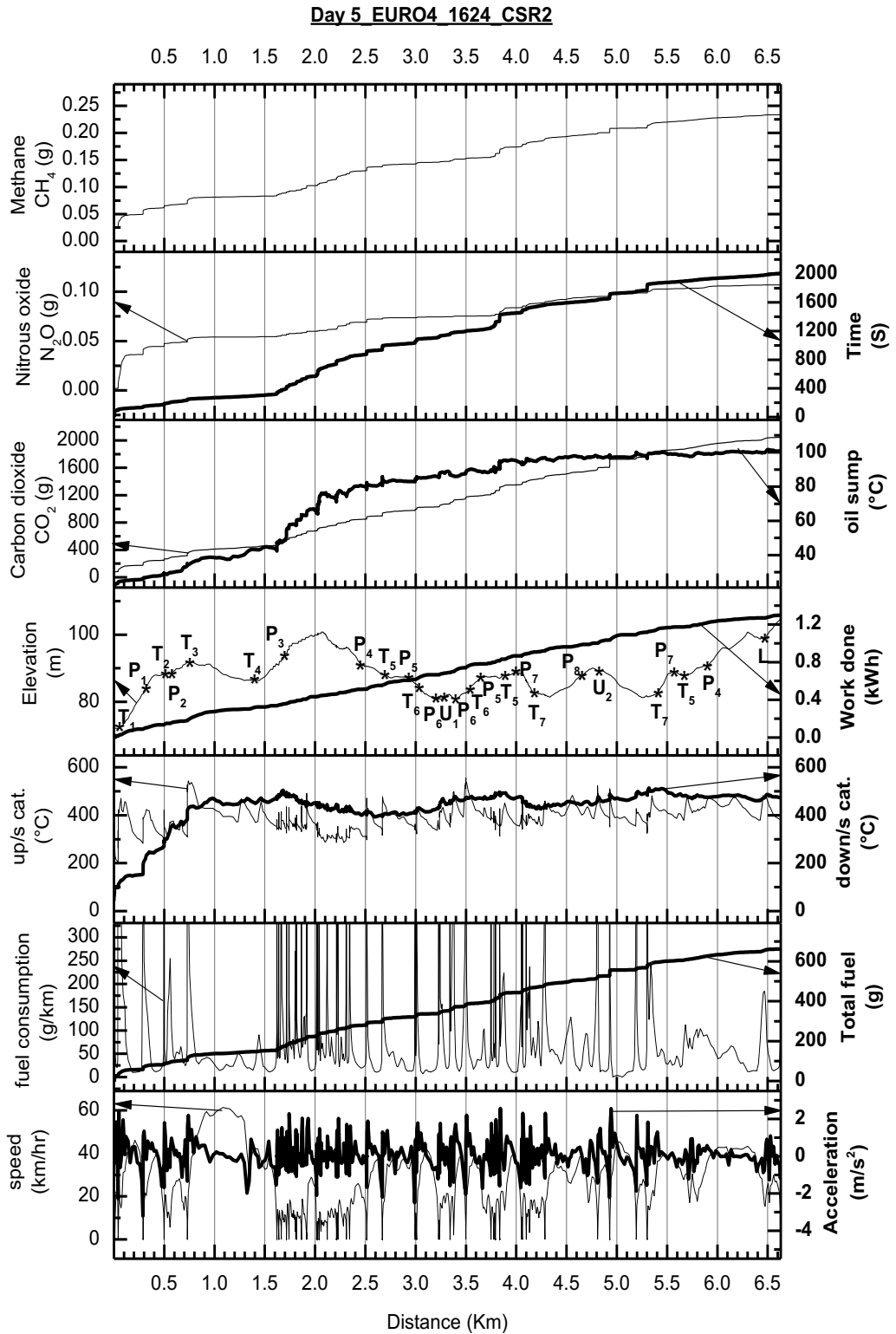


Figure 6-2 GHG Vs time profiles for the congested trip 16:24.



**Figure 6-3 GHG Vs distance profiles for the free flow trip 11:50a.**



**Figure 6-4 GHG Vs distance profiles for the congested trip 16:24.**

#### 6.4.4 Nitrogen compound emissions



Figure 6-5 and Figure 6-6 show the mass emission rate (g/s) and cumulated mass emissions for five nitrogen compounds as a function of time, together with some driving parameters. Figure 6-6 shows more nitrogen species spikes than Figure 6-5, which is a free-flowing trip. Also Figure 6-6 shows more spikes for lambda, VSP, fuel consumption, velocity and acceleration as it is a congested trip. Figure 6-7 and Figure 6-8 show the cumulative mass emission (g) as a function of the distance travelled for five nitrogen compounds. Figure 6-7 shows that the mass of N<sub>2</sub>O, NO, NO<sub>2</sub>, NH<sub>3</sub> and HCN were 0.05, 0.5, 0.01, 0.4 and 0.008 g respectively. Total fuel was 450 g and cumulative work done was 0.95 kWh. Whereas a higher value except HCN were similarly shown in Figure 6-8, which is a congested trip where the mass of N<sub>2</sub>O, NO, NO<sub>2</sub>, NH<sub>3</sub> and HCN were 0.11, 0.9, 0.03, 0.7 and 0.008 g respectively. Total fuel was 680 g and cumulative work done was 1.3 kWh. One of the main purposes of these diagrams is to illustrate the effect of pollutant accumulation on congested traffic. The longer the vehicle remains still, the higher the accumulated emissions. All the major step rises in any emissions are linked to stoppages of the vehicle. As the traffic lights, pedestrian crossing lights, left or U-turns are marked in the diagrams, the accumulation of pollution can then be determined.

NH<sub>3</sub> is an abundant nitrogen compound emitted from the exhaust gases and has a value of 0.05~0.11 g/km (see Table 6-2). Bielaczyc et al, (2012) [88] investigated NH<sub>3</sub> emissions from EURO5, 4 and 3 emission compliance SI passenger cars, using the NEDC test cycle. They reported much lower NH<sub>3</sub> emissions from all three vehicles. Table 6-3 compared NH<sub>3</sub> emissions from Bielaczyc's work with this research. The make and model of the EURO4 passenger car in Bielaczyc's paper is unknown and therefore direct comparison may be difficult as the tailpipe NH<sub>3</sub> emissions may be related to the type of the TWC. However, the gap between their results from NEDC and the realistic driving cycle in this research is too large to be attributed to the possible difference in catalyst technology and type. The frequent stop and start, the much harsher acceleration and deceleration, the greater and more transient power demands for engine under realistic driving conditions presented in this study are important parameters, causing high tailpipe NH<sub>3</sub>

emissions. Karlsson et al, (2004) [118] compared NH<sub>3</sub> emissions with NEDC and UDC (Urban Driving Cycle) of FTP-75 and observed much higher NH<sub>3</sub> emissions from UDC than from NEDC due to harsher accelerations in the UDC. This is consistent with this study's finding, i.e. rapid and harsh accelerations are the main causes of NH<sub>3</sub> emissions.

Day 2 EURO4 1150 CSR2

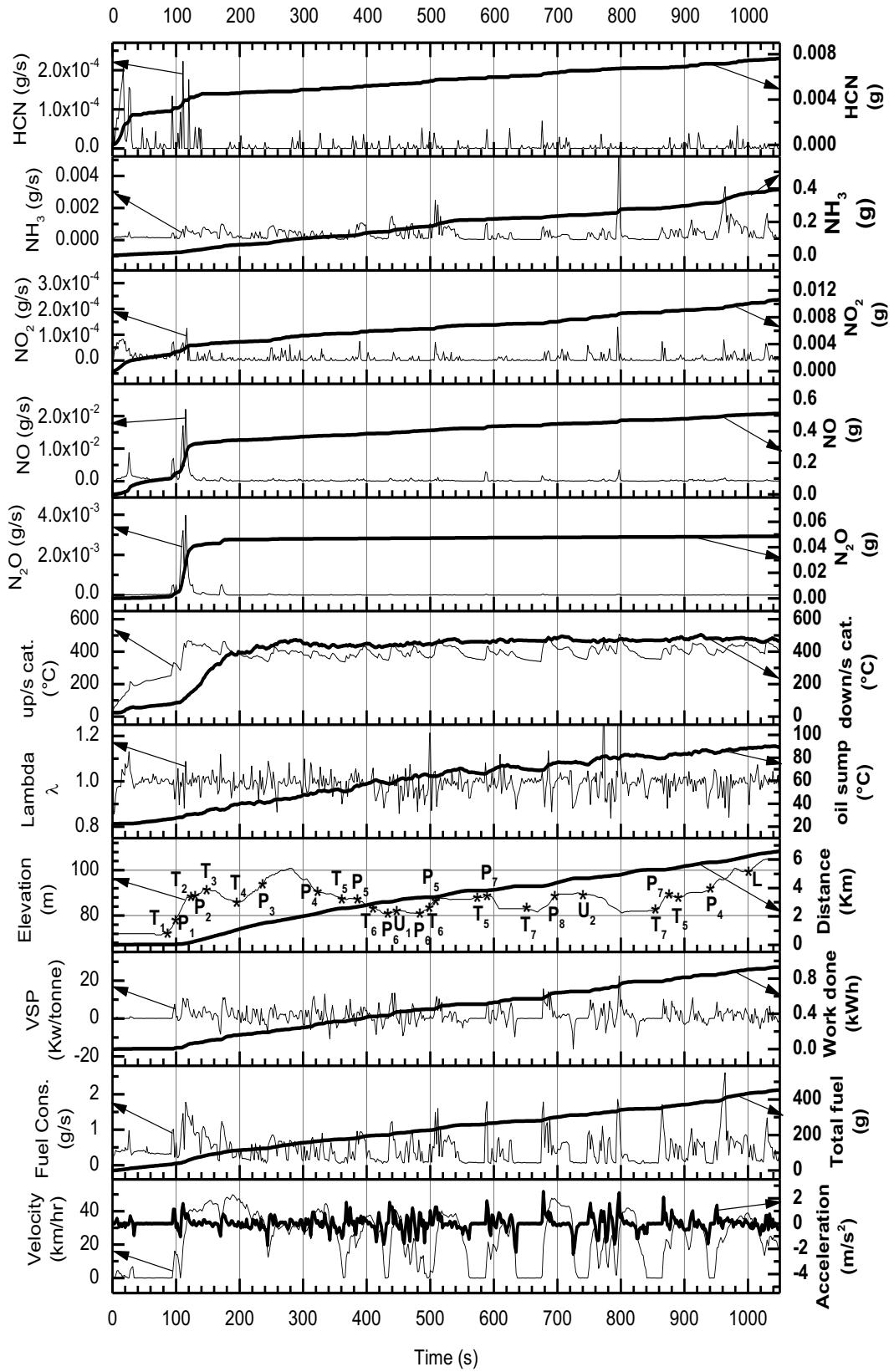


Figure 6-5 Nitrogen species vs time profiles for the free flow trip 11:50.

Day 5 EURO4 1624 CSR2

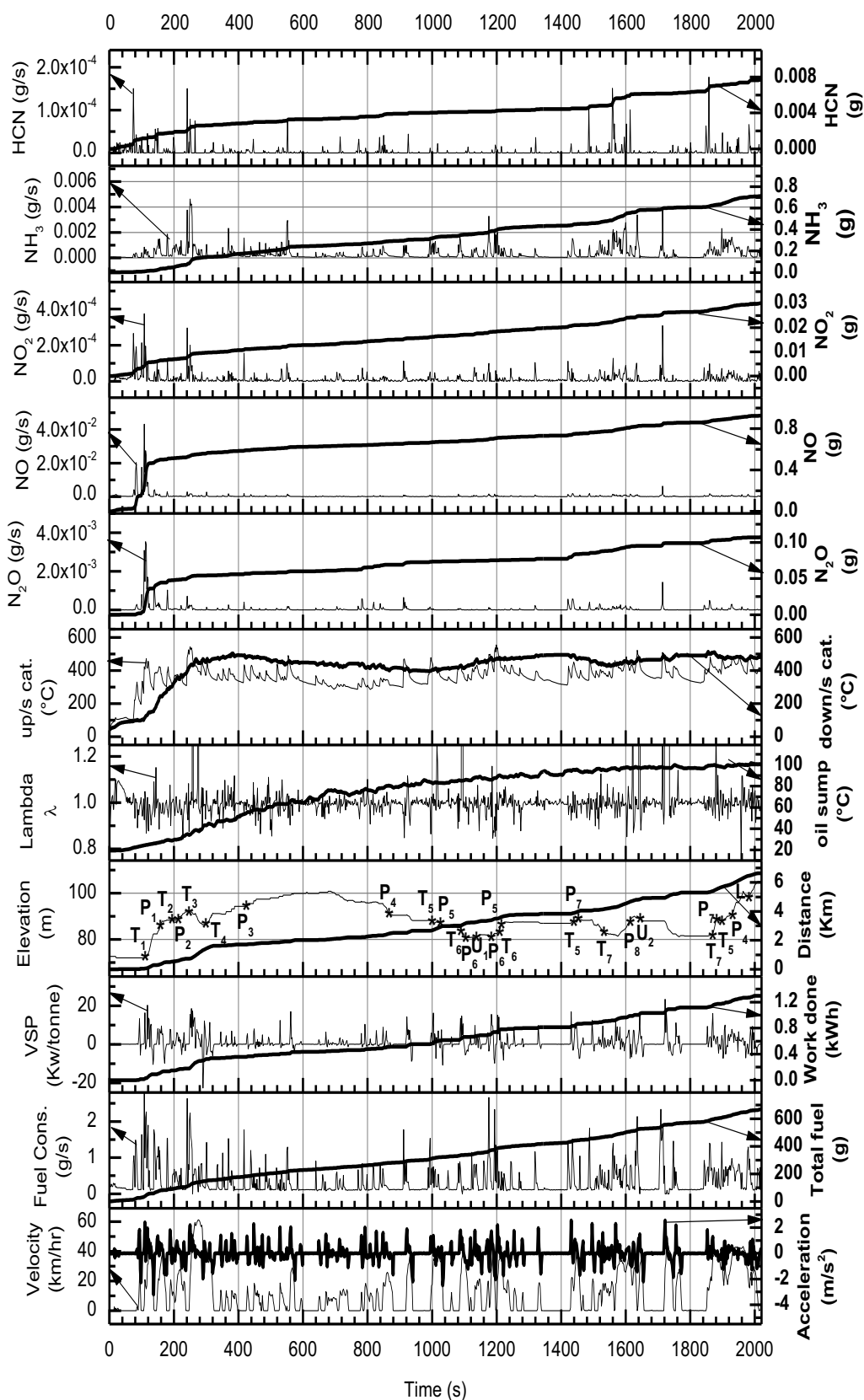


Figure 6-6 Nitrogen species Vs time profiles for the congested trip 16:24.

The peak NH<sub>3</sub> emission rate (g/s) from eight trips in Figure 6-5 and Figure 6-6 are generally in the range of 2~4 mg/s, well aligned with the reported data from Heeb [112]. Using the German highway cycle (BAB).

**Table 6-3 Comparison of NH<sub>3</sub> emission (mg/km) from reference [88] and this research**

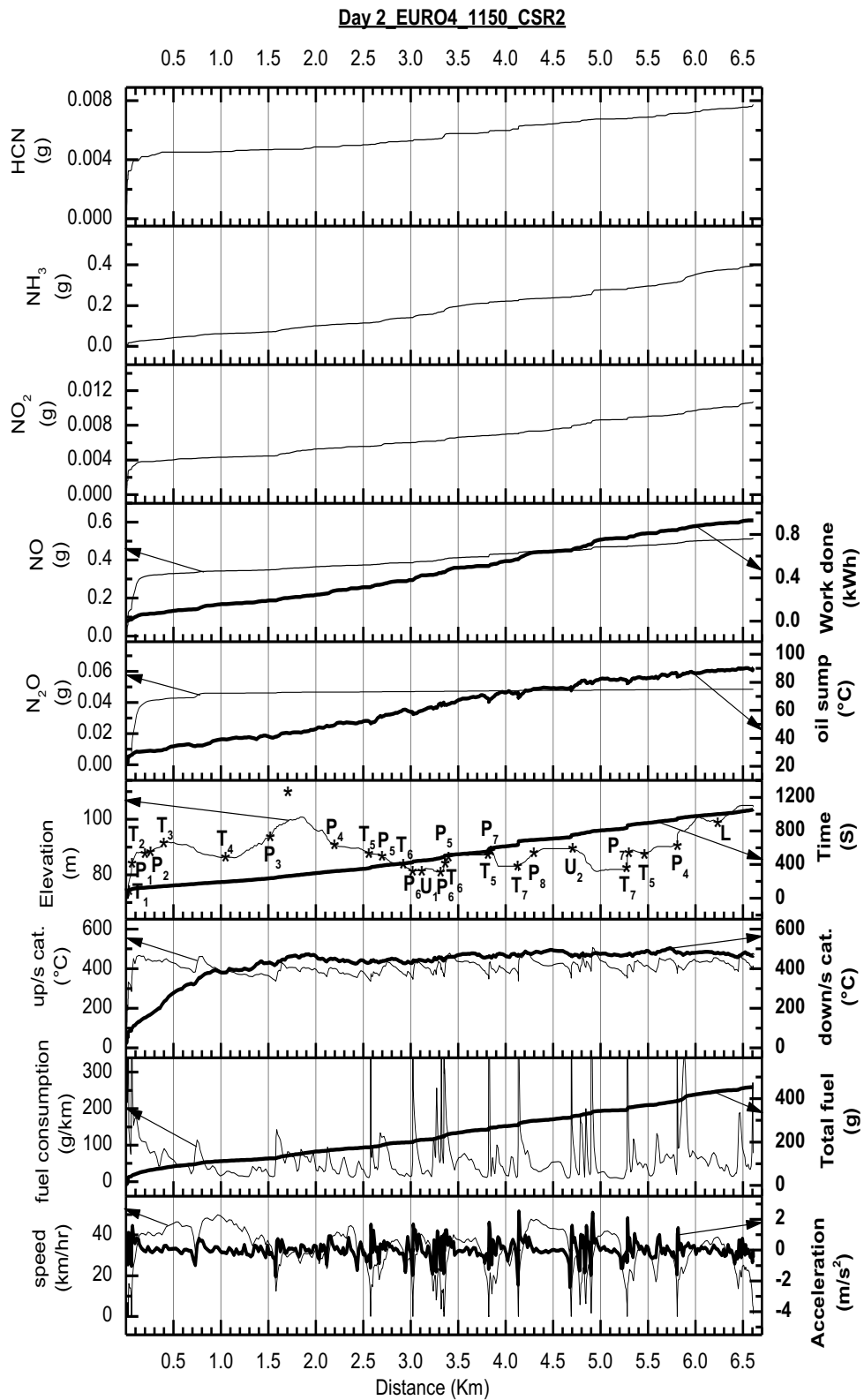
CYCLE	EURO 5	EURO4	EURO3	EURO4
NEDC	5.27	2.91	16.52	
UDC	6.7	4.13	19.21	
EUDC	4.46	2.2	14.99	
LHC (THIS WORK)				60~108

The peak mass emission rate of HCN was generally around 1 mg/s. These values are significantly higher than those obtained by using Euro 1 and 2 SI cars and close to the values of a high-mileage pre-Euro SI car reported by Karlsson [118]. The high HCN emissions from the Euro4 SI car may be related to the high NH<sub>3</sub> emissions, as both are by-products of de-NO<sub>x</sub> and reduction reactions across the TWC. However, the detailed mechanism on the formation of HCN through the TWC is not clear.

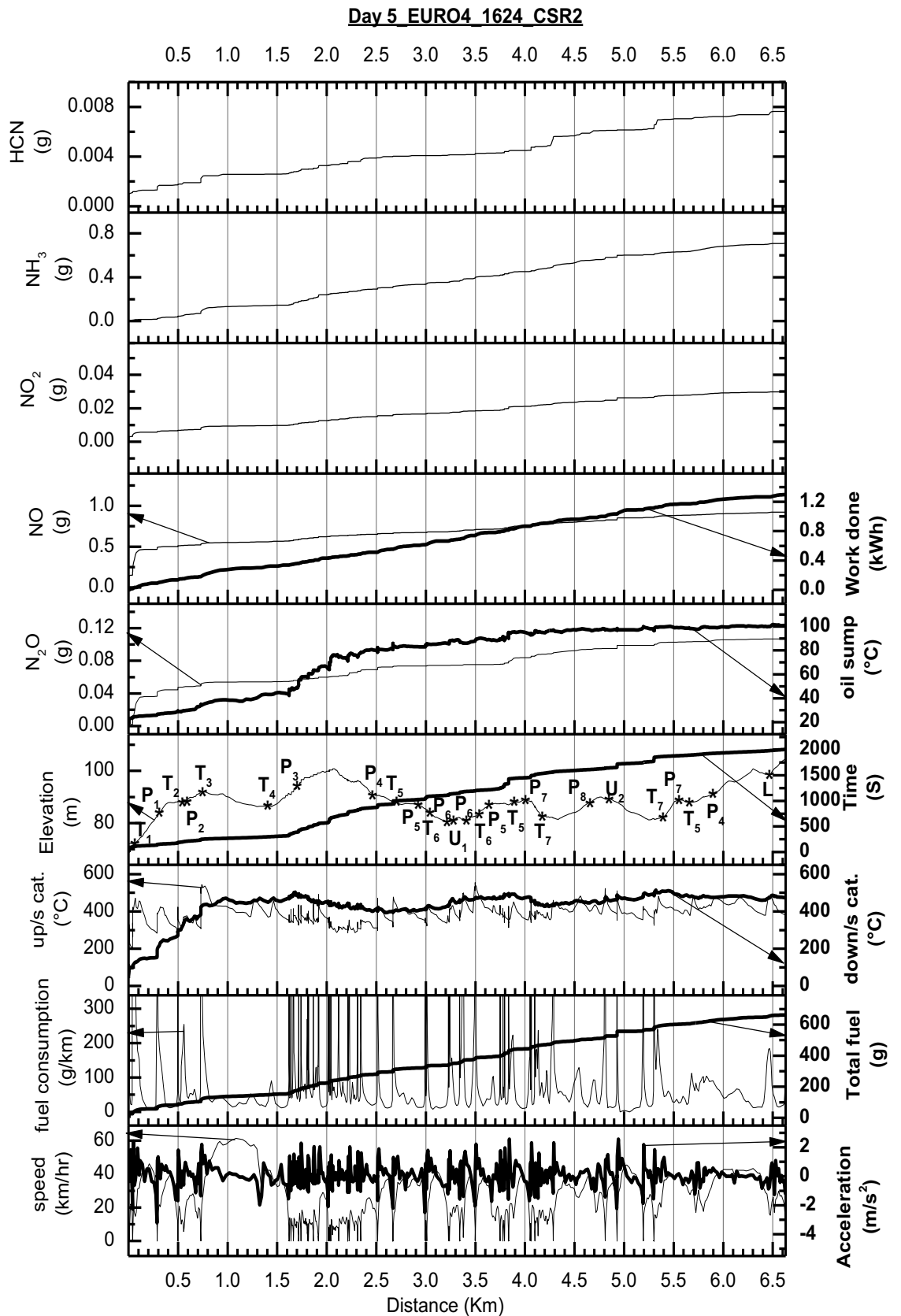
The NO<sub>2</sub> emissions are generally low for all the trips but the fraction of NO<sub>2</sub> in NO<sub>x</sub> is higher than those generally recognized values [112], which were <1%. The possible reasons for this are that the journeys presented in this paper were mostly in congested situations and thus have more decelerations (lean spikes), which resulted in further oxidation of NO.

N<sub>2</sub>O is usually formed when the TWC temperature is within certain ranges (250~450 C). The downstream of TWC gas temperature was measured in this research. The N<sub>2</sub>O emissions had an initial spike in the first 250 seconds for all the journeys after the engine started. However, there were very few obviously detectable N<sub>2</sub>O emissions during the remainder of the trips. This indicated that when the catalyst temperature was higher than 450 C, N<sub>2</sub>O formation across the TWC was trivial.

All the nitrogen compound emissions are related to the accelerations and positive VSP, even when there was no lambda deviation from 1, but not all the accelerations produce emission spikes.



**Figure 6-7 Nitrogen species vs distance profiles for the free flow trip 11:50.**



**Figure 6-8 Nitrogen species vs distance profiles for the congested trip 16:24.**

### 6.4.5 Legislated emissions

Figure 6-9 and Figure 6-10 show the mass emission rate (g/s) and cumulated mass emissions for legislated emissions as a function of time along with some driving parameters. Figure 6-10 shows more legislated emission spikes than Figure 6-9, which was a free-flowing trip. Also Figure 6-10 shows more spikes for lambda, VSP, fuel consumption, velocity and acceleration, as it was a congested trip. Figure 6-11 and Figure 6-12 show the cumulative mass emission (g) as a function of the distance travelled for legislated emissions. Figure 6-11 shows that the mass of CO, NO<sub>x</sub> and THC were 9.5, 0.8 and 2g respectively. Total fuel was 450 g and cumulative work done was 0.95 kWh. Whereas a higher value shows in Figure 6-12, which was a congested trip, the mass of CH<sub>4</sub>, N<sub>2</sub>O and CO<sub>2</sub> were 17, 1.4 and 3.2 g respectively. Total fuel consumption was 680 g and cumulative work done was 1.3 kWh.



Day 2 EURO4 1150\_CSR2

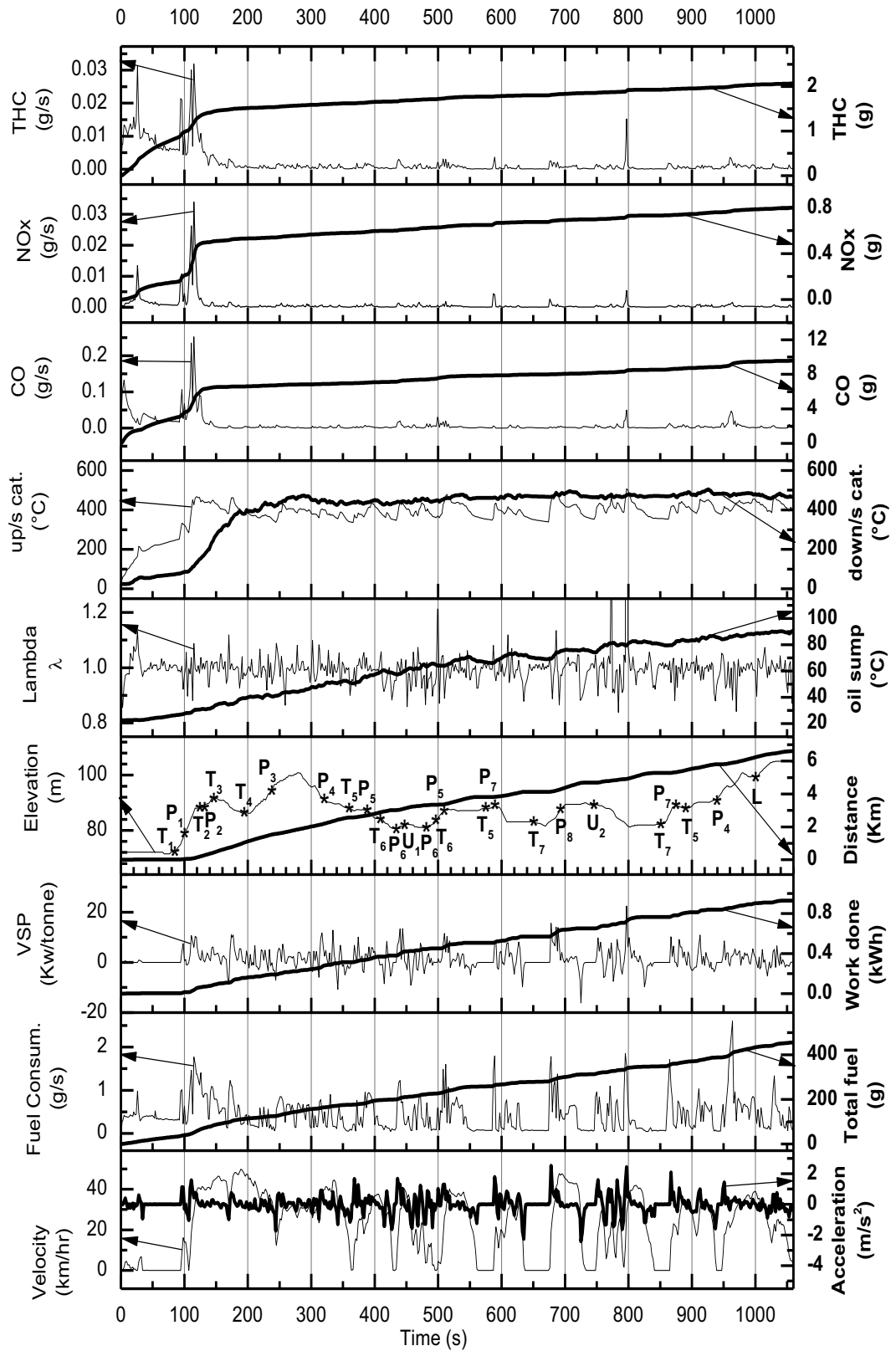


Figure 6-9 Legislated species vs time profiles for the free flow trip 11:50.

Day 5 EURO4 1624 CSR2

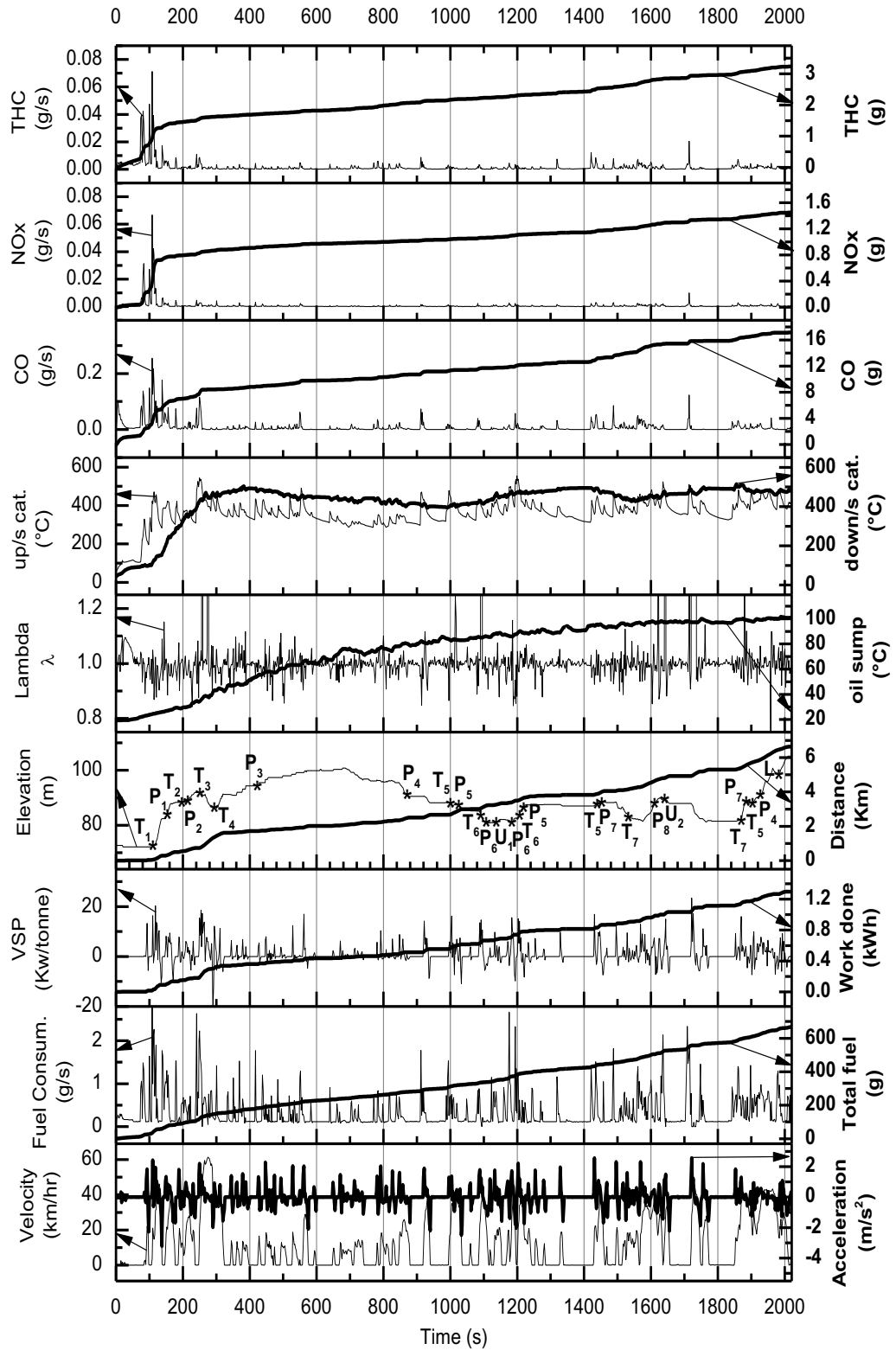
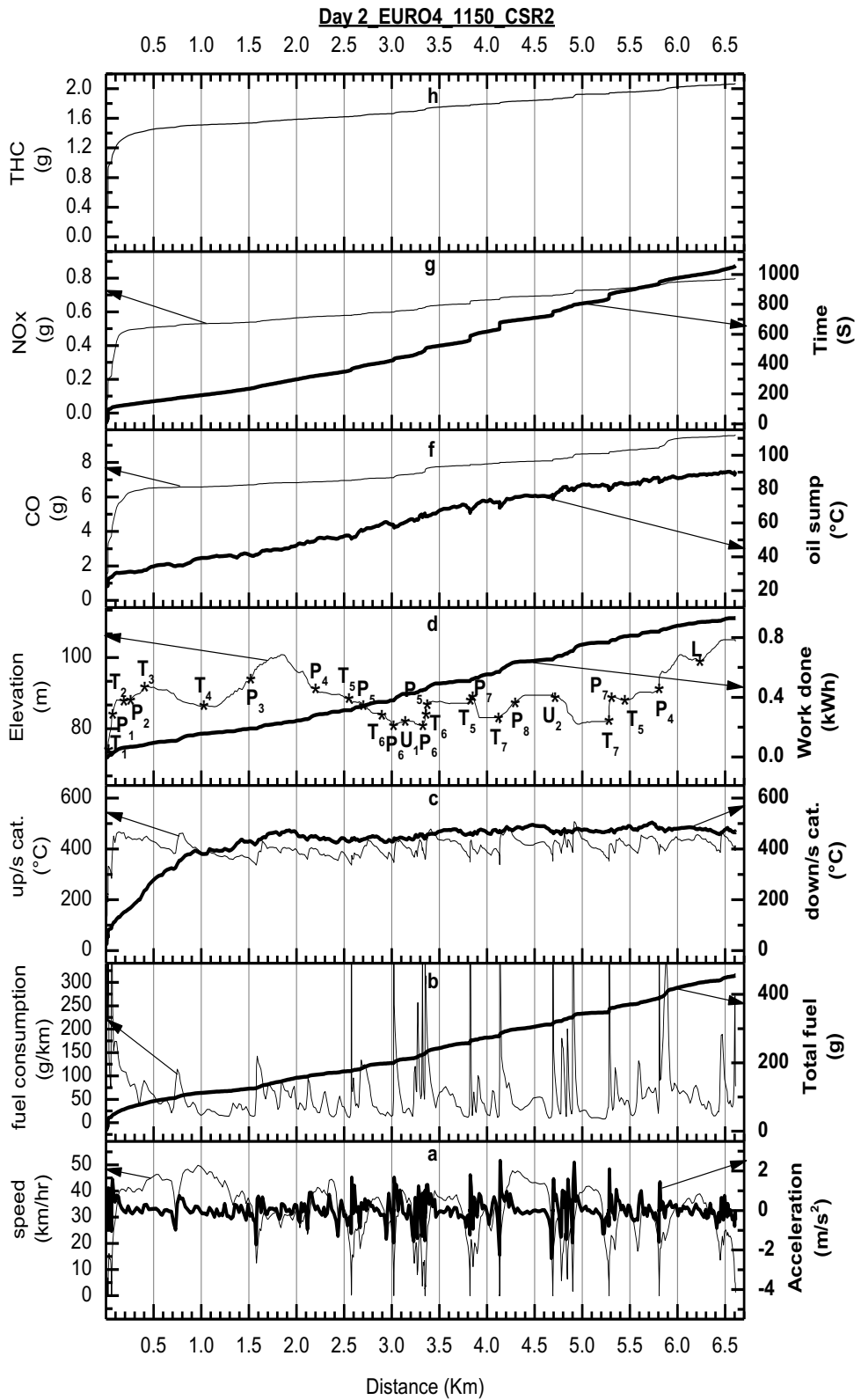
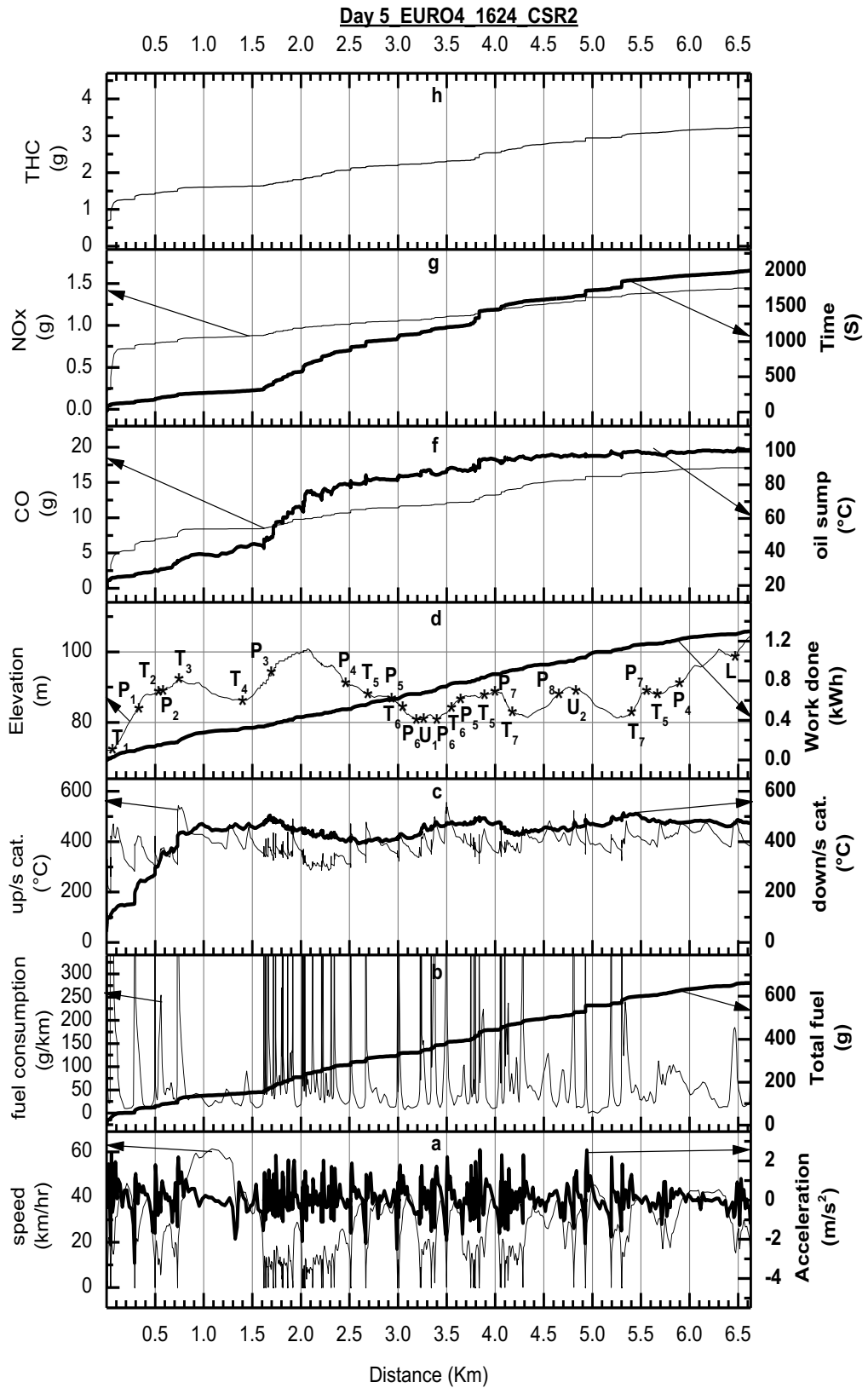


Figure 6-10 Legislated species vs time profiles for the congested trip 16:24.



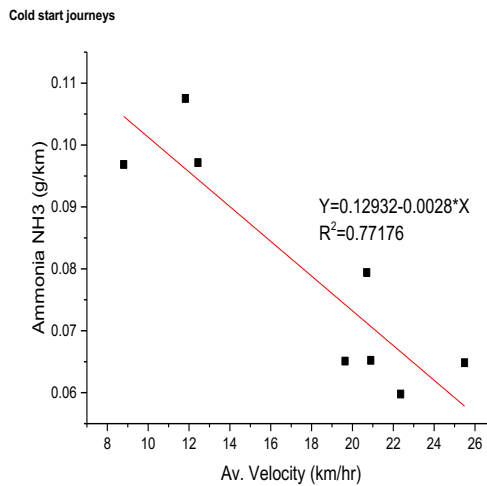
**Figure 6-11 Legislated species vs Dist. profiles for the free flow trip 11:50.**



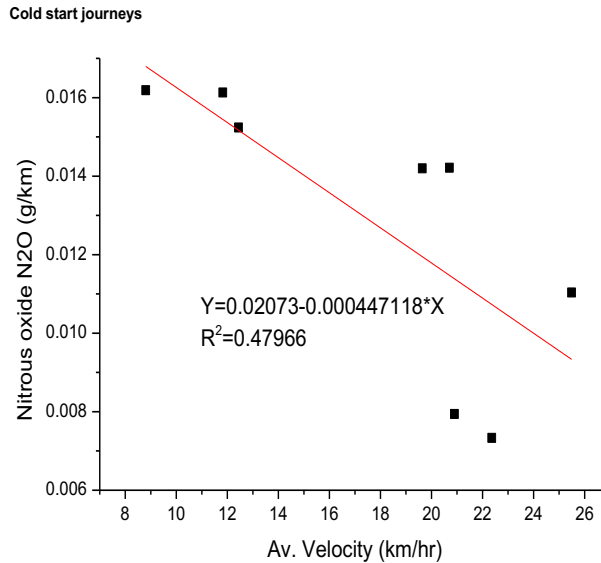
**Figure 6-12 Legislated species vs Dist. profiles for the congested trip 16:24.**

#### 6.4.6 Correlations between emissions and driving parameters

Figure 6-13 shows the correlation between trip NH<sub>3</sub> emissions in terms of g/km Vs average speed for eight trips. Additionally, a good linear correlation is observed. Similarly a good linear correlation between THC emissions and Vs average speed is observed as shown in Figure 6-15. Also, a good linear correlation between CO<sub>2</sub> emissions is observed as shown in Figure 6-14. Also, a good linear correlation between CH<sub>4</sub> emissions Vs average speed is observed as shown in Figure 6-17, whereas a moderate linear correlation between N<sub>2</sub>O emissions, vs average speed is observed as shown in Figure 6-14. However, the type approval CO<sub>2</sub> emission data for this make and model is 179 g/km based on the NEDC driving cycle [111] but the driving cycles in this study were urban cycles, so for the sake of being equitable, the results from this study can be only compared to NEDC urban part.



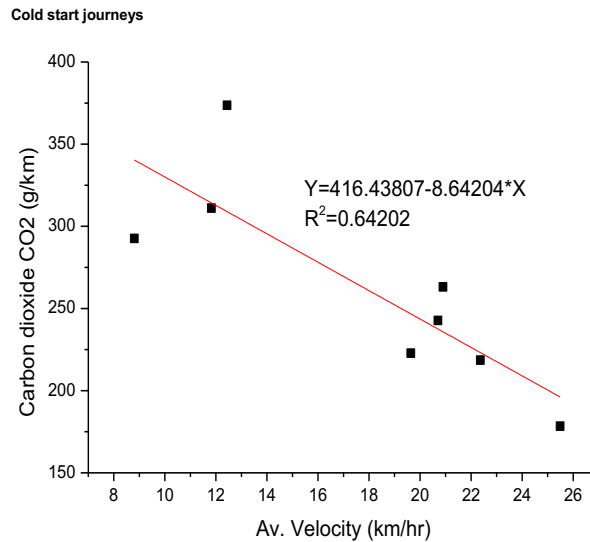
**Figure 6-13 Trip mean NH<sub>3</sub> emissions vs vehicle's average trip velocity.**



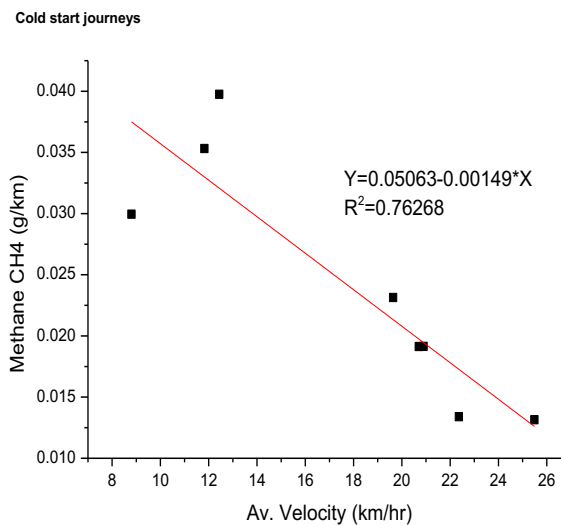
**Figure 6-14 Trip mean N<sub>2</sub>O emissions vs vehicle's average trip velocity.**

Based on the ratio of the combined and urban part fuel consumption from NEDC, which was 1.36 g/km, it is estimated that the NEDC urban part CO<sub>2</sub> for this model of vehicle is 244 g/km. The CO<sub>2</sub> emissions from this study are within a range of 178-374 g/km. This indicated that the realistic CO<sub>2</sub> emissions in the densely populated areas could be much higher than the legislated cycle results, which will depend on the severity of congestion. It can be seen in Table 6-1 that only four of those very congested journeys, namely (0722\_CSR2), (1624\_CSR2), (1620\_CSR3) and (1620\_CR3s), produced higher than NEDC urban part certified CO<sub>2</sub> emissions' values. Figure 6-16 demonstrated the correlation of journey average velocity with journey average CO<sub>2</sub> emissions. It shows that CO<sub>2</sub> (g/km) was higher than 244 g/km when the journey average velocity was slower than 20 km/h.

N<sub>2</sub>O and CH<sub>4</sub> have a much higher global warming potential (GWP) compared to CO<sub>2</sub> and their GWP index is about 300 and 35 relative to CO<sub>2</sub> respectively. However, due to the very low mass emissions, their contributions to GWP are only 0.1-0.4% and thus negligible.



**Figure 6-15 Trip mean CO<sub>2</sub> emissions Vs vehicle's average trip velocity.**



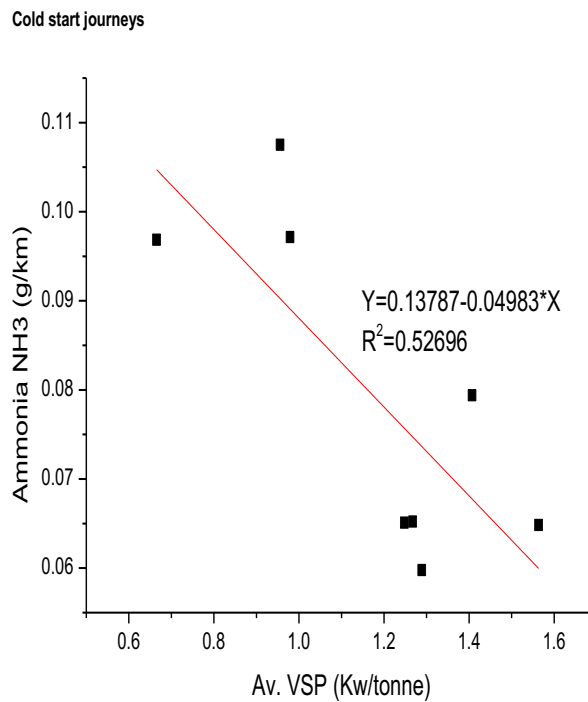
**Figure 6-16 Trip mean CH<sub>4</sub> emissions vs vehicle's average trip velocity.**

Interestingly, the reductions in NH<sub>3</sub>, N<sub>2</sub>O, THC, CO<sub>2</sub> and CH<sub>4</sub>, with increased average velocity might be due to reduced congestion and more free-flowing driving and thus fewer rich spikes in lambda. The reduction in N<sub>2</sub>O with increased average velocity is probably due to the fact that the catalyst temperatures exceeded the N<sub>2</sub>O formation window.

Figure 6-18, Figure 6-19 and Figure 6-20 indicate the relationship between emissions of NH<sub>3</sub>, CO<sub>2</sub> and CH<sub>4</sub>, Vs average vehicle specific power (VSP) for

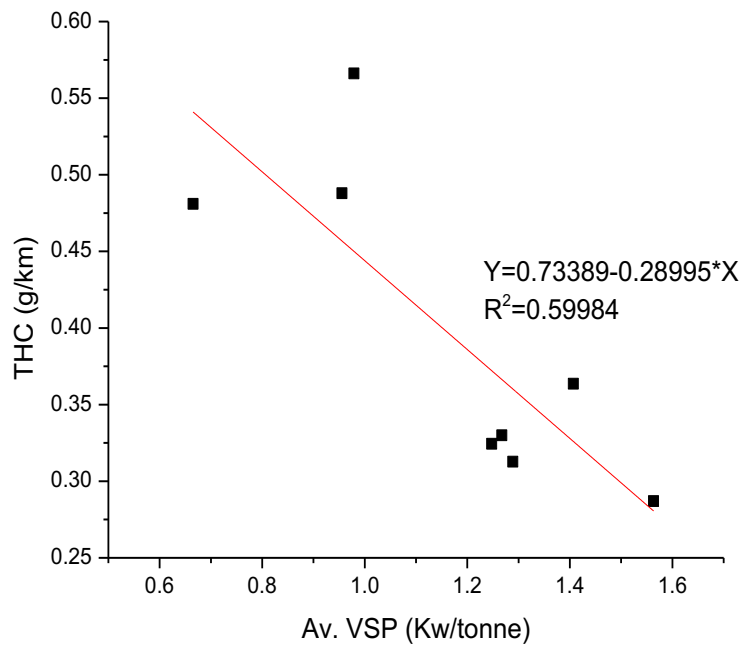
eight trips respectively. A moderate linear correlation is observed in these figures.

Figure 6-18 presents the correlation between trip THC emissions in terms of g/km, Vs average vehicle specific power (VSP) for eight trips. A good linear correlation is observed. The values of VSP are determined by travel velocity. The results in Figure 6-4, Figure 6-6, Figure 6-8, Figure 6-10, Figure 6-12 and Figure 6-14 are warm start and not truly cold start tests as the car was stopped for approximately 2.5 hours from previous tests, and the oil sump temperature was around 50-60°C at the start of the tests. If the tests were conducted with the vehicle soaked long enough, the emissions and fuel consumption would be even higher than what was presented.

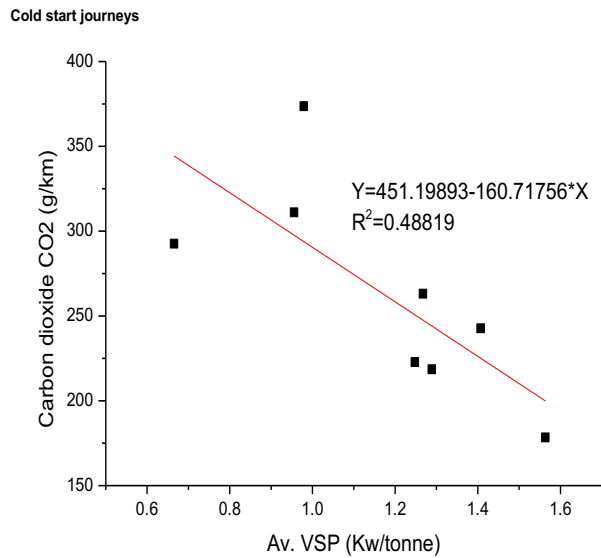


**Figure 6-17 Trip mean NH<sub>3</sub> emissions vs vehicle's average trip velocity.**



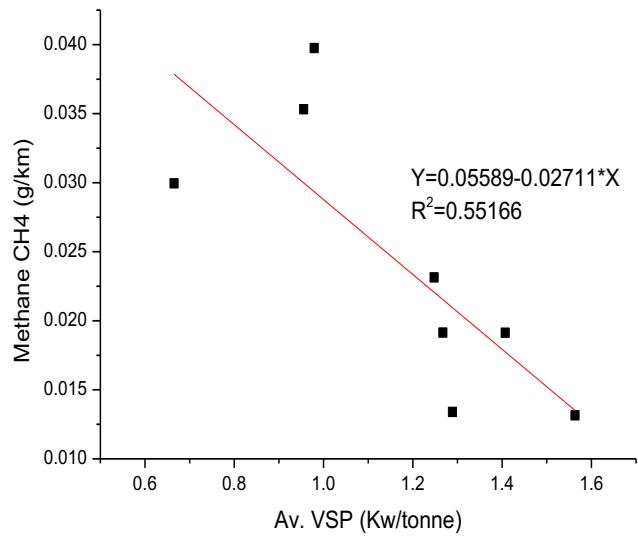


**Figure 6-18 Trip mean THC emissions vs vehicle's average trip vehicle specific power.**



**Figure 6-19 Trip mean CO<sub>2</sub> emissions vs vehicle's average trip vehicle specific power.**

Cold start journeys



**Figure 6-20 Trip mean CH<sub>4</sub> emissions vs vehicle's average trip vehicle specific power.**

## 6.5 Conclusions

Greenhouse gases (GHG), nitrogen compound emissions (HCN, NO, NO<sub>2</sub>, N<sub>2</sub>O and NH<sub>3</sub>) and legislated emissions from a EURO4 SI passenger car were measured using a portable FTIR system. The vehicle was driven on realistic driving cycles (route CSR1, CSR2, CSR3 and CSR3s) using the routes located in a densely populated area of Leeds representing a typical urban road network. Eight realistic emission tests were conducted at different times, such as rush hours in the morning, lunch time, evening, and off-peak time. The emissions were presented in ppm, g/s and g/km. The correlations between emissions and trip average velocity, acceleration and VSP were analysed. The following conclusions were observed:

- The light-off time for the TWC was approximately 200 seconds for the free-flowing trips and 350 seconds for congested trips. Congested trips show more emissions and driving parameters' spikes (lambda, VSP, fuel consumption, velocity and acceleration) than the free-flowing trips.
- Fuel consumption in congested traffic is much deteriorated. Fuel economy has difficulty in achieving the certified values in congested urban traffic. The idling fuel consumption accounted for 7~28% of the total fuel consumption, which will also cause an increase of 7~28% in CO<sub>2</sub> emissions. The total fuel consumption for congested traffic could be doubled when compared to the free-flowing trip. CO<sub>2</sub> showed good correlation with the average velocity and a moderate linear correlation with average VSP. The long stoppage time (idle) in a traffic queue can seriously reduce the engine's thermal efficiency. In this study, the thermal efficiency of the engine was 14-20% significantly lower than the theoretical values. CO<sub>2</sub> emissions were 178-373 g/km from this study. The type approval CO<sub>2</sub> for this make and model of vehicle is 179 g/km based on NEDC cycle (the NEDC urban part CO<sub>2</sub> is estimated at 244 g/km based on the fuel consumption ratio). This would result in an underestimation of CO<sub>2</sub> emissions for emission inventories.
- VSP, representing the power demand to move a vehicle is dominantly affected by the accelerations in urban driving conditions. The value of average

VSP and average VSP+ can be employed as indicators of traffic congestions. The minimum values for free-flowing VSP could be 1.3 for average VSP and 3 for average VSP+, whereas the minimum values for congested flow VSP could be 1 for average VSP and 2.1 for average VSP+.

- From this study, the journey average CH<sub>4</sub> was 0.013 g/km for free-flowing traffic and 0.035 g/km for congested traffic.
- CH<sub>4</sub> emissions can be very low when the engine is hot in congested traffic. CH<sub>4</sub> showed good correlation with the average velocity and a moderate linear correlation with average VSP.
- The N<sub>2</sub>O emissions had an initial spike during the first 250 seconds and for all the journeys after the engine was started was then trivial when TWC get hot even in very congested traffic. N<sub>2</sub>O showed a moderate correlation with the average velocity.
- From this study, THC showed good correlation with the average velocity and a moderate linear correlation with average VSP. THC emissions were 0.29-0.57 g/km, about 60% more in congested traffic.
- NO and NH<sub>3</sub> emissions are the most abundant nitrogen species in the tailpipe and could be detected from all the trips. HCN was generally very far below the detection limit during most of the journeys and only had occasional detectable spikes at harsh accelerations and at the beginning of the trips.
- NH<sub>3</sub> emission is one of the most abundant nitrogen species in the tailpipe and can be detected from all the trips. NH<sub>3</sub> emissions from this research were significantly higher than some reported data from other Euro 4 SI cars using NEDC due to heavy traffic and pedestrian crossings leading to frequent stops and starts. and harsher accelerations. NH<sub>3</sub> showed good correlation with the average velocity and a moderate linear correlation with average VSP.

- The results of mass emissions as a function, of distance travelled, showed clear evidence of the accumulation of emissions during vehicles' stoppage periods at traffic lights and in queues.

Finally, from this study CO emissions were observed to be 1.45-2.66 g/km.

## **7 Chapter Seven: Real driving emissions (RDE) in congested traffic: a comparison of cold and hot start**

### **7.1 Results and discussions**

#### **7.1.1 Examples of real driving emission data vs time and distance**

Two of the thirty-seven data sets are shown in detail in odd number figures from Figure 7-1 to Figure 7-11 each graph represents a low-congestion journey and the even number figures Figure 7-2 to Figure 7-12 represent an example of a high-congestion journey, for the same journey B (1-3-2-4 in Figure 7-27). The results are shown firstly as emissions vs time and then as emissions vs distance. The twelve graphs show three sets of data: figures from Figure 7-1 to Figure 7-4 we can see the GHG emissions, CO<sub>2</sub>, CH<sub>4</sub> and N<sub>2</sub>O; also it is clear from Figure 7-5 to Figure 7-8 the nitrogen speciation NO, NO<sub>2</sub>, NH<sub>3</sub>, HCN, and for completeness N<sub>2</sub>O again; then we can see from Figure 7-9 to Figure 7-12 show the legislated emissions THC, CO and NO<sub>x</sub>. Also, every graph has the vehicle parameters of velocity, acceleration, fuel consumption, gradient, lambda, VSP, and oil and catalyst temperature. In all the data plots, instantaneous and cumulative mass emissions are shown.

The hot start is shown by the lubricating oil temperature and by the catalyst temperature. The oil sump temperature is 95°C at the start of the tests and increases to 105°C within 20s. The catalyst temperature is initially at approximately 300°C but increases to 400°C in the catalyst outlet within 10-20s. In the lower congestion journey, the catalyst inlet and outlet temperatures remain above 400°C for most of the journey and the outlet temperature was 500 °C. The catalyst temperature was significantly lower for the high-congestion journey and the inlet temperature was consistently below 400°C , and the outlet temperature was only above 400°C for short periods of time. This will mean that at high congestion, the catalyst efficiency will not be at its optimum and this contributes to the consistently higher emissions of all species for the more congested journeys. There was also a significant 'cold start' effect in all the emissions, and there are always  $\lambda$  variations during the initial hot start. The impact on emissions is that the start period contributes significantly to the total journey mass emissions.

Day 6 EURO4 0913 B

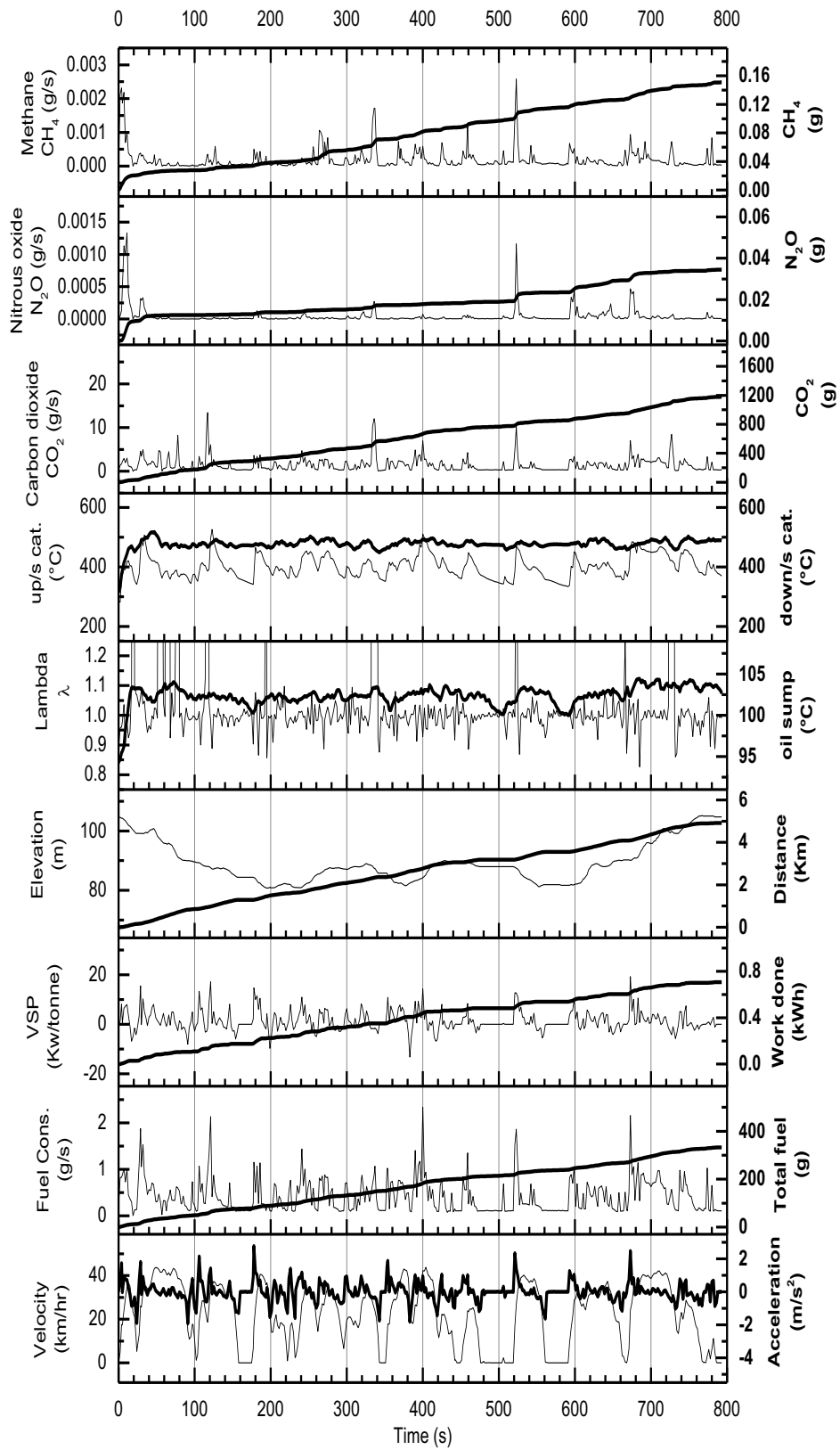
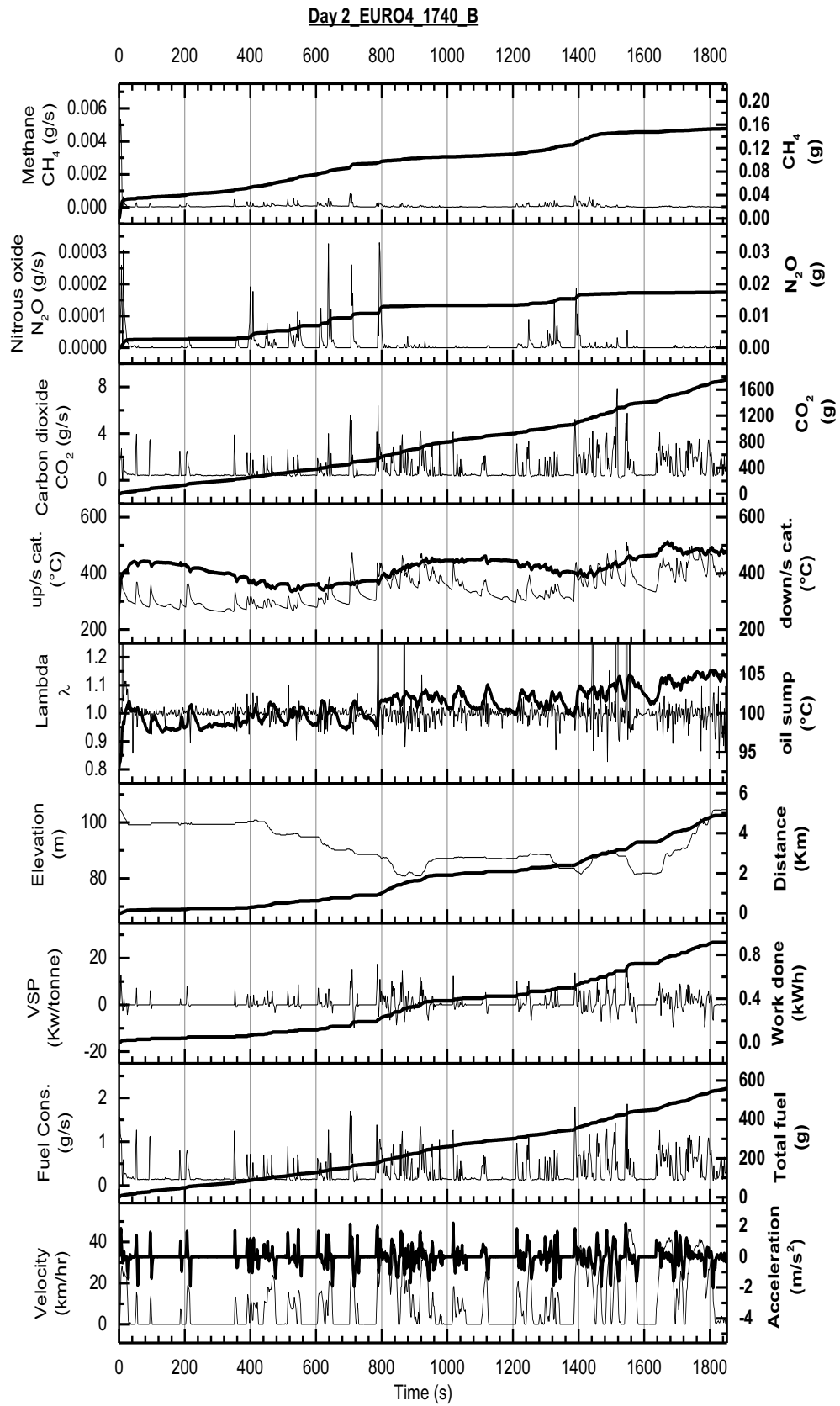
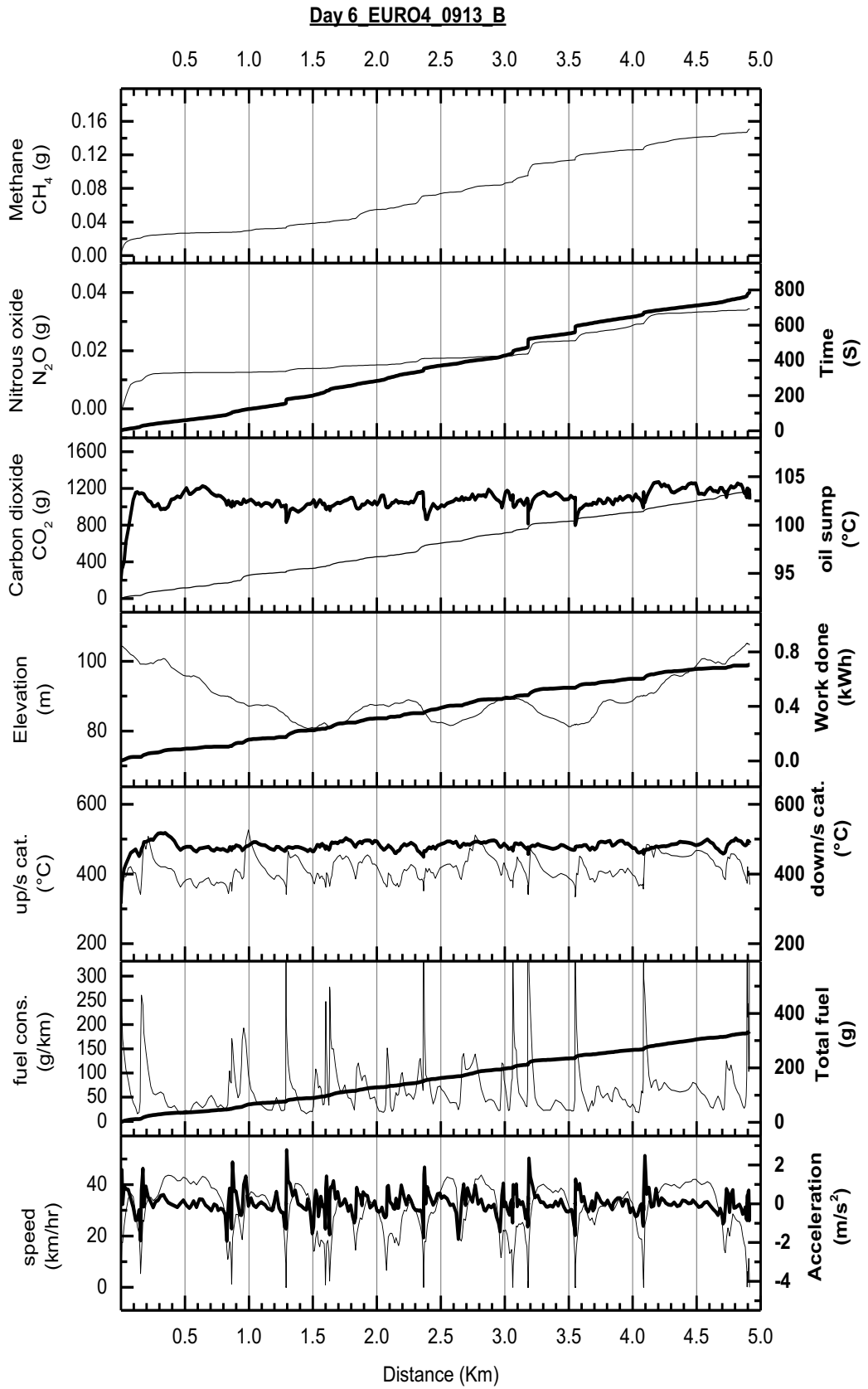


Figure 7-1 GHG vs time profiles for low congested trip 9:13B.

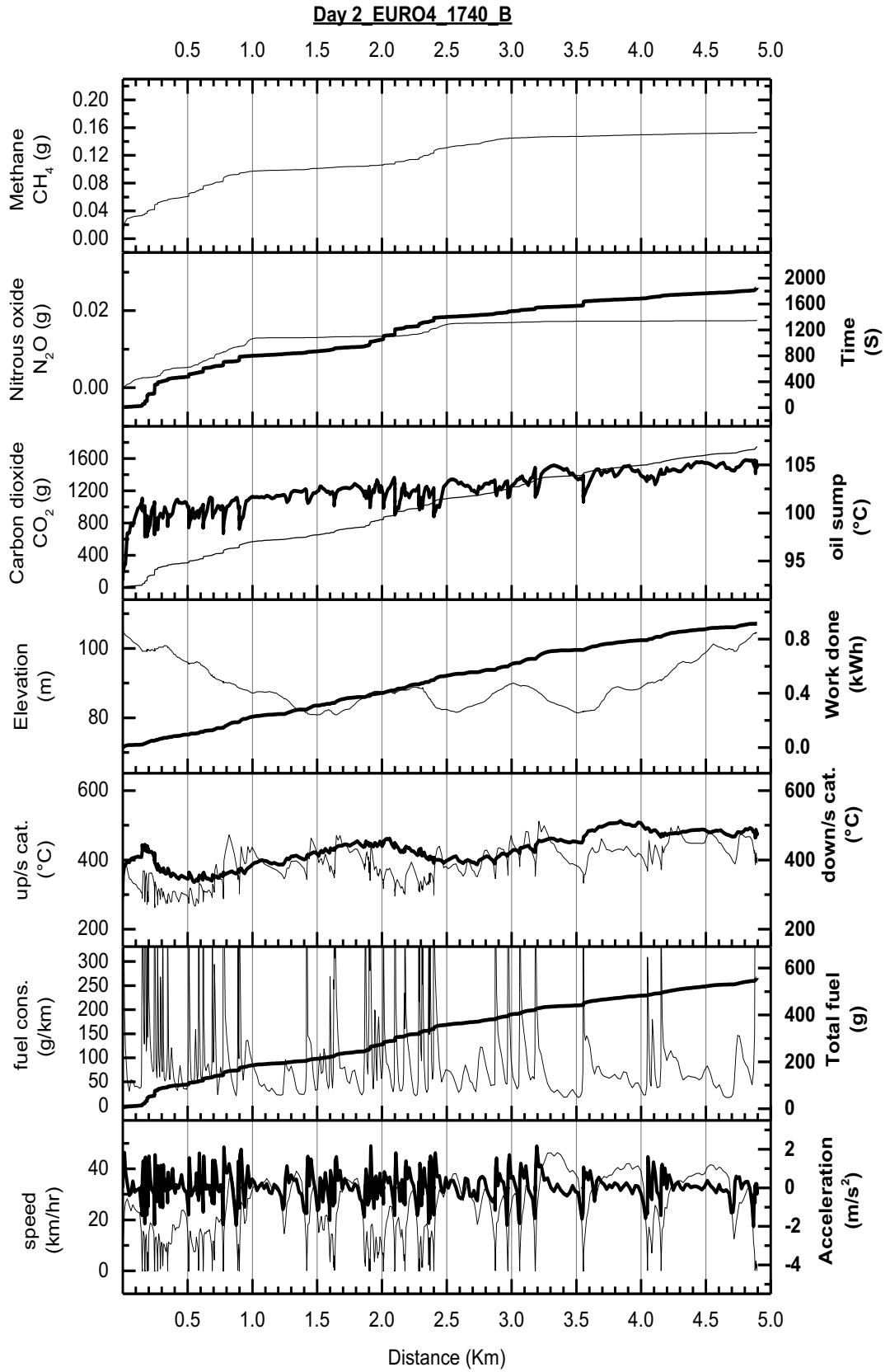


**Figure 7-2 GHG vs time profiles for high congested trip 17:40B.**

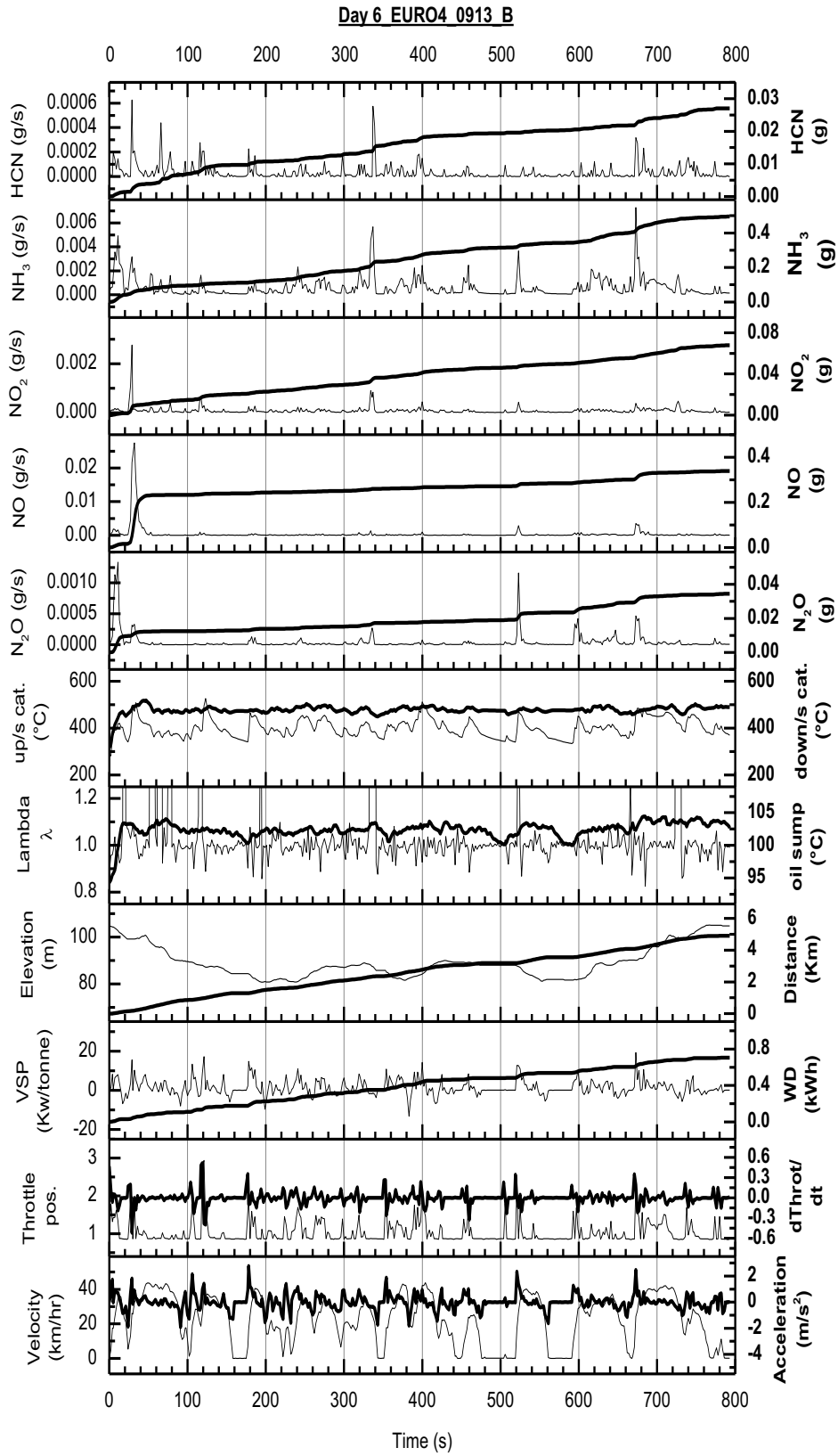




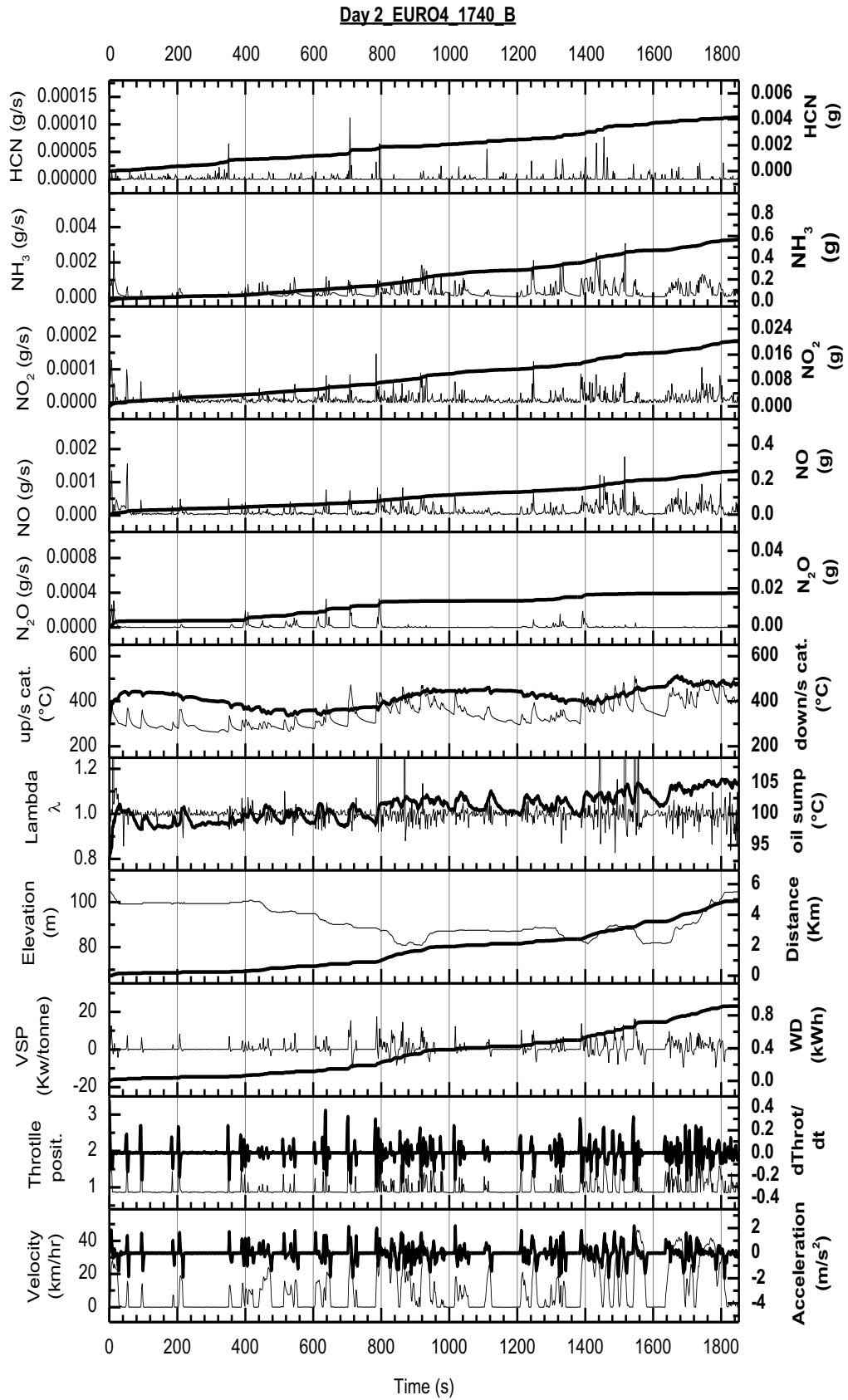
**Figure 7-3 GHG vs distance profiles for low congested trip 9:13B.**



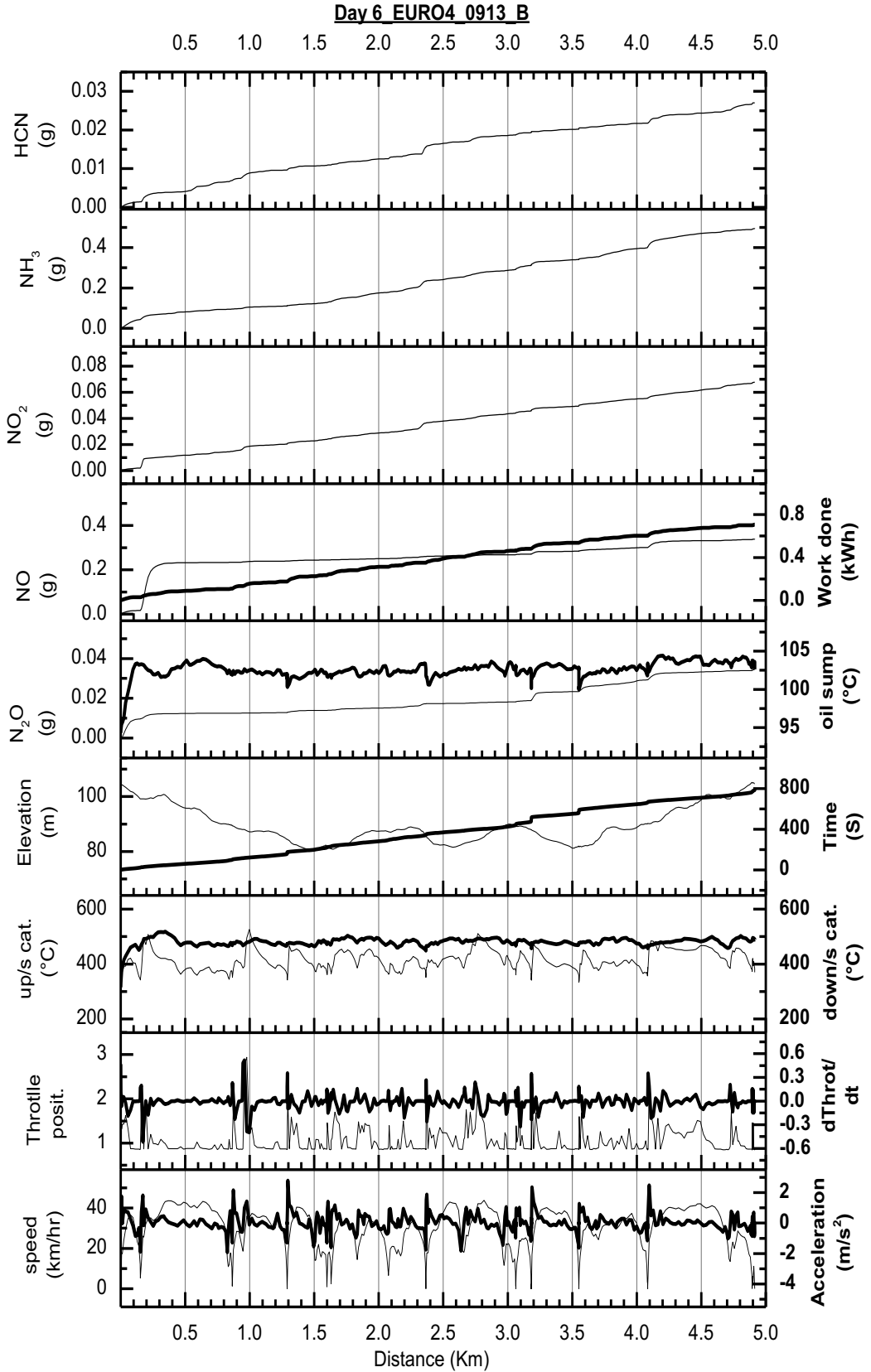
**Figure 7-4 GHG vs distance profiles for high congested trip 17:40B.**



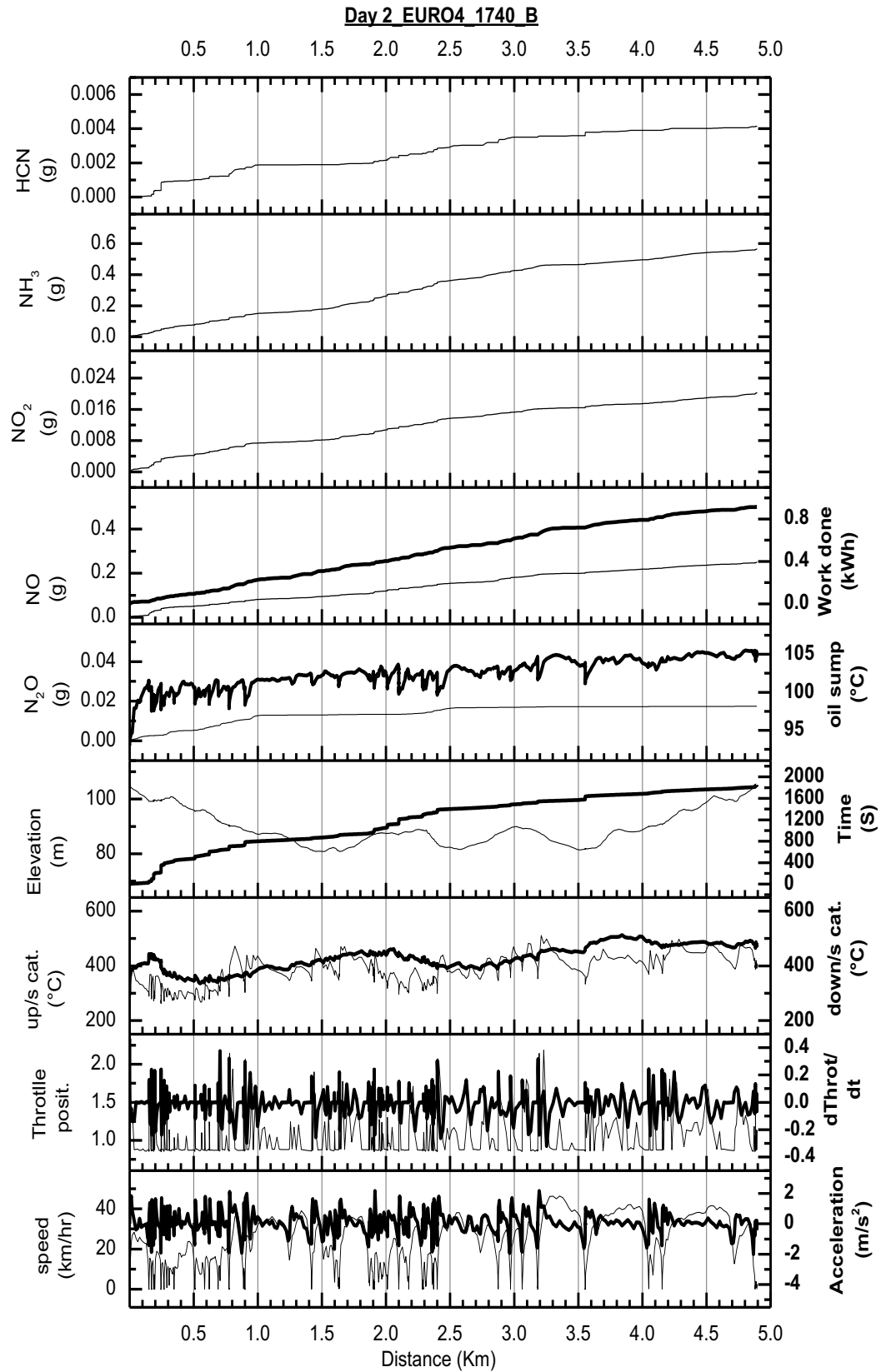
**Figure 7-5 Nitrogen species vs time profiles for low congested trip 9:13B.**



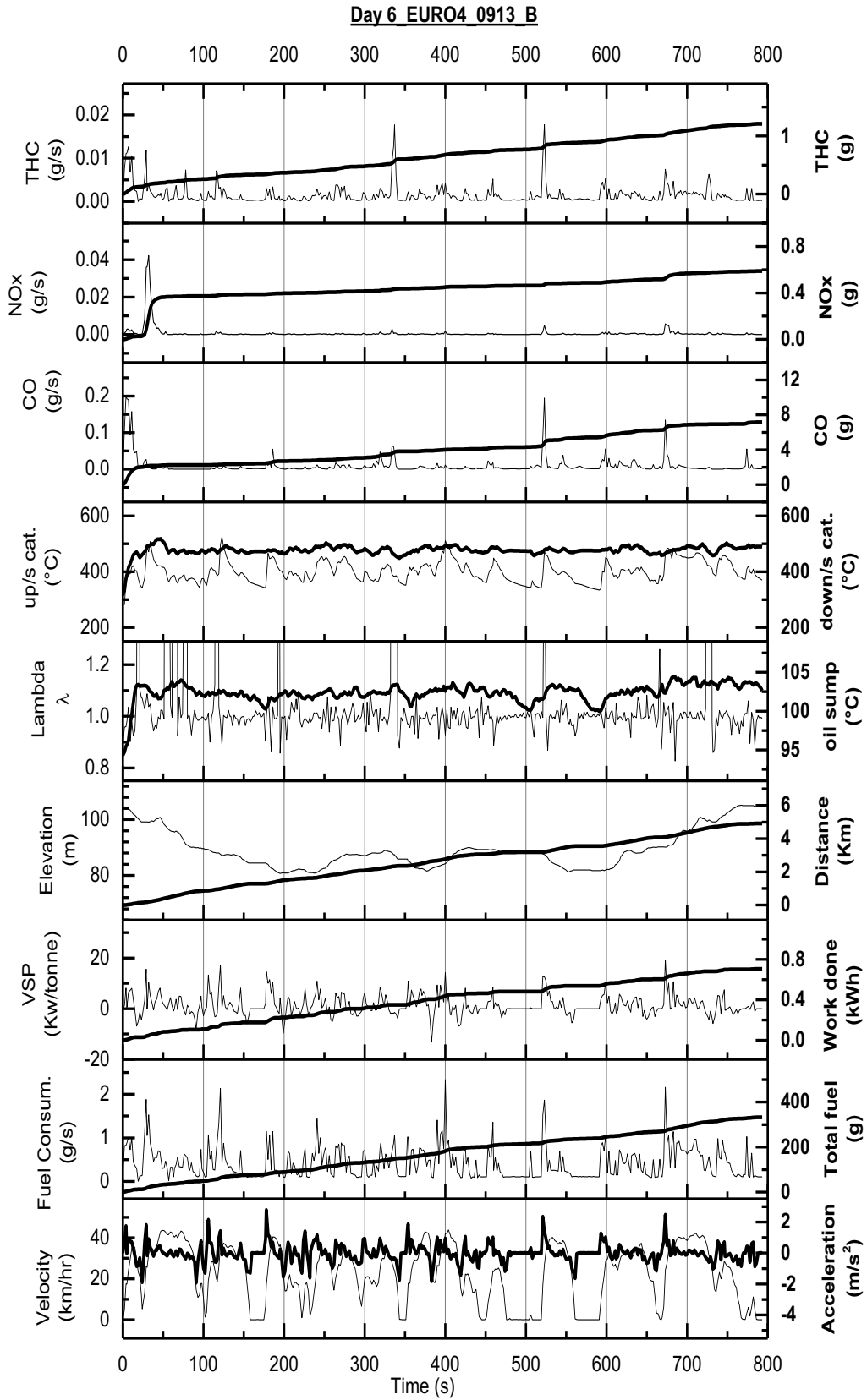
**Figure 7-6 Nitrogen species vs time profiles for high congested trip 17:40B.**



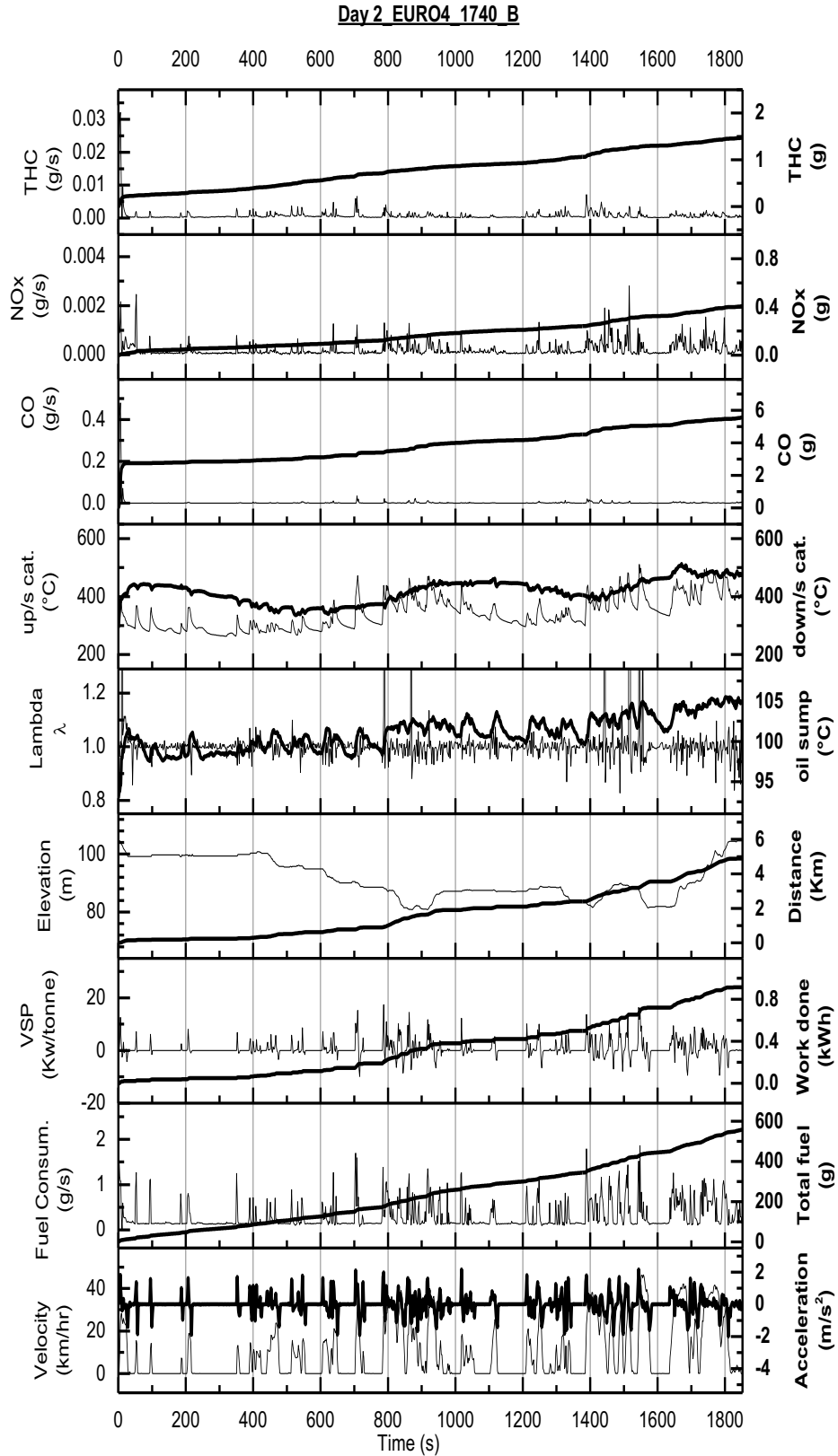
**Figure 7-7 Nitrogen species vs distance profiles for low congested trip 9:13B.**



**Figure 7-8 Nitrogen species vs distance profiles for high congested trip 17:40B.**

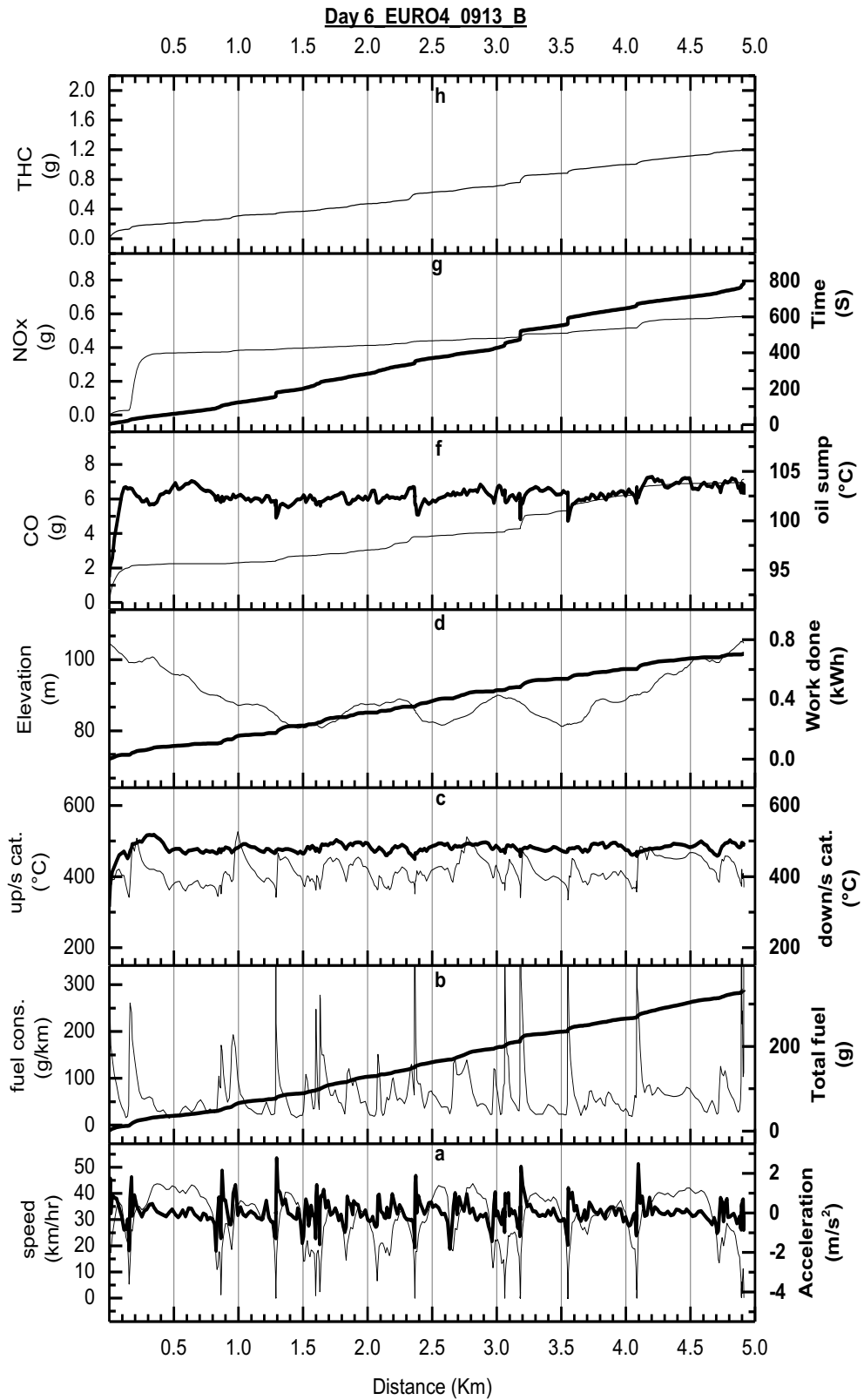


**Figure 7-9 Legislated species vs time profiles for low congested trip 9:13B.**

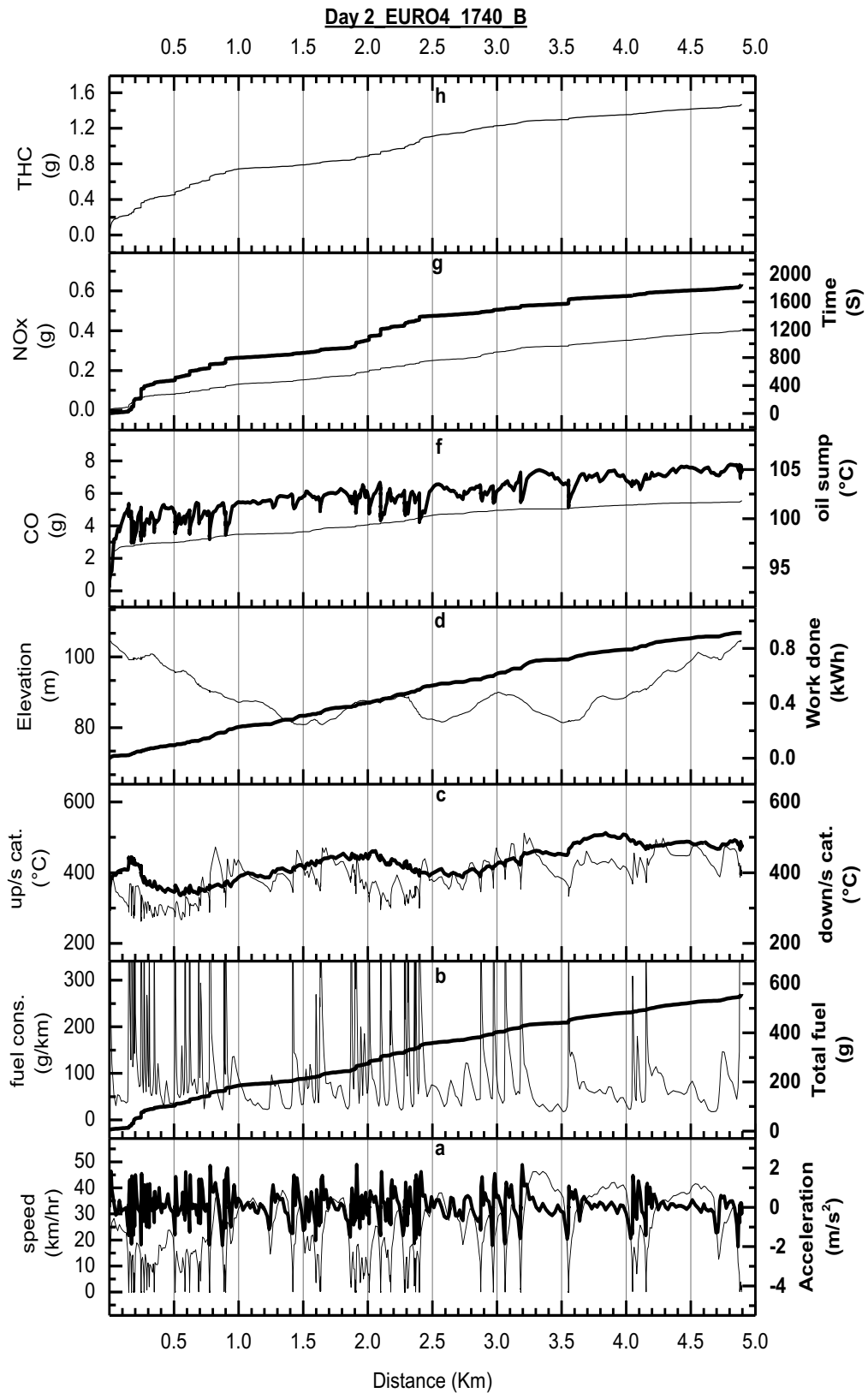


**Figure 7-10 Legislated species vs time profiles for high congested trip 17:40B.**





**Figure 7-11 Legislated species vs distance profiles for low congested trip 9:13B.**



**Figure 7-12 Legislated species vs distance profiles high congested trip 17:40B.**

Two effects occur here, the catalyst temperature may be below 400°C and the  $\lambda$  can be rich or lean for a short period. In Figure 7-9, with low congestion, there is a significant NO<sub>x</sub> peak that is associated with a lean excursion and loss of NO<sub>x</sub> TWC control. This is two-thirds of the total journey emissions. The highly-congested journey has better initial  $\lambda$  control and no 'start' effect on the total NO<sub>x</sub>, as shown in Figure 7-10. For the remainder of the journey, the NO<sub>x</sub> is higher with congestion by a factor of 2, but the total NO<sub>x</sub> was still higher for the low congestion due to the initial lean  $\lambda$  excursion. The distance plots show that these periods of high emissions occur when the vehicle is almost stationary and all released into the atmosphere as a local high concentration and not dispersed by the movement of the vehicle. This difference in the 'start' emissions was mainly due to the vehicle being effectively idle for the congested traffic, where  $\lambda$  control was good compared with an initial acceleration followed by a deceleration event in the less-congested traffic. The lean  $\lambda$  excursion then occurred during this first strong deceleration event. Event differences, give a strong variation in emissions for each journey, even in the case of the same journey average velocity.

Figure 7-5 to Figure 7-8 also have the throttle position and rate of change of throttle position, which is one measure of 'jerk'. The opening of the throttle is the power demand input and the output of this action is vehicle acceleration. Thus, Figure 7-5 to Figure 7-7 show that opening the throttle coincides, after a short delay, with the vehicle acceleration and the fuel-flow increase. Differences in throttle movement for the same vehicle speed and acceleration result in emissions variations that could be reduced if the throttle was not a direct input to the engine power. Drive by wire engine control technology, that treats the throttle as an input demand, can control acceleration and therefore constant velocity operation is a more consistent method with lower emissions and lower fuel consumption as a consequence.

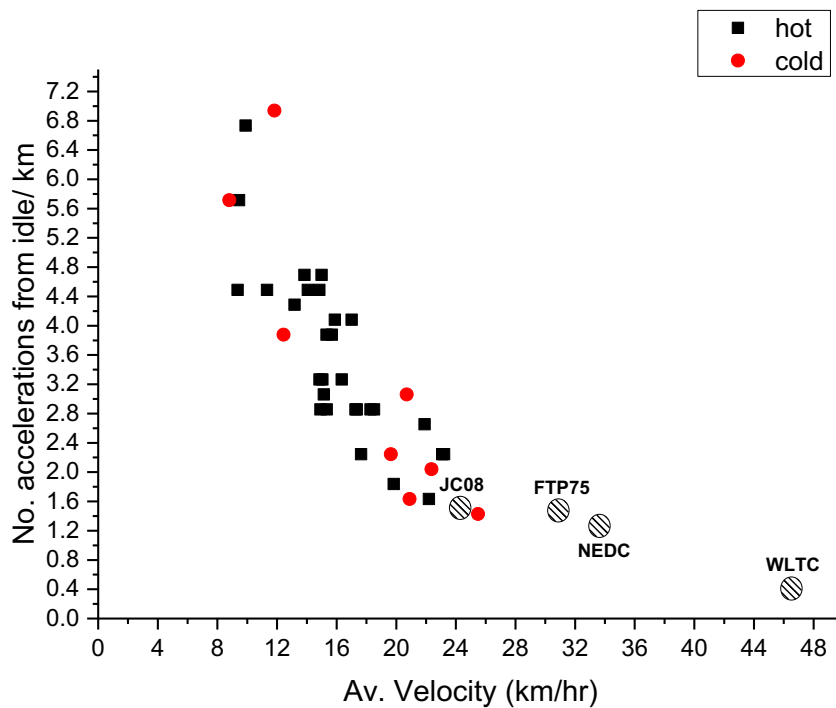
A common feature of these two journeys is that the emissions are generated by specific road events and that, between the transient events, the emissions were low. The same occurs for fuel consumption and CO<sub>2</sub> emissions, where each acceleration is accompanied by a spike in fuel consumption and CO<sub>2</sub>

emissions so that the CO<sub>2</sub> mass emissions from the journey are controlled by the number of stop/start events, or other accelerations, with low consumption between these events. In congested traffic the number of events were higher, due to the greater number of stop/starts. This is the key action of congested traffic, an increase in the number of stop/starts as the mean velocity decreases and the congestion increases.

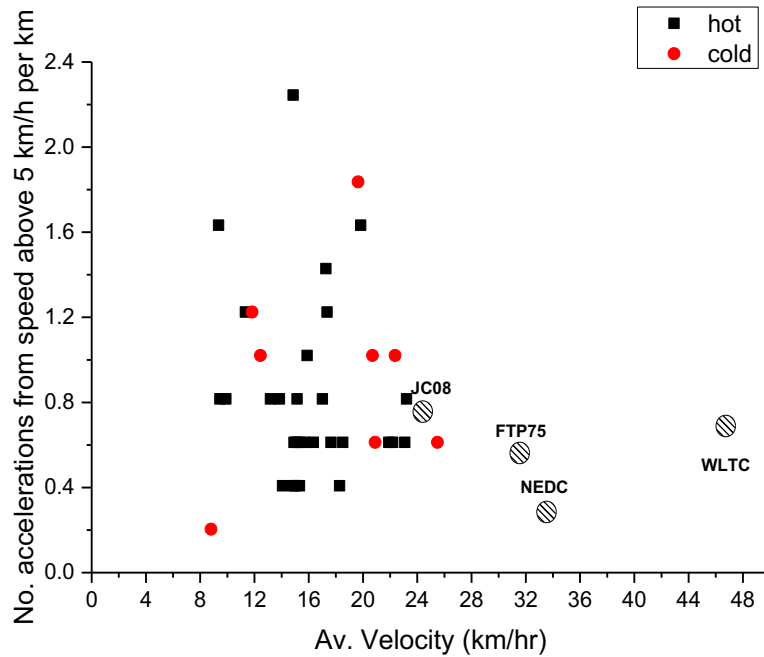
For all the twenty-nine hot start journeys and eight cold start journeys, the number of accelerations from idle per km are shown in Figure 7-13 as a function of the mean journey speed. This is the total number of events over the 5 km journey divided by the journey length, not individual km by km number of starts from idle. Figure 7-13 shows that the cold start data is not different from the hot start in terms of the number of stops that contribute to a particular average speed. A stop event has been defined as the instantaneous speed of the vehicle falling below 5 kph. The subsequent acceleration is then essentially from stationary. The duration of the stop events is seen in the time plots in figures numbers as Figure 7-1, Figure 7-2, Figure 7-5, Figure 7-6, Figure 7-9 and Figure 7-10, but the distance plots Figure 7-3, Figure 7-4, Figure 7-7, Figure 7-8, Figure 7-11 and Figure 7-12 show each stop as a spike to zero velocity in the velocity v. distance plots.

None of the legislated test cycles has transient events that have any of the features of highly-congested traffic in Figure 7-1 to Figure 7-12. This is shown in Table 7-1 Table 1 in terms of the number of stop/start events in legislated test cycles, and these are compared with the present work in Figure 7-13. For the present 5km journey length, the number of stop/start events was 1.4 - 7/km. The NEDC, FTP75 and JCO9 test cycles have 1.3-1.5/km accelerations from idle which is at the lowest level of those seen in the present work, as shown in Figure 7-13. The new test cycles WLTC and RDE, that are intended to be more realistic, are actually less realistic as they have higher mean velocities and fewer stop/starts i.e. journeys without junctions and traffic lights, as shown in Table 7-1 and Figure 7-13.

Realistic driving certainly includes accelerations from vehicle speeds above 5 kph and the number of these per km are shown as a function of the average velocity in Figure 7-14, with a comparison with data from the test cycles. The number of these acceleration events is low compared to those in Figure 7-13 and similar to those for starts from idle for journeys with average velocities above 24 kph. Figure 7-14 shows that the number of accelerations starting from >5kph are not correlated by the mean velocity and are variable, mainly due to the actions of the traffic in front of the vehicle. Figure 7-14 also shows that the test cycles are all at the lowest end of the range of accelerations/km in the present work.



**Figure 7-13 Number of accelerations from idle vs mean trip velocity for cold and hot start trips.**



**Figure 7-14 Number of accelerations not from idle ( $\geq 5$  kph initial vehicle speed) vs mean trip velocity for cold and hot start trips.**

The WLTC has more accelerations from  $>5$  kph than from  $<5$  kph, which is different from the other test cycles and the present realistic driving results.

A further feature that causes the congested traffic to have high emissions is that the temperature upstream of the TWC is below  $400^{\circ}\text{C}$  for most of the journey, as shown in Figure 7-2. The downstream temperature in congested traffic is about  $400^{\circ}\text{C}$ , indicating some heat release at the catalyst, but the efficiency will be lower than for low congestion where Figure 7-1 shows the upstream catalyst temperature was fluctuating around  $400^{\circ}\text{C}$  and downstream of the catalyst was  $500^{\circ}\text{C}$ .

The stop/start actions of the vehicle in congested traffic makes it difficult to keep  $\lambda=1$ . Figure 7-1 and Figure 7-2 show that for low congestion the deviations from  $\lambda=1$  are greater than for high congestion. This is due to the higher acceleration and deceleration rates under lower congestion conditions. These greater transient events lead to greater deviations from  $\lambda=1$ , with each high acceleration giving a locally rich mixture and each harsh deceleration giving a lean  $\lambda$  deviation. Emission spikes then line up with these  $\lambda$  deviations, as shown in Figure 7-1 to Figure 7-12.

### 7.1.2 Emissions as a function of congestion

The journey average emissions and other vehicle movement parameters are summarised for all thirty-seven journeys in Table 7-1 to Table 7-3 Appendices A-C. Figure 7-15 shows the cumulative CO<sub>2</sub> emissions for each journey as a function of the mean journey velocity (or congestion) for both hot and cold starts. Figure 7-15 shows that the CO<sub>2</sub> emissions are a linear function of the average journey speed with no significant difference for hot or cold starts. The variability in the data is due to differences in local traffic conditions for each journey for the same mean velocity and Figure 7-13 shows that the key variable factor is the number of stop/start events. All the measured data were above the certified NEDC CO<sub>2</sub> levels for this Euro 4 Ford Mondeo vehicle of 179 g/km. However, the data show that at the mean velocity of 33.6 kph ,in the NEDC, the present trends would be in agreement and perhaps below the certified value.

The stop/start events shown in Figure 7-13 reduce the mean velocity and increase the CO<sub>2</sub> emissions. Every acceleration from idle in Figure 7-1 to Figure 7-12 shows a corresponding peak in the fuel consumption and CO<sub>2</sub> emissions. Between the CO<sub>2</sub> spikes, associated with acceleration from idle, the CO<sub>2</sub> emissions were very low. The reason that many drivers complain that certified emissions on the NEDC or FTP75 are not reproduced in realistic driving in urban areas is that the test cycles do not reproduce the congested traffic conditions of urban driving. The WLTC and RDE proposals will cause this to deteriorate as they are emphasising high-speed high-power events that are irrelevant to urban driving, but are relevant to overall fuel consumption and CO<sub>2</sub> emissions. As over 50% of journeys are <5km in the USA[23], it likely that drivers who complain about fuel consumption being greater than that stated for the vehicle have evaluated their fuel consumption in congested urban driving.

The legislated emissions of CO, THC and NO<sub>x</sub> are shown as a function of the mean journey speed in Figure 7-16 to Figure 7-18. For all three pollutants, the cold start journeys had significantly higher emissions than for the hot starts. The reason was that the time to achieve the 400°C catalyst inlet temperature

was longer under cold start [30]. For mean journey velocities above 16kph, the CO emissions were below the Euro 4-6 limits, but at higher congestion were above the limits. The high CO emissions under high-congestion conditions were due to the greater number of stop/starts shown in Figure 7-13 with the rich excursion that accompany each acceleration leading to peaks in the CO emissions. For example Figure 7-9. shows that each acceleration was accompanied firstly by a rich excursion and then by a lean excursion quite close to a peak in the CO following the rich excursion. However, there were relatively few CO peaks in low-congestion conditions of Figure 7-9 and less than there were rich excursions to about  $\lambda=0.9$ . The reason for the relatively few CO emissions peaks is that TWC have ceria that stores oxygen, so that CO and HC oxidation can continue for a time during a rich excursion. For CO and HC to slip this control the rich residence time needs to be greater than the stored ceria can control, and this only occurs for a few of the rich excursion events.

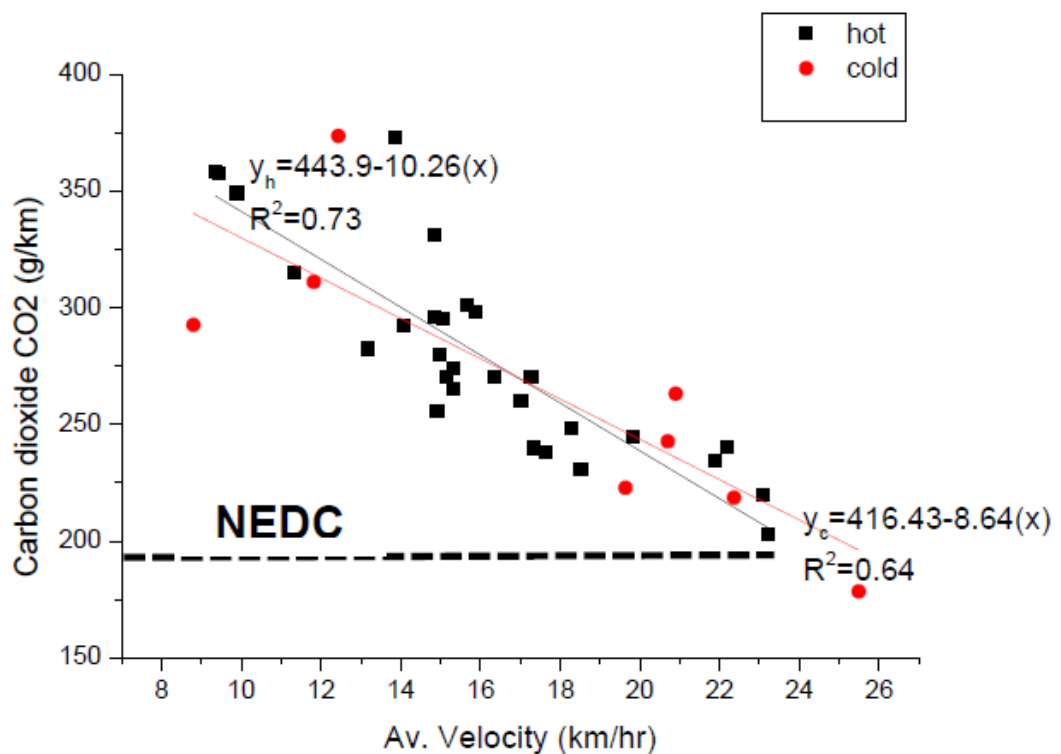


Figure 7-15 Trip mean CO<sub>2</sub> emissions vs vehicle's average trip velocity.



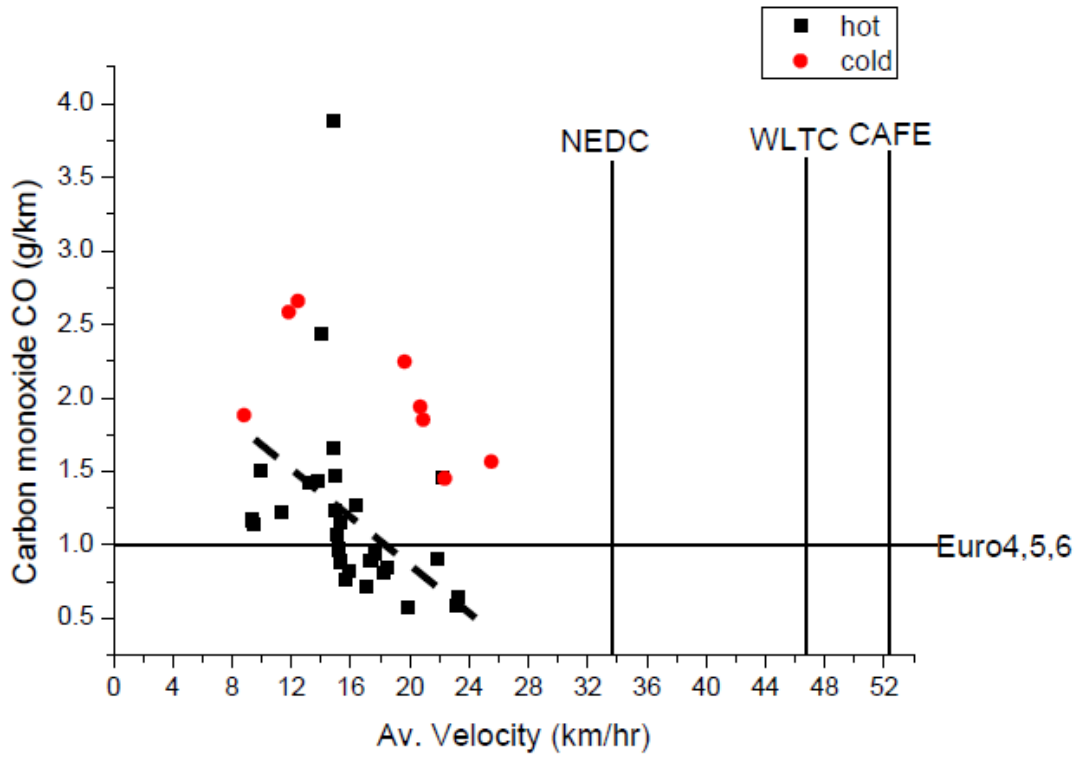


Figure 7-16 Trip mean CO emissions vs vehicle's average trip velocity.

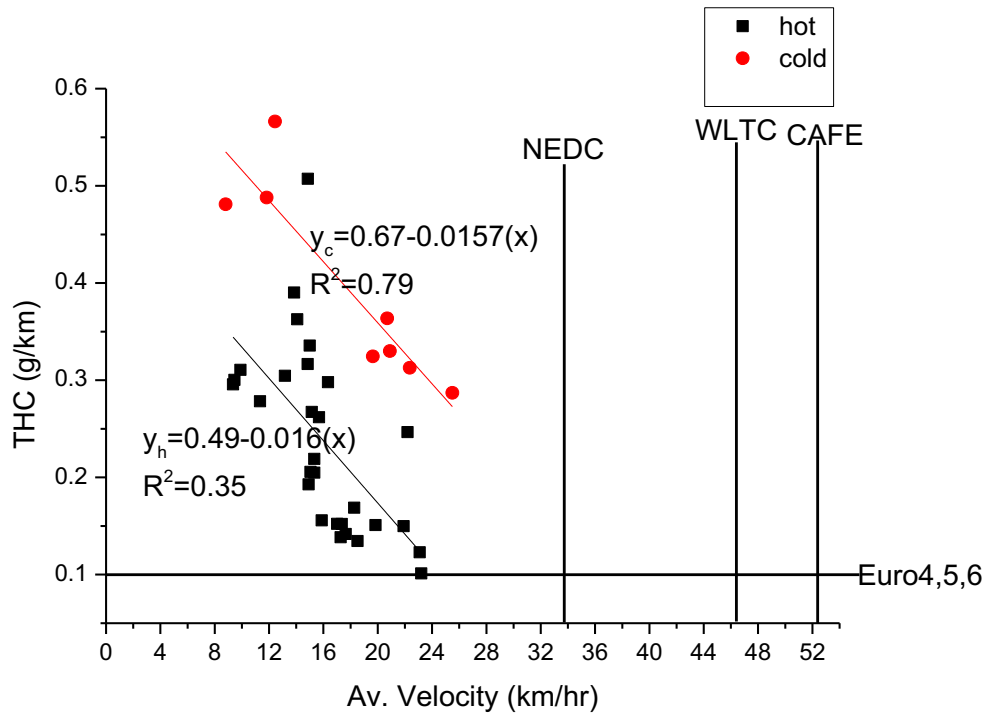


Figure 7-17 Trip mean THC emissions vs vehicle's average trip velocity.

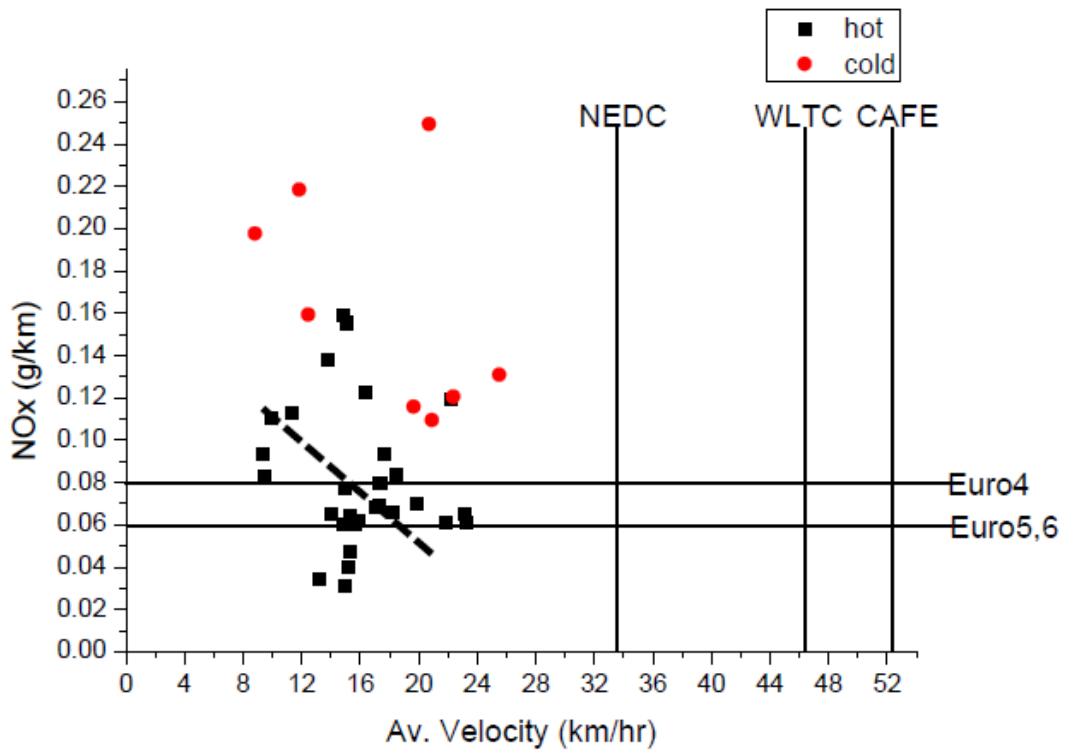


Figure 7-18 Trip mean NO<sub>x</sub> emissions vs vehicle's average trip velocity.

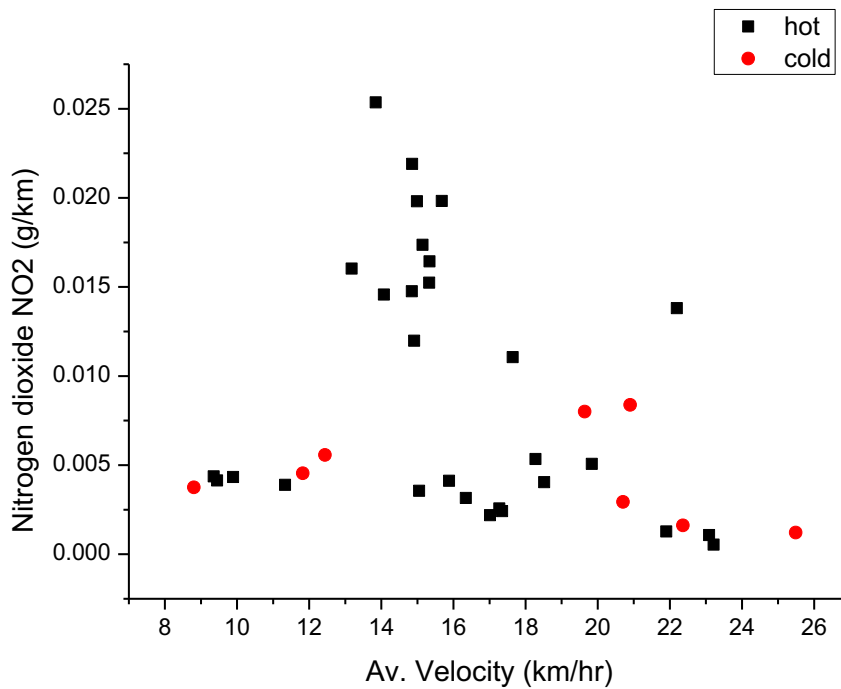


Figure 7-19 Trip mean NO<sub>2</sub> emissions vs vehicle's average trip velocity.

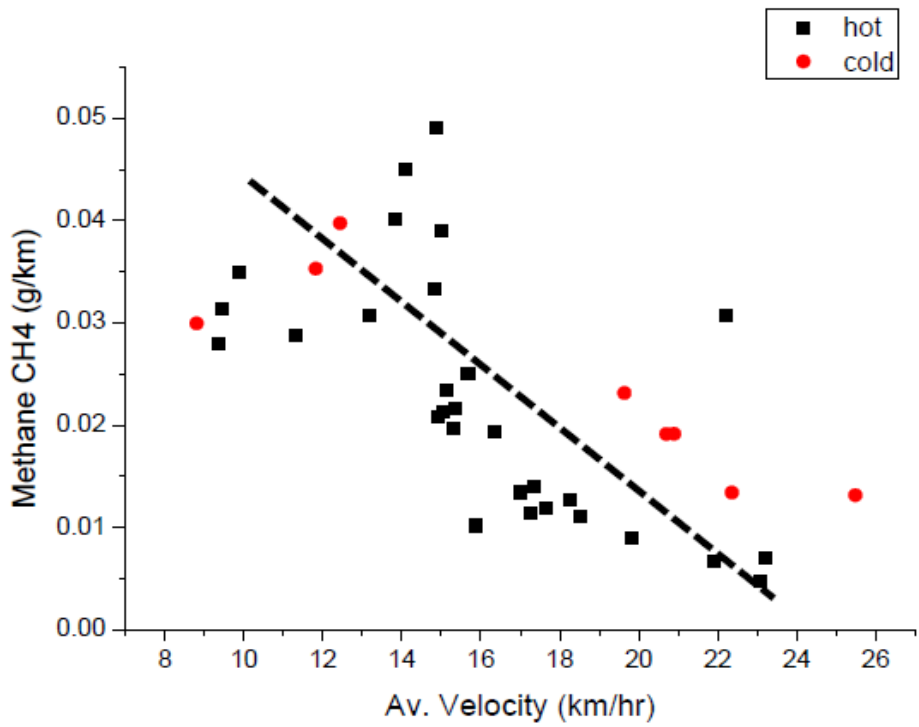


Figure 7-20 Trip mean CH<sub>4</sub> emissions vs vehicle's average trip velocity.

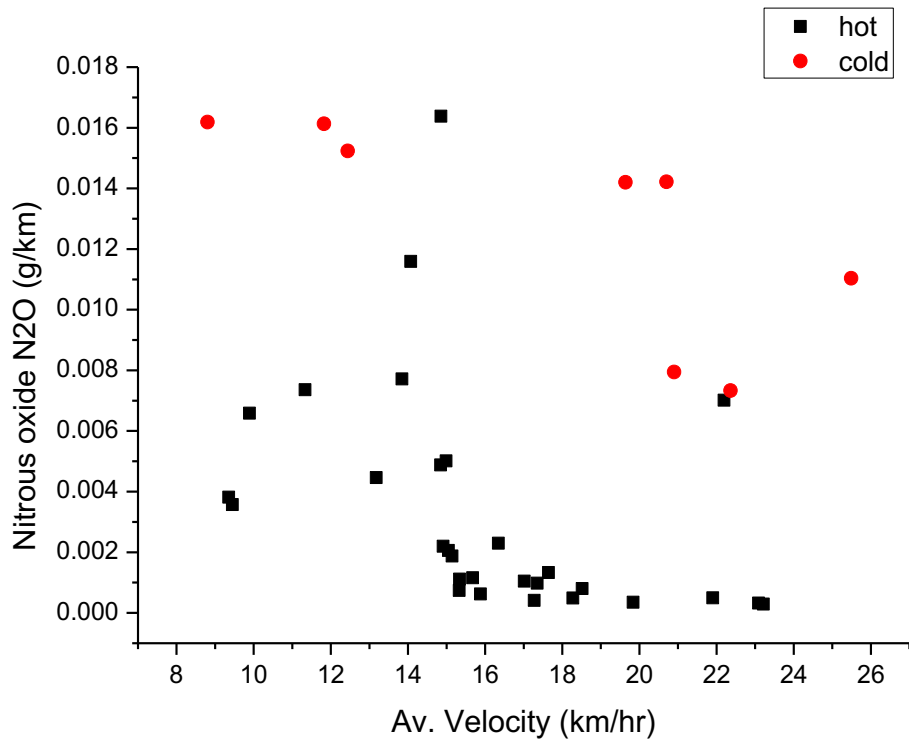


Figure 7-21 Trip mean N<sub>2</sub>O emissions vs vehicle's average trip velocity.

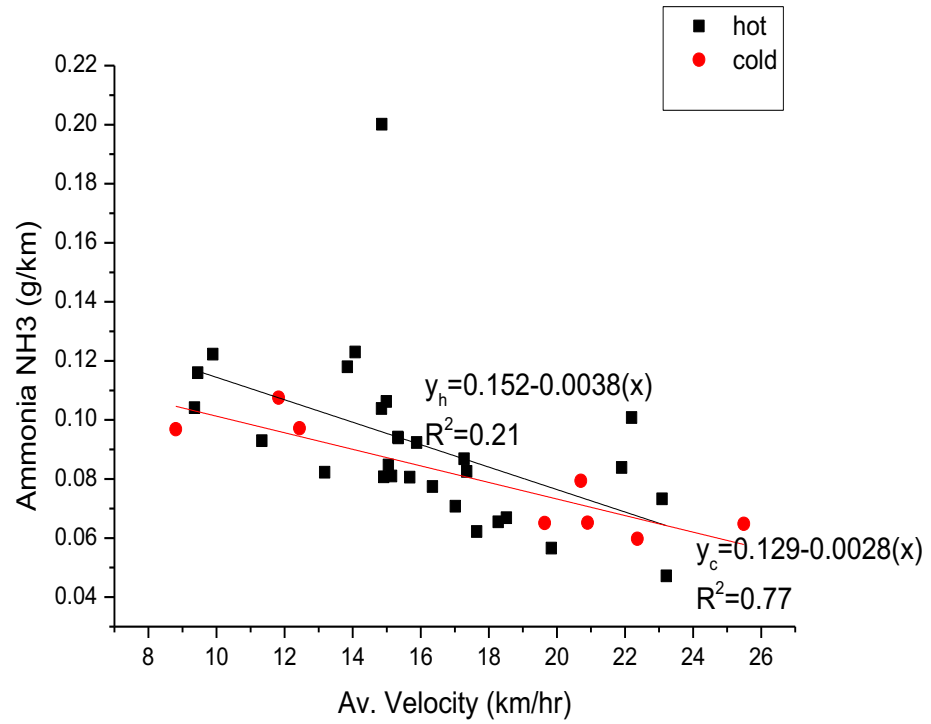


Figure 7-22 Trip mean NH<sub>3</sub> emissions vs vehicle's average trip velocity.

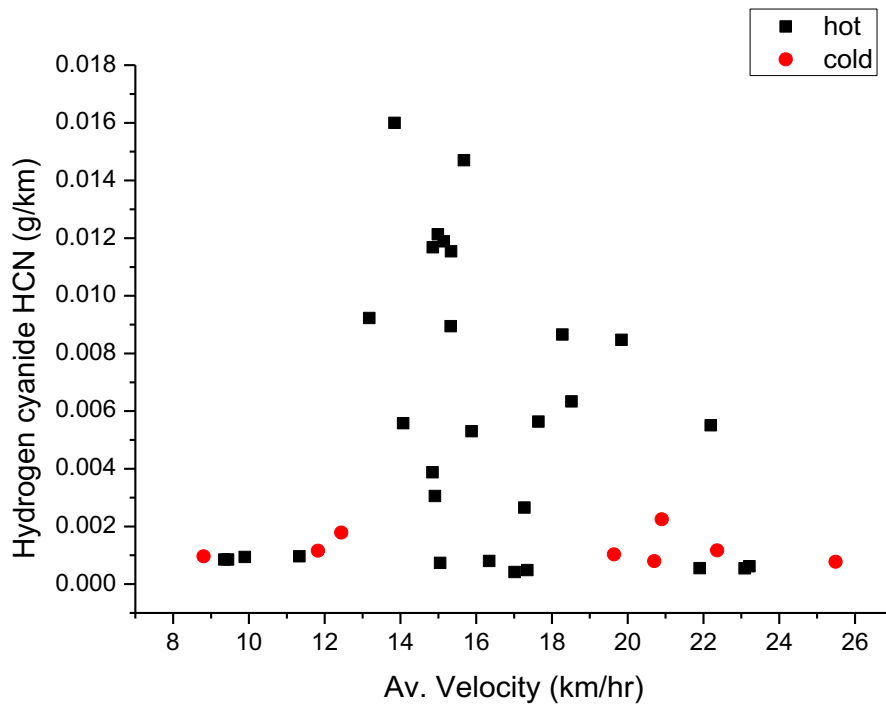


Figure 7-23 Trip mean HCN emissions vs vehicle's average trip velocity.

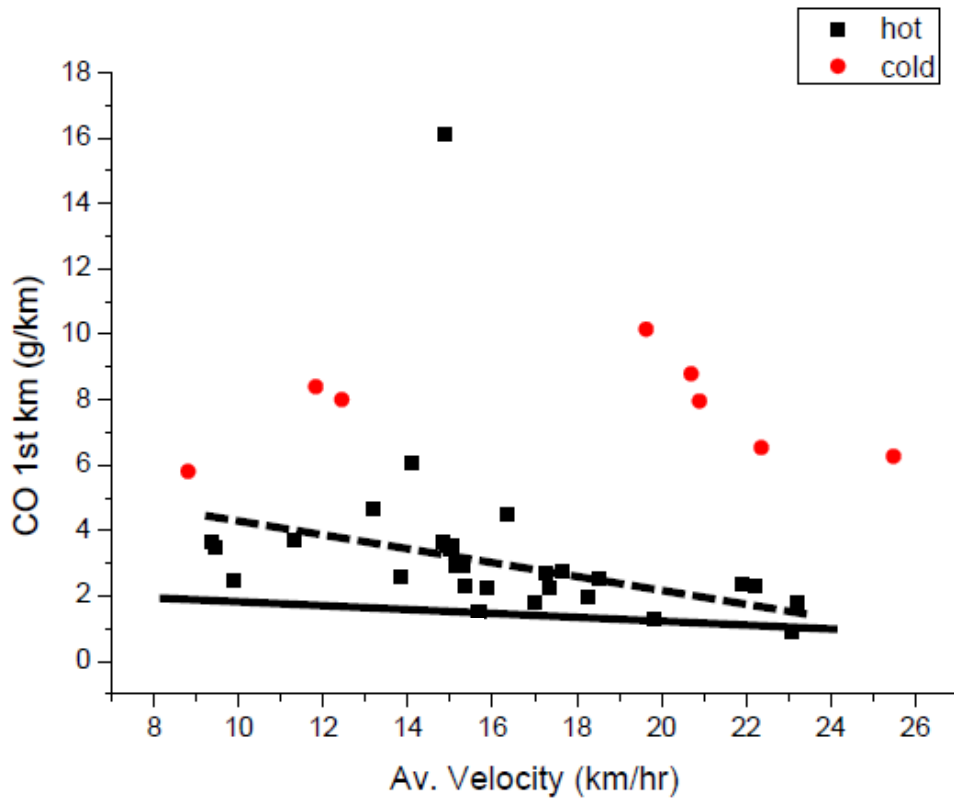


Figure 7-24: Hot and cold CO emissions for the first km vs mean speed.

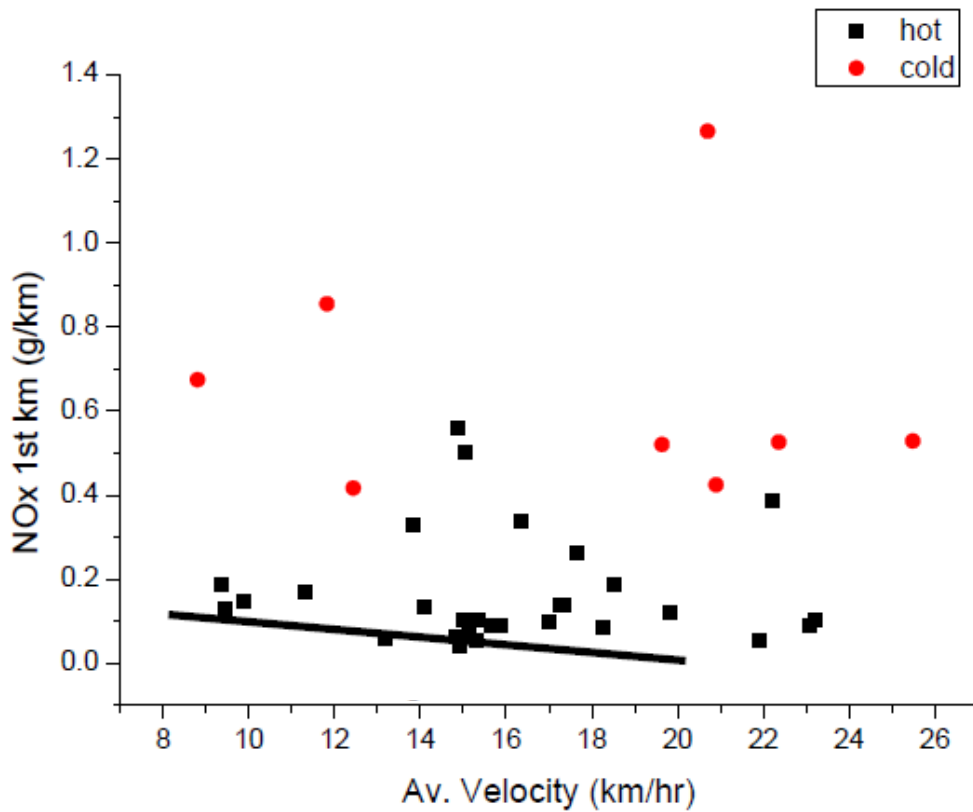


Figure 7-25: Hot and cold NOx emissions for the first km vs mean speed.

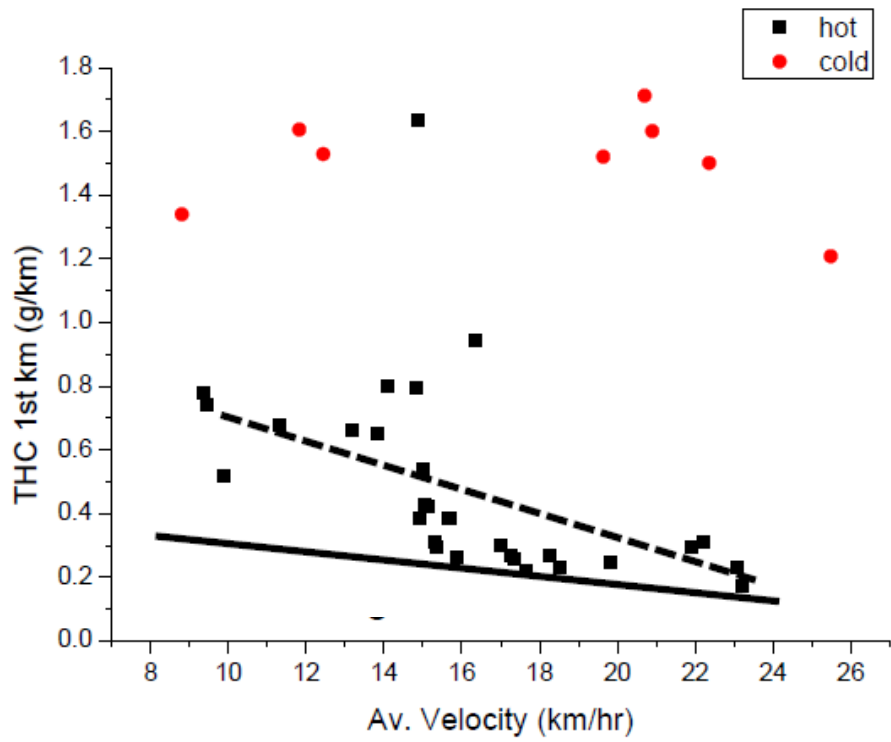


Figure 7-26: Hot and cold THC emissions for the first km vs mean speed.



**Figure 7-27: Congested traffic driving route.**

For most of the time, the CO was close to zero, so that the CO emitted was mainly due to that emitted in the acceleration transients. At the start of the journey, in Figure 7-9, the engine calibration was rich for a short period and a large CO peak resulted from this. Figure 7-9 shows that one-third of the total CO was emitted during the ‘hot’ start, even though the catalyst temperature was at 400°C during that period. This was surprising, as this engine has a lean cold start strategy[5], so a rich hot start was not expected, although a hot start is not part of the NEDC procedures.

The second largest CO peak in Figure 7-9 was at 520s and is difficult to explain. Around this peak there were significant  $\lambda$  changes, with a rich peak just before the acceleration event where fuel had been injected as an attempt to accelerate, but no acceleration occurred (a typical congested traffic event). However, this fuel was not burnt in the engine and the catalyst had a temperature minimum of 300°C, but there was no HC or CO peak as the ceria would have sufficient oxygen to oxidise the CO and HC. However, there then followed a rapid acceleration with a lean and rich excursion (gear change) and

the rich event then produced CO and HC as the ceria had insufficient oxygen stored to oxidise the CO and HC. The net result was a large CO and HC peak at this acceleration event.

These examples illustrate that realistic emissions are dominated by transient events caused by the traffic congestion, but not all transients give a CO, HC or NO<sub>x</sub> peak. Each transient in congested traffic has complex events around it that are usually controlled by the TWC, being the high engine out emissions from the transient events. The emissions are linked to the success of  $\lambda=1$  control during the greater transients in congested-traffic driving. If congested traffic is not part of regulated test cycles such as WLTC and RDE and the existing NEDC, then there is no requirement for manufacturers to develop  $\lambda$  control systems that will cope with congested traffic conditions.

The hydrocarbon emissions (HC) shown in Figure 7-17 and the cold start emissions were significantly higher than the hot start, but both correlate well with the journey average velocity or congestion. The HC emissions would meet Euro 4-6 requirements for average speeds above 25 kph. Most of the HC emissions occur in specific transient events with low or zero emissions between the events. This has been discussed in relation to the CO emissions above.

The NO<sub>x</sub> emissions in Figure 7-18 show a poor correlation with mean velocity and are dominated by the wide data scatter between journeys. Examination of Figure 7-9, as a typical transient NO<sub>x</sub> trace, shows that most (63%) of the NO<sub>x</sub> in this case, was generated 40s after the hot start. This event occurred with the catalyst seeing  $\lambda=1$  operation but with a lean excursion either side of this. The acceleration event that generated this peak NO<sub>x</sub> was the highest in the journey and had a peak power of 17kW/tonne or 23.4 kW for this vehicle. The acceleration occurred for a very short duration near idle condition, where the fuel had been cut off and then the maximum fuel flow for the whole journey was injected. During this transient, the TWC temperature at the inlet increased from 350 to 520°C. This illustrates how specific events in congested traffic can dominate the journey emissions. For the remainder of the journey there were



six events that generated  $\text{NO}_x$  at a low level. All these events coincided with a lean excursion at the catalyst. The number of stop/start events control the  $\text{NO}_x$  generation and the variability in this, for the same mean journey velocity, gives the variability in the  $\text{NO}_x$ .

The vehicle specific power, VSP, was dominated, in the present work, by the velocity times acceleration term in Equation (3-2), as the changes in elevation were low and the velocities were low and consequently, the aerodynamic drag term was low. The results in Figure 7-9 and Figure 7-10 show that power demand is intermittent in congested traffic. Figure 7-10 shows that, for highly-congested traffic, each power demand produced a  $\text{NO}_x$  increase. However, for lower congestion, in Figure 7-9, the link between peaks in VSP and  $\text{NO}_x$  was not as clear because there were relatively few  $\text{NO}_x$  peaks but many peaks in the VSP. For the 1.4 tonne vehicle employed in the present work, the power variation in Figure 7-9 and Figure 7-10 was from 7 – 25 kW with a lot of zero power at idle conditions. The peak engine power for this vehicle was 100kW and the powers used in congested traffic were very low, where the thermal efficiency for SI engines is very poor. This results in high  $\text{CO}_2$  emissions as discussed above.

The  $\text{NO}_2$  results in Figure 7-19 show little correlation with the average journey velocity. Compared with the  $\text{NO}_x$  results in Figure 7-18, the proportion of  $\text{NO}_2/\text{NO}_x$  varies from 5 to 15%. Figure 7-5 shows that the  $\text{NO}_2$  emission events coincide with the  $\text{NO}_x$  emission peaks and that these occur with lean excursions, which provide the necessary oxygen for the catalyst to convert  $\text{NO}$  to  $\text{NO}_2$ . The very short duration of the lean excursion events in realistic driving causes the generation of  $\text{NO}_2$  to be a low proportion of the total  $\text{NO}_x$ . Figure 7-19 also shows that the cold start had no significant influence on  $\text{NO}_2$  for the same journey congestion.

The  $\text{CH}_4$  GHG emissions in Figure 7-20 correlate reasonably well with the journey average velocity or congestion, but there is a wide scatter which shows a dependence on the number of individual events. The  $\text{CH}_4$  emissions are approximately 10% of the total HC emissions. In terms of GHG  $\text{CO}_2$

equivalence, the CH<sub>4</sub> emissions were approximately 0.4% of the total. For higher journey average speeds and less congestion, Figure 7-20 shows that CH<sub>4</sub> emissions would be close to zero. Figure 7-1 and Figure 7-2 show that the CH<sub>4</sub> emissions occur at specific events that correlate with the CO<sub>2</sub> emissions and the fuel flow peaks. The events follow a lean/rich  $\lambda$  variation associated with a gear change just before the acceleration. For the more congested journey in Figure 7-2 the CH<sub>4</sub> peaks were lower and their correlation with other events was less clear. Figure 7-20 also shows that the cold start had no significant influence on CH<sub>4</sub> emissions even though it did on the total HC emissions in Figure 7-17.

The N<sub>2</sub>O GHG emissions in Figure 7-21 show high values at low mean velocity. The peak N<sub>2</sub>O at lower journey average speeds was approximately 0.8% of the total GHG equivalence. This means that non-CO<sub>2</sub> GHGs are only about 1.2% of the total GHG equivalence in the worst case of low-speed congested traffic. At higher speeds (above 20 kph), the present results indicate that they will be negligible. Figure 7-21 shows that the cold start N<sub>2</sub>O results are higher than for the hot start and continue to be significant at higher journey average velocities. N<sub>2</sub>O emissions are controlled by TWC temperatures, as is known from their measurement under cold start on the NEDC and in other realistic driving journeys [2, 27, 45, 46, 52]. Figure 7-5 and Figure 7-6 show that N<sub>2</sub>O occurs at specific events and the highest generation was at the hot start, where the catalyst temperature was increasing from 300 to 400°C, and there was a rich start. The largest other N<sub>2</sub>O peak was at 520s in Figure 7-5, and this occurred after a lean/rich  $\lambda$  excursion which occurs at a gear change at the start of the acceleration. The catalyst inlet temperature was increasing from 350°C to 450°C during this acceleration event.

The NH<sub>3</sub> emissions are shown in Figure 7-22 and decreased, roughly linearly, as the mean velocity increased. There was no cold start effect, indicating that NH<sub>3</sub> generation was not dependent on catalyst temperature. Figure 7-5 and Figure 7-6 show that the NH<sub>3</sub> emissions occurred at many individual events, but there was a large formation rate after the hot start and at 340 and 680s as shown in Figure 7-5. The significant feature on these two occasions was that

before the event there was a deceleration to a short idle period, and afterwards a strong acceleration. If the idle period is longer, then the ammonia peak is absent or is lower. Both events have lean/rich operation through a gear change with the  $\text{NH}_3$  occurring during the rich excursion. Clearly better  $\lambda$  control during gear changes and acceleration could reduce the ammonia formation. Comparison of Figure 7-22 and Figure 7-18 show that the  $\text{NH}_3$  in Figure 7-22 is very close to the trend line in Figure 7-18. and hence have similar emissions to that of  $\text{NO}_x$ .

The HCN emissions are shown in Figure 7-23 and there is no correlation with the mean vehicle speed and no influence of a cold start. As explained above, HCN requires an NO peak and HC peak together and a rich mixture. Figure 7-5 and Figure 7-9 show that these conditions are met for the main HCN peaks in Figure 7-5. The events occur during a throttle demand increase at the start of a high acceleration. The rapid throttle opening gives a transient lean mixture as the air increases more quickly than the  $\lambda$  control can increase the fuel. The fuel increases, and is then over-rich to respond to the initial lean mixture, resulting in a transient rich excursion. The acceleration is also accompanied by a gear change. The whole transient event takes less than 10s but the consequences are significant HCN emissions. The other pollutants are also related to this type of event, as discussed above.

### **7.1.3 Emissions during the first minute and first 0.5 km of travel**

The above emissions were the total emissions over the whole 5 km journey on a mass/km basis. However, using g/km data in air quality modelling assumes that the emissions are uniform across the journey. This is a major problem for legislated emissions, as where catalysts are the key emissions control device, as in the TWC for SI engine and the SCR or  $\text{NO}_x$  trap catalyst for lean burn diesel  $\text{NO}_x$  control, the cold start period dominates the emissions, and typically most of the emissions in the test cycle occur over the first km. If the catalyst is hot and the  $\lambda$  control is good then there are negligible CO, HC and  $\text{NO}_x$  emissions over the rest of the journey in modern SI vehicles. This is particularly the case for CO and HC but for  $\text{NO}_x$  there is often a lower

proportion of the total emissions during the cold start period. However, it is the case that with a cold start test, the longer the test duration is, the lower is the impact of the cold start. Thus the 23 km length of the WLTC and the 90km length of the RDE relative to the 11km length of the NEDC, will for the same total mass emissions (during cold start), reduce the g/km emissions. The WLTC and RDE test procedures may be better for CO<sub>2</sub> emissions but they will not produce realistic urban driving emissions for NO<sub>x</sub>, CO and HC.

The higher emissions during cold start in comparison with hot start for the first minute of the present 5km congested traffic journeys is shown in Figure 7-24 to Figure 7-26 for CO, NO<sub>x</sub> and HC emissions respectively as a function of the mean velocity over the first minute of driving. All three results showed, as expected, that cold starts produced higher emissions, particularly for HC. The cold start results show little correlation with average speed during the first minute, but the hot start results do show a reduction in CO and HC as the average speed is increased. The hot start NO<sub>x</sub> results show no correlation with average speed. However, what was not expected was that the hot start emissions in the first minute were significantly higher than that the average values for the full 5 km journey, as shown in Figure 7-24 to Figure 7-26. The results in Figure 7-1 and Figure 7-2 show that for both low and high congestion, the hot start had lube oil >90°C and the catalyst downstream temperatures 400-500°C for high and low congestion. The only catalyst temperature that was low was the inlet temperature which for low congestion started at 300°C and increased to 500°C in the first minute. For the high-congestion case in Figure 7-2 the upstream catalyst temperature started at 400°C and was reduced to 300°C, and then increased to 350°C in the first minute. These conditions are far from a cold start, but the periods of inlet temperature <300°C could impact the emissions for a TWC.

The variation in  $\lambda$  during the first minute was more important than the catalyst inlet temperature. In Figure 7-1 with low congestion, there was a high acceleration and deceleration in the first 60s. This initial starting  $\lambda$  was rich and then became lean followed by a short period at  $\lambda=1$  and then a lean period, all in 60s. For the high congestion case in Figure 7-2 the hot start was

less transient. The starting  $\lambda$  was lean, as for the cold start strategy, then the acceleration made the mixture rich and after 25s to 60s,  $\lambda=1$  applied. Thus in the first 60s the vehicle movement was more transient than on average for the rest of the 5 km. This was because there has to be a first acceleration after the hot start and this is always in the first 30s, and may be followed by deceleration as the first right hand turn is approached. For the remainder of the test route the occurrence of accelerations from idle is more random.

The first 60s for the low congestion journey in Figure 7-9 was 7.5% of the total journey time. In this time, 25% of the total journey CO and HC occurred with 66% of the  $\text{NO}_x$ . For the high-congestion case in Figure 7-10 the first 60s was only 3.3% of the total journey time but it produced 36% of the HC, 30% of CO and 10% of the  $\text{NO}_x$  for the whole journey. Thus, the reason for the emissions being higher in the first 60s than for the whole journey, as shown in Figure 7-24 to Figure 7-26, was that the vehicle movement was more transient and the  $\lambda$  control was more variable than for the journey as a whole. Although it appears that there was a hot start effect, this was not due to cold lube oil or cold catalyst. This illustrates that in a vehicle journey in congested traffic, the emissions vary with the local congestion. This is important where there is a roadside air monitor, as in the present work at Headingley. This will respond to local emissions for the traffic conditions in that area. Analysis of the present data for the section of road adjacent to the roadside, the air quality monitor shows that it is located at the most congested part of the route with the highest local traffic emissions.

## 7.2 Conclusions

1. Air quality exceedances in cities occur at local roadside measurements stations due to the presence of locally congested traffic with higher emissions than on the test cycles.
2. Existing test cycles have low levels of congested driving and the WLTC and proposed RDE have even lower congestion than the NEDC. The European RDE has no congestion and no cold start and is thus not very real world.
3. The road studied had 1000 cars/hour in single lane traffic at the peak congestion times and peak emissions occurred at peak congestion with the lowest average journey speed.
4. The number of stop/starts per km in the congested traffic driving varied from 1.5 to 7 and had a good correlation with the average journey speed. The NEDC, FTP75 and JC09 test cycles had stop/starts of 1.3-1.5/km, which for the same average speed agrees with the present work. It is the lower average speeds in congested traffic that increases the emissions, but this is due to the increased number of stop/start events and the associated higher emissions in these events.
5. In the highest traffic congestion emissions for a hot start were a multiple of the regulated NEDC emissions of 1.5, 3 and 2 for CO, HC and NO<sub>x</sub> respectively and for cold start were about 2.5, 5 and 3 times the NEDC CO, HC and NO<sub>x</sub> respectively.
6. For cold starts the average journey emissions were higher than for hot starts due to the catalyst warm-up period that is longer in real world congested traffic driving than on the NEDC.
7. The vehicle specific power, VSP kW/tonne or m<sup>2</sup>/s<sup>3</sup>, can be calculated from the vehicle velocity and acceleration and the road altitude gain and the aerodynamic drag. In the present work the velocity times acceleration term dominated as elevation changes were low and average speeds were low. At high congestion peaks in VSP correlated with peaks in NO<sub>x</sub>, but this relationship was not as clear for lower congestion.
8. NH<sub>3</sub> emissions were measured at about the same mass emissions level as for NO<sub>x</sub>. The NH<sub>3</sub> was formed in specific transient events that resulted

in rich excursions. This was a harsh acceleration from idle and gave a short duration lean mixture followed by a rich excursion before the  $\lambda=1$  control stabilised. The rich excursion gave a pulse of  $\text{NH}_3$  and the lean excursion gave a pulse of  $\text{NO}_x$ . The  $\text{NH}_3$  and  $\text{NO}_x$  emissions were of a similar mass magnitude.  $\text{NH}_3$  emissions from SI engines are high and unregulated, whereas  $\text{NH}_3$  slip from diesel SCR deNO<sub>x</sub> catalysts is regulated at a relatively low level that is below the  $\text{NH}_3$  emissions from SI engines.

9. HCN formation at a TWC requires a reaction between HC and NO and thus HCN only occurs where a HC peak and  $\text{NO}_x$  peak coincide. Examples where this occurred were found in the transient tests.
10. Greenhouse gases  $\text{CH}_4$  and  $\text{N}_2\text{O}$  occurred in specific congested traffic transient events. In terms of  $\text{CO}_2$  equivalent emissions  $\text{CH}_4$  was 0.4% of the total GHG emissions and  $\text{N}_2\text{O}$  was 0.8%. For less congested conditions both GHGs were even lower contributors to the total GHG emissions.

**Table 7-1 Summary of driving parameters and emissions species for compared journey.**

Journey	0913_B	1908_B	1334_A	1215_A	1734_B	1701_A	1740_B	1704_A
Av. Velocity (km/hr)	22.194	21.902	18.274	17.349	11.333	9.892	9.449	9.355
Max Velocity (km/hr)	43.780	50.920	50.830	46.830	44.220	46.960	46.330	45.390
Min Velocity (km/hr)	0.000	0.000	0.000	0.000	0.000	0.000	0.000	0.000
Av. Acceleration (m/s <sup>2</sup> )	0.4636	0.4830	0.4662	0.4254	0.4012	0.4334	0.3646	0.3535
Max Acceleration (m/s <sup>2</sup> )	2.778	2.494	2.497	2.337	2.212	2.325	2.167	2.585
Max Deceleration (m/s <sup>2</sup> )	-1.917	-3.082	-2.057	-2.075	-2.560	-2.243	-2.001	-2.806
Av. VSP (Kw/tonne)	1.32	21.58	19.49	18.75	17.04	17.59	17.44	21.41
Min VSP (Kw/tonne)	-13.23	-13.94	-14.41	-14.22	-13.02	-10.04	-9.90	-14.98
Av. VSP+ (Kw/tonne)	3.16	3.22	3.00	2.60	1.90	1.86	1.62	1.62
Av. VSP- (Kw/tonne)	-2.03	-2.41	-2.47	-2.07	-1.75	-1.52	-1.74	-1.64
Power output+ (KWh)	0.71	0.77	0.84	0.79	0.88	0.97	0.91	0.93
Power output- (KWh)	-0.25	-0.26	-0.30	-0.27	-0.30	-0.33	-0.32	-0.32
Total stoppage time (s)	159	222	338	368	766	914	1057	1029
stoppage time (%)	20.05	27.72	35.17	36.26	49.64	51.20	57.07	55.09
Cruise%	47.04	48.19	35.95	31.63	17.17	13.45	14.42	12.79
Total fuel consumption (g)	333.00	338.03	380.54	380.85	485.47	561.60	557.75	558.81
Av. fuel consumption (g/s)	0.42	0.42	0.40	0.38	0.31	0.31	0.30	0.30
Idle fuel consumption (g)	37.21	51.56	59.84	65.03	134.75	161.08	170.97	169.64
Idle fuel consumption (%)	11.18	15.25	15.72	17.07	27.76	28.68	30.65	30.36
Journey Av. fuel consumption (g/km)	67.77	69.08	77.69	77.67	99.24	17.92	113.97	114.05
Fuel economy (mile/UKG)	30.09	29.51	26.24	26.25	20.54	17.92	17.89	17.88
Overall thermal efficiency (%)	0.17	0.19	0.18	0.17	0.15	0.14	0.13	0.13
Total Distance (km)	4.91	4.89	4.90	4.90	4.89	4.90	4.89	4.90
Carbon dioxide CO2 (g/km)	240.07	234.20	248.28	239.93	315.15	349.19	357.63	358.17
Nitrous oxide N2O (g/km)	0.007	0.000	0.000	0.001	0.007	0.007	0.004	0.004
Methane CH4 (g/km)	0.031	0.007	0.013	0.014	0.029	0.035	0.031	0.028
Nitrogen monoxide NO (g/km)	0.07	0.04	0.04	0.05	0.07	0.07	0.05	0.06
Nitrogen dioxide NO2 (g/km)	0.014	0.001	0.005	0.002	0.004	0.004	0.004	0.004
Ammonia NH3 (g/km)	0.10	0.08	0.07	0.08	0.09	0.12	0.12	0.10
Hydrogen cyanide HCN (g/km)	0.0055	0.0006	0.0087	0.0005	0.0010	0.0009	0.0009	0.0008
Nox (g/km)	0.12	0.06	0.07	0.08	0.11	0.11	0.08	0.09
Total HydrocarbonTHC (g/km)	0.25	0.15	0.17	0.15	0.28	0.31	0.30	0.30
Carbon monoxide CO (g/km)	1.46	0.91	0.81	0.90	1.22	1.50	1.14	1.17
Carbon dioxide CO2 idle%	4.59	8.50	13.58	15.88	21.24	19.62	26.65	25.14
Nitrous oxide N2O idle%	2.80	1.16	3.17	6.53	17.83	4.09	5.99	4.41
Methane CH4 idle%	6.90	4.95	4.03	11.24	21.59	19.57	23.90	28.66
Nitrogen monoxide NO idle%	0.93	7.57	14.89	12.57	17.98	16.00	24.17	24.07
Nitrogen dioxide NO2 idle%	4.29	4.54	12.74	14.53	19.05	17.97	23.91	20.33
Ammonia NH3 idle%	3.61	6.88	9.73	12.97	16.46	16.51	20.61	21.71
Hydrogen cyanide HCN idle%	3.41	9.64	17.44	15.48	19.43	18.48	39.27	33.56
Nox idle%	1.31	7.51	14.72	12.63	18.01	16.08	24.15	23.78
Total HydrocarbonTHC idle%	5.39	5.87	11.36	12.66	20.33	17.79	23.32	26.77
Carbon monoxide CO idle%	5.35	5.26	4.99	8.50	9.33	8.28	9.49	14.71
Congestion	0.54	0.54	0.62	0.64	0.76	0.79	0.80	0.81
Number of stops	9	9	19	15	39	47	37	42
Journey duration (s)	793	801	961	1015	1543	1785	1852	1868



**Table 7-2 Summary of driving parameters and emissions species for all journeys part A.**

Journeys	D1 1975 A	D1 1941 B	D6 0013 B	D1 1008 B	D2 1316 B	D2 1256 A	D2 1334 A	D3 0746 A	D3 1215 A	D3 1235 B	D2 1213 A	D3 1256 A2	D2 1234 B	D3 0853 B	D3 0830 A
Avg Velocity (km/hr)	23.09	23.21	22.19	21.90	19.84	18.32	18.27	17.64	17.35	17.01	17.27	16.35	15.88	15.68	15.34
Max Velocity (km/hr)	49.42	52.24	43.78	50.92	49.31	48.67	50.83	44.04	46.83	46.61	46.81	43.87	50.37	45.76	43.48
Min Velocity (km/hr)	0.00	0.00	0.00	0.00	0.00	0.00	0.00	0.00	0.00	0.00	0.00	0.00	0.00	0.00	0.00
Avg Acceleration (m/s <sup>2</sup> )	0.47	0.43	0.46	0.48	0.44	0.43	0.47	0.40	0.43	0.47	0.43	0.42	0.44	0.45	0.38
Max Acceleration (m/s <sup>2</sup> )	2.29	2.11	2.78	2.49	2.35	2.42	2.50	2.57	2.34	2.68	2.60	2.37	2.43	2.76	2.17
Max Deceleration (m/s <sup>2</sup> )	-1.90	-4.03	-1.92	-3.08	-4.30	-1.80	-2.06	-2.35	-2.08	-2.23	-1.82	-2.46	-2.39	-2.71	-1.91
Avg VSP (Kw/tonne)	1.56	1.44	1.32	1.47	1.39	1.20	1.27	1.08	1.17	1.22	1.11	1.13	1.19	1.10	0.96
Max VSP (Kw/tonne)	20.61	22.96	19.26	21.58	18.10	25.76	19.49	19.08	18.75	18.43	21.19	20.76	21.41	18.47	16.83
Min VSP (Kw/tonne)	-13.11	-13.54	-13.23	-13.94	-15.01	-11.21	-14.41	-13.49	-14.22	-11.39	-15.62	-11.84	-13.29	-22.33	-12.02
Avg VSP+ (Kw/tonne)	3.65	3.21	3.16	3.22	2.99	2.89	3.00	2.59	2.60	2.78	2.65	2.52	2.63	2.02	2.21
Avg VSP- (Kw/tonne)	-3.01	-2.48	-2.03	-2.41	-2.48	-0.74	-2.47	-2.13	-2.07	-2.15	-2.02	-2.29	-2.39	-2.45	-1.98
Power output+ (Kw/h)	0.83	0.75	0.71	0.77	0.80	0.81	0.84	0.76	0.79	0.85	0.78	0.83	0.89	0.91	0.75
Power output- (Kw/h)	-0.31	-0.25	-0.25	-0.26	-0.27	-0.30	-0.30	-0.27	-0.27	-0.29	-0.28	-0.28	-0.31	-0.35	-0.26
Total stoppage time (s)	167.00	176.00	159.00	222.00	235.00	276.00	338.00	281.00	368.00	298.00	289.00	368.00	354.00	368.00	392.00
Total stoppage time (%)	21.89	22.80	20.05	27.72	26.49	28.93	35.17	28.30	36.26	28.82	27.87	34.17	31.72	32.74	34.03
Cruise%	46.13	47.15	47.04	48.19	41.38	36.06	35.95	33.30	31.63	31.24	33.37	34.35	29.39	28.29	27.26
Total fuel consumption (g)	339.30	316.96	333.00	338.03	370.32	363.70	380.54	380.79	380.85	400.33	420.25	411.16	454.73	430.35	399.75
Avg fuel consumption (g/s)	0.44	0.41	0.42	0.42	0.42	0.38	0.40	0.38	0.38	0.39	0.41	0.38	0.41	0.38	0.35
Min fuel consumption (g)	41.90	42.56	37.21	51.56	50.07	62.81	59.84	60.76	65.03	67.36	61.19	76.41	74.38	78.45	84.84
Max fuel consumption (g)	12.35	13.43	11.18	15.25	13.52	17.27	15.72	15.95	17.07	16.83	14.56	18.58	16.36	18.23	21.22
Journey Avg fuel consumption (g/km)	69.00	63.57	67.77	69.08	75.46	74.09	77.69	77.53	77.67	81.61	84.42	83.65	91.71	87.67	81.27
Fuel economy (mile/UKG)	29.55	32.07	30.09	29.51	27.02	27.52	26.24	26.30	26.25	24.98	24.15	24.37	22.23	23.26	25.09
Overall thermal efficiency (%)	0.20	0.19	0.17	0.19	0.18	0.18	0.18	0.16	0.17	0.17	0.15	0.16	0.16	0.17	0.15
Total Distance (km)	4.92	4.99	4.91	4.89	4.91	4.91	4.90	4.91	4.90	4.91	4.98	4.91	4.96	4.91	4.92
Carbon dioxide CO2 (g/km)	219.70	202.63	240.07	234.20	244.86	230.84	248.28	237.88	239.93	260.33	270.06	270.46	298.43	300.95	265.10
Nitrous oxide N2O (g/km)	0.0003	0.0003	0.0070	0.0005	0.0003	0.0008	0.0005	0.0013	0.0010	0.0010	0.0004	0.0023	0.0006	0.0012	0.0011
Methane CH4 (g/km)	0.00	0.01	0.03	0.01	0.01	0.01	0.01	0.01	0.01	0.01	0.01	0.02	0.01	0.03	0.02
Nitrogen monoxide NO (g/km)	0.04	0.04	0.07	0.04	0.04	0.05	0.04	0.05	0.05	0.04	0.04	0.08	0.04	0.03	0.03
Nitrogen dioxide NO2 (g/km)	0.001	0.001	0.014	0.001	0.005	0.004	0.005	0.011	0.002	0.002	0.003	0.003	0.004	0.020	0.016
Ammonia NH3 (g/km)	0.07	0.05	0.10	0.08	0.06	0.07	0.07	0.06	0.08	0.07	0.09	0.08	0.09	0.08	0.09
Hydrogen cyanide HCN (g/km)	0.0005	0.0006	0.0055	0.0006	0.0085	0.0063	0.0087	0.0056	0.0005	0.0004	0.0027	0.0008	0.0053	0.0147	0.0115
NOx (g/km)	0.07	0.06	0.12	0.06	0.07	0.08	0.07	0.09	0.08	0.07	0.07	0.12	0.06	0.06	0.06
Total Hydrocarbon THC (g/km)	0.12	0.10	0.25	0.15	0.15	0.13	0.17	0.14	0.15	0.15	0.14	0.30	0.16	0.26	0.22
Carbon monoxide CO (g/km)	0.58	0.65	1.46	0.91	0.58	0.85	0.81	0.94	0.90	0.72	0.89	1.27	0.82	0.77	0.89
Congestion	0.52	0.52	0.54	0.54	0.59	0.61	0.62	0.63	0.64	0.65	0.64	0.66	0.67	0.67	0.68
Number of stops	15.00	11.00	9.00	9.00	15.00	15.00	19.00	12.00	15.00	22.00	19.00	22.00	23.00	23.00	25.00
Journey duration (s)	763.00	772.00	793.00	801.00	887.00	954.00	961.00	1000.00	1015.00	1034.00	1037.00	1077.00	1116.00	1124.00	1152.00

**Table 7-3 Summary of driving parameters and emissions species for journey part B**

Journeys	D3 0807_B	D3 1318_B	D4 0852_A	D5 1337_B	D4 0753_A	D5 1247_B	D5 1222_A	D6 0849_B	D5 1311_A	D4 0825_B	D5 1734_B	D5 1701_A	D2 1740_B	D2 1704_A
Avg Velocity (km/hr)	15.33	15.05	15.14	14.99	14.91	14.86	14.85	14.07	13.84	13.18	11.33	9.89	9.45	9.36
Max Velocity (km/hr)	45.48	47.24	43.28	48.07	47.35	43.63	46.85	50.17	49.57	42.76	44.22	46.56	46.33	45.39
Min Velocity (km/hr)	0.00	0.00	0.00	0.00	0.00	0.00	0.00	0.00	0.00	0.00	0.00	0.00	0.00	0.00
Avg Acceleration (m/s <sup>2</sup> )	0.43	0.43	0.43	0.44	0.39	0.41	0.48	0.42	0.51	0.40	0.40	0.43	0.36	0.35
Max Acceleration (m/s <sup>2</sup> )	2.65	2.52	2.34	2.38	2.75	2.33	2.63	2.37	2.58	2.40	2.21	2.32	2.17	2.58
Max Deceleration (m/s <sup>2</sup> )	-2.04	-3.13	-2.35	-2.96	-2.21	-2.50	-2.97	-1.98	-3.11	-2.37	-2.56	-2.24	-2.00	-2.81
Avg VSP (Kw/tonne)	1.01	1.08	1.05	1.09	1.00	1.08	1.19	1.02	1.12	0.90	0.87	0.81	0.72	0.73
Max VSP (Kw/tonne)	19.25	21.19	17.04	21.38	21.94	21.05	22.90	15.62	18.70	16.90	17.04	17.59	17.44	21.41
Min VSP (Kw/tonne)	-14.77	-13.31	-14.64	-15.38	-10.67	-12.36	-11.63	-11.76	-14.03	-10.22	-13.02	-10.04	-9.90	-14.98
Avg VSP+ (Kw/tonne)	2.39	2.44	2.42	2.45	2.15	2.36	2.70	2.34	2.65	2.06	1.90	1.86	1.62	1.62
Avg VSP- (Kw/tonne)	-1.81	-2.12	-1.91	-2.08	-2.03	-2.24	-2.23	-2.27	-2.21	-1.74	-1.75	-1.52	-1.74	-1.64
Power output+ (Kw/Wh)	0.80	0.85	0.82	0.87	0.80	0.86	0.96	0.90	0.99	0.80	0.88	0.97	0.91	0.93
Power output- (Kw/Wh)	-0.28	-0.30	-0.29	-0.30	-0.28	-0.31	-0.33	-0.34	-0.35	-0.28	-0.30	-0.33	-0.32	-0.32
Total stoppage time (s)	339.00	393.00	364.00	410.00	430.00	427.00	457.00	496.00	521.00	506.00	766.00	914.00	1057.00	1029.00
stoppage time (%)	29.35	33.82	31.14	34.83	36.26	35.94	38.37	39.49	40.99	37.93	49.64	51.20	57.07	55.09
Cruise%	26.58	26.16	26.63	27.80	25.97	25.34	28.21	27.55	24.15	20.99	17.17	13.45	14.42	12.79
Total fuel consumption (g)	418.99	427.84	425.30	428.84	405.07	440.08	447.34	448.29	498.69	442.85	485.47	561.60	557.75	558.81
Avg fuel consumption (g/s)	0.36	0.37	0.37	0.36	0.34	0.37	0.38	0.36	0.39	0.33	0.31	0.31	0.30	0.30
Idle fuel consumption (g)	83.34	77.56	77.03	82.77	90.65	82.64	88.57	96.99	100.65	102.37	134.75	161.08	170.97	169.64
Idle fuel consumption (%)	19.89	18.13	18.11	19.30	22.38	18.78	19.80	21.63	20.18	23.12	27.76	28.68	30.65	30.36
Journey Avg fuel consumption (g/km)	85.03	87.54	86.33	87.43	82.27	89.90	90.77	91.28	101.72	90.45	99.24	17.92	113.97	114.05
Fuel economy (ml/e/UKG)	23.98	23.29	23.62	23.32	24.78	22.68	22.46	22.34	20.04	22.54	20.54	17.92	17.89	17.88
Overall thermal efficiency (%)	0.16	0.16	0.16	0.16	0.16	0.16	0.17	0.16	0.16	0.15	0.15	0.14	0.13	0.13
Total Distance (km)	4.93	4.89	4.93	4.90	4.92	4.90	4.93	4.91	4.90	4.90	4.89	4.90	4.89	4.90
Carbon dioxide CO2 (g/km)	274.34	295.52	270.18	279.77	255.40	331.31	295.83	292.11	372.81	282.50	315.15	349.19	357.63	358.17
Nitrous oxide N2O (g/km)	0.0007	0.0021	0.0019	0.0050	0.0022	0.0164	0.0049	0.0116	0.0077	0.0045	0.0074	0.0066	0.0036	0.0038
Methane CH4 (g/km)	0.02	0.02	0.02	0.04	0.02	0.05	0.03	0.04	0.04	0.03	0.03	0.03	0.03	0.03
Nitrogen monoxide NO (g/km)	0.02	0.10	0.01	0.04	0.01	0.09	0.03	0.03	0.07	0.01	0.07	0.07	0.05	0.06
Nitrogen dioxide NO2 (g/km)	0.015	0.004	0.017	0.020	0.012	0.022	0.015	0.015	0.025	0.016	0.004	0.004	0.004	0.004
Ammonia NH3 (g/km)	0.09	0.08	0.08	0.11	0.08	0.20	0.10	0.12	0.12	0.08	0.09	0.12	0.12	0.10
Hydrogen cyanide HCN (g/km)	0.0089	0.0007	0.0119	0.0121	0.0031	0.0117	0.0039	0.0056	0.0160	0.0092	0.0010	0.0009	0.0009	0.0008
NOx (g/km)	0.05	0.16	0.04	0.08	0.03	0.16	0.06	0.07	0.14	0.03	0.11	0.11	0.08	0.09
Total Hydrocarbon THC (g/km)	0.20	0.21	0.27	0.34	0.19	0.51	0.32	0.36	0.39	0.30	0.28	0.31	0.30	0.30
Carbon monoxide CO (g/km)	1.15	1.07	0.97	1.47	1.24	3.88	1.66	2.43	1.44	1.42	1.22	1.50	1.14	1.17
Congestion	0.68	0.69	0.68	0.69	0.69	0.69	0.69	0.71	0.71	0.73	0.76	0.79	0.80	0.81
Number of stops	30.00	23.00	24.00	25.00	21.00	21.00	27.00	32.00	32.00	28.00	39.00	47.00	37.00	42.00
Journey duration (s)	1155.00	1162.00	1169.00	1177.00	1186.00	1188.00	1191.00	1256.00	1271.00	1334.00	1543.00	1785.00	1852.00	1868.00

## **8 Chapter Eight: Micro trip analysis of emissions under real world congested driving**

### **8.1 Introduction**

The emissions from vehicles in real world driving are of current concern, as they are often higher than on legislated test cycles and this may explain why air quality in cities has not improved in proportion to the reduction in automotive emissions. This has led to the Real Driving Emissions (RDE) legislation in Europe. RDE involves journeys of about 90km with roughly equal proportion of urban, rural and motorway driving. However, air quality exceedances occur in cities with urban congested traffic driving as the main source of the emissions that deteriorate the air quality. Thus the emissions measured on RDE journeys may not be relevant to air quality in cities. A Temet FTIR and Horiba exhaust mass flow measurement system was used for the mass emissions measurements in a Euro 4 SI vehicle. A 5km urban journey on a very congested road was undertaken 29 times at various times so that different traffic congestion was encountered. Each journey was split into ten sections of about 0.5km in order that the location and traffic conditions of the highest emissions could be determined. It was found that low speed stop-start traffic has much higher emissions than freely moving traffic and most of the higher emissions on the longer 5km journeys occurred in relatively short sections of slow moving stop/start traffic.

Real world driving uses different powers, different average speeds, different traffic congestion conditions, different road gradients, different maximum acceleration rates, different cold start conditions, different numbers of stop/start events and occurs at different ambient temperatures and pressures than on test cycles and will inevitably have different emissions, as all these factors influence the emissions. This applies equally to spark ignition and diesel engines [5, 6, 8, 9, 14, 35, 105, 122-125] This work concentrates on the influence of congested traffic on SI vehicle emissions.

The road on which this research was undertaken was the subject of a city of Leeds traffic and congestion study [107, 108, 120]. The air quality in the same

area was monitored and compared with traffic emission modelling results. These modelled results were based on traffic counts and the certified emissions on the NEDC test cycle. The modelled NO<sub>2</sub> concentrations were 47% lower than actually measured results in the area and 28% lower for the city centre site [120]. The NO<sub>2</sub> measurements showed 14 sites in Leeds above the EU limit where the model only predicted 4 sites in exceedance. The high NO<sub>2</sub> in the area was attributed to traffic congestions, as there are no industrial air pollution sources. Leeds as a population of 750,000 with the several large towns to the north, Ilkley, Otley, Harrogate all of which would feed traffic into central Leeds down the road studied.

Legislated test cycles such as the NEDC and FTP75 were not designed to produce data for air quality modelling, but to compare cars A, B, C etc. with a reference standard, on identical test cycle basis. It is important that the test cycle is representative of real world driving with cold start, stop/starts, acceleration and deceleration, and transient operation comparable to real world driving. This is why purely steady state testing ceased to be the only

**Table 8-1 Comparison of key parameters in test cycles and in real world driving.**

Test Cycle	NEDC	FTP	JC09	WLTC	RDE[18-20]	[17]
Mean Vel. km/h	33.6	31.5	24.4	46.5	30- 110	5–26
Congest.	30%	34%	49%	3%	0%	90-46%
Max. Acc. m/s <sup>2</sup>	1	1.5	1.7	1.7	1.5	2.2–2.8
Dist., km	11	12	8.2	23.3	80-90	5
No. Acc. /km	1.3	1.5	1.5	0.4	~0.2	1.4-7

method of emissions testing for heavy duty vehicles in 2000 and was abandoned for fuel economy testing for passenger cars in 1993. However, if the test cycle conditions are well removed from current real world driving, then there is concern that the emissions on the legislated test cycle may be too low and result in air quality not being improved as intended. This has led to the development of the WLTC test procedures and real world emissions measurement using portable emissions measurement systems (PEMS) [30, 98, 126] or Real driving emissions test procedures (RDE) [127-129].

Table 8-1 compares some key test parameters between the test cycles and typical RDE data, which are mainly taken from Hausberger et al. [127]. Key differences in the WLTC and RDE legislation and the existing NEDC, FTP and JC09 are the higher average speeds and the complete lack of congested driving. The longer distances of the cycles means that the cold start portion, which lasts about 1km [30], is a lower proportion of the whole cycle. This means that the cold start emissions are divided by a longer distance to produce apparently lower emissions, but actually the same emissions over the first km. The WLTC has a higher mean velocity than the NEDC or FTP, double the test distance and a quarter of the number of starts from idle. All this leads to lower emissions than the NEDC [31], as shown by Williams et al. [32] for Euro 6 vehicles.

Liu et al. [23] analysed data for USA vehicle trips with 1851 trips using 292 passenger car vehicles driving a total of 25,000km. 50% of the trips were <4km, 25% were 4-8km and only 25% were for distances >8km. This justifies the use of a 5km trip distance in the previous work of the authors [30, 107, 126] and in this work. The trip analysis of Liu et al. [23] also shows the unrealistic trip distance in RDE test procedures, as <1% of journeys were of this length.

The RDE test procedures are weighted to higher vehicle speeds using higher engine powers, where for SI engines the catalyst will always be hot and lambda 1 control is precise. This results in SI engine vehicles always meeting the NEDC legislation under RDE conditions. However, it will be shown that under congested traffic conditions emissions can be well above the NEDC values.

The objective of this work is to further analyze the real world emissions data of Khalfan et al. [98] by splitting the 5 km journey into ten sections of about 0.5km. The 29 repeat journeys then give 29 measured emissions for each 0.5 km section. This will enable the most congested traffic part of the journey to be assessed for emissions. It will be shown that the most congested sections of the 5km journey dominate the total emissions for the journey.

## 8.2 Congested traffic in urban area

The severity of congestion in traffic could be indicated by average velocity of the traffic. However, the average velocity is related to the speed limit of particular roads. So a universal congestion factor is used for the indication of congestion and defined as follows:

$$\text{Congestion factor (CF)} = 1 - (\text{Ave. Speed} / \text{legal speed limit}) \quad (8-1)$$

It is generally regarded as congested traffic if the CF is less than 0.5, i.e. the average speed of a journey is lower than the half of the speed limit of the road. If the CF is 0, it means that the average speed is equal to the speed limit of the road, i.e. no congestion.

The legal speed for the road investigated in this study is 48 km/h. The average speed on the NEDC is 33.6 km/h and is an average congestion of 30%. For the urban part only of the NEDC the average speed is 17.2 km/h and congestion is 64% which is more reasonable. However, in this work congestion levels up to 90% have been measured and 95% in the worst congested parts of the route. The new WLTP is little improvement on the NEDC as the average speed is higher, which is the main reason why it has been found to give lower emissions than on the NEDC for many vehicles [98, 127].



**Figure 8-1 Map and notations of the driving route.**

**Table 8-2 Directions of the two driving routes.**

Driving cycle (route)	Direction
A	1-2-3-4
B	1-3-2-4

Features of congested roads:

1. A high traffic flow
2. Frequent junctions on the route with traffic joining and leaving the main flow. Main flow stops to let in vehicles from the right or left, at the discretion of the drivers in the main flow. Each car joining causes main traffic to halt.
3. Traffic lights at major junctions and pedestrian crossings. All traffic now halts periodically. For high traffic flows it can take several stop/starts to get through. The process of starting and moving about 10m is very energy intensive with high emissions.
4. Traffic joining and leaving flows that can be comparable with the main flow.
5. Traffic mean velocity decreases as congestion increases.



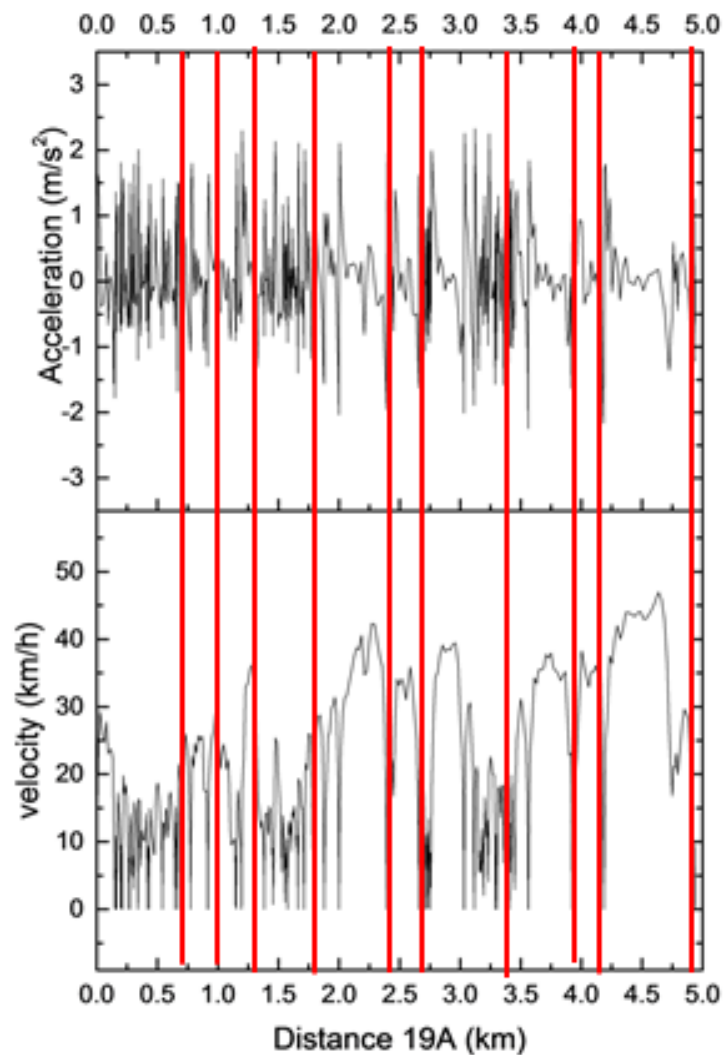


**Table 8-3 Journey sections for locations in previous map.**

A journey					
Section	Section start	Section end	same section	Section	Distance km
<b>S1</b>	1	3	<b>S1=S10</b>	<b>S1</b>	<b>0.719</b>
<b>S2</b>	3	4	<b>S2=S9</b>	<b>S2</b>	<b>0.24</b>
<b>S3</b>	4	6	<b>S3=S6</b>	<b>S3</b>	<b>0.289</b>
<b>S4</b>	6	8	<b>S4=S5</b>	<b>S4</b>	<b>0.535</b>
<b>S5</b>	8	9	<b>S7=S8</b>	<b>S5</b>	<b>0.684</b>
<b>S6</b>	9	11		<b>S6</b>	<b>0.244</b>
<b>S7</b>	11	15		<b>S7</b>	<b>0.662</b>
<b>S8</b>	15	19		<b>S8</b>	<b>0.586</b>
<b>S9</b>	19	20		<b>S9</b>	<b>0.202</b>
<b>S10</b>	20	22		<b>S10</b>	<b>0.739</b>

The mean emissions for the complete 5 km route have been previously presented for hot and cold starts [13]. This work showed high emissions for congested traffic with low mean journey speeds. Two complete journey velocity and acceleration plots as a function of distance for the complete 5km route are shown in Figure 8-3 and Figure 8-4 for high and low congestion respectively. These are both for route A in Table 8-2 and are two of the 29 hot start journeys made on this route.

This work splits these journeys into 10 sections and analyses the mean emissions for each section. This enabled the most congested portion of the 5km route to be identified and the range of mean velocities in the previous work [107] to be extended. The key points in the 5km loop journey in Figure 8-1 are shown in Figure 8-2 and the sections of the journey are summarized in Table 8-3, which are the same sections for journey A and B. Table 8-3 shows that there are five sections on the journey, but travelled in the opposite direction on the return journey, where different traffic flows and different actions at traffic lights and pedestrian crossings occur.

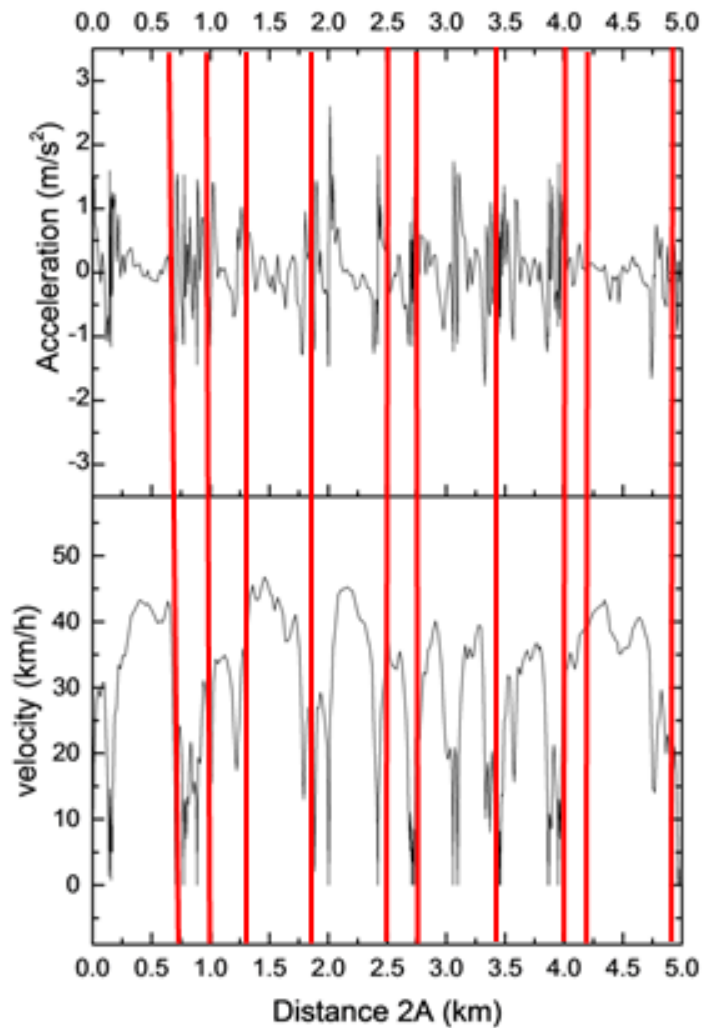


**Figure 8-3 Velocity and acceleration records for high congestion (6 stop/starts per km) as a function of distance showing the 10 stages in Table 8-3.**

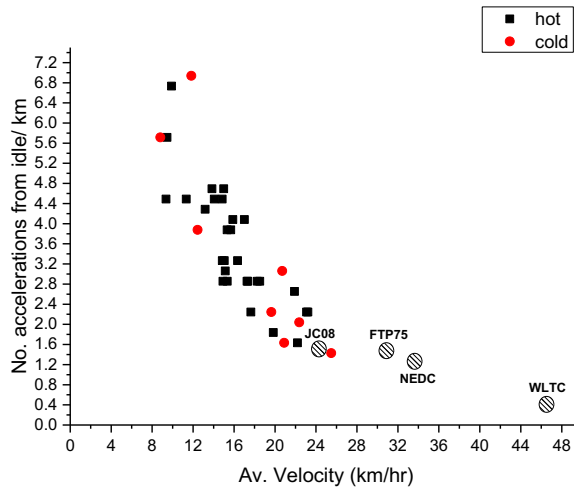
Thus the return journeys have been treated as a separate journey and thus the results are presented for the 10 sections of the journey. The Headingley roadside air quality monitor is between points 19 and 20 in Figure 8-2 and hence  $S_2$  and  $S_9$  are the two parts of the journey that pass the roadside monitor. The data for  $S_9$  will be presented later to show the high emissions local to the monitor. The 10 sections of the journey in Table 8-3 can be seen in terms of velocity and acceleration in Figure 8-3 & Figure 8-4, for high and low congestion respectively. For each of these sections the 29 repeat journeys have been separated into 10 sections giving 290 data points for average fuel consumption and emissions for each section.

## 8.4 The Number of stop/starts

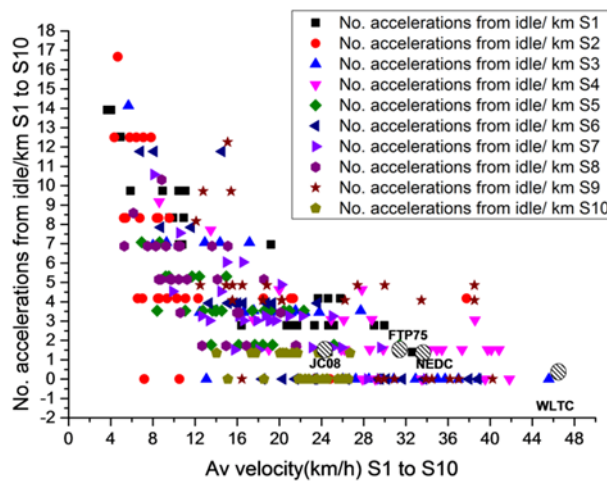
Examples of the instantaneous emissions have been published by the authors for cold [30] and hot starts [98] and will not be repeated here. This paper includes a more detailed analysis of the hot start data than the mean journey emissions [30, 98].



**Figure 8-4 Velocity and acceleration records for low congestion (2.4 stop/starts per km) as a function of distance showing the 10 stages in Table 8-3.**



**Figure 8-5 Number of accelerations from idle vs mean trip velocity for cold and hot start trips.**



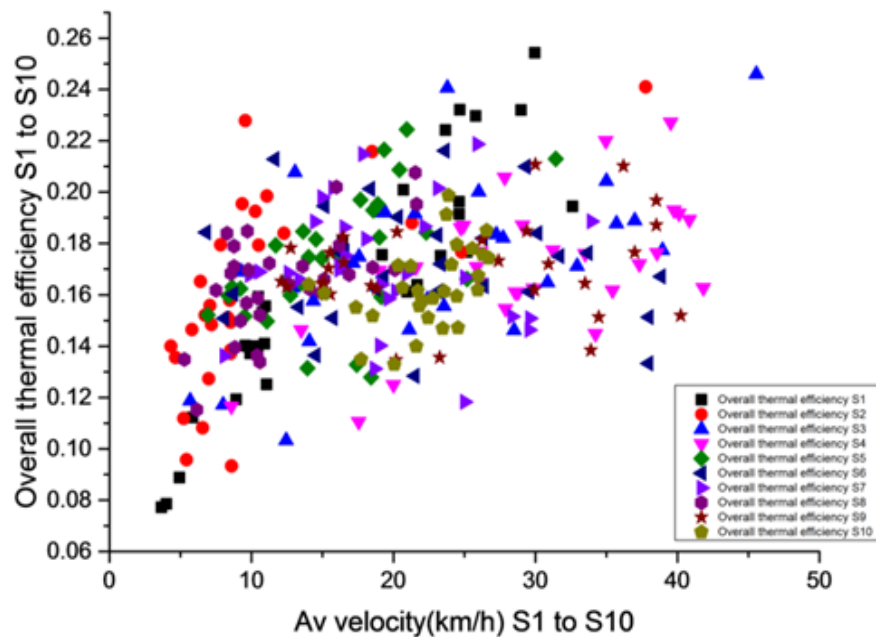
**Figure 8-6 Number of accelerations from idle (<5km/h) per km for the 10 journey sections in Table 8-3.**

Figure 8-5 shows the number of starts from idle (<5 km/h) for the 29 hot start and 8 cold start 5km journeys [107]. This shows that low average speeds are associated with a high number of stop/starts in journeys with high congestion and low mean velocities. Figure 8-5 also shows the number of stop/starts in the various test cycles in Table 8-1 and this shows that none of these test cycles includes the traffic conditions involved in congested traffic in cities, with large numbers of stop/starts per km. The WLTC, which is supposed to be more real world than the NEDC, has fewer stop/starts and a higher average speed and hence is not representative at all of congested traffic driving. As a

consequence data from WLTC tests and NEDC tests on the same vehicles show lower emissions and lower CO<sub>2</sub> for the WLTC [31, 32]. Thus the WLTC is not going to give data that explains why air quality in cities is not improving in proportion to the improvement in vehicle emissions. This will only come from studying the congested traffic in the vicinity of the air quality monitoring stations in cities, as in the present work.

Hybrid vehicles are particularly suitable to stop/start congested traffic conditions, as all the starts will use stored energy and not fuel burnt in an engine. Conversely, hybrid vehicles will have little benefit on the WLTC as there are few stop/starts and high average speeds. If representative stop/starts for congested traffic are not in the test cycles for passenger car vehicles then there is little incentive to develop hybrid technologies. The emission of stop/start congested traffic from RDE test cycles means that Hybrid vehicles will be disadvantaged relative to non-hybrids on the RDE journeys.

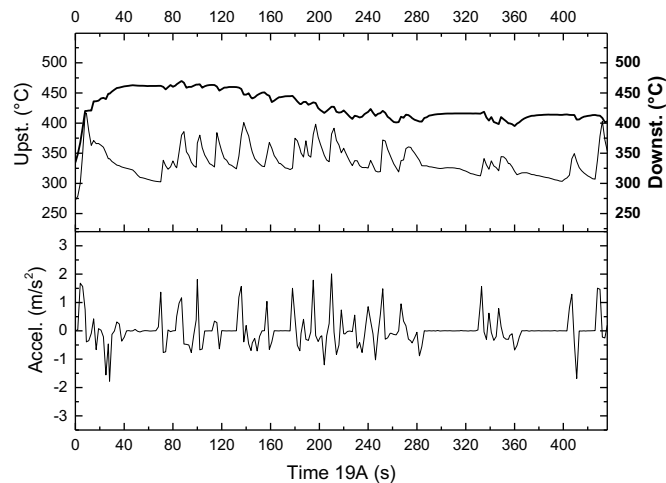
Figure 8-6 shows the number of stop/starts per km as a function of the mean velocity of each stage, for the 10 journey sections with 29 hot start journeys in each (290 data points). Figure 8-6 shows a wider range of mean velocities from 4 to 46 km/h, instead of 8.5 – 25 km/h in Figure 8-5. At the higher mean velocities the number of stop/starts reduces to those in the test cycles, one journey section having conditions close to the WLTC in terms of the mean velocity and number of stop/starts per km. Figure 8 6 also shows that the number of stop/starts per km had a greater range from 0 – 17, compared with 1.3 – 7 in Figure 8 5. Twenty one the 290 journeys had a number of stop/starts >10 per km or one stop/start every 100m on average. This is mainly caused by queuing at traffic lights in congested traffic. At 5 km/h a 100m distance takes 139s and this is similar to the green on time at traffic lights. On the tested route the traffic lights are computer controlled to maximize the traffic flow in the direction into the city centre in the morning and out of the city centre in the afternoon, so that the green on period is variable.



**Figure 8-7 The average thermal efficiency for each journey section as a function of the average velocity.**

Figure 8-6 shows the general trend of Figure 8-5, that higher average speeds is accompanied by few stop/starts. However, at low mean velocities, such as 8 km/h, the number of stop/starts varies from 0 to 12/km for journey 2 in Table 8-3. This is the section that leads up to a set of traffic lights. In contrast section 1 has a number of stop/starts per km that increase as the mean velocity decreases. The reason for this difference in two connected sections of the journey is then in times of high congestion the traffic queue backs up to  $S_1$  and there is a large number of stop/start movements, as shown in Figure 8-3. However,  $S_2$  can move slowly or quickly depending on whether the lights or on green. Figure 8-3 shows  $S_2$  with a relatively high velocity, compared with the stop/start traffic in  $S_1$  for the same journey. This was due to the lights changing to green, with them on red when the vehicle was in  $S_1$  on the same journey. Figure 8-4 shows the reverse situation with relatively free moving traffic in  $S_1$  and stop/start traffic in  $S_2$ . The section of the journey  $S_3$  also shows in Figure 8-6 a wide range of stop/starts per km and this is again due to this section have a second set of traffic lights at the road junction at the end of this section. This  $S_3$  section of the journey has mean velocities from 13 to 46 km/h with no stop/starts. These are all journey with green traffic

lights at the end of  $S_3$  and the velocity decreases as the traffic load increases. Higher number of start in  $S_3$  occur when the traffic light are on red for part of the time.



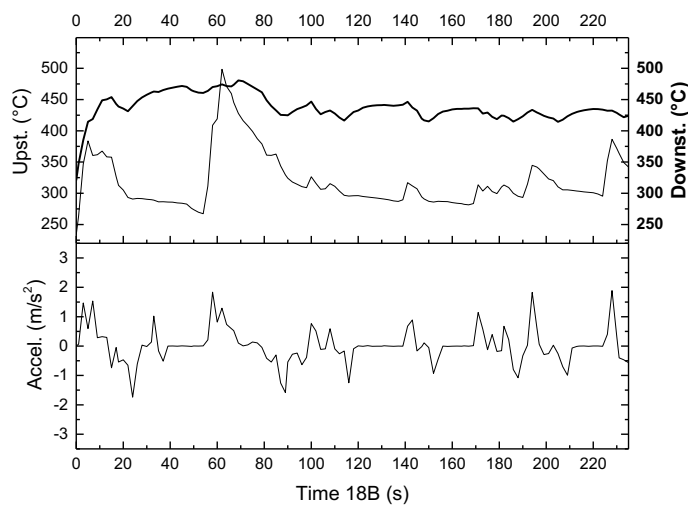
**Figure 8-8 TWC upstream and downstream temperature for highly congested traffic.**

The VSP data from Equation (3-2), was used to determine the total MJ power output for each section of the journey, for all 29 journeys. The fuel flow rate data was used to determine the total fuel consumed during each section of the journey and this was converted to MJ of input energy using a fuel CV of 43 MJ/kg. This enabled the average thermal efficiency for each section of the journey to be determined and this is shown in Figure 8-7 as a function of the mean velocity for each section. The results in Figure 8-7 show a very wide data scatter, which is due to the influence of the proportion of idle. Idle has no power output, but does consume fuel and has emissions. So the impact of idle is to reduce the thermal efficiency and to reduce the mean journey speed. Comparison of Figure 8-7 and Figure 8-6 shows that at the lowest thermal efficiency of 8% at 4 km/h there were 14 starts from idle per km and the proportion of time at idle in this journey would be high. In contrast there was a journey at 10 km/h that had a thermal efficiency of 23% because there were no starts from idle and hence no idle period in the journey. In contrast a journey with an average velocity of 9 km/h had a thermal efficiency of 9.5% because it had 12.5 starts from idle per km. Thus it is not the low average

velocity that causes low thermal efficiencies and high CO<sub>2</sub> but the frequency of the stop/start motion per km.

## 8.5 The TWC temperature during the hot start

Although the test were carried out with a prior journey to warm up the engine lube oil, coolant and TWC, it was found that the hot start resulted in the TWC upstream temperature being lower than the downstream temperature for a significant part of the SI journey. Typical results of the catalyst front and downstream temperatures and the associated vehicle acceleration are shown in Figure 8-8 for a stop/start congested traffic journey and in Figure 8-9 for a less congested journey. These results were unexpected, as the downstream was above 400°C within 10s, but the upstream temperature struggled to reach 400°C and was cooled by the exhaust flow. The upstream temperature varied with acceleration, as this is a power demand and the exhaust temperature increases with power. The net result is that there is a cold start effect, even when the catalyst is hot when the Journey starts. This means that the cold start actions of late spark timing and hydrocarbon storage are not active when the catalyst is hot initially. The catalyst is then cooled by the low power exhaust flow in congested traffic. It will be shown in the results below, that journey S<sub>1</sub> has high emissions than all the other journeys, due to the catalyst not being hot enough at the front brick during hot start.



**Figure 8-9 TWC front and downstream temperature for lower congestion then in Figure 8-8.**



## **8.6 The emissions alongside the roadside air quality monitoring station.**

The average CO<sub>2</sub>, total hydrocarbons (THC), CO and NO<sub>x</sub> emissions as g/km are shown as a function of the mean speed for S<sub>2</sub> in Figure 8-10 to Figure 8-13 and for S<sub>9</sub> in Figure 8-14 to Figure 8-17. These two sections are the north and south direction traffic that passes the roadside air quality monitor that exceeds the European air quality standards for NO<sub>x</sub> and PM at peak traffic times of the day. It was also found, as shown in Figure 8-18 to Figure 8-21, that the worst traffic emissions were for S<sub>1</sub> that contains upstream queuing traffic from the lights at the end of S<sub>2</sub>. The 290 data points for all 29 journeys over S<sub>1</sub> – S<sub>10</sub> are shown for the four legislated pollutants in Figure 8-22 to Figure 8-25. All the results show several journeys with mean emissions below the NEDC but the majority of the mean emissions for all four pollutants were above the NEDC for low average speeds caused by the stop/start motion of the congested traffic.

### **8.6.1 CO<sub>2</sub> emissions**

These results show that congestion was very bad for CO<sub>2</sub> emissions and fuel economy. Figure 8-18 shows that for S<sub>1</sub> there were only 4 of the 29 journeys where the CO<sub>2</sub> emissions were <180 g/km, certified on the NEDC for this vehicle. These four journeys occurred for average speeds above 23 km/h. However, there were 5 journeys above 23 km/h with higher CO<sub>2</sub> emissions than 180 g/km. At the lowest mean velocities there was a wide range of journey CO<sub>2</sub>, but Figure 8-18 shows for S<sub>1</sub> there were journeys where the CO<sub>2</sub> was x3 of the NEDC value and these were in the velocity range 4 – 12 km/h, with a high number of stop/starts.

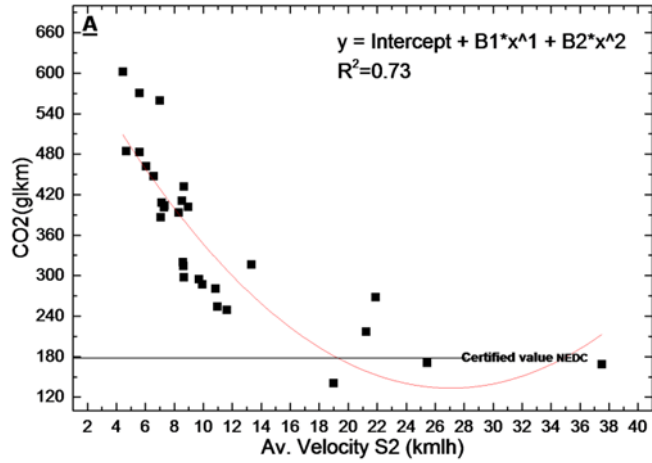


Figure 8-10  $CO_2$  emissions for  $S_2$  vs the mean velocity for  $S_2$ .

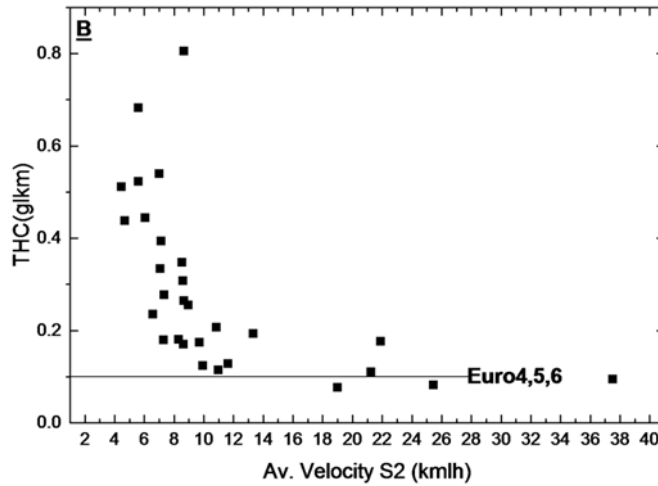


Figure 8-11 THC emissions for  $S_2$  vs the mean velocity for  $S_2$ .

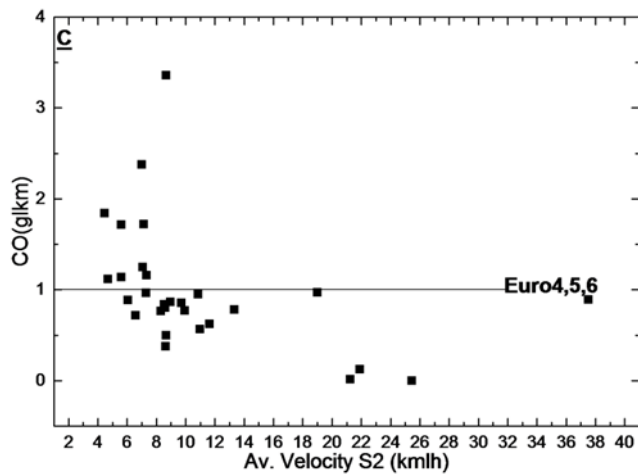


Figure 8-12 CO emissions for  $S_2$  v. the mean velocity for  $S_2$ .

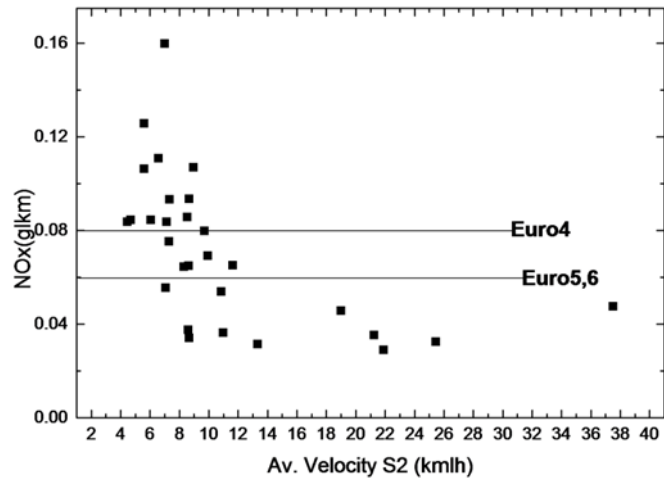


Figure 8-13 NO<sub>x</sub> emissions for S<sub>2</sub> vs the mean velocity for S<sub>2</sub>.

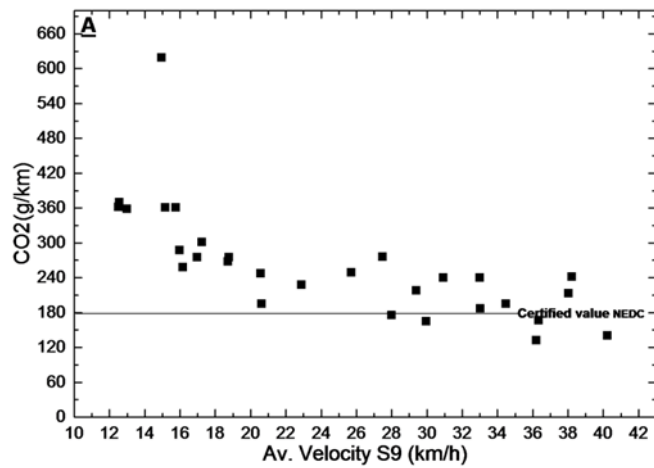


Figure 8-14 CO<sub>2</sub> emissions for S<sub>9</sub> v. the mean velocity for S<sub>9</sub>.

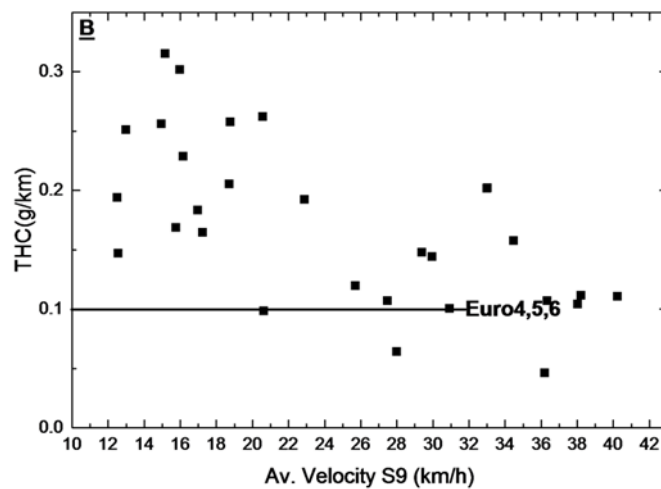


Figure 8-15 THC emissions for S<sub>9</sub> vs the mean velocity for S<sub>9</sub>.

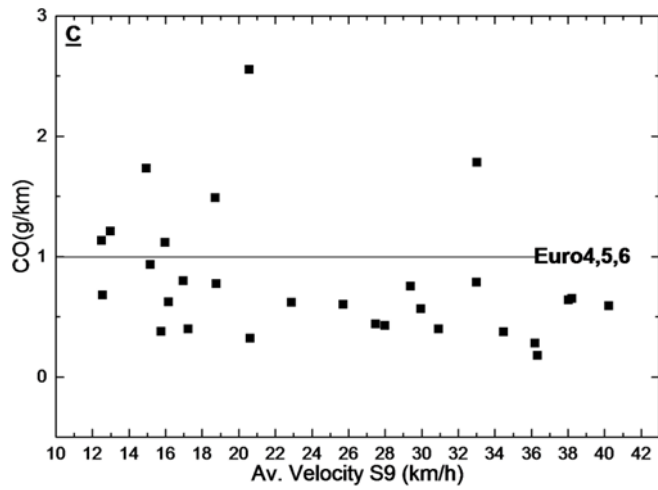


Figure 8-16 CO emissions for S<sub>9</sub> vs the mean velocity for S<sub>9</sub>.

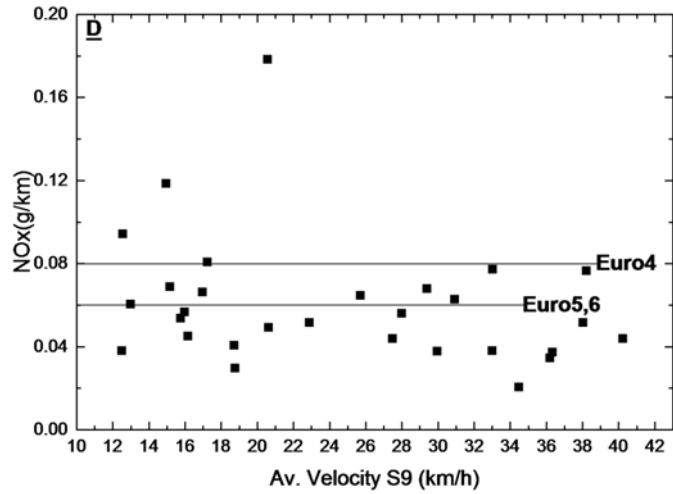


Figure 8-17 NO<sub>x</sub> emissions for S<sub>9</sub> vs the mean velocity for S<sub>9</sub>.

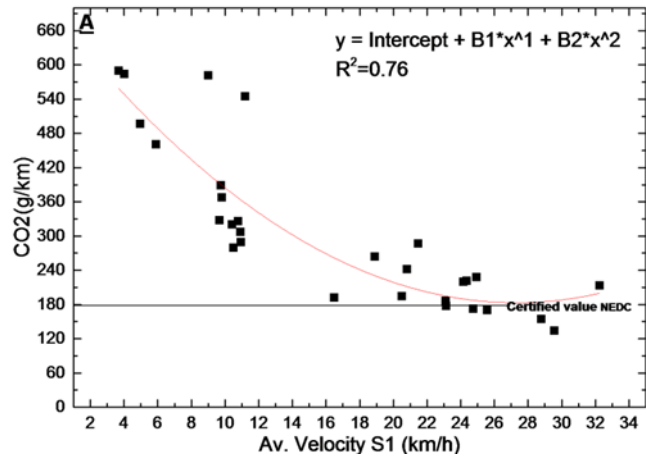


Figure 8-18 CO<sub>2</sub> emissions for S<sub>1</sub> v. the mean velocity for S<sub>1</sub>.

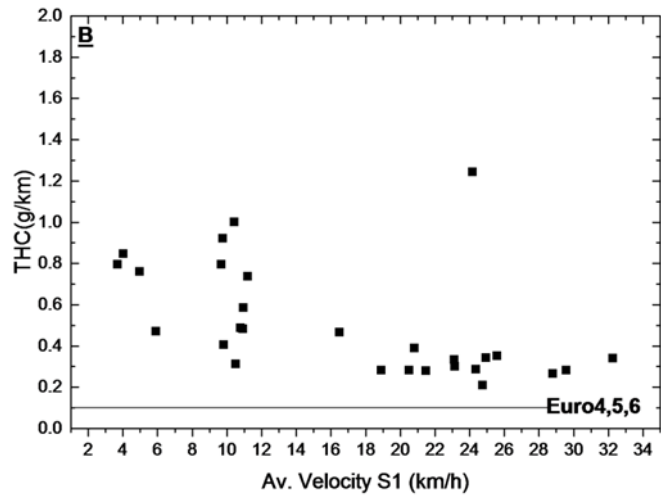


Figure 8-19 THC emissions for S<sub>1</sub> v. the mean velocity for S<sub>1</sub>.

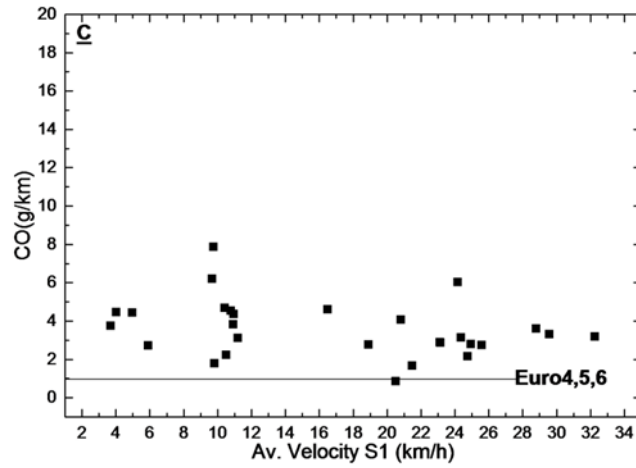


Figure 8-20 CO emissions for S<sub>1</sub> vs the mean velocity for S<sub>1</sub>.

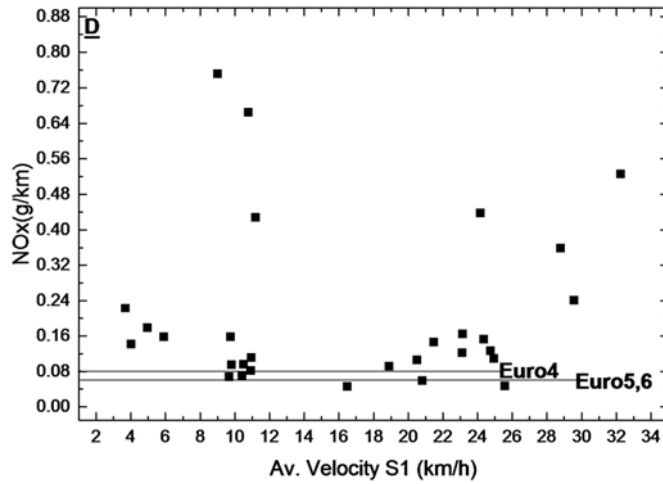


Figure 8-21 NO<sub>x</sub> emissions for S<sub>1</sub> vs the mean velocity for S<sub>1</sub>.

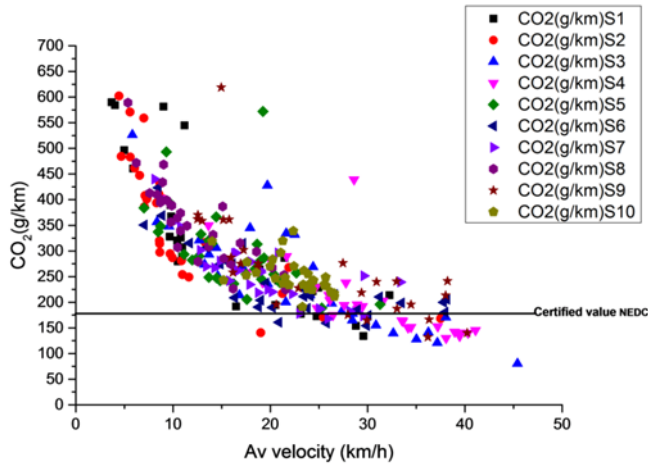


Figure 8-22 CO<sub>2</sub> emissions for S<sub>1</sub>-S<sub>10</sub> vs the mean velocity.

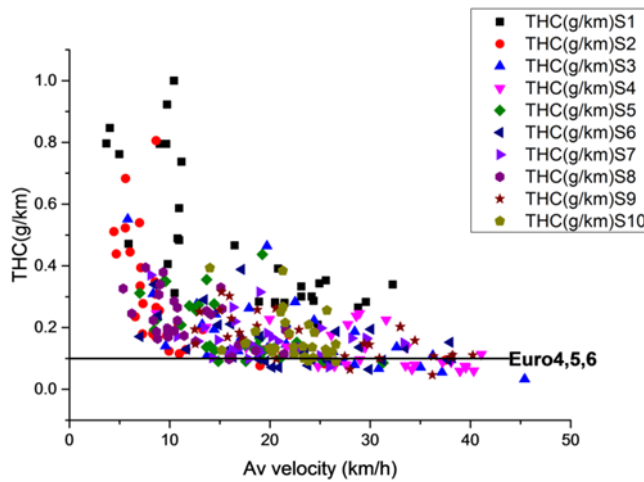


Figure 8-23 THC emissions for S<sub>1</sub> – S<sub>10</sub> vs the mean velocity.

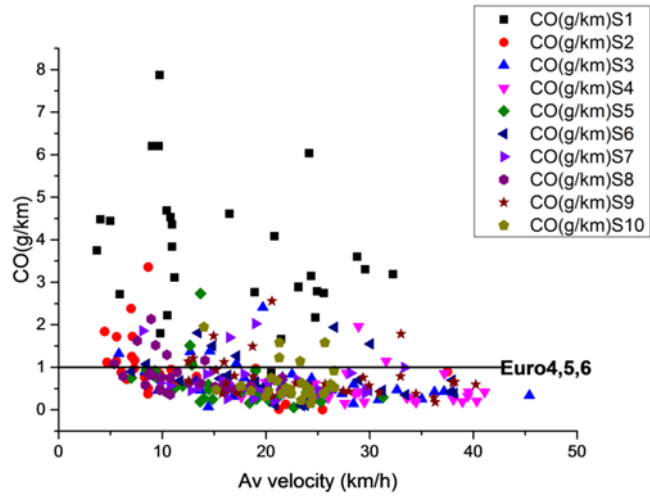


Figure 8-24 CO emissions for S<sub>1</sub>-S<sub>10</sub> vs the mean velocity.

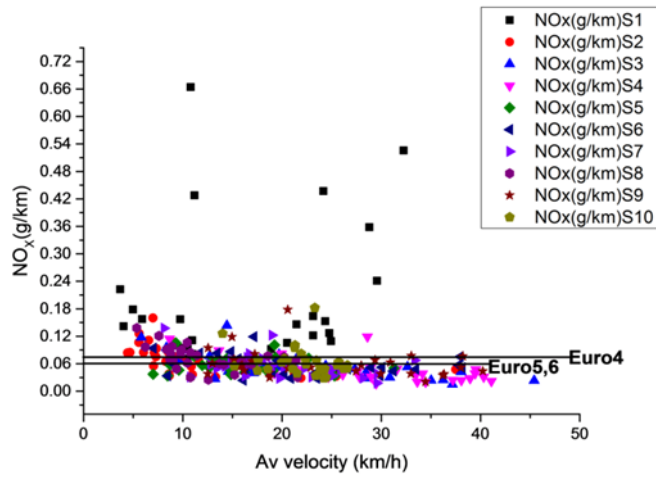


Figure 8-25 NO<sub>x</sub> emissions for S<sub>1</sub> – S<sub>10</sub> v. the mean velocity.

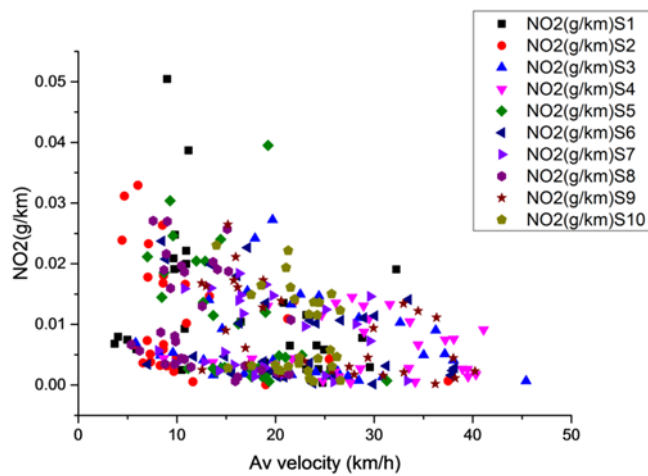
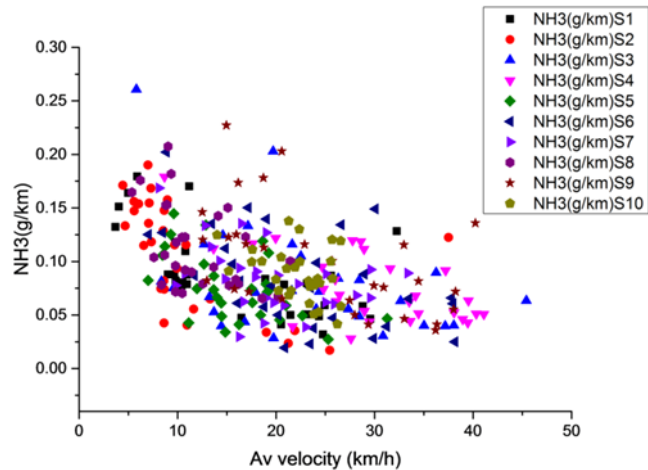


Figure 8-26 NO<sub>2</sub> emissions for S<sub>1</sub>-S<sub>10</sub> vs the mean velocity.



**Figure 8-27 NH<sub>3</sub> emissions for S<sub>1</sub> – S<sub>10</sub> vs the mean velocity.**

For the journey section by the road side air quality monitor, S<sub>2</sub> and S<sub>9</sub>, most of the journeys had CO<sub>2</sub> emissions >180 g/km for the NEDC. In Figure 8-10. for S<sub>2</sub> only 3 of the 29 data points were below 180 g/km and these were for mean velocities >19 km/h. However, for 22 km/h Figure 8-10 shows that there were two journeys with CO<sub>2</sub> emissions above the NEDC value. At low velocities with congested traffic Figure 8-10 shows that journey S<sub>2</sub> had 3 trips with x3 the NEDC CO<sub>2</sub>. Similarly, for the traffic travelling into the city on route S<sub>9</sub>, Figure 8-14 shows that there were 5 journeys where the CO<sub>2</sub> was below that NEDC for mean velocities above 28 km/h, but in the speed range 30-40 km/h there were 7 journeys with higher CO<sub>2</sub> than on the NEDC. For S<sub>9</sub> there was only one journey at 15 km/h that had x3 the NEDC CO<sub>2</sub>.

For S<sub>2</sub> the CO<sub>2</sub> emissions do not meet those certified under the NEDC until the mean velocity was 25 km/h. This was mainly due to the high traffic flows in the evening period. However, the inward traffic flow is worse for CO<sub>2</sub> in S<sub>9</sub>, where the mean velocity has to be above 38 km/h before the NEDC CO<sub>2</sub> is reached. The mean velocity on the NEDC is 33.6 km/h and these higher CO<sub>2</sub> at lower mean speeds would be expected from the greater number of stop/starts per km that give rise to the lower velocities. For the outward journey S<sub>1</sub> had a mean velocity of 25 km/h before the CO<sub>2</sub> emissions were equal to or less than those certified for the NEDC. However, in the opposite flow of this same section of road, S<sub>10</sub>, the results were that the NEDC CO<sub>2</sub> was never



achieved, as the highest velocity in this section in the 29 repeat journeys was 27 km/h.

### **8.6.2 THC emissions**

The THC emissions for S<sub>2</sub> and S<sub>9</sub> by the roadside air quality monitor are shown in Figure 8-11 and Figure 8-15. For S<sub>2</sub> the journey mean velocity range was 4 – 38 km/h and all the data was well above the NEDC limit below a speed of 18 km/h. There were five journeys in the speed range 4-8 km/h with >x5 NEDC THC. As many of the individual HC that were measured were toxic, such as benzene, 1, 3 butadiene and aldehydes, these exceedances of NEDC standards in low speed congested traffic are a potential health concern. For the S<sub>9</sub> section the average speeds varied from 12 – 40 km/h and the higher minimum journey speed than for S<sub>2</sub> was due to the absence of a near traffic light ahead of the flow as the next traffic lights were about 1km ahead and congestion would only reach the S<sub>9</sub> section in the peak early morning traffic flow at 8am. Due to access to the instrumented vehicle no measurements were made at 8am. All the high congestion was measured around 5pm and this peaked in the northerly direction on section S<sub>2</sub>. Figure 8-15 shows that for S<sub>9</sub> there were only two journeys with the THC <NEDC values and these occurred at mean speeds >28 km/h. However, there were 9 journeys between 28 and 40 km/h that were at or above the NEDC level.

The first journey after the cold start in S<sub>1</sub> had the highest THC emissions, as shown in Figure 8-19, that were higher than for any other journey as shown in Figure 8-23. All 29 were >NEDC THC over the velocity range 4 – 32 km/h and 9 were >x5 the NEDC limit. It was shown above that S<sub>1</sub> also had the highest CO<sub>2</sub> emissions and it will be shown below that it had the highest CO and NO<sub>x</sub> emissions. It was shown in Figure 8-8 and Figure 8-9 that the intended hot start had problems with the low engine powers cooling the upstream of the catalyst, even though the downstream of the catalyst was above 400°C. The vehicle had been stationary for about 15 mins. prior to the start of the test while the FTIR and data loggers were set up. The vehicle start and acceleration resulted in the front and downstream of the catalyst being above

400°C within 10s of the start. However, once the speed was reduced on entry into congested traffic the upstream of the catalyst was cooled by the lower temperature exhaust flow, as shown in Figure 8-8 and Figure 8-9. The net result was a cold start influence on the THC, even though the catalyst was initially hot. This cold start influence is also shown in the CO and NO<sub>x</sub> results, as discussed below.

The THC for all 29 journeys for all 10 sections are shown as a function of the mean journey speed for that section in Figure 8-23. This shows a very wide variation in THC for the same mean velocity. This was due to differences in the number of stop/starts and the start acceleration magnitude, caused by the presence of other traffic. For most journeys the NEDC THC limit was exceeded and only about 10% of the data was below the NEDC limit and this occurred over the speed range 15 – 45 km/h. But there was more data in the speed range 15 – 40 km/h that had THC >NEDC levels.

The reason for the higher THC in real world driving than on the NEDC are due to several influences. The low engine powers used at the low average speeds in real world driving result in higher engine out emissions. This can result in the ability being compromised of the oxygen storage ceria to oxidize HCs during rich excursions.

### **8.6.3 CO emissions**

The CO emissions are shown for the section S<sub>2</sub> in Figure 8-12 and most of the data was < NEDC values apart from in the low mean velocity range of 4-8 km/h where there were 9 journeys with CO above the NEDC. This is in contrast to the THC emissions where most of the data was above the NEDC limit. This difference is due to the lower TWC light off temperature for CO compared with THC. The CO in the southbound traffic in the same section, S<sub>9</sub> route, is shown in Figure 8-16 CO emissions for S<sub>9</sub> vs the mean velocity for S<sub>9</sub> and most of the data here is < NEDC, apart from 9 journeys with CO above the NEDC limit. The data had no correlation with the journey mean velocity.

These low CO for the two lanes of travel by the roadside air quality monitor indicates no problem on average of enhanced CO emissions.

The CO emissions for the first section of the journey, S<sub>1</sub>, are shown in Figure 8-20 CO emissions for S<sub>1</sub> vs the mean velocity for S<sub>1</sub> and all the 29 journeys were above the NEDC limit. Much of the CO data was x4 above the NEDC limit and some was x6 above the limit. This was a similar pattern to the THC data and the reason was that in this first section the catalyst was hot at the downstream face but not at the upstream face and this led to a significant catalyst warm-up period, as discussed above. Figure 8-24 CO emissions for S<sub>1</sub>-S<sub>10</sub> vs the mean velocity shows that for the other 9 journey sections, the CO was mainly <NEDC. If S<sub>1</sub> is ignored then only 17% of the rest of the data was above the NEDC limit across the 4 – 35 km/h speed range. The proportion of the data >NEDC was higher at low speeds, but there were high CO journeys up to 32 km/h.

#### **8.6.4 NO<sub>x</sub> emissions**

The NO<sub>x</sub> emissions for S<sub>2</sub> are shown in Figure 8-13 NO<sub>x</sub> emissions for S<sub>2</sub> vs the mean velocity for S<sub>2</sub> and they were all <Euro 6 for journey speeds >12 km/h 38% of the 29 journeys were <Euro 6 NO<sub>x</sub> across all speed ranges. However, there were a significant number of journeys in congested traffic with mean velocities in the range 4 – 8 km/h, with NO<sub>x</sub> up to x2 Euro 6 NO<sub>x</sub>. Part of the reason for low NO<sub>x</sub> is the low engine powers used in congested traffic, as engine out NO<sub>x</sub> increases with increased power, as the peak temperature increases with power. Also at low powers EGR levels are higher which reduces CO<sub>2</sub>, due to lower pumping power with a more open inlet throttle for the same power. For the opposite direction journeys on route S<sub>9</sub> in Figure 8-17 NO<sub>x</sub> emissions for S<sub>9</sub> vs the mean velocity for S<sub>9</sub>, 59% of the 29 journeys had NO<sub>x</sub> below Euro 6 levels and 90% were below Euro 4 NO<sub>x</sub> levels. This low NO<sub>x</sub> occurred for journey average speeds from 12 to 40 km/h. The S<sub>9</sub> journeys into the city were less congested than the outward S<sub>2</sub> journey, but this was because the most congested times into the city centre at 8am were not measured. There were three journeys with speeds <20 km/h where the NO<sub>x</sub>

was very high. On average journeys in S<sub>2</sub> and S<sub>9</sub> close to the roadside air quality monitor had NO<sub>x</sub> emissions at or below the Euro 4-6 NO<sub>x</sub> levels.

For the first journey section S<sub>1</sub> in Figure 8-21 NO<sub>x</sub> emissions for S<sub>1</sub> vs the mean velocity for S<sub>1</sub> 83% of the 29 journeys had NO<sub>x</sub> emissions above the Euro 6 emissions level. The NO<sub>x</sub> emissions were much higher than for the S<sub>2</sub> and S<sub>9</sub> journeys and Figure 8-25 NO<sub>x</sub> emissions for S<sub>1</sub> – S<sub>10</sub> v. the mean velocity shows that the S<sub>1</sub> NO<sub>x</sub> was much higher than for all the other 9 journey sections. The reason for this was as discussed above, there was a cold start effect for the TWC that was hot on the downstream but cooled on the upstream by the low temperature exhaust gases at the low powers used in congested traffic. Figure 8-25 NO<sub>x</sub> emissions for S<sub>1</sub> – S<sub>10</sub> v. the mean velocity shows that with the exception of section S<sub>1</sub> most of the NO<sub>x</sub> emissions for the other sections were below the Euro 6 level. The data above the Euro 6 level were confined to the 4 – 29 km/h mean velocity region and would not be seen on an RDE cycle as these low mean velocities are omitted from the RDE cycles.

These NO<sub>x</sub> emissions show that SI vehicles are unlikely to be the source of elevated roadside NO<sub>x</sub>, even in congested traffic and diesel vehicles are more likely to be responsible. Hadavi et al [123] for a Euro 3 diesel in the same congested section of this journey, S<sub>2</sub>, measured NO<sub>x</sub> emissions of 1.9 – 3.0 g/km at mean average velocities of 5.1 – 6.4 km/h. These were between 2.9 and 4.6 times the NEDC level for this vehicle of 0.65 g/km. These diesel emissions at Euro 3 are much greater than for the SI engine in Figure 8-25 NO<sub>x</sub> emissions for S<sub>1</sub> – S<sub>10</sub> v. the mean velocity which for the same mean velocity was about 0.12 g/km over an order of magnitude less than for the diesel results. With de NO<sub>x</sub> catalysts at Euro 6 for diesels the NO<sub>x</sub> emissions should be similar to Euro 4 SI emissions. However, real world measurement of Euro 6 vehicle emissions [100, 127, 130] have shown a major problem of much higher emissions than certified for. The main reason for this is low exhaust temperatures at the low average speeds of congested traffic, as shown by Hadavi et al. [123]. This means that the de NO<sub>x</sub> catalysts are not active in congested traffic. Also if high speed journeys are undertaken, as in

the RDE test cycles, then the high powers can reach catalyst temperatures where the de NO<sub>x</sub> efficiency reduces.

#### 8.6.4.1 NO<sub>2</sub> and NH<sub>3</sub> Emissions

The NO<sub>2</sub> emissions from lambda 1 SI vehicles are normally assumed to be low, but there are relatively few measurements to demonstrate this. The NO<sub>2</sub> emissions measured on the 10 journey sections with 29 repeat journeys is shown in Figure 8-26 NO<sub>2</sub> emissions for S1-S10 vs the mean velocity. Most of the data was below 10% of Euro 4 NO<sub>x</sub>, but there were a number of journeys where the NO<sub>2</sub> was 25% of the total NO<sub>x</sub> and this is similar to the proportion in diesel engines [123]. However, the higher total NO<sub>x</sub> for diesels means that the NO<sub>2</sub> emissions will also be higher even if the proportion is similar to some real world congested traffic SI vehicle emissions. Thus the direct contribution of SI NO<sub>2</sub> to roadside NO<sub>2</sub> measurements is significant, but is not greater than the direct NO<sub>2</sub> emissions from diesels.

The ammonia emissions for all the journeys are shown in Figure 8-27 NH<sub>3</sub> emissions for S1 – S10 vs the mean velocity. The ammonia emissions are shown to be high and of the same order as the NO<sub>x</sub> emissions. Approximately 50% of the ammonia data is higher than the NO<sub>x</sub> limit of Euro4 and 50% is lower. There were some journeys in which the ammonia emissions were very low.

Ammonia is generated across TWCs by the reaction in Equation (8-2).



This occurs in local rich excursions during acceleration, which generate the hydrogen to react with NO. The large number of accelerations during congested traffic driving results in high NH<sub>3</sub> emissions.

### 8.6.5 Greenhouse gas emissions (GHG)

The greenhouse gas emissions from vehicle exhaust gases are CO<sub>2</sub>, CH<sub>4</sub> and N<sub>2</sub>O and the CO<sub>2</sub> emissions have already been presented in Figure 8-22. The CH<sub>4</sub> and N<sub>2</sub>O GHG emission are shown as a function of the average velocity in Figure 8-28 and Figure 8-29. This shows that both emissions increase for low average velocities and for high congestion. However, the variability is very high at all average velocities and only above 35 km/h are there no very high emissions. For methane and N<sub>2</sub>O the first stage S<sub>1</sub> of the hot start journeys have the highest emissions. This is associated with the unusual TWC temperatures with the upstream showing a cold start feature while the downstream remained hot. N<sub>2</sub>O emissions are sensitive to the catalyst temperature and have a high production of N<sub>2</sub>O during the 250 – 350 °C temperature window that the upstream of the catalyst experiences during the first stage of the journey after the hot start. Methane emissions follow the trends of the total hydrocarbons in Figure 8-23 with a similar spread of data and S<sub>1</sub> having the highest emissions. Typical high level emissions during congested traffic would be 0.05 g/km for methane and 0.01 for N<sub>2</sub>O. Using GHG equivalence factors of x 30 for methane and x300 for N<sub>2</sub>O this converts to 1.5 g/km CO<sub>2</sub> for methane and 3 g/km CO<sub>2</sub> for N<sub>2</sub>O. This is a total of 4.5 g/km which is about 1% of the congested traffic CO<sub>2</sub> emissions but 2.5% of the certified CO<sub>2</sub> emissions for this vehicle. Thus other GHGs than CO<sub>2</sub> are not really an issue in real world driving and there is little reason to regulate them, as the US has done, apart from when NG is used as the fuel and CH<sub>4</sub> emissions can be very high.

### 8.6.6 Toxic gas emissions

The five toxic gases that are regulated in the USA, benzene, toluene, 1,3 butadiene and formaldehyde are shown as a function of the average vehicle speed in Figure 8-30 to Figure 8-33.

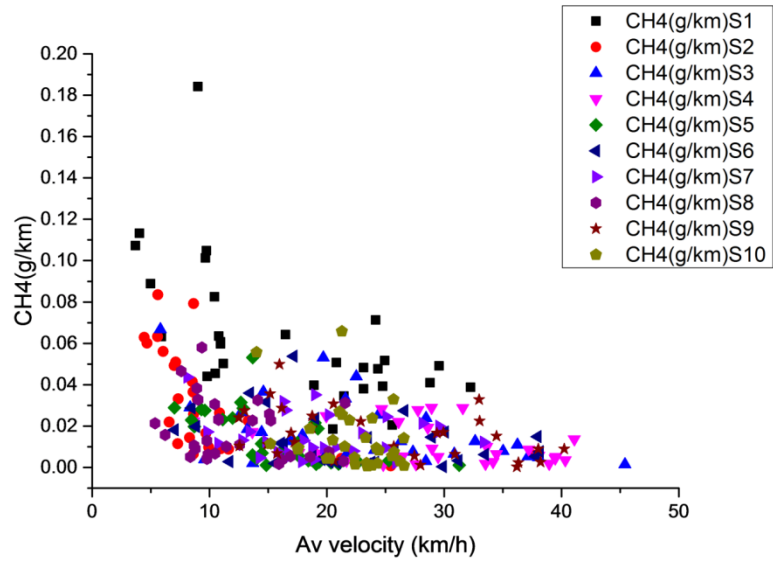


Figure 8-28 CH<sub>4</sub> emissions as a function of the average velocity.

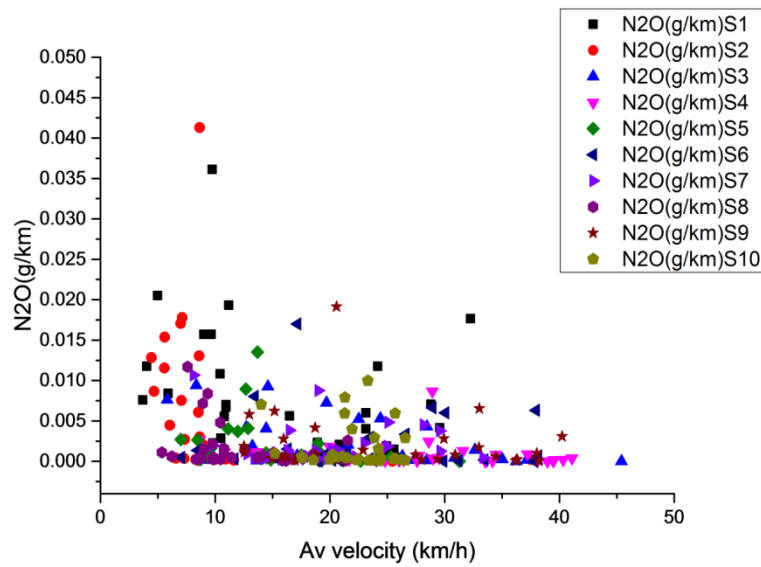


Figure 8-29 N<sub>2</sub>O emissions as a function of the average velocity.

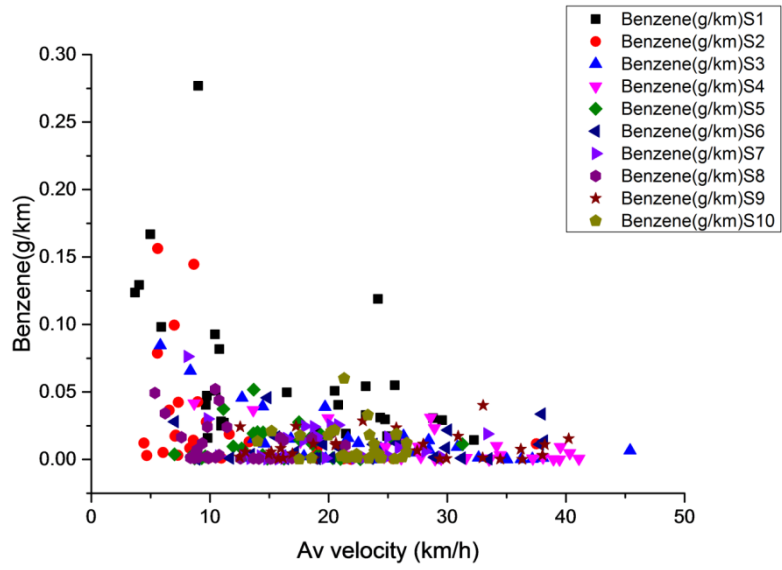


Figure 8-30 Benzene emissions as a function of the average velocity.

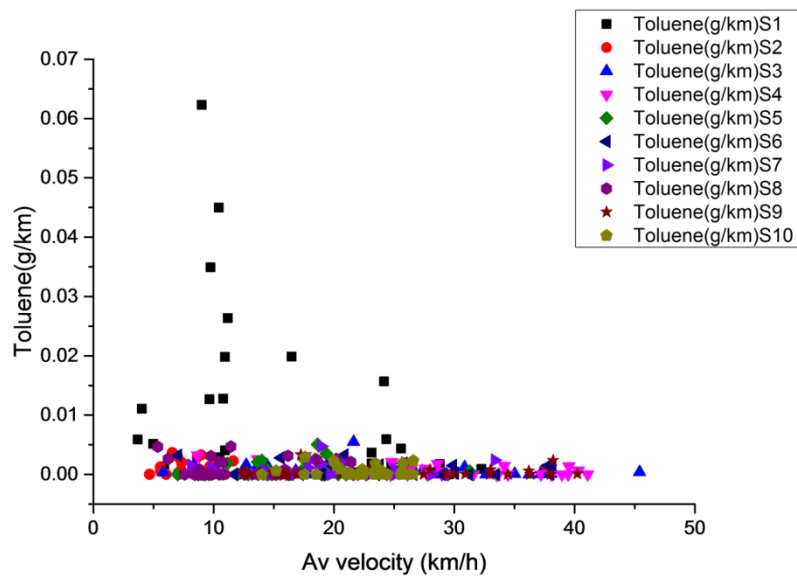


Figure 8-31 Toluene emissions as a function of the average velocity.



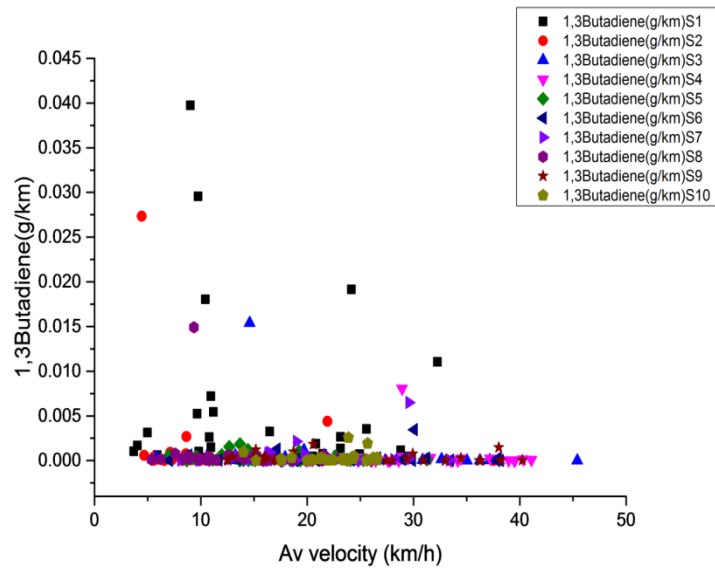


Figure 8-32 1, 3Butadiene emissions as a function of the average velocity.

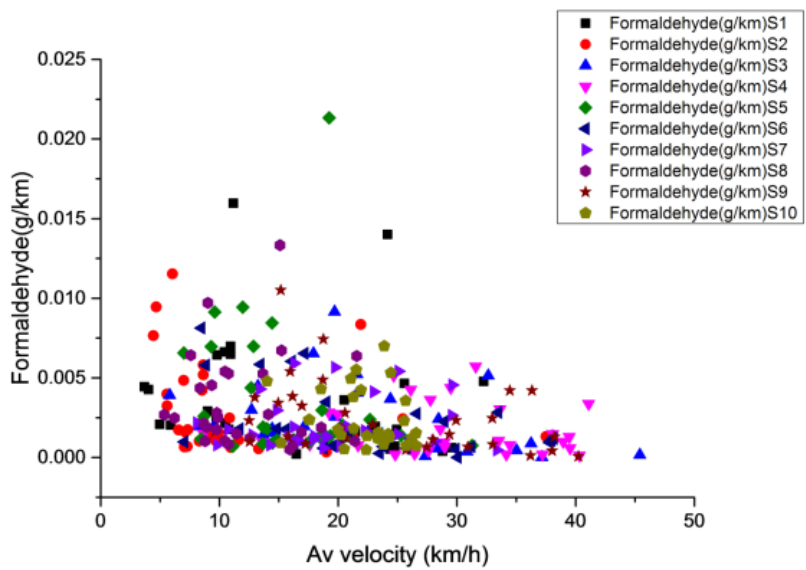


Figure 8-33 Formaldehyde emissions as a function of the average velocity.

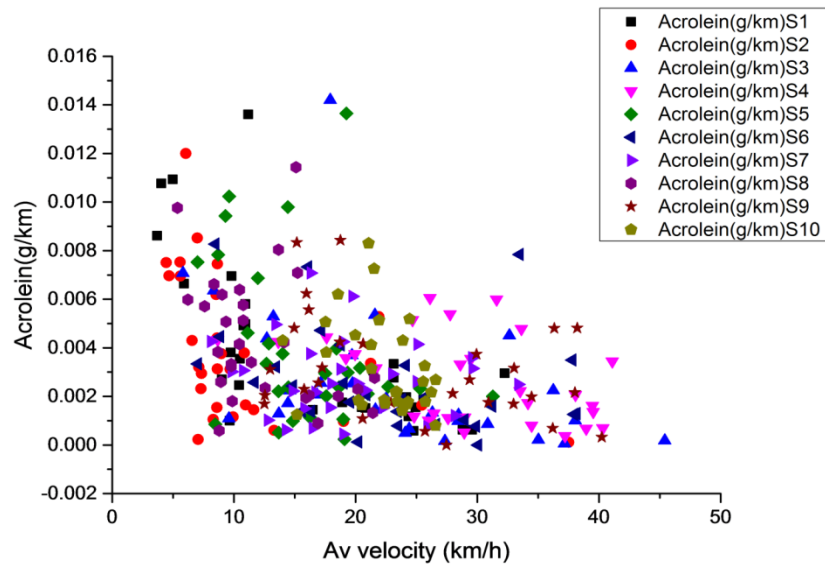


Figure 8-34 Acrolein emissions as a function of the average velocity.

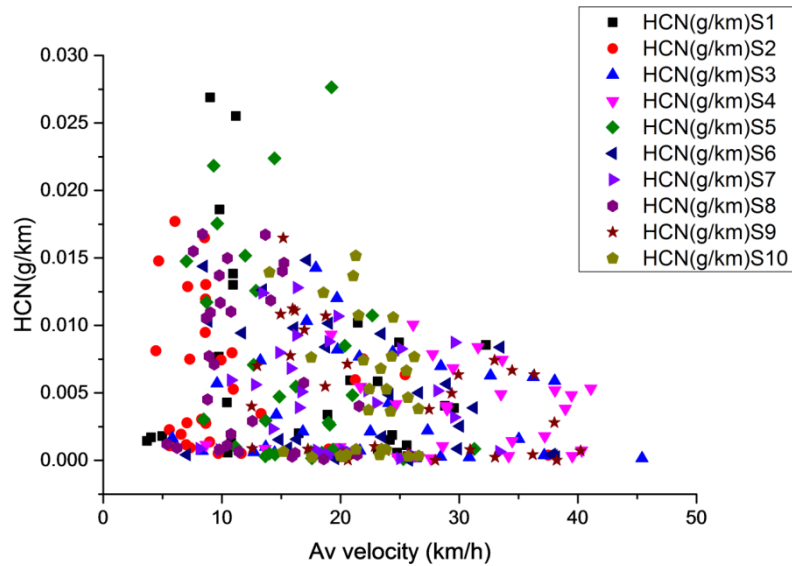


Figure 8-35 HCN emissions as a function of the average velocity.

Acetaldehyde was not emitted in significant quantities. Two other important toxic gases are shown in Figure 8-34 and Figure 8-35: acrolein and HCN. The toxic hydrocarbons follow the trend for hydrocarbons, with higher emissions

at low mean velocities and high congestion. However, the normal level of these toxic hydrocarbons would be zero if the TWC was hot and operational at  $\lambda=1$ . The results in Figure 8-30 to Figure 8-32 are close to zero but with occasional events that cause the emissions to vary widely and this occurs across the speed range, but more frequently at low speeds. The biggest occurrence of the high emissions is on journey section  $S_1$  after the hot start and where the traffic is very congested. This is particularly so for Toluene and 1,3 Butadiene, which have very few events with high values in other sections of the journey. Benzene emissions were higher than methane and the levels are significant as benzene is a known toxic to humans and is emitted in a densely populated area. EU gasoline specifications allow up to 0.9% of benzene in gasoline and so the source of the benzene is unburnt fuel. The TWC clearly is not as effective at oxidizing benzene as it is for toluene and 1,3 butadiene. The second highest emitter of benzene is  $S_2$  and  $S_3$  which are very congested parts of the route and span the region of two sets of traffic lights and two major road junctions. Figure 8-8. shows that in congested stop/start traffic the upstream temperature of the catalyst is well below the hydrocarbon light off temperature. It is likely that the light off temperature for benzene is higher than for n-alkanes and hence benzene is more sensitive to cool catalyst than other components of the exhaust gases.

A key feature of these specific hydrocarbons is that they account for a major part of the total hydrocarbons. If the data point at 10 km/h with the maximum UHC in Figure 8-23 of 1 g/km, then it can be seen in Figure 8-28 and Figure 8-30 to Figure 8-32 that this consists of 0.18 g/km of methane, 0.28 g/km of benzene, 0.06 g/km of toluene and 0.04 g/km of 1,3 butadiene. This is 0.56 g/km of these four hydrocarbons or 56% of the total. The emissions of methane and benzene each exceed the regulated emissions for total hydrocarbons. If the last data point at 45 km/h is taken then it is entirely benzene as the level is 0.01 g/km of total HC and this is the emissions level of benzene and all the other three UHC are zero. If we take the highest data point at 38 km/h at 0.14 g/km total UHC, then the benzene emissions are 0.03 in Figure 8-30. Methane is 0.017 g/km, toluene is 0.001 g/km and 1,3 butadiene is zero. The total is 0.048 g/km and at this data point other

hydrocarbons must be of more significance. If we look at another high data point on  $S_2$  at 10 km/h which has 0.8 g/km in Figure 8-23, the total of the other HC methane and the 3 toxic HC is 0.224 g/km, with benzene being the largest at 0.14 g/km.

It is thus clear that the toxic hydrocarbons are a significant fraction of the total hydrocarbons and occur through oxidation slippage at the TWC. If the above data points are looked at on the  $NO_x$  emissions in Figure 8-25 they do not occur as high peaks. This indicates that during that particular journey section the catalyst was operating slightly rich, which will give good  $NO_x$  removal but the hydrocarbon removal will depend on the efficiency of the hydrocarbon absorbers used in TWC to achieve oxidation of hydrocarbons during rich excursions. However, HC absorbers are specific to different hydrocarbons and it could be that in this case the absorber is not as good for benzene as for other hydrocarbons.

Figure 8-33 and Figure 8-34 show that aldehyde emissions are significant across all the speeds tested with only a weak increase at low speeds with congested stop/start traffic. The two aldehydes are emitted in roughly similar quantities and were extremely variable. Some journeys had 0.001 g/km emissions and others had 10 - 20 times this level. It is possible that the source of the aldehydes is the ethanol that forms about 5% of gasoline in the year the tests were undertaken. The other source of aldehydes is partial oxidation of hydrocarbons, but a source based on the ethanol in the fuel is more likely. It is clear that the TWC is not as effective in removing aldehydes as it is in oxidizing hydrocarbons.

The final toxic species is HCN in Figure 8-35. This occurs as part of  $NO_x$  formation chemistry in rich mixtures through the reaction  $HC + NO_x > HCN$ . It is thus linked to the slippage of hydrocarbons. Figure 8-35 shows that HCN formation occurs across the speed range with only a weak increase in low speed congested traffic. It is rarely zero and will be a significant environmental source of HCN emissions. Clearly to control HCN formation at the catalyst better  $\lambda=1$  control is required and this is a feature of Euro 5 and 6 vehicles. It

can be seen that congested traffic is a significant source of toxic emissions of benzene, 1,3 butadiene, toluene, acrolein, formaldehyde and HCN. All of these emissions are currently unregulated in Europe and are not required to be measured as part of air quality. However, they are all related to the total hydrocarbon emissions and understanding why there are such high exceedances of the regulated UHC levels in congested traffic is the key to understanding the source of the toxic emissions.

### **8.6.7 The role of idle in reducing the mean speed and increasing emissions**

A key source of variability in the data for the different sections of the route for the same mean speed is the proportion of time at idle. It has been analyzed for its 29 repeat journeys to investigate the impact of removing the fuel consumption and emissions during idle. The technology to do this, stop/start control, is not in production in about half of all new vehicles. By determining the proportion of time at idle in all the journeys a new average speed can be determined that is based on the ratio of the distance travelled to the time to travel that distance less the time spent at idle. Also the emission and fuel consumption during idle can be summated and deducted from the total emissions and fuel consumption. The following graphs show the effect that stop/start control would have in the present congested traffic journey.

Figure 8-36 shows the % of the time spent at idle as a function of the mean journey speed including the idle time. This clearly shows that the % of time spent at idle increases as the average and this data together with that for the US FTP and Japan J09 is shown in Figure 8-36 It is clear that in the present congested traffic the proportion of idle is higher than on test cycles because the average speed is lower. However, the test cycles % idle is similar to that found in the S<sub>8</sub> route but occurs at a higher speed.

Figure 8-37 shows that corrected CO<sub>2</sub> emissions, deducting the CO<sub>2</sub> emitted during idle, as a function of the mean moving vehicle speed (with the time spent at idle ignored). This simulates the action of a stop/start control. The CO<sub>2</sub> g/km are all still above the NEDC value for this vehicle of 180 g/km, but

the emissions are lower than in Figure 8-22. At the lowest speed the CO<sub>2</sub> emissions in Figure 8-37 are 260 g/km compared with 450 g/km in Figure 8-22. The fuel consumption during idle is shown in Figure 8-38 as a function of the % of time at idle. The corrected fuel consumption is shown as a function of the corrected mean journey speed, ignoring the fuel consumption and time at idle, is shown in Figure 8-39.

These results show that the use of stop/start engine controls will have a much more significant influence on fuel consumption and CO<sub>2</sub> emissions in congested traffic than on the FTP or NEDC or WLTC. This has led to the impact of this technology being underestimated as the benefits are always only quoted based on NEDC or FTP test cycles. At the most congested condition in the S8 journey in Figure 8-38 and Figure 8-39 the fuel saving by using engine off at idle would be 31%. At the lowest congestion it would be 6% fuel saving. A plug in HEV has been measured to have 14% fuel saving with stop/start 10.stop/start, which will be for the NEDC. Wishart [131] has measured on on-road benefit of stop-start at 9.7%, close to the minimum saving determined from the present results. They had NEDC benefits from 10.3% to 12.2% for three vehicles. However, they had some real world tests that no significant benefit of stop/start controls. Mueller [132] for the NEDC reported CO<sub>2</sub> reduction of about 4% for the NEDC and FTP test cycles. However, for real world driving on the Stuttgart RDE found 8% fuel savings from stop/start in city driving. However, all these results are for low congestion driving and the present results indicate a much greater benefit in highly congested traffic.

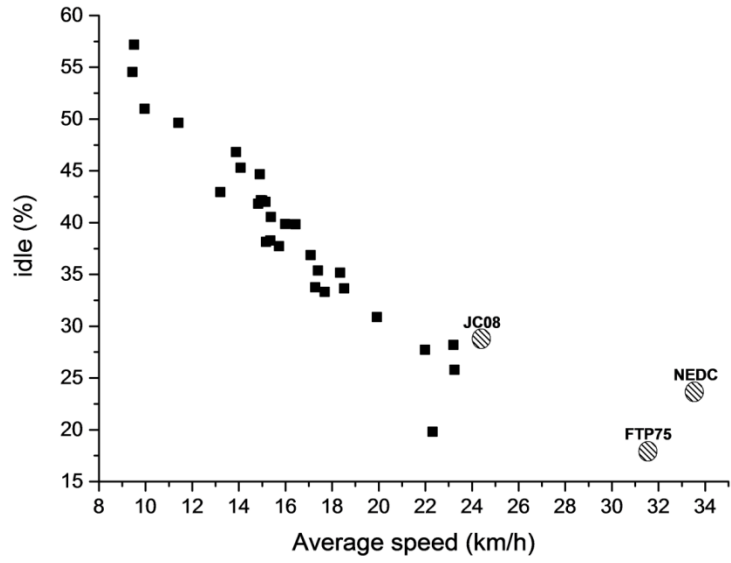


Figure 8-36 Idle percentage as a function of the average velocity.

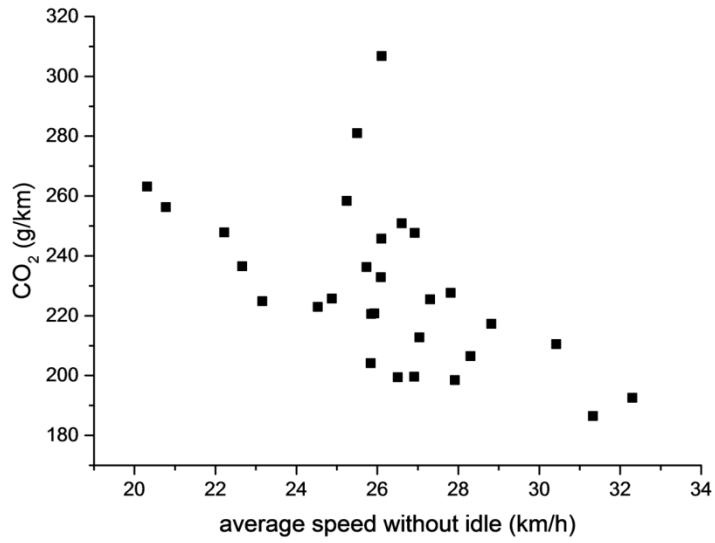
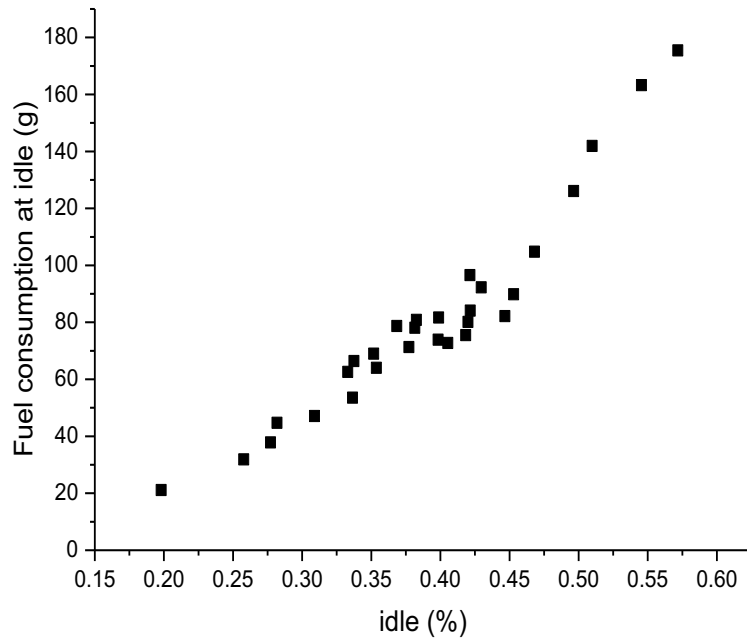
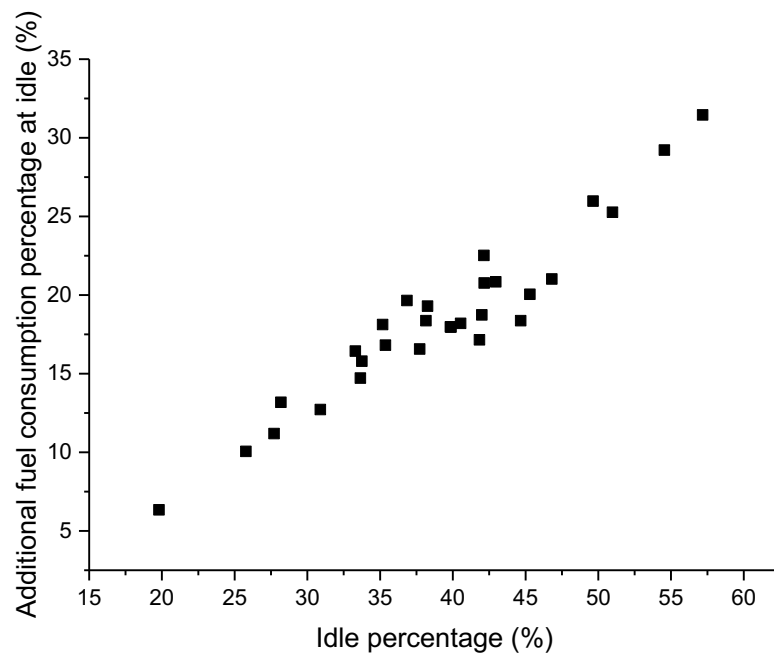


Figure 8-37 CO<sub>2</sub> as a function of the average velocity without idle.



**Figure 8-38 Fuel consumption at idle as a function of idle percentage.**



**Figure 8-39 Additional fuel consumption as a function of idle percentage.**



## 8.7 Conclusions

1. Emissions from low speed congested traffic are responsible for elevated air pollution at roadside air quality monitoring stations and for air quality exceedances in cities.
2. 50% of passenger car journeys in cities are 5km or less [23] in the real world and this should be the distance used for real world emissions studies and include congested traffic, if air quality issues are to be addressed.
3. The WLTC and RDE test procedures involve higher speeds and no congested traffic driving and in the case of the RDE no cold start. They are thus test cycles which will not produce data relevant to explaining why air quality in cities is improving much more slowly than vehicle test cycle emissions are being reduced.
4. Congested traffic journey studied had a mean vehicle speed range of 4-45 km/h, depending on the time of the day and the traffic congestion. The prime reason for high CO<sub>2</sub> emissions in congested traffic was the large numbers of stop/starts and the low thermal efficiencies at the low engine powers used in low speed congested traffic driving.
5. There was a significant 'cold start' effect, even though the TWC was at 400°C within 10s of the hot start. The low exhaust temperatures with the low powers used in congested traffic driving resulted in the cooling of the upstream of the catalyst and a loss of catalyst efficiency. It took between 100 and 400s for the upstream of the catalyst to reach 400°C after the hot start in congested traffic.
6. The congested traffic emissions of CO were very high relative to the Euro 4-6 levels for mean vehicle speeds <10 km/h. For THC the emissions were high over a wider range of speeds up to 30 km/h and this was due to the higher catalyst light off temperature for THC compared with CO. Above these speeds the emissions of CO and THC were well below Euro 4-6 levels.
7. NO<sub>2</sub> emissions were significant in congested traffic driving and were >10% of Euro 4 NO<sub>x</sub> and for some highly congested journeys >25% of NO<sub>x</sub>. Thus SI vehicles are not negligible direct emitters of NO<sub>2</sub>.

8. Ammonia emissions were similar to the  $\text{NO}_x$  emissions, due to rich excursions during acceleration. In this vehicle the calibration of the TWC lambda control was biased 2% rich to maximize  $\text{NO}_x$  reduction, but this created high levels of  $\text{NH}_3$ .
9. Greenhouse gas emissions of  $\text{CH}_4$  and  $\text{N}_2\text{O}$  are only 1% in total of the  $\text{CO}_2$  equivalent emissions in the present real world congested traffic driving and are thus not significant.
10. Toxic gas emissions of benzene are significant in real world driving, toluene and 1,3 butadiene are of lesser importance. The TWC appears not to control benzene as well as it does other hydrocarbons. The benzene emissions are a significant health concern that is currently not regulated or measured in current or future test cycles.
11. Aldehyde and HCN emissions were significant at all speeds in congested traffic and are a significant health concern.
12. The use of engine shut off at idle was shown to have a good potential to reduce emissions in real world congested traffic driving and the benefit on  $\text{CO}_2$  emissions was significantly greater than has been reported for NEDC and FTP tests.

## 9 Chapter Nine: Conclusion and future work

### 9.1 Conclusions

The VW scandal alerted the entire world regarding vehicle real world driving emissions and their impact on urban air quality. The scandal itself exposed a cheating behaviour trying to defeat the emission legislation. However, it is a well-known fact that legislative test cycles are not fit for air quality legislations. The emissions from vehicles in real world driving are of current concern, as they are often higher than on legislated test cycles and this may explain why air quality in cities has not improved in proportion to the reduction in automotive emissions. This has led to the Real Driving Emissions (RDE) legislation in Europe. It has been recognised that the transport sector is one of the major contributors to urban pollutions. So the information on real world transient emissions linked to traffic movements are essential for accurate assessment of impacts of transport on urban air quality. The purpose of this research was to investigate the real world tail pipe emissions under different traffic conditions (very congested at rush hours and less congested at off-peak hours) using a SI passenger car equipped with an on-board multi-gas real time FTIR emission analyser. Typical urban routes located in a busy residential area and a major transport link road to Leeds city centre were designed to represent typical urban driving conditions. Low air quality in cities occur at local roadside measurements stations due to the presence of locally congested traffic with higher emissions than that on the test cycles. Real driving emission are strongly influenced by driving behaviour such as aggressive driving with high acceleration/deceleration. Also ambient temperature has big impact on real driving emission, which affects catalyst light off, water and lube oil warm-up times and thus during of cold start. Moreover the real diving emissions increased with congested traffic in urban driving with low average speed and more stop/starts influence of other drivers and traffic lights, road junctions.

The road studied had 1000 cars/hour in single lane traffic at the peak congestion times and peak emissions occurred at peak congestions with the lowest average journey speed and these peak emissions multiplied with number of lanes in other area got many lane. Note that spark ignition(SI) vehicles are sensitive to quality of  $\lambda$  control, i.e. the deviation of  $\lambda$  values from stoichiometric value. Using software for live traffic monitoring and prediction to avoid congested traffic must be mandatory on all vehicles as this has a lot of benefits to reduce emissions. So it should encourage automotive industrial to build vehicles with live traffic display software by reducing the tax for cars have this kind of technology. Also stop start control of engines is important to reduce emissions as the fuel cut off technology can reduce about 20% of fuel and emissions. Furthermore use of engine shut off at idle was shown to have a good potential to reduce emissions in real world congested traffic driving and the benefit on CO<sub>2</sub> emissions was significantly greater than has been reported for NEDC and FTP tests.

Catalysts light off time in RDE with cold start was a major factor. This light off time varied depending on the traffic conditions. The light-off time for the TWC in congested traffic is 75% more than free-flowing traffic. Thus influence the emissions due to the catalyst warm-up period that is longer in real world congested traffic driving than that on the NEDC. If we compare the legislated cycles with congested real world driving we see that current driving cycles do not represent real driving emissions especially in congested traffic as real average speed less than that of standard driving cycles. In other words, existing test cycles have low levels of congested driving. The WLTC and proposed RDE have even lower congestion than the NEDC. The European RDE has no congestion and no cold start and is thus not very real world. The WLTC and RDE test procedures involve higher speeds and no congested traffic driving and in the case of the RDE no cold start. They are thus test cycles which will not produce data relevant to explaining why air quality in cities is improving much more slowly than vehicle test cycle emissions are being reduced. The number of stop/starts per km in the congested traffic driving varied from 1.5 to 7 and had a good correlation with the average journey speed. The NEDC, FTP75 and JC09 test cycles had stop/starts of 1.3-

1.5/km, which for the same average speed agrees with the present work. It is the lower average speeds in congested traffic that increases the emissions, but this is due to the increased number of stop/start events and the associated higher emissions in these events. In the highest traffic congestions the emissions for a hot start were a multiple of the regulated NEDC emissions of 1.5, 3 and 2 for CO, HC and NO<sub>x</sub> respectively and for cold start were about 2.5, 5 and 3 times of the NEDC CO, HC and NO<sub>x</sub> values respectively.

50% of passenger car journeys in cities are 5km or less [23] in the real world and this should be the distance used for real world emissions studies and include congested traffic, if air quality issues are to be addressed. Fuel consumption in congested traffic is much increased. Fuel economy has difficulty in achieving the certified values in congested urban traffic. The total fuel consumption for congested traffic could be doubled when compared to the free-flowing trips. The long stoppage time (idle) in a traffic queue can seriously reduce the engine's thermal efficiency. The vehicle specific power, VSP kW/tonne or m<sup>2</sup>/s<sup>3</sup>, can be calculated from the vehicle velocity and acceleration and the road altitude gain and the aerodynamic drag. In the present work the velocity times acceleration term dominated as elevation changes were low and average speeds were low. VSP, representing the power demand to move a vehicle is dominantly affected by the accelerations in urban driving conditions. The value of average VSP and average VSP+ can be employed as indicators of traffic congestions, which is proportional to vehicle specific power values as high values mean free flow traffic.

## 9.2 Future work

1. Carry out tests using euro 6 vehicles with portable emissions measurement system in urban areas and compare with previous results.
2. Investigation on modern hybrid vehicles with portable emissions measurement system in urban areas and compare with previous results.
3. Further investigate emissions during accelerations events, Working on the acceleration event and their effect on emissions as the acceleration is most sensitive factor with emissions amount specially in congested urban area.
4. It will be beneficial to reduce transport emission if more studies about idle event and associated emissions especially in urban congested area can be conducted so as to fully quantity the benefit of using cut off technology at idle event to reduce fuel consumptions and emissions.
5. Develop new system that can integrate software and hardware to draw and display all parameters such as velocity, acceleration, fuel consumption, VSP, lambda, oil sump temperature, water temperature, upstream catalyst, downstream catalyst in considerations of times and distances with emission amount in one graph to know exactly which parameters effect the emissions amount.
6. Investigations on decelerations event and their effect on emissions and powers available to catch.
7. Investigate the feature of intersections/junction in urban transport networks, and their effect on emissions and fuel consumptions.
8. Assess the effect of introducing new European RDE legislation on real world emissions.

## Reference

1. Transport, D.f., *review of methods used to measure hot exhaust emission factors, including test cycles and data collection methods*. 2009.
2. Gupta, H.N., *Fundamentals of internal combustion engines*. 2012: PHI Learning Pvt. Ltd.
3. Reif, K., *Gasoline Engine Management*. 2015: Springer.
4. Transport, D.f., *a review of methodologies of modelling cold-start emissions*. 2009.
5. Daham, B., et al., *Comparison of real world emissions in urban driving for euro 1-4 vehicles using a PEMS*. 2009, SAE Technical Paper.
6. Li, H., et al., *Characterization of Regulated and Unregulated Cold Start Emissions for Different Real World Urban Driving Cycles Using a SI Passenger Car*. 2008, SAE Technical Paper.
7. Schneider, S.H., *The Global Warming Debate Heats Up: An Analysis and Perspective*. National Center for Atmospheric Research, 1999.
8. Wang, A., et al., *On-road pollutant emission and fuel consumption characteristics of buses in Beijing*. *Journal of Environmental Sciences*, 2011. 23(3): p. 419-426.
9. Wang, X., et al., *Impacts of different emission sources on air quality during March 2001 in the Pearl River Delta (PRD) region*. *Atmospheric Environment*, 2005. 39(29): p. 5227-5241.
10. Wargo, J., L.E. Wargo, and N. Alderman, *The harmful effects of vehicle exhaust: a case for policy change*. 2006: Environment & Human Health.
11. Institute, V.T.P.
12. Pundir, B., *Engine emissions: pollutant formation and advances in control technology*. 2007: Alpha Science International, Limited.
13. Toyota.
14. Li, H., et al., *Impact of Driving Cycles on Greenhouse Gas (GHG) Emissions, Global Warming Potential (GWP) and Fuel Economy for SI Car Real World Driving*. *International Journal of Fuels and Lubricants*, 2009. 1(1)): p. 1320-1333.
15. Bosch, R., *Gasoline-engine Management: Basics and Components*. 2001: Sae Soc Of Automotive Eng.
16. Andrews, G.E., et al., *The effect of ambient temperature on cold start urban traffic emissions for a real world SI car*. 2004.
17. Gurney, M. and J. Allsup, *Predictability of emissions from in-use vehicles at low-ambient temperature and alternate driving cycle based on standard tests*. 1989, Warrendale, PA; Society of Automotive Engineers.
18. Hawirko, J.D. and M.D. Checkel, *Quantifying vehicle emission factors for various ambient conditions using an on-road, real-time emissions system*. 2003, SAE Technical Paper.
19. Larson, R.E., *Vehicle Emission Characteristics under Cold Ambient Conditions*. 1989, SAE Technical Paper.
20. Bielaczyc, P., *Future developments in WLTP and RDE - PEMS (PN)*. 2016.
21. Laurikko, J. and P. Aakko, *The effect of ambient temperature on the emissions of some nitrogen compounds: a comparative study on low-*

- medium-and high-mileage three-way catalyst vehicles.* 1995, SAE Technical Paper.
22. Laurikko, J. and N.-O. Nylund, *Regulated and unregulated emissions from catalyst vehicles at low ambient temperatures.* 1993, SAE Technical Paper.
  23. Liu, Z., A. Ivanco, and Z.S. Filipi, *Impacts of Real-World Driving and Driver Aggressiveness on Fuel Consumption of 48V Mild Hybrid Vehicle.* SAE International Journal of Alternative Powertrains, 2016. 5(2016-01-1166).
  24. Li, H., et al., *Study of the emissions generated at intersections for a SI car under real world urban driving conditions.* 2006, SAE Technical Paper.
  25. Li, H., et al., *Analysis of Driving Parameters and Emissions for Real World Urban Driving Cycles using an on-board Measurement Method for a EURO 2 SI car.* 2007, SAE Technical Paper.
  26. Li, H., et al., *Impact of traffic conditions and road geometry on real world urban emissions using a SI car.* 2007, SAE Technical Paper.
  27. Figliozzi, M.A., *The impacts of congestion on time-definitive urban freight distribution networks CO 2 emission levels: Results from a case study in Portland, Oregon.* Transportation Research Part C: Emerging Technologies, 2011. 19(5): p. 766-778.
  28. Lenaers, G., *Real life CO 2 emission and consumption of four car powertrain technologies related to driving behaviour and road type.* 2009, SAE Technical Paper.
  29. Barth, M. and K. Boriboonsomsin, *Real-world carbon dioxide impacts of traffic congestion.* Transportation Research Record: Journal of the Transportation Research Board, 2008(2058): p. 163-171.
  30. Khalfan, A., H. Li, and G. Andrews, *Cold Start SI Passenger Car Emissions from Real World Urban Congested Traffic.* SAE technical paper series, 2015.
  31. Marotta, A., et al., *Gaseous Emissions from Light-Duty Vehicles: Moving from NEDC to the new WLTP test procedure.* Environmental science & technology, 2015. 49(14): p. 8315-8322.
  32. Williams, R., et al., *Effect of Diesel Properties on Emissions and Fuel Consumption from Euro 4, 5 and 6 European Passenger Cars.* 2016, SAE Technical Paper.
  33. Della Ragione, L. and G. Meccariello, *GPS Signal Correction to Improve Vehicle Location and Related Emission Evaluation.* Journal of Statistical Science and Application, 2015. 3(3-4): p. 50-61.
  34. Sullivan, F., *Real Driving Emissions: Implementation and Its Impact on Current Technology.* 2017.
  35. Przybyla, G., et al., *Real World Diesel Engine Greenhouse Gas Emissions for Diesel Fuel and B100.* 2013, SAE Technical Paper.
  36. Dietrich Schwela, O. Zali, and a.P. Schwela, *Motor vehicle air pollution public health impact and control measures.* World Health Organization and ECOTOX.
  37. Guy Hytchcock, B.C., Duncan Kay, Charlotter Brannigan and Dan Newman, *Air Quality and Road Transport, Impacts and Solutions.* RAC Foundation, 2014.
  38. Woodcock, J., et al., *Prentice, and Ian Roberts. 2007. "Energy and Health 3: Energy and Transport."* Lancet. 370(9592): p. 1078-88.



39. Corsmeier, U., et al., *Comparison of measured and model-calculated real-world traffic emissions*. Atmospheric Environment, 2005. 39(31): p. 5760-5775.
40. Uherek, E., et al., *Transport impacts on atmosphere and climate: Land transport*. Atmospheric Environment, 2010. 44(37): p. 4772-4816.
41. Department for Environment, F.a.R.A., *Air quality statistics in the UK 1987 to 2015*. National Statistics, 2015.
42. Sharaf, J., *Exhaust Emissions and its Control Technology for an Internal Combustion Engine*. International Journal of Engineering Research and Applications, 2013. 3(4).
43. Asif Faiz, C.S.W.a.M.P.W., *Air Pollution from Motor Vehicles Standards and Technologies for Controlling Emissions*. 1996.
44. Technology, P.o.o.S.a., *Air quality in the UK*. 2012. 188.
45. House of Commons Environment, F.a.R.A.C., *Air Quality*. Report, 2015-2-16.
46. Godleski, J.J., et al., *Mechanisms of morbidity and mortality from exposure to ambient air particles*. Research Report (Health Effects Institute), 2000(91): p. 5-88; discussion 89-103.
47. Burnett, R.T., et al., *Associations between ambient particulate sulfate and admissions to Ontario hospitals for cardiac and respiratory diseases*. American journal of epidemiology, 1995. 142(1): p. 15-22.
48. Reddy, M.S. and C. Venkataraman, *Inventory of aerosol and sulphur dioxide emissions from India: I—Fossil fuel combustion*. Atmospheric Environment, 2002. 36(4): p. 677-697.
49. Hao, J., et al., *A study of the emission and concentration distribution of vehicular pollutants in the urban area of Beijing*. Atmospheric Environment, 2000. 34(3): p. 453-465.
50. Kim, J.J., et al., *Traffic-related air pollution near busy roads: the East Bay Children's Respiratory Health Study*. American journal of respiratory and critical care medicine, 2004. 170(5): p. 520-526.
51. Agarwal, A.K., *Biofuels (alcohols and biodiesel) applications as fuels for internal combustion engines*. Progress in energy and combustion science, 2007. 33(3): p. 233-271.
52. Moriarty, P. and D. Honnery, *The prospects for global green car mobility*. Journal of Cleaner Production, 2008. 16(16): p. 1717-1726.
53. Institute, V.T.P., *Transportation Cost and Benefit Analysis II – Air Pollution Costs*. 2015.
54. Sher, E., *Handbook of air pollution from internal combustion engines: pollutant formation and control*. 1998: Academic Press.
55. Andrews, G.E., et al., *Influence of ambient temperature on cold-start emissions for a Euro 1 SI car using in-vehicle emissions measurement in an urban traffic jam test cycle*. 2005, SAE Technical Paper.
56. Weingart, P., A. Engels, and P. Pansegrau, *Risks of communication: discourses on climate change in science, politics, and the mass media*. Public understanding of science, 2000. 9(3): p. 261-283.
57. Cox, R.A., R.G. Derwent, and M.R. Williams, *Atmospheric photooxidation reactions. Rates, reactivity, and mechanism for reaction of organic compounds with hydroxyl radicals*. Environmental Science & Technology, 1980. 14(1): p. 57-61.
58. Haagen-Smit, A., *Chemistry and physiology of Los Angeles smog*. Industrial & Engineering Chemistry, 1952. 44(6): p. 1342-1346.

59. Hoffmann, T., et al., *Formation of organic aerosols from the oxidation of biogenic hydrocarbons*. Journal of Atmospheric Chemistry, 1997. 26(2): p. 189-222.
60. Ostro, B.D., et al., *Asthmatic responses to airborne acid aerosols*. American journal of public health, 1991. 81(6): p. 694-702.
61. Raizenne, M.E., et al., *Acute lung function responses to ambient acid aerosol exposures in children*. Environmental health perspectives, 1989. 79: p. 179.
62. Pereda-Ayo, B. and J. R., *NOx Storage and Reduction for Diesel Engine Exhaust Aftertreatment*. 2013.
63. Andrews, P.G.E., *CO Formation in SI engines*. 2008, University of Leeds, ERRI, SPEME, UK.
64. Eastwood, P., *Critical topics in exhaust gas aftertreatment*. 2000.
65. Prof. Gordon E. Andrews, *The Kinetics of NOx and CO Formation in SI and Diesel engines* 2008, University of Leeds, UK.
66. Mueller Associates Inc. Baltimore, M., *Indoor Air Quality Environmental Information Handbook: Combustion Sources*. 1985, Brookhaven National Laboratory Upton: Syscon Corporation Washington, DC, New York.
67. Wylie, W. and V. Armstrong. *Exposure guidelines for residential indoor air quality*. in *Transactions of an APCA Specialty Conference, Indoor Air Quality in Cold Climates: Hazards and Abatement Measures*. 1986. Air Pollution Control Association Pittsburgh.
68. Andrews, P.G.E. *Engine Emissions Measurement* 2012. ERRI, SPEME, University of Leeds.
69. Agentschap NL, M.v.E.Z., Landbouw en Innovatie, *Hydrocarbon emissions from gas engine CHP-units 2011 measurement program*. 2011.
70. Heywood, J.B., *Internal combustion engine fundamentals*. Vol. 930. 1988: Mcgraw-hill New York.
71. Harrison, R.J., *Chemicals and gases*. Primary Care: Clinics in Office Practice, 2000. 27(4): p. 917-982.
72. Auckenthaler, T.S., *Modelling and Control of Three-Way Catalytic Converters*. Thesis, SWISS FEDERAL INSTITUTE OF TECHNOLOGY ZURICH, 2005.
73. Seijger, G.B.F., *Cerium-ferrierite catalyst systems for reduction of NOx in lean burn engine exhaust gas*. 2002: TU Delft, Delft University of Technology.
74. INC., D.R., *Reduction in Emissions with Catalytic Converters*. 2010.
75. E. P. Brandt, Y.W.a.J.W.G., *Dynamic Modeling of a Three-Way Catalyst for SI Engine Exhaust Emission Control*. IEEE Transactions on Control Systems Technology, 1999.
76. Pontikakis, G.N., G.S. Konstantas, and A.M. Stamatelos, *Three-Way Catalytic Converter Modeling as a Modern Engineering Design Tool*. Journal of Engineering for Gas Turbines and Power, 2004. 126(4): p. 906.
77. UNICORE, P.m., *Catalytic Converter*. 2015.
78. Heck, R.M. and R.J. Farrauto, *Automobile exhaust catalysts*. Applied Catalysis A: General, 2001. 221(1): p. 443-457.
79. Bera, P. and M. Hegde, *Recent advances in auto exhaust catalysis*. Journal of the Indian Institute of Science, 2010. 90(2): p. 299-325.

80. Chang, C.-F., et al., *Air-fuel ratio control in spark-ignition engines using estimation theory*. Control Systems Technology, IEEE Transactions on, 1995. 3(1): p. 22-31.
81. Usami, J. and M. Nishiwaki, *Method of compensating output of air/fuel ratio sensor for variation in the current sensitivity to oxygen*. 1993, Google Patents.
82. Tunestål, P., et al., *Hydrogen addition for improved lean burn capability of slow and fast burning natural gas combustion chambers*. 2002, SAE Technical Paper.
83. Cairns, A. and H. Blaxill, *The effects of combined internal and external exhaust gas recirculation on gasoline controlled auto-ignition*. 2005, SAE Technical Paper.
84. Government, L.
85. Heeb, N.V., et al., *Three-way catalyst-induced formation of ammonia—velocity- and acceleration-dependent emission factors*. Atmospheric Environment, 2006. 40(31): p. p. 5986-5997.
86. Heeb, N.V., C.J. Saxer, A.-M. Forss, and S. Brühlmann, *Correlation of hydrogen, ammonia and nitrogen monoxide (nitric oxide) emissions of gasoline-fueled Euro-3 passenger cars at transient driving*. Atmospheric Environment, 2006. 2006 40(20): p. 3750-3763.
87. Heeb, N.V., et al., *Trends of NO-, NO2-, and NH3-emissions from gasoline-fueled Euro-3- to Euro-4-passenger cars*. Atmospheric Environment, 2008. . 42(10): p. 2543-2554.
88. Bielaczyc, P., et al., *A comparison of ammonia emission factors from light-duty vehicles operating on gasoline, liquefied petroleum gas (LPG) and compressed natural gas (CNG)*. SAE International Journal of Fuels and Lubricants, 2012. 5(2): p. 751-759.
89. Hu Li, A.K., and Gordon Andrews, *Determination of GHG Emissions, Fuel Consumption and Thermal Efficiency for Real World Urban Driving using a SI Probe Car*. SAE International, 2014. 7(3 ).
90. Khalfan, A., H. Li, and G. Andrews, *Speciation of nitrogen compounds in the tailpipe emissions from a SI car under real world driving conditions*. SAE International Journal of Engines, 2014. 7(4): p. 1961-1983.
91. Bosch, R., *Bosch Automotive Handbook, ser. Bosch Invented for life*. 2011, Wiley.
92. Kühlwein, J., J. German, and A. Bandivadekar, *Development of test cycle conversion factors among worldwide light-duty vehicle CO2 emission standards*. ICCT, Washington, DC, USA, 2014.
93. Leeds, D.H.L.U.o., *Real world in vehicle emission measurements SEME 5400 mini-transport project*.
94. (ACEA), T.E.A.M.A., *Car Emissions Testing Facts*. 2016.
95. Commission, E., *The Clean Air Policy Package Impact Assessment*. 2013.
96. Bielaczyc, P., *Current developments in WLTP test cycle and comparison of vehicles on NEDC and WLTP Current developments in RDE legislation and testing (PEMS) for Euro 6c and Euro 6d Bosmal* . 2016.
97. Agency, E.E., *Air quality in Europe*. 2013.
98. Khalfan, A., H. Li, and G. Andrews. *Real Driving Emissions in Congested Traffic: A Comparison of Cold and Hot Start*. in Conference

- Proceedings SAE International Powertrain, Fuels and Lubricants Meeting*. 2016. SAE International.
99. Gordon E. Andrews, Hu Li, A.S.H., Ahmad Khalfan, School of Chemical and Process Engineering, University of Leeds. 3rd International Conference on Real Driving Emissions, Berlin, Germany, *RDE in Congested Traffic with Cold Start*. 2015.
  100. Weiss, M., et al., *Will Euro 6 reduce the NO<sub>x</sub> emissions of new diesel cars?—Insights from on-road tests with Portable Emissions Measurement Systems (PEMS)*. Atmospheric Environment, 2012. 62: p. 657-665.
  101. Nakamura, H., et al., *Development of a wet-based NDIR and its application to on-board emission measurement system*. 2002, SAE Technical Paper.
  102. Li, H., et al., *Analysis of Driving Parameters and Emissions for Real World Urban Driving Cycles using an on-board Measurement Method for a EURO 2 SI car*. SAE Technical Paper Series 2007-01-2066/JSAE 20077353, in *The JSAE International Fuels and Lubes Conference 2007*, SAE International/JSAE: Kyoto, Japan.
  103. Li, H., et al., *Impact of Traffic Conditions and Road Geometry on Real world Urban Emissions Using a SI Car*. SAE Technical Paper Series 2007-01-0308, in *Emissions measurement and testing, 2007 (SP-2089)*. 2007, SAE International.
  104. Tziraks, E., et al., *Vehicle Emissions and Driving Cycles: Comparison of the Athens Driving Cycle (ADC) with ECE-15 and European Driving Cycle (EDC)*. Global Nest, 2006. 8(3): p. 282-290.
  105. Wyatt, D.W., H. Li, and J. Tate, *Examining the Influence of Road Grade on Vehicle Specific Power (VSP) and Carbon Dioxide (CO<sub>2</sub>) Emission over a Real-World Driving Cycle*. 2013, SAE Technical Paper.
  106. Fonseca, N., J. Casanova, and M. Valdés, *Influence of the stop/start system on CO<sub>2</sub> emissions of a diesel vehicle in urban traffic*. Transportation Research Part D: Transport and Environment, 2011. 16(2): p. 194-200.
  107. Council, L.C., *Leeds NGT Trolleybus Public Inquiry TWAO Doc.C-1-8 Leeds Transport Model—Forecasting and NGT Central Case*. 2014.
  108. Council, L.C., *Leeds NGT Trolleybus Public Inquiry TWAO Doc.C-1-3 Leeds Transport Model—Update*. 2014.
  109. Van De Vate, J.F., *Comparison of energy sources in terms of their full energy chain emission factors of greenhouse gases*. Energy Policy, 1997. 25(1): p. 1-6.
  110. Weisser, D., *A guide to life-cycle greenhouse gas (GHG) emissions from electric supply technologies*. Energy, 2007. 32(9): p. 1543-1559.
  111. Agency, D.f.T.V.C., *New car fuel consumption and emissions figures 2005*. 2005.
  112. Heeb, N.V., et al., *Trends of NO-, NO<sub>2</sub>-, and NH<sub>3</sub>-emissions from gasoline-fueled Euro-3-to Euro-4-passenger cars*. Atmospheric Environment, 2008. 42(10): p. 2543-2554.
  113. Finlayson-Pitts, B.J. and J.N. Pitts, *Tropospheric air pollution: ozone, airborne toxics, polycyclic aromatic hydrocarbons, and particles*. Science, 1997. 276(5315): p. 1045-1051.
  114. UN, *Guidance documents and other methodological materials for the implementation of the 1999 Protocol to Abate Acidification*,

- Eutrophication and Ground-level Ozone (Gothenburg Protocol)*  
Gothenburg Protocol United Nations Economic Commission for Europe, 1999.
115. Heeb, N.V., et al., *Three-way catalyst-induced formation of ammonia—velocity-and acceleration-dependent emission factors*. Atmospheric Environment, 2006. 40(31): p. 5986-5997.
  116. Heeb, N.V., et al., *Correlation of hydrogen, ammonia and nitrogen monoxide (nitric oxide) emissions of gasoline-fueled Euro-3 passenger cars at transient driving*. Atmospheric Environment, 2006. 40(20): p. 3750-3763.
  117. Liu, I.O. and N.W. Cant, *The formation and reactions of hydrogen cyanide during isobutane-SCR over Fe-MFI catalysts*. Catalysis Surveys from Asia, 2003. 7(4): p. 191-202.
  118. Karlsson, H.L., *Ammonia, nitrous oxide and hydrogen cyanide emissions from five passenger vehicles*. Science of the Total Environment, 2004. 334: p. 125-132.
  119. Coelho, M.C., et al., *Assessing methods for comparing emissions from gasoline and diesel light-duty vehicles based on microscale measurements*. Transportation Research Part D: Transport and Environment, 2009. 14(2): p. 91-99.
  120. Council, L.C., *Leeds NGT Trolleybus Public Inquiry TWAO Doc. A-08c-1 Air Quality*. 2013.
  121. Taylor, G.W. and S. Stewart, *Cold start impact on vehicle energy use*. 2001, SAE Technical Paper.
  122. Tzirakis, E., et al., *Vehicle emissions and driving cycles: comparison of the Athens driving cycle (ADC) with ECE-15 and European driving cycle (EDC)*. Global NEST Journal, 2006. 8(3): p. 282-290.
  123. Hadavi, S.A., et al., *Comparison of gaseous emissions for B100 and diesel fuels for real world urban and extra urban driving*. SAE International Journal of Fuels and Lubricants, 2012. 5(2012-01-1674): p. 1132-1154.
  124. Hadavi, S., et al., *Diesel Cold Start into Congested Real World Traffic: Comparison of Diesel and B100 for Ozone Forming Potential*. 2013, SAE Technical Paper.
  125. Hadavi, S.A., et al., *Diesel Cold Start into Congested Real World Traffic: Comparison of Diesel, B50, B100 for Gaseous Emissions*. 2013, SAE Technical Paper.
  126. Li, H., A. Khalfan, and G. Andrews, *Determination of GHG emissions, fuel consumption and thermal efficiency for real world urban driving using a SI probe car*. SAE International Journal of Engines, 2014. 7(3): p. 1370-1381.
  127. S. Hausberger, S., Blassnegger, J., Lipp, S. , *Experience with Current RDE Legislation. Proc. 3rd Conf. on Real Driving Emissions*. 2015.
  128. Merkisz, J., Pielecha, J. and Fuc, P., *Selected Investigations of Exhaust Emissions Measurements in Vehicle Real Operating Conditions and their Practical Implications. Proc. Conf. on Real Driving Emissions*. 2015.
  129. Bielaczyc, P.A., *Comparison of RDE Testing with the WLTP as Evaluation Tools for Emissions and Fuel Consumption. Proc. 3rd Conf. on Real Driving Emissions*. 2015.
  130. Mamakos, A.a.M., U. JRC report 72196

131. Wishart, J., et al., *Quantifying the Effects of Idle-Stop Systems on Fuel Economy in Light-Duty Passenger Vehicles*. 2012, SAE Technical Paper.
132. Mueller, N., et al., *Next Generation Engine Start/Stop Systems: "Free-Wheeling"*. SAE International Journal of Engines, 2011. 4(2011-01-0712): p. 874-887.